Second Series *October, 1928* *Vol. 32, No. 4*

THE

PHYSICAL REVIEW

THE ORIGIN OF THE COSMIC RAYS

By R. A. Millikan and G. H. Cameron

Abstract

Maximum energy released by atomic-disintegration (radioactivity.)—From Einstein's equation $Mc^2 = E$ and Aston's curve the maximum possible energy that can be released in radioactive changes can be computed. The theoretical and experimental values are in satisfactory agreement.

Energy released in step-by-step atom-building.—No step-by-step atom-building process can produce rays as penetrating as the observed cosmic rays. The absence of the radiations corresponding to such step-by-step processes probably means that atom-building does not in general occur in this way.

The creation of helium out of hydrogen.—About 80 percent of the observed cosmic rays appear to be due to the act corresponding to the sudden union of four positive and two negative electrons into the nucleus of the atom of helium. This produces a cosmic ray of absorption coefficient $\mu = 0.30$ per meter of water.

The creation of oxygen and silicon out of hydrogen.—The observed cosmic rays of absorption coefficients $\mu = 0.08$ and $\mu = 0.04$ appear to be produced by the sudden building of positive and negative electrons into atoms of oxygen and silicon, the former act giving rise to a ray of absorption coefficient $\mu = 0.08$, the latter to $\mu = 0.04$. This last is a definitely observed ray having an energy corresponding to the fall of an electron through 216,000,000 volts.

Possible rays due to the creation of iron and to the annihilation of hydrogen.—The cosmic-ray indications are reconcilable with the view that iron is produced by the union in a single act of positive and negative electrons into the atom of iron, but the cosmic rays show no direct indications of the transformation of the whole mass of the hydrogen atom into radiation.

Synthetic cosmic-ray curves.—The observed cosmic-ray curve can be built up fairly satisfactorily by the assumption that the relative intensities of the cosmic rays reaching the earth's atmosphere are proportional to the abundance of the common elements in meteorites and the earth's crust, 96 percent of these bodies being made of the four elements, oxygen, magnesium, silicon and iron.

The kinetics of atom-building.—While the kinetics of atom-building are more bothersome than the thermodynamics, with suitable assumptions, presented herewith, they may not offer wholly insuperable difficulties.

The place of origin of the cosmic rays.—Evidence is presented to show that cosmic rays do not originate in the stars, but only in the depths of space where temperature and densities are practically zero.

Cosmic rays and the Second Law of Thermodynamics.—The observed properties of cosmic rays, indicating that the creation of the common elements occurs only in interstellar or intergalactic space, suggest the possibility of avoiding the "wärmetod," and of regarding the universe as already in "the steady state."

1. Introduction

IN PRECEDING papers[1] we have presented an ionization-depth curve of high "resolving power" and have shown that this curve indicates a cosmic-ray spectrum consisting of two main sets of bands nearly three octaves apart, the long wave-length band which is responsible for most of the ionization in the atmosphere having an absorption coefficient of about $\mu=0.35$ while the short wave-length band is resolvable into two wave-lengths of the values $\mu=0.08$ and $\mu=0.04$, the first having an intensity about half that of the second.

These results were obtained from an empirical analysis of the ionization-depth curve and entirely without the guidance of any theory. They represented solely the general type of solution demanded by the nature of the curve itself. This solution had at once one consequence of great significance. For it required us to discard the suggestion which we had made earlier that these rays might be due to the impact of very high speed (up to 216,000,000 volt) electrons against the nuclei of atoms. For any such cause would produce a *general* cosmic-ray radiation instead of a spectrum consisting of bands. *The existence of cosmic-ray bands, definitely shown by our curve, demands that the cosmic rays originate in some nuclear act or acts having sharply defined energy-values translatable, like quantum jumps, into spectral-line frequencies.*

2. General Significance of a Banded Cosmic-Ray Spectrum

After we had made the foregoing empirical analysis, prepared the foregoing paper in essentially the form in which it appears in the Physical Review for June 1928, and presented the results (Feb. 16, 1928) in detail to the physics seminar at the Norman Bridge Laboratory, our minds being up to this time completely unbiased by any knowledge as to whether bands might be expected, or if so where they might occur, we set at the task of seeing whether we could find any theoretical justification for their existence, or for their energy-values.

If the Einstein special theory of relativity may be taken as a sound basis of reasoning—and no results predicted by it have ever thus far been shown to be incorrect, while it has many striking successes to its credit—then it follows that radiant energy can never escape from an atomic system without the disappearance of an equivalent amount of mass from that system, these relations being contained in the now well-known and universally-used equation of Einstein (1905) $Mc^2=E$, where M is mass in grams, c is the velocity of light in centimeters per second, and E is energy in ergs.

[1] Millikan and Cameron, Nature Jan. 7, 1928, Science Apr. 13, 1928, 401, Phys. Rev. **31,** 921 (1928). The analysis of the curve into three definite spectral bands was presented at the Physics seminar of the California Institute Feb. 16, 1928. The proof that these bands constitute the signals of atom-building processes was presented publicly to the California Institute Associates on March 16th and carried in Associated Press reports the next day March 17, 1928.

Now, through the recent, very exact work of Aston[2] supplemented by preceding atomic weight determinations, we know the mass of every one of the atoms with a great deal of certainty, and we can therefore compute the amount of ether-wave energy that can be generated by any sort of atomic transformation that can take place, and knowing this energy we can compute, with the aid of the Einstein equation, the frequency, and with the aid of the Dirac formula,[3] the penetrating power of any rays resulting from all possible atomic transformations. *Such studies reveal the fact that there are no possible transformations capable of yielding rays of the enormous penetrating power observed by us except those corresponding to the building up or creation of the abundant elements like helium, oxygen, silicon and iron out of hydrogen, or in the case of the last two elements out of helium.*

The entire annihilation of hydrogen by the falling completely together of its positive and negative electrons might be an additional possibility, but it can be eliminated in this case for two excellent reasons. The first of these reasons is that there is practically no place whatever for such a radiation in the *observed* ionization-depth curve, for it would be between four and five times more penetrating than the radiation that has the smallest absorption coefficient mentioned above. The ionization due to it, if it exists, would then have to be included in the 2.4 ions which represents the "zero of the electroscope."[1] But this 2.4 ions is only about one-tenth of the observed ionization at the top of the curve, viz. 21 ions, this topmost reading corresponding to a depth of 1 m below the surface of Gem Lake (Alt. 9000 ft.). So that this hypothetical radiation can have nothing to do with the observed ionization-depth curve much above the reading 2.4; and below it there is of course room only for a radiation relatively negligible in intensity in comparison with the softer rays that are responsible for the observed curve.

The second reason is that this hypothetical radiation, if it were present, would of necessity be homogeneous and could not therefore exhibit the banded structure shown by the observed cosmic rays. Whether then this act of the entire annihilation of the hydrogen atom through the coming into complete coincidence of the positive and negative electrons takes place or not, it can certainly be eliminated as a cause of the *observed* cosmic rays. There remains, then, as shown more in detail below, no other atomic transformation in which sufficient mass disappears to create the observed cosmic rays except the aforementioned *atom-building* processes.

3. Energy Released in Atomic Disintegrating Processes—Radioactivity

It is easy to show that no *radioactive* change will suffice for the generation of the cosmic rays, since the Einstein equation tells us that in no case can a radioactive transformation produce rays of more than from one-fourth to one-twenty-fifth of the observed penetrating power. This can be

[2] Aston, Proc. Roy. Soc. **A115,** 487 (1927).
[3] Dirac, Proc. Roy. Soc. **A111.** 423 (1926).

seen from a glance at Aston's curve which for convenience is reproduced herewith (Fig. 1). The radioactive, or *disintegrating* process is always one in which the products of the disintegration are either an alpha particle and an atom of atomic weight four units lower than the parent atom, or else a beta particle and an atom of practically the same atomic weight as the parent atom. In the latter case there has been no *measurable* change in mass, and this is of course also true when the radioactive process emits both beta and gamma rays, so that the only *measurable* source of radioactive energy of any sort is the change in mass associated with the expulsion of an alpha ray. The case of the radioactivity of potassium and rubidium, which emit only beta rays, is no exception to this rule since with methods thus far available there is no measurable change in mass involved in these activities—a fact altogether in keeping with the minute evolution of energy that accompanies them.

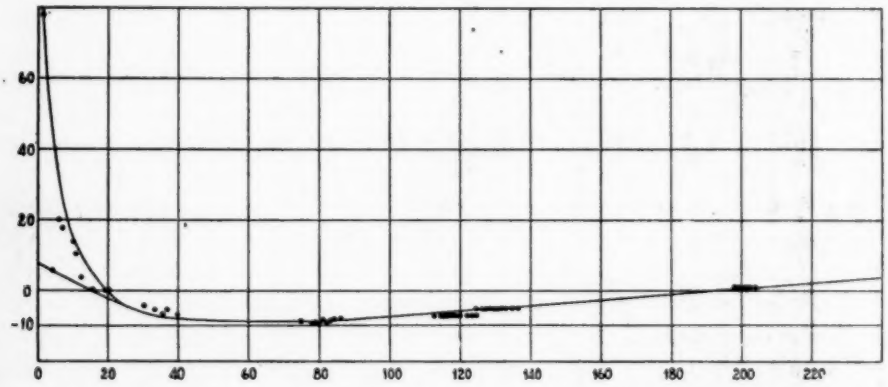

Fig. 1. Aston's mass spectrograph curve. Abscissas: mass numbers of the elements; Ordinates: $(m-1)\times 10^4$ where m is the mass of the hydrogen nucleus in the atom considered.

There can now be but little doubt that the mass of the hydrogen nucleus in all the atoms lies very close to Aston's smooth curve shown in Fig. 1; and if this is so it follows at once that no atom of atomic weight less than 80 can possibly be radioactive in the sense of emitting alpha rays. For the curve up to its lowest point, or minimum, which is reached at about atomic weight 80, requires that the total mass after such hypothetical alpha-ray emission from an atom lighter than one of atomic weight 80, be *greater than* the total mass before the act. This of course means that no act calling for the emission of energy can take place. In other words, the disintegration, by the emission of alpha rays or of hydrogen nuclei, of all atoms of atomic weight less than 80 must be an *endothermic*, not an *exothermic* process, i. e. *it is one that cannot take place at all of itself.*

This disposes quite effectively of the suggestion made many times within the past thirty years that there is the possibility of obtaining energy out of the *disintegration* of the common elements. If Aston's curve is even approximately correct it is only very heavy elements that can possibly

evolve energy through disintegrating, and *there are no abundant elements at all above atomic weight 80.* The whole of such elements taken together constitute not one percent of all matter.[4]

The condition which must be satisfied in order that even a heavy atom may liberate energy through the emission of an alpha particle may be seen at once from Aston's curve. *Such liberation can only happen in that part of the curve that is rising so rapidly with increasing atomic weight that*

$$n\Delta y > 4\times(0.00054 - y_n)$$

in which n is the atomic weight of the atom ejecting the alpha ray, Δy is the difference in ordinate between $(n-4)$ and n, y_n is the ordinate corresponding to the atomic weight n, and 0.00054 is the value of y for helium (See Fig. 1), i.e. it is the mass of the hydrogen nucleus as it appears within the alpha particle.

This equation not only shows that it is the very heavy atoms alone that can disintegrate with the ejection of alpha rays and the evolution of energy, but it enables us to compute the maximum hardness, or penetrating power, of any radiations that can be produced by the process of radioactive disintegration.

Thus when thorium, for example, throws off an alpha particle, since the curve shows that at $n=232$, $y_n=0.00031$, the *increase* in the mass of the alpha particle per gram-atom by virtue of the fact that it has escaped from the nucleus is

$$4(0.00054-0.00031)=0.00092$$

The *loss* in mass of the residue of the disintegrating thorium atom

$$n\Delta y=0.000034\times 228=0.007752.$$

Therefore the total loss in mass through the emission of the alpha ray is

$$0.00775-0.00092=0.00683 \text{ grams per gram-atom.}$$

By Einstein's equation the total energy available for emission in any form because of this loss of mass is $0.00683c^2$ ergs per gram-atom. The total energy that can be given off in each act of ejection of an alpha particle is this divided by the Avogadro number 6.062×10^{23} or 1.004×10^{-5} ergs. Now the highest speed alpha ray known to be given off from radium, according to Kovarik and McKeehan's recent tables, has an energy of 7,700,000 volts which is equivalent to 1.2×10^{-5} ergs.[5] ThC′ ejects in one instance an alpha ray with 14 percent more energy than this. Similarly according to the same tables the "upper limit" for the speed of a beta ray ejected by any of the disintegration products of thorium or radium is 7,540,000 volts or

[4] F. W. Clark, Chem. News, **123**, 341 (1921) shows that the nine elements—O, Si, Al, Fe, Ca, Na, K, H and Te—all light elements—constitute 98% of the earth's crust.

[5] Kovarik and McKeehan, Nat. Res. Council Report on Radioactivity, p. 68.

again 1.2×10^{-5} ergs[6] so that *Einstein's equation predicts very beautifully quite within the limits of reliability of Aston's measurements of mass, the maximum energy available in the radioactive process.*

In general it is the loss of mass when the alpha particle is ejected that must furnish the energy not only for the alpha ray, but also for the beta and gamma rays, since these last two ejections by themselves involve no appreciable loss of mass. Hence most of the alpha, beta and gamma rays given off by the radioactive process will contain very much less energy than the foregoing maximum value, as the radioactive tables show is in fact the case. There are actually no gamma rays from radium or thorium that correspond to an energy of more than about 2,000,000 volts,[7] and these (from RaC and ThC″) have an absorption coefficient of 4.0 per meter of water,[8] which means that they are completely absorbed, i.e. reduced to less than say 2 percent of their initial value, in going through one meter of water. It is not strange that the hardest gamma ray has only about one-fourth the energy of the swiftest alpha and beta rays, since Meitner[9] Ellis[10] and Rutherford[11] have shown that the emission of a charged particle is the primary act in the radioactive process, the emission of a gamma ray being a secondary phenomenon.

The Einstein equation then, taken in connection with Aston's determinations of the precise mass relations of the atoms, not only shows that the property of radioactivity involving the emission of alpha rays must be limited to a very few, very heavy and relatively very rare atoms, for all of the very heavy atoms are non-abundant, but it predicts altogether satisfactorily the observed energy-characteristics of the radiations emitted. The important point for the present argument is that these considerations show that almost all conceivable atomic disintegrating processes involve the *input*, i.e. the *absorption*, rather than the emission of energy, and that none of the few possible exothermic disintegrating processes can in any case give rise to an ethereal radiation of greater energy than would correspond to the fall of an electron through about 8,000,000 volts. A radiation of this theoretical upper limit of penetrating power for a ray arising from a radioactive transformation would be four times as penetrating as the hardest observed rays from RaC or ThC″, i.e. it would pass through approximately four meters of water before becoming completely absorbed (reduced to less than 2 percent of its initial value). *The cosmic rays found by us to pass through eighteen times this amount of matter or 70 meters of water must therefore have an entirely different origin. They correspond to the fall of an electron through 216,000,000 volts and cannot be produced by any atomic disintegrating process whatever since there is no such process that can liberate enough mass to supply the needed energy.*

[6] Kovarik and McKeehan, Nat. Res. Council Report on Radioactivity, p. 92.
[7] Kovarik and McKeehan, l.c. p. 122 also Meyer and v. Schweidler, Radioaktivität, p. 641.
[8] Kovarik and McKeehan, l.c. p. 114.
[9] Meitner, Zeits. f. Physik **26**, 169 (1924).
[10] Ellis and Wooster, Proc. Camb. Phil. Soc. **22**, 844 (1925).
[11] Rutherford and Wooster, Proc. Camb. Phil. Soc. **22**, 834 (1925).

4. Inadequacy of Any Step-by-Step Building-up Process

On the other hand Aston's curve and Einstein's equation show that the process of *building-up* of the more abundant elements out of positive and negative electrons is not only a process capable of producing rays of the observed penetrating power, but that it is the only atomic process capable of producing such rays. This will be discussed quantitatively in §§5 and 6. The foregoing qualitative situation alone, however, is probably sufficient to warrant the conclusion that the observed cosmic rays are the signals sent out through the ether announcing the continuous creation of the heavier elements out of the lighter.

But the Aston curve and the Einstein equation also bring with them entirely new knowledge as to the precise nature of the atom-building processes, namely they show that the atom-building process that results in the observed cosmic rays cannot be one in which positive electrons are added *in successive unit steps* to form the heavier elements out of the lighter. For the Aston curve shows that the maximum mass that could disappear if an element like iron were thus formed by the addition of one hydrogen nucleus to the nucleus of the atom just below iron in the atomic-weight series would be

$$0.00778+0.0008=0.00858 \text{ grams per gram-atom.}$$

This is an energy of the same general magnitude as that found above to be released in the disintegration of thorium (viz. 0.00683). Hence the ether wave sent out when such an act occurred would have but little more penetrating power than that computed above, even if the whole energy of a radioactive change could be concentrated in a gamma ray. As above shown such a ray would be completely absorbed in about four meters of water.

The foregoing argument holds with approximately the same cogency for the formation of any atom whatever by the addition to the atom next below it in the atomic-weight series of one hydrogen nucleus; although in the single case of the formation of carbon out of boron by the addition of one positive electron the energy released would be (See Aston's points)

$$11\times 0.0007+0.0076=0.0153$$

or a little under twice that just computed for the similar formation of iron. But even this radiation would be completely absorbed in about eight meters of water so that *even it could not get into the general region of our cosmic-ray measurements.*

The argument is obviously still more cogent against the generation of the cosmic rays by the process of the building-up of the heavier atoms through the step-by-step addition of an alpha particle to the nuclei of the lighter atoms, since the largest energy that could be released by this process would correspond to a disappearance of mass equal to

$$4(0.00054+0.0008)=0.0054 \text{ grams per gram-atom}$$

and this would produce a radiation that would be completely absorbed in about $4\times0.0054/0.0068$ or three meters of water. *The observed cosmic rays cannot then be produced by any atom-building process involving so small a disappearance of mass as that corresponding to the addition of either a single hydrogen nucleus or a single helium nucleus to any atom to produce the atom one or four units heavier respectively.*

The results obtained by Millikan and Bowen in the flight of their sounding balloon carrying recording electroscopes 0.92 of the way to the top of the atmosphere enable us to go even farther, and to assert that no radiation *of strong intensity* comes into the earth's atmosphere of a penetrating power between that of the hardest gamma rays and that of the observed cosmic rays, since any strong rays which could penetrate more than 80 cm of water (the amount of matter above the highest point reached in the highest balloon flight) would have discharged the electroscope toward the top of its flight. All of the foregoing radiations, computed on the basis of the assumption of a step-by-step atom-building where either the positive electron, or the alpha particle, is the unit considered to be consecutively added, would correspond to radiations of hardness intermediate between gamma rays and our observed cosmic rays. We may therefore conclude *not only that such atom-building acts do not produce the observed cosmic rays, but also that none of these atom-building acts which could send rays into the earth's atmosphere in this region of frequencies have anything like the probability of occurrence in the heavens that is possessed by the more energetic acts about to be considered.*

5. Quantitative Evidence for the Creation in a Single Act of Helium out of Hydrogen

The foregoing evidence has consisted chiefly in the elimination of other possibilities than those herewith urged; but the direct computation from Einstein's equation of the penetrating powers of the observed cosmic rays furnishes quantitative evidence of a still higher order of certainty.

If all the atoms are built up out of positive and negative electrons, as isotope-evidence indicates is the case, and if step-by-step atom-building, with either hydrogen nuclei or alpha particles as units, must be eliminated, for the reasons detailed in §4, as the source of the cosmic rays, then obviously the first and most fundamental atom-building process that is to be looked for is the instantaneous binding of four positive electrons by two negatives, so as to create *in a single act* the nucleus of helium. The subsequent union of a number of such helium nuclei into heavier elements, if it occurs, would in any event have to be of much less frequent occurrence than the primary one of helium-building out of hydrogen, since it is obliged to use the results of a number of these primary acts for its own existence. Or again, if the heavier elements are built up directly out of hydrogen without going through the intermediary process of the formation of helium, the increased complexity of the process with increasing atomic weight would lead to the expectation that the most frequent occurrence would be the helium-

building one. The whole case then for atom-building must rest quite largely upon whether the radiation corresponding to this particular liberation of energy is found in great abundance in the cosmic rays. The way in which the observed rays respond to this test is most illuminating, as the following shows.

According to Einstein's equation and Aston's findings the loss in mass due to this sort of a helium-building act is

$$4\times 1.00778-4\times 1.00054=0.029 \text{ grams per gram-atom}$$

and the radiant energy released each time this act happens is

$$(0.029\times 9\times 10^{20})/(6.062\times 10^{23})=4.3\times 10^{-5} \text{ ergs}$$

The frequency of the ether wave produced is obtained from $E_1-E_2=h\nu$ i.e. $\nu=(4.3\times 10^{-5})/(6.547\times 10^{-27})=6.57\times 10^{+21}$ which corresponds to $\lambda=0.00046$A. To find the absorption coefficient of an ether wave of this energy (or wave-length) we may use with a great deal of confidence Dirac's relativity-quantum-mechanics formula[12] viz:

$$\frac{\mu}{\rho}=\frac{ZN}{A}\,\frac{2\pi e^4}{n^2c^4}\,\frac{1+\alpha}{\alpha^2}\left\{\frac{2(1+\alpha)}{1+2\alpha}-\frac{1}{\alpha}\log(1+2\alpha)\right\}$$

in which Z is the atomic number (for water, 10), A the atomic weight (18), e the charge on the electron (4.774×10^{-10}), m the electronic mass (9.05×10^{-28}), $c=3\times 10^{10}$, and

$$\alpha=h/mc^2=0.0242/\lambda=53$$

These figures yield $\mu/\rho=0.0030$, *or* 0.30 *per meter of water, in place of the value* 0.35 *which we arrived at purely empirically.*

The two figures agree well within the limits of experimental uncertainty at the upper end of the curve, for it will be remembered that in this region the observed slope of the curve gave $\mu=0.22$ and that the figure 0.35 was arrived at by first subtracting from the observed ionization that due to the more penetrating components as determined by the lower end of the curve, and then finding what coefficient would best reproduce *the residuals*. Errors in the correct assignment of the wave-lengths and intensities of these more penetrating components would influence somewhat, though not largely, the residuals and the coefficient computed from them; so that the above agreement may be taken as at present quite satisfactory. We hope, however, soon to have data which will enable us to make the argument somewhat more precise.

There is one further source of some little uncertainty which should be mentioned before stressing the quantitative agreements. It is found in the fact that Dirac's formula gives the value of μ for a homogeneous, monochromatic radiation, while our measurements are made upon rays some of which have degenerated into secondaries (of one-half the value of $h\nu$)[13]

[12] Dirac, Proc. Roy. Soc. **A111.** 423 (1926).

[13] Millikan and Cameron, Phys. Rev. **28,** 866 (1926).

tertiaries ($h\nu/4$), etc. This should not vitiate the foregoing comparison provided the following condition, probably satisfied in this case, has been met. We have earlier pointed out[13] that after a given primary radiation has gone far enough through matter to get *into equilibrium* with its secondaries, the composition of the beam, or the ratio of the energy of any secondary to that of the primary, thenceforth remains unchanged. As soon as this state is attained the coefficient of absorption of the mixed beam must obviously be the same as that of the primary. It is only when the originally monochromatic beam is *starting* on its path through matter that its absorption coefficient will be different from, and somewhat less than, that of the mixed beam. We assume then in the foregoing that near the earth's surface, where the measurements here considered are made, this condition of equilibrium between secondaries and primary has been attained. Even if this were not so the error thus introduced, were it as high as thirty or forty per cent, would not entirely vitiate the argument here in review for the building, through one single energy-transformation of helium out of hydrogen—an act which releases the cosmic ray for which μ is about 0.30. For the great strength of that argument is found not merely in one quantitative fit, but rather in the agreement between quite a group of experimental facts, as set forth in (1) below, and the set of theoretical facts set forth in (2) below.

1. Our experimental curve combined with the Millikan-Bowen high-flight data shows that the great bulk of the cosmic-ray ionization of the atmosphere from one meter below the top down to 10 or 12 meters below it is in fact carried *by one single monochromatic radiation of about* $\mu = 0.3$ per meter of water. Only at great depths, i.e. from 25 to 70 meters below the top, after the foregoing radiation has been all absorbed, (see Fig. 2), does another ray come into the picture, and this has at least four times the penetrating power of the foregoing radiation so that this radiation for which μ is approximately 0.3 per meter of water stands out quite alone on the wave-length scale, and of great intensity.

2. From a theoretical point of view the atom-building process that creates helium out of hydrogen ought to be the most common one taking place in the universe, both because it is the first and most elementary atom-building process that can occur, and also because there is abundant evidence that the alpha particle (helium nucleus) formed by this process appears in the constitution of many atoms. Further the theoretical value of the absorption coefficient in water of the radiation produced by this particular atom-building act is in fact exactly $\mu = 0.3$ per meter. Still further *there are no abundant elements* between helium, atomic weight 4, and oxygen (or nitrogen) of atomic weight about four times as much, so that the helium-building cosmic ray ought to stand out quite alone, *as it actually does*, with nothing nearer it on either side, i.e. of higher frequency or lower frequency, than a ray four times more penetrating. All of the foregoing theoretical facts in (2) are then precisely in accord with the experimental facts in (1). The abundance of this radiation, its isolated position in the spectrum, and

the numerical value of its absorption coefficient all unite to form a powerful argument for the interpretation here given, even though the uncertainties in the exact numerical relationships have not yet been completely removed.

6. Quantitative Evidence for the Building of Oxygen out of Hydrogen

Only second in cogency to the atom-building argument drawn from the upper end of our curve is that which comes from a comparison of the penetrating powers represented by the lower end of the curve with the energies released by the building of all of the small number of *abundant* elements out of hydrogen.

Bowen's discovery[14] that nebulium consists of oxygen and nitrogen, when combined with the enormous extent of these nebulosities, some of them being visible at least 20°—many many light-years—away from the exciting star, means that these two gases are enormously abundant in the heavens. No other lines are found in the nebulae except hydrogen and helium, both very strong, and carbon, very weak. So far then as evidence from the nebulae goes, the only possible cosmic radiations to look for would be those corresponding to the creation of oxygen, nitrogen and carbon out of hydrogen, or else out of helium. Now the energy released by the formation of oxygen out of hydrogen is

$$16 \times 0.00778 = 0.1245 \text{ grams per gram-atom.}$$

This should give rise to a radiation having, by Dirac's formula, an absorption coefficient $\mu = 0.074$ per meter of water, while the radiation produced by the similar formation of nitrogen, releasing 0.108 g per gram-atom should correspond to $\mu = 0.086$. *The mean of these two is* 0.08 *in exact coincidence with one of the two coefficients, in addition to* $\mu = 0.35$, *that we found we had to introduce to fit our experimental curve.*

The creation of carbon, relatively non-abundant, out of hydrogen, an act releasing 0.0933 g per gram-atom would produce merely a slight broadening of this band on the long wave-length side, unobservable with our limited resolution. It is our judgment, then, that the foregoing quantitative agreement, taken in connection with the fact that theoretically this band for which μ is about 0.08, (henceforth, merely for convenience, called "the oxygen band,") should stand out quite alone between the helium band and the silicon band (see below) is sufficient to warrant the conclusion that the direct formation by a single act of oxygen, (and nitrogen), out of hydrogen actually takes place.

The other way by which oxygen might be formed, namely by the union of four helium atoms, would release an energy per gram-atom equal to $0.00054 \times 16 = 0.00858$ g. This is almost exactly that computed on p. 539 for the maximum possible energy released in a radioactive change, the resulting radiation having a sufficient hardness to be completely absorbed in 4 meters of

[14] Bowen, Astroph. Jour. **67**, 1 (1928).

water. In other words this radiation, if it is produced, would not get into our region of observation at all. If it were abundant, however, it would have made its presence known in the Millikan and Bowen high balloon-flight. And indeed, it may be that the reason our observed helium band had a coefficient 0.35, when the computed came out 0.30, is that there is some weak radiation of the sort here considered in the upper regions of our atmosphere; for so far as the data obtained in mountain lakes are concerned the value $\mu = 0.30$ reproduces the observed points altogether satisfactorily as may be seen from the synthetic curve shown in Fig. 2 (see below). But this coefficient $\mu = 0.30$ yields, as we have indicated heretofore, an *integrated* ionization some thirty percent lower than that observed in the Millikan and Bowen high balloon-flight[15] and this was the sole reason that we pushed the value above $\mu = 0.30$ in originally fixing upon the empirical values of the coefficients that best fitted our data.[16]

So far then as the gaseous elements are concerned *there are only two possible frequency bands which could be formed by any conceivable atom-building process suitable to produce the cosmic rays observable at the earth's surface*, for there are no abundant gases save hydrogen, oxygen and nitrogen, and helium, all extraordinarily abundant in comparison with other elements, and these two bands are actually found in the cosmic rays just where they belong, viz. at about $\mu = 0.30$ and $\mu = 0.08$. The oxygen band then, though less certainly established than the helium band, adds no little strength to the interpretation of the cosmic rays herewith being presented.

7. Quantitative Evidence for the Building of Silicon out of Hydrogen

Turning next to the solid elements there are just three ways of estimating their abundance, viz. (1) the composition of meteorites, (2) the constitution of the earth, (3) the spectroscopy of the stars, and these all tell roughly the same story. Thus 95% of the weight of all meteorites [17] consists of the four elements, oxygen (54%) magnesium (13%), silicon (15%), and iron (13%), while 76% of the earth's crust[18] is composed of the three elements oxygen (55%), silicon (16%), aluminum (5%), no other element rising to over 2%. Iron constitutes only 1.5% of the crust but it is supposed to be very largely represented in the interior. The evidence from the spectroscopy of the stars is less definite, but it too assigns a very great abundance to the foregoing elements, and gives no others a prominent place unless they be calcium and sodium. Calcium constitutes 1.5% of the earth's crust and 1% of meteorites, while sodium is 2% of the earth's crust and negligible in meteorites. Silicon then appears to be the next most abundant element to oxygen, the only others that need to be considered at all being aluminum

[15] Millikan and Cameron, Phys. Rev. **31**, 921 (1928).

[16] This is why our original tables, Phys. Rev. **31**, 929 (1928), show that our so-called experimental values at the top of the curve are higher than our computed values.

[17] Harkins, Phil. Mag. **42**, 313 (1921).

[18] Cecilia H. Payne, Stellar Atmospheres, Harvard Univ. Press, 1925, p. 5.

and magnesium. But for the purposes of the cosmic rays, aluminum and silicon are altogether identical, their atomic weights being 27 and 28 respectively, while magnesium, atomic weight 24 is so close to them that it releases practically the same mass when it is formed out of hydrogen. In other words *there are no elements between oxygen and iron the formation of which out of hydrogen could give rise to cosmic rays of appreciable intensity except silicon and its immediate neighbors*, and these should give rise to a cosmic-ray band which for covenience we shall call the *silicon band*, because of the fact that silicon is by far the most influential element in it.

The energy released by the formation of silicon out of hydrogen should, according to Aston's curve and Einstein's formula be

$$28(0.00778+0.00050)=0.232 \text{ g per gram-atom}$$

According to Dirac's formula this should have an absorption coefficient of $\mu=0.041$ per meter of water. This is exceedingly close to the empirical coefficient 0.04 which actually carries our curve from 30 meters down to 70 meters below the top of the atmosphere Its energy corresponds to the fall of an electron through 216,000,000 volts. There is no uncertainty at all about the presence in the cosmic rays of a radiation of about this penetrating power, but here again the exactness of the quantitative agreement is less significant than the fact that the elements are so distributed in abundance that this silicon band is the first which can appear, in appreciable intensity, harder than the oxygen band, or better that silicon (and its neighbors) is the only element which can produce a cosmic-ray band between that of oxygen and that of iron where a cosmic-ray band certainly appears.

There is, however, just one other way in which silicon might be formed and produce a radiation of cosmic-ray hardness, namely by the instantaneous union of seven alpha particles, or helium atoms, into an atom of silicon. This act would release an energy per gram-atom of

$$28(0.00054+0.00050)=0.029$$

which is exactly the same as that released (0.029) when four hydrogen atoms unite to form helium. This radiation would then be indistinguishable from the helium band, but at the very most it could only be one-seventh as common an occurrence, since at least seven helium atoms must form out of hydrogen before it can take place. The possibility of its occurrence could not then affect in any significant way the interpretations made above.

8. The Formation of Iron

Thus far we have found all three of the cosmic-ray bands the theoretical existence of which we have predicted from the abundance of the elements, the Aston curve, and the Einstein and Dirac formulas.

There is but one more possible cosmic-ray frequency, of appreciable intensity, higher than that due to the formation of silicon out of hydrogen,

namely that due to the formation of iron out of hydrogen, for there are no abundant elements between silicon and iron and none of larger atomic weight than iron. Calcium and potassium, astrophysically somewhat common, may be thought of as providing merely a weak satellite on the high frequency side of the silicon band, while nickel and titanium are identifiable, from the cosmic-ray standpoint, with iron. The hypothetical band due to the formation of iron out of hydrogen corresponds to a release of energy equal to

$$56(0.00778+0.00080)=0.48 \text{ g per gram-atom}$$

and would have an absorption coefficient $\mu=0.019$. Such a radiation could be brought to light with certainty only by making very careful measurements on the shape of the curve at its lower end. The resolving power of our present curve is insufficient to make it possible to assert that it shows the existence of such a radiation. However, we may assert that our curve is not inconsistent with it and even that its introduction improves somewhat the fit of our experimental and theoretical points as will be seen from the discussion of the next section.

As in the case of silicon there is just one other way in which iron might be produced with a sufficient disappearance of mass to produce a radiation of cosmic-ray hardness, namely through the union of fourteen helium atoms in a single act into one atom of iron. This would release an energy equal to

$$56(0.00054+0.00080)=0.075 \text{ g per gram-atom}$$

which gives a radiation practically identical with that produced by the formation of carbon out of hydrogen. In other words it would be a part of the oxygen band already found. We have nothing to show that this process may not take place. Incidentally iron might also be formed by the union of two atoms of silicon, but this act would release

$$56(0.00080-0.00050)=0.0168 \text{ g per gram-atom}$$

and would give rise to a radiation capable of penetrating 8 meters of water (See p. 539). The Millikan and Bowen experiments show that there is no abundant radiation of this sort though there may be a weak one. Also the formation of iron by the union of four atoms of nitrogen, an act releasing

$$56(0.0008+0.0002)=0.056 \text{ g per gram-atom}$$

would give rise to a radiation about twice as penetrating as that produced by the formation of helium out of hydrogen. Our curve does not bring to light evidence of any abundant radiation of this type.

9. The Prediction of the Cosmic-Ray Curve

It will be clear from the foregoing analysis that if we make the assumption that elements are now being created at a rate roughly proportional to the abundance of their occurrence in nature, the problem of predicting the

origin of the cosmic rays is enormously simplified by the fact that, broadly speaking, there are only four abundant elements besides the primordial hydrogen, which appears in great abundance everywhere in the heavens, namely helium, oxygen, silicon and iron.

The first two of these, helium and oxygen, can only be formed in one particular way, namely by the coming together in one act of the requisite number of hydrogen atoms, if the mass released is to be such as to give rise to radiations of cosmic-ray hardness. That this mode of coming together actually occurs is further attested by the quantitative agreements between the observed and the computed penetrating powers.

In the case of silicon there are just two different possible modes of formation, viz., first the foregoing one, twenty-eight atoms of hydrogen uniting in one act to form silicon, and second, the union in one act of seven alpha particles to form one atom of silicon. There is *direct, positive* evidence that the first mode of formation occurs, the ray of just the predicted penetrating power actually appearing in our curve. There is no direct evidence that the second mode does not occur, since it would produce a radiation of the same hardness as does the formation of helium out of hydrogen—the most abundant cosmic ray,—but there is a little indirect evidence that it is less likely to occur than the first mode. This is found in the fact that *oxygen* is not formed abundantly, if at all, by the union of four alpha particles as the Millikan and Bowen balloon flight showed (See above p. 544), and if four alpha particles do not unite frequently to form oxygen, there is even less reason to suppose that seven will unite frequently to form silicon.

In the case of the last of the abundant elements, iron, there are a considerable number of possible modes of its formation; but the one which, by analogy with oxygen and silicon, we shall take as most likely of occurrence is its direct formation in one act out of hydrogen.

In endeavoring then to predict from a theoretical standpoint our cosmic-ray curve we have taken the mean proportions in which oxygen, silicon (i.e., silicon+aluminum+magnesium), and iron are found in meteorites and in the earth's crust, viz., 55%, 26% and 7% respectively. Assuming that these three atoms are being formed out of hydrogen in these proportions,we have computed with the aid of the Gold tables the relative intensities of these three frequency bands *after the three radiations corresponding to them, viz. those for which* $\mu=0.08$, $\mu=0.04$ *and* $\mu=0.02$ *have traversed 30 meters of water.* The foregoing sequence of numbers is thus reduced to the sequence O 1.4, Si 2.9, Fe1 .8, i.e., oxygen and iron have about the same influence and silicon has approximately twice that of either of them. We have then divided up our observed cosmic-ray intensity at 30 meters in about these proportions, the ionization at a depth of 30 m being taken as a starting point merely because the ionization due to the helium band ($\mu=0.30$) would have entirely disappeared at this depth. As a matter of fact the observed ionization at 30 m was 1.79 ions of which we gave 0.45 each to oxygen and to iron and the remainder, twice as much, to silicon, these being roughly the proportions

given by the abundance of these elements in meteorites and the earth after the radiations have been filtered through 30 meters of water.

TABLE I. *Comparison of observed and computed ionization*

Depth	Iron $\mu = .02$	Silicon .04	Oxygen .08	Helium .30	Total Sum	Exp'l Curve
70	0.13	0.10	0.015		0.245	0.16
60	0.18	0.17	0.03		0.38	0.24
50	0.24	0.28	0.07		0.59	0.44
40	0.32	0.47	0.19		0.98	0.85
30	0.45	0.84	0.50		1.79	1.79
20	0.64	1.52	1.42	0.12	3.70	3.95
15	0.83	2.09	2.46	0.65	6.03	6.24
12	0.89	2.56	3.50	1.90	8.85	8.60
10	0.96	2.94	4.46	3.84	12.20	12.20
9	1.01	3.17	5.06	5.62	14.86	16.05
7	1.10	3.69	6.55	12.18	23.52	
5	1.23	4.34	8.64	27.6	41.81	
3	1.37	5.24	11.75	64.4	82.76	
2	1.46	5.75	13.9	105.1	126.21	192.0*

* This point is obtained from the Millikan and Bowen sounding-balloon data. The experimental error may possibly be as high as 30%. Also, as indicated above, there may be some weak softer rays coming into the top of the atmosphere.

Having thus fixed a starting point, i.e., a value of the ionization I at some point for each of these three radiations, we have computed, with the aid of

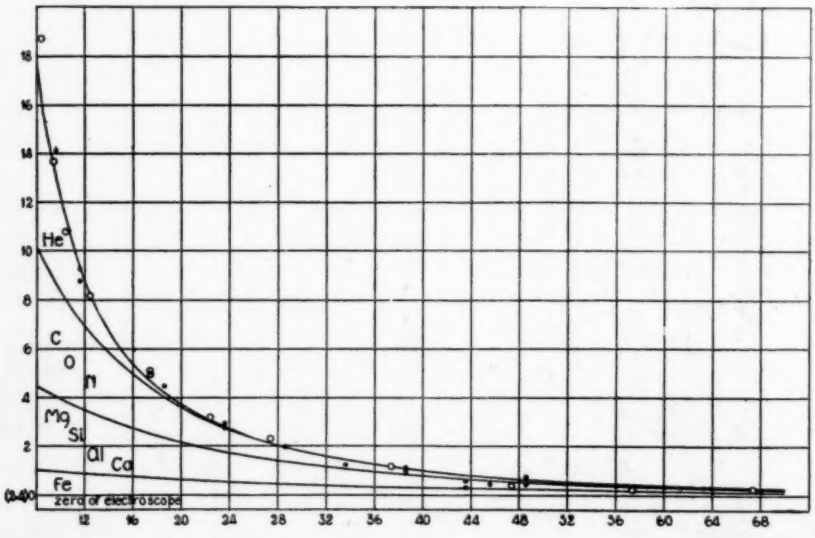

Fig. 2. Comparison of experimental data with a built-up curve compounded from four absorption coefficients. Abscissas: depth in equivalent meters of water beneath surface of atmosphere; Ordinates: ionization in ions per cc per second. Dots are readings in Lake Arrowhead; circles, Gem Lake.

the Gold table and the known absorption coefficient for each radiation, viz., $\mu = 0.08$, $\mu = 0.04$, $\mu = 0.02$, the complete ionization curve for each radiation

at all depths. The results are shown in Table I and graphically in Fig. 2. In Fig. 2 the area between the zero horizontal line and the first curve above it represents the ionization due to the formation of iron; the area between the iron line and the curve above it represents the ionization due to silicon, and that between the silicon line and the one above it the ionization due to oxygen. We then took the difference between the reading on this upper line, at 10 m, and the observed ionization at 10 m to fix a starting point, or an I, for helium, and with this starting point, the coefficient $\mu = 0.30$ and the Gold table we computed the ionization at all depths due to the formation of helium. The area between the upper two curves represents this ionization. It will be seen that the upper curve, built up in this theoretical way, fits the observed points about as satisfactorily as any curve which could be drawn through them. There is no very great importance to be attached to this synthetic curve, since the mean proportions in which elements occur in meteorites and the earth is not definitely known to be a measure of the abundance of their formation. The curve and table are of some significance, however, first in emphasizing the fact that the four elements, helium, oxygen, silicon and iron are all that are needed to build up the observed cosmic-ray curve; second, in showing pictorially and tabularly how the ionization due to the formation of these four elements varies with depth, for example the total ionization at all depths due to iron is so small that it does not make a great deal of difference whether it is considered or not, while the curves and table show at once that at the top of the atmosphere more than 80% of all the ionization is due to the helium band; third, in showing that there is perhaps a little direct evidence for the formation of iron out of hydrogen since the significant experimental points at 12 m, quite accurately determined, are fitted better when we add the iron coefficient 0.02, than they were when we were locating all our coefficients purely empirically.[19]

10. Thermodynamic and Kinetic View-points as to the Origin of Cosmic Rays

The argument for the sort of interpretation of the cosmic rays herewith suggested has been thus far wholly a thermodynamic one. We have not troubled ourselves at all with the mechanism of atom-building, but have confined our attention to seeing what sort of atomic transformations and combinations were demanded in order to satisfy what we consider to be the fundamental and necessary energy relations. This mode of attack has been the most infallible that physics has thus far devised, but the kinetics of the situation ought not to be wholly ignored.

At first sight these seem to present great difficulties. For first, it has been assumed that positive electrons are able to rush together against their mutual repulsions and, under the inducement of a number of negatives not more than half the number of positives for the lighter atoms, to become

[19] In table IV Phys. Rev. **31**, 929 (1928) at the one point at 12m the agreement between computed and observed readings scarcely fell within the limits of observational uncertainty. This is rectified above without throwing any points on the curve outside that limit.

locked in a new nucleus which always has a net positive charge of from 2 to 92. The evidence is strong that the inverse square law holds for the mutual repulsions of such systems, at least up to distances of the order of 10^{-12} cm. The introduction of the idea of the spinning electron, which makes of it a magnetic doublet, each side of which is capable of attracting an opposite pole with a force that varies with the inverse cube of the distance, may help in the picturing of a mechanism by which one negative can bind two positives, as it does in helium for example, and also in explaining the fact that energy is evolved rather than absorbed in the formation of helium out of hydrogen; but it does not provide any escape from the conclusion that, up to distances of the order of nuclear dimensions, work should be required to bring a new positive up to the distances at which the nucleus-building polar forces can act. Further, this work should in general be so enormous that no known temperatures could be of any avail in providing the requisite kinetic energies to bring a new positive up to within nuclear distances of another positively charged nucleus which might bind it. This will be obvious from the fact that at the highest estimated temperatures in the interior of stars, viz., 40,000,000°C, the wave-length of maximum energy in the black-body radiation curve is at only about 1A, not enough even to strip the *k* electrons from the heavier atoms, for it takes an energy corresponding to from 0.2A to 0.7A to do even that, to say nothing of pushing nuclei up to distances of 10^{-13} cm at which they might conceivably unite. *These considerations seem to us to show that high temperatures cannot be expected to help at all in the solution of the problem of nucleus-formation. They are probably inimical to such formation.*

The second difficulty which the kinetics of atom-building encounters is that of explaining how four positive and two negative electrons can possibly *chance* to come together at a given instant, at the same spot, and under suitable conditions for uniting into an atom of helium; and this difficulty is, of course, progressively increased in going to the consideration of oxygen, silicon and iron.

Our own way out of the first difficulty is to assume, as elaborated below, that nucleus-building is a phenomenon which, in some as yet unknown way, is favored by the extreme and thus far unexplored conditions of *low temperature and density* existing in interstellar space.

A possible way of escape from the second difficulty is the following; without at this moment hazarding a judgment as to where positive and negative electrons come from—through the condensation of radiation or otherwise—we may at least affirm that they exist in great numbers throughout space. Under the influence of their mutual attractions a positive and a negative begin to fall together in quantum-jumps, and in so doing they give rise to the spectrum of atomic hydrogen so conspicuous in the heavens. When the negative has reached the inmost quantum orbit, it has still not approached close enough to the positive to have occasioned any appreciable loss in mass. This normal atomic hydrogen may next be supposed to gather in another positive electron thus producing ionized molecular hydrogen, a

system which the positive-ray spectrograph shows to be a stable one. Up to this point there has not been sufficient closeness of approach between any positives and negatives to cause appreciable loss in mass. Two of these ionized hydrogen systems may then be assumed to come together. Under nearly all conditions of such impact they may if desired be considered to rebound in accordance with the usual assumptions of the kinetic theory of gases. But let it be now imagined that once in a long, long time the conditions of approach governed by the unknown probability law above suggested are just right for the four positives and the two negatives to clamp themselves together into a helium nucleus. Practically the whole change in mass will then occur at this instant of clamping so that the radiation given out will have the full value 4 (0.00778 − 0.00054), and the necessity of having six electrons (four positives and 2 negatives) *happen to find* themselves at the same spot at the same time has been avoided. They have been *gathered in* by a step-by-step process, but the clamping, or nucleus-building, has all taken place at one instant. These considerations may be extended to oxygen silicon and iron, and *it may well be that the loose clustering which precedes clamping may be facilitated by the exceedingly low temperatures that exist in interstellar space*. In other words energy of impact may well be inimical to the *clustering* which, according to the suggestion herewith put forth, would have to precede nucleus-building. It might be interesting to see whether even in the laboratory hydrogen at liquid helium temperatures will show any tendency to be transformed into helium.

After all, the problem of the kinetics of atom-building need not be so different from the kinetics of complex-molecule-building or crystal-building. If in the latter case the atoms take their assigned places one at a time, then the two problems would, indeed, be essentially different, but if a large group of them fall into position at the same instant the two problems would not be altogether dissimilar. Again crystal-building is facilitated by low temperature not by high, and as will appear more fully in the next section, this seems to be also a definitè characteristic of the process of atom-building.

11. The Place of Origin of the Cosmic Rays

All observers are now agreed that if there be any directional effect at all in the cosmic rays it is but a slight one. We, ourselves, have not yet detected any favored direction whatever, though Kolhörster[20] and Büttner[21] report doing so. In any case the rays certainly come into the earth *nearly* equally from all directions. This means that they are either formed (1) out in the interplanetary and interstellar spaces, including of course the nebulous regions above the earth, or else (2) in stars that are more or less uniformly distributed throughout the heavens. These are the only two possible alternatives. In both of these localities matter exists under extreme and as yet unexplored conditions, and in view of the history of the last thirty years of physics, it would no longer be surprising if matter were again found to

[20] Kolhörster, Sitz. Ber. d. Preuss. Akad. **34,** 366 (1923).
[21] Büttner, Zeits. f. Geophys. **21,** 87 (1926); **21,** 291 (1926).

behave in some hitherto unknown and unexpected way as a new field of observation is entered.

Of the two foregoing alternatives we think it possible to eliminate the first and to establish the second with considerable definiteness, and that for the two following reasons.

First. If the mere presence of matter in large quantities and at high temperatures favored in any way the atom-building processes which give rise to the cosmic rays, then it is obviously to be expected that the sun, in view of its closeness, would send to the earth enormously more of them than could any other star. But the fact is that all observers are agreed that the change from midday to midnight does not influence at all the intensity ofthe cosmic rays.[22] This can only mean that *the conditions existing in and about the sun, and presumably also in and about other stars as well, are unfavorable to the atom-building processes which give rise to these rays.*

Since, however, the rays do come to us at all times, day and night, and, according to all observers, at least very nearly equally from all directions—according to some as accurately so as they have as yet been able to make the measurements—there is scarcely any escape from the conclusion that *the atom-building processes giving rise to the cosmic rays are favored by the conditions existing in interstellar space.* If then, in going from a point in interstellar space toward the center of a star the favorable conditions for atom-building existing in outer space have disappeared as the surface of the star is reached, it is well-nigh inconceivable that they will again reappear in penetrating from the surface to the center—a path along which the changes in physical conditions all continue unchanged in direction. So that from the foregoing we may not only conclude quite definitely that the stars are not the sources of the cosmic rays, but also that the main *atom-building processes probably do not take place inside of stars at all.*

Second. The foregoing conclusions may also be arrived at from an entirely different mode of approach, namely from our measurements upon the absorption coefficients and the total energy content of the cosmic rays.

The hardest rays which we have observed are completely absorbed (reduced to say 2% of their initial intensity) in going through 70 meters of water. This means that, even if the atom-building processes went on inside a star, the resulting cosmic radiations could not possibly get out, but would all be frittered away in heat[23] before emergence, save in the case of those rays that originated in the star's very outermost skin—a skin equivalent in absorbing power to a hundred or so meters of water.

But we have also found that the total energy coming into the earth's atmosphere in the form of cosmic rays is about one-tenth the total heat and light energy coming to the earth from the stars exclusive of the sun.[24] This

[22] R. A. Millikan and G. H. Cameron, Phys. Rev. **31**, 169 (1928).

[23] It is important to remember that, as we have already shown, Phys. Rev. **28**, 866 (1926), rays of this kind become frittered away into heat in this passage through matter *without any change in the quality* (i.e. frequency or absorption coefficient) *of the residual beam.*

[24] R. A. Millikan, and G. H. Cameron, Phys. Rev. **31**, 929 (1928).

last fact means that *if the cosmic rays have their origins within the stars they cannot, even at the points of their origin, have an intensity more than ten times that which they have when they reach the earth's atmosphere, for if they had the cosmic-ray energy transformed into heat by absorption on the way out would yield a total heat outflow from the stars larger than the observed ten to one ratio.* In other words, if the stars are the sources of the observed cosmic rays, it follows from our measurements on absorption coefficients and on total energy content that the total heat output of the stars must be furnished by the atom-building processes going on in their merest outer skins of a thickness equivalent in absorbing power to about a hundred meters of water, and that therefore no atom-building processes, nor any other activities capable of furnishing heat, can then be going on in their interiors.

It is, however, so altogether absurd to suppose that atom-building processes are going on actively at the surface of a star and down to a depth of a hundred meters, and then suddenly stop there that we are forced back by this present mode of approach to the same conclusion arrived at from the direct determination of the lack of cosmic-ray activity of a particular star, the sun, namely to the conclusion that *the observed cosmic rays do not originate in the stars at all, but that they must originate under the extreme influences of exactly the opposite sort existing in interstellar space.*

These considerations bring us then from two entirely new points of view to the conclusion that the heat output of the stars must be derived from an entirely different source from the atom-building processes which produce the cosmic rays. Jeans[25] and Eddington,[26] from other considerations, based wholly upon the lifetimes of the stars, have repeatedly emphasized the necessity of finding a source for this output other and greater than the process of atom-building, but we can now go further and say that the process of energy emission by atom-building does not take place in the stars at all, or at least in such amount as to make the stars an appreciable factor in the output of cosmic rays, for if it did the stars would have to be radiating heat much faster than is the case.

As is well known, Eddington and Jeans have found this new source of stellar heat *not in an atom-building process, but rather in an atom-annihilating process* which they assume to be going on in the interior of stars, positive electrons being thought to be continually transforming their entire mass into ether waves in accordance with the demands of Einstein's equation. As indicated above, we have sought in vain among our cosmic rays for a ray of penetrating power corresponding to this act. It will be recalled that the mass which disappears in the creation out of hydrogen of one gram-atom of silicon—this produced the hardest cosmic ray that we can say with certainty that we have yet observed, for the iron rays are still to some degree hypothetical—was 0.23 g. The complete annihilation of the mass of hydrogen would obviously then produce, in accordance with Einstein's equation, a ray having approximately 4 times (accurately 1.0778/0.23 times) the energy and

[25] J. H. Jeans, Problems of Cosmogony and Stellar Dynamics, Cambridge, 1919, p. 286.
[26] A. S. Eddington, The Internal Constitution of the Stars, Cambridge, 1926, Chap. XI.

penetrating power of our hardest definitely observed ray. *Our failure to find this ray, however, is no argument at all against the existence of the process in the interior of stars* where the pressures are colossal and the densities may be enormous. Indeed our failure to find this ray means rather that, if the act occurs at all, as Eddington and Jeans think it must, it is obliged to occur precisely in the interior of stars where the resulting radiation is hidden away behind an impenetrable screen of matter—a screen that transforms all its energy into heat before the ray can get out. If the cosmic rays originate within the stars they would of course be similarly screened.

On the other hand, that the atom-building processes responsible for the cosmic rays, as distinct from the atom-destroying process just considered, actually occur, as our experiments definitely show, *outside the stars*, or at least where the rays produced by them can get to us, and in an energy that is of the same order of magnitude as that of the heat poured out by the star, is an extraordinarily illuminating fact. For it suggests at once, when combined with Eddington's argument, the following incomplete cycle each element in which now has the *experimental* credentials indicated in the brackets:

(1) Positive and negative electrons exist in great abundance in interstellar space (see the evidence of the spectroscope).

(2) These electrons condense into atoms under the influence of the conditions existing in outer space, viz., absence of temperature and high dispersion (see the evidence of the cosmic rays).

(3) These atoms then aggregate under their gravitational forces into stars (see the evidence of the telescope).

(4) In the interior of stars, under the influence of the enormous pressures, densities and temperatures existing there, an occasional positive electron, presumably in the nucleus of a heavy atom, transforms its entire mass into an ether pulse the energy of which, when frittered away in heat, maintains the temperature of the star and furnishes most of the supply of light and heat which it pours out (see the evidence of the lifetimes of the stars—Eddington-Jeans).

The foregoing is as far as the experimental evidence enables us to go, but the recent discovery of the second element of the above unfinished cycle, namely that the supply of positive and negative electrons is being used up continually in the creation of atoms the signals of whose birth constitute the cosmic rays, at once raises imperiously the question as to why the process is still going on at all after the eons during which it has apparently been in process—or better *why the building stones of the atoms have not all been used up long ago*. And the only possible answer seems to be to complete the cycle, and to assume that these building stones are continually being replenished throughout the heavens by the condensation with the aid of some as yet wholly unknown mechanism of radiant heat into positive and negative electrons.

This is a new mode of approach to a conclusion, a portion of which at least is old. For the Einstein assumption itself that mass is convertible into

radiant energy, requires the existence also of the inverse process, unless the validity of the Second Law of Thermodynamics in its most widely accepted form is to be denied. In other words, in the strict thermodynamic sense there can be no such thing as *equilibrium* within a closed system containing radiation and matter unless the convertibility of mass into radiant energy is a reversible process. The effort to work out the thermodynamics of a cycle containing this process has recently been made by Stern[27] Tolman[28] Zwicky.[29]

But we have in the foregoing gone farther than they. For the mere assumption of the reversibility of the foregoing process is not sufficient of itself to avoid the "wärme-tod," i.e., the ultimate disappearance of all available energy. The essence of the Second Law lies in the assumption that an isolated system tends towards a state of uniform temperature characterized by the black-body law of distribution of radiant energies and of gas-molecular velocities. The mere assumption that radiant energy is transformable into atoms in no way modifies the consequences of the Second Law, provided the atoms, when created out of radiation, are endowed with the kinetic energies appropriate to the temperature of the radiation out of which they have been formed, and they must on the average be so endowed if Second Law reasoning is to be used, since otherwise temperature differences would establish themselves in an enclosure once brought to a uniform temperature. Indeed, from the Einstein point of view radiation is essentially corpuscular in its very nature.

On the other hand, if the universe is to be treated as a closed system the only way to avoid the "wärme-tod" is to assume that after potential energy has been once transformed into heat, it can somehow, somewhere in the universe go back again completely into the potential form—in particular that the *kinetic energy of light-quants* is actually re-transformable in toto into the *potential energy of statically attracting systems*. This is the essence of the assumption that we have made above in supposing that only under the conditions of temperature and pressure existing in inter-stellar space, radiant energy is transformed into *positive and negative electrons* which can then fall together under the influence of their mutual attractions, aggregate in turn into the heavier atoms, and then develop new "hot spots" in space, (stars) as these atoms rush together, and in so doing re-transform their potential energies again into heat. This is a violation of the Second Law of Thermodynamics as applied to the universe, and, it is this violation that we have been led to suggest by the observed properties of the cosmic rays; but we leave the Second Law intact for all the purposes of the small scale, terrestrial phenomena for which it has been used so successfully in the past. *The essentially new element that we have introduced is the experimental observation that the creative, or atom-building, processes do not appear to take place at all in the stars*, or in those parts of the universe where matter is found in appreciable densities and temperatures, but only in the interstellar or

[27] O. Stern, Zeits. f. Elektrochemie, **31**, 448 (1925).
[28] Richard C. Tolman, Proc. Nat. Acad. **14**, 268, 348, 353 (1928).
[29] F. Zwicky, Proc. Nat. Acad. July, 1928.

intergalactic spaces where densities and temperatures are essentially zero. Our *experimental evidence* does not, indeed, extend to the creation of the lightest element, hydrogen, out of radiation, but the inclusion of this also among the creative processes going on only in interstellar space is a natural extension of our observational data on the other abundant elements, for hydrogen is well-nigh inevitably being created in those portions of space in which the elements that use it for their building material are also being created. But in making this extension we are denying the reversibility at ordinary temperatures and pressures of the process of the transformation of matter into radiation. This is why our conclusion differs from that of Stern and Tolman and why we are able to regard the universe as in a steady state now, though a state not satisfying the condition of microscopic reversibility.

In a certain formal sense our assumption may be considered as *not* a violation of the Second Law since, in accordance with the Carnot's statement of that law, viz.: efficiency $=(T_1-T_2)/T_1$, heat is indeed transformed completely into work *when* T_2 *is at absolute zero.* Nevertheless we have in our assumption denied the applicability of the usual thermodynamical reasoning to *cosmical* processes. This is, however, not the first time that doubts as to the legitimacy of applying such reasoning to the cosmos as a whole have been expressed. Our assumption is scarcely more radical than was Einstein's assumption of 1905, and it is certainly one the validity of which cannot be denied until we have more information than we now have about the behavior of matter in interstellar space. Indeed it seems to us the least radical of the three possible hypotheses between which a choice must in any case be made by all who admit the validity of Einstein's equation, $Mc^2=E$. These three hypotheses are as follows:

1. The first is that of Jeans and others that electrons, and hence atoms and molecules, are convertible into radiant energy, but that the process is nowhere reversible. A very recent statement of Jeans reads[30] "Thus observation and theory agree in indicating that the universe is melting away into radiation. Our position is that of polar bears on an iceberg that has broken loose from the ice pack surrounding the pole and is inexoraby melting away as the iceberg drifts to warmer latitudes and ultimate extinction."

This is the old hypothesis of the "wärme-tod." It conflicts with no observed facts, and before the advent of Einstein it was a necessary consequence of the Second Law *provided the universe were treated as a closed system.* Scientists, however, have always objected that such treatment represents an extravagant and illegitimate extrapolation from our very limited mundane experience, and modern philosophers and theologians have also objected on the ground that it overthrows the doctrine of Immanence and requires a return to the middle-age assumption of a Deus ex machina. Since the advent of Einstein it meets the further difficulty that it injects into modern thermodynamics one single process which violates the principle of "microscopic reversibility" required by the modern statement of the Second Law.

[30] J. H. Jeans, Nature **121**, 467 (1928).

2. The second possible hypothesis is that of Stern, Tolman and Zwicky that the foregoing processes are all everywhere reversible. This hypothesis keeps the Second Law intact, including microscopic reversibility, denied by Jeans' assumption, but so far as can now be seen, it does not avoid the "wärme-tod," and it is not favored by the evidence herewith presented that the atom-building processes which give rise to the cosmic rays do not seem to be taking place everywhere, e.g., in the stars, but do seem to be taking place solely in the depths of space.

3. The third hypothesis,—that herewith presented,—is just as radical as (1), but no more so, in denying microscopic reversibility, but it provides an escape sought in vain by both (1) and (2) from the "wärme-tod." Also it is just as radical as (2) but no more so in assuming that radiant energy can condense into atoms somewhere, but it is in better accord with the cosmic-ray evidence that the atom-creating processes seem to take place only in interstellar space.

NORMAN BRIDGE LABORATORY OF PHYSICS,
CALIFORNIA INSTITUTE.
PASADENA, CALIFORNIA.
July 9, 1928.

THEORY OF X-RAY DIFFRACTION IN LIQUIDS

By G. W. Stewart

Abstract

There are numerous experimental results in the diffraction of x-rays in liquids that seek explanation by an adequate theory. They may be enumerated at least in part as follows: (1) small scattering intensity near zero diffraction angle, (2) a principal maximum in the intensity-diffraction-angle curve corresponding to distance of molecular separation, (3) the position of this chief maximum as independent of the length of the molecule which forms a straight chain, (4) the variation of the position of a second diffraction peak with carbon content in the case of a normal hydrocrabon or a derivative of a hydrocarbon in a manner that makes the variation of the corresponding "planar" distance (computed by Bragg's Law) with carbon content in the straight chain, a linear one, (5) the similarity of the foregoing variation in solid and liquid saturated normal fatty acids, (6) the agreement of the molecular separation computed by Bragg's Law and other experiments upon the cross-sectional area of straight chain molecules, (7) the alteration in computed separation by attached branches, (8) the presence of three peaks apparently corresponding to three dimensions of a branched chain molecule, (9) the agreement among the computed cross-sectional areas of the three straight carbon chains, normal paraffins, saturated nomal fatty acids and normal alcohols.

The theories of Raman and Ramanathan and of Zernike and Prins give a fairly good account of the first two phenomena just mentioned. But the conception of molecular non-crystalline groupings in the liquid makes possible the use of the crystal powder theory as an idealized one for liquids. It is found that, used as an approximation, this theory explains all the above phenomena.

The Ehrenfest formula, intended by its author for gases but which has been used to obtain the mean molecular separation in liquids, and which varies from Bragg's Law by about 19 percent, cannot be so applied to liquids.

X-RAY diffraction in non-crystalline substances is of increasing interest both from a theoretical and from a practical point of view. The theory of diffraction in liquids presents several difficulties. The molecules are not spherical, the law of force from which the spacial distribution of molecules might be obtained is not known, and probability theorems are not easily applicable to regions which are comparable in dimensions to the distance of separation of the molecule. It is the purpose of the present paper to discuss the present status of the theory of diffraction in liquids, but in so doing the details of current theories will necessarily be omitted.

Theory of Raman and Ramanathan. Perhaps the most complete theory is that of Raman and Ramanathan.[1] The expression they deduce for the intensity of the x-rays of wave-length λ scattered at angles between θ and $\theta+d\theta$ is

$$C_1 \exp\left[-\frac{1}{16}\frac{N}{RT\beta}\lambda_0^3\left(1-\frac{\lambda_1^3}{\lambda_0^3}\right)^2\right] \qquad (1)$$

[1] Raman and Ramanathan, Proc. Ind. Assoc. for Cultiv. Science, VIII, II p. 127 (1923).

wherein N is Avagadro's constant, R the gas constant for a gram molecule, β the isothermal compressibility, λ_0 the mean distance between neighboring molecules in the fluid and λ_1 the wave-length of the "structural spectrum" responsible for the scattering of the incident radiation and related thereto by the equation $\lambda = 2\lambda_1 \sin \theta/2$. This expression does give a diffraction-intensity curve that closely resembles those found in liquids. Its exact form seems, however, not so important as other aspects of the contribution of Raman and Ramanathan.

These authors point out that at small angles of scattering there is an analogy with the optical scattering problem. By reference to the work of Lorentz and the use of the statistical thermodynamical theory of light scattering developed by Smoluchowski and Einstein, it is shown that thermal fluctuations of density will produce scattering. Moreover, if the x-ray scattering occurs at a small angle the optical theory can be applied to x-rays. For example in benzene, if $\lambda = 0.71$A, $\theta = 10'$ the thickness of a slab with a path difference of λ would be 239A and hence would contain enough molecules to make the probability considerations apply. Hence the scattering of x-rays would be treated as in optics. But, in magnitude, the scattering from a liquid would be less than from a gas of the same number of molecules. This is because the compressibility is relatively small in a liquid. For benzene the scattering would be one-fortieth of the value in a gas where it is proportional to the number of molecules per unit volume. Thus the reason for the small scattering of x-rays in the region of 0° scattering angle is explained.

By a further discussion the authors of this theory show that, as the angle θ increases, the intensity of scattering increases until $\lambda/(2 \cdot \sin \theta/2)$ is equal to the mean distance of separation of the molecules, at which angle there is a maximum scattering. The explanation of the small intensity near 0° and the presence of a maximum at an angle such that $\lambda = 2\lambda_0 \sin \theta/2$ where λ_0 is the mean molecular distance, is a valuable contribution.

But when Raman and Ramanathan subsequently apply probability considerations developed for a continuum to discrete particles separated by a distance comparable to the volume involved, and thus secure Eq. (1), they probably go beyond what might be called a theory. Eq. (1) is then, in the writer's view, interesting but not acceptable. Nevertheless, Raman and Ramanathan have given the most satisfactory discussion of the problem up to the present time. They have accounted for small scattering near 0° and the presence of a maximum at an angle related to the mean separation of molecules by Bragg's crystal-diffraction law. Variation in density caused by thermal elastic waves explains the interference phenomenon.

Theory of Zernike and Prins. Inasmuch as the law of force between molecules is not known, it would be advisable to express the intensity of scattering as a function of the space distribution of molecules and the angle, and then to ascertain this space distribution by observation of the

intensity. This Zernike and Prins[2] have done. The result of their development gives the final equation

$$rg_0(r) = (1/2\pi^2) \int_0^\infty ds \cdot s \cdot i(s) \sin(sr) \tag{2}$$

wherein r is the distance from a given molecule, $g_0(r)$ is a probability distribution function, s is $4\pi\sin(\phi/2)/\lambda$ with ϕ the angle of diffraction and λ the wave-length, and $i(s)$ is defined as follows

$$i(s) = \frac{I(\phi) - NA^2/2}{NA^2/2} \tag{3}$$

In Eq. (3) N is the number of molecules considered, A is the scattering amplitude of each one, $I(\phi)$ is the actual scattering at the angle ϕ. These authors consider the molecules to be distributed along a straight line with a probable variation in their distance of separation, this variation to be the same as the variation of the free path of a gas molecule in terms of the mean free path. Then by treating the scattering as from a unidimensional grating, an expression for the $I(\phi)$ is found. The reasoning is then extended to three dimensions and the above form of Eq. (2) adopted because of our ignorance of $g(r) = g_0(r) + \rho$, or the probability distribution of molecule centers. It is in fact the probability that in an element of volume dv, which is at a distance r from the central point of any given molecule, another molecular center is found. The authors show that for a small angle of scattering or a large wave-length, the scattered intensities from the fluid and the gas (of the same number of molecules) have the ratio of the compressibilities in these two states. This point agrees with the discussion of Raman and Ramanathan. Moreover, in the discussion of the unidimensional grating, Zernike and Prins show that, with the unidimensional grating and the assumed law of separation as stated, the scattering from the molecules at large values of ϕ approximates $NA^2/2$, whereas at small angles it becomes $NA^2l^2/2(l+a)^2$, where l is the mean separation of molecules and a is the molecular diameter. The latter expression is small if l is relatively small. This again accounts for the small scattering at small angles. The curve of intensity of scattering of the one-dimensional grating as a function of ϕ, shows a series of maxima and minima, decreasing in magnitude as ϕ increases.

The theory of Zernike and Prins adds to the earlier work of Raman and Ramanathan chiefly in the form of Eq. (2), which supplies a method of obtaining $g_0(r)$ and finally $g(r)$ from the observed scattering. But the method does not seem practical. It assumes the function to be symmetrical in r, which, in general, will be contrary to fact. For elongated molecules this variation from assumption may and probably would nullify the entire method.

[2] Zernike and Prins, Zeits. f. Physik, **41** p. 184 (1927).

Ehrenfest formula. In connection with other theories the formula of Ehrenfest[3] will be cited, not because he intended it to be applied to liquids, which he did not, but because it has been so used by several investigators.[4] Consider the scattering by two electrons at a distance a apart. It is shown that the intensity at an angle ϕ, $I(\phi)$ is

$$I(\phi) \propto (1+ \sin 2\pi\rho/2\pi\rho) \text{ where } 2\pi\rho \text{ is } (4\pi a/\lambda) \sin \phi/2 \qquad (4)$$

This function has maximum values for $2\pi\rho = 0.0$, 7.72, 14.07, etc. Hence the first maximum is at $\phi = 0°$. The second is at

$$(4\pi a/\lambda) \sin \phi/2 = 7.72, \text{ or, } a = \lambda/2 \times 0.812 \sin \phi/2 \qquad (5)$$

Eq. (5) cannot be used to ascertain the distance of separation of two scattering centers in a liquid because the assumptions of the scattering occurring by independent pairs of centers is not met. Indeed, Ehrenfest states clearly that the formula cannot apply to liquids. For a fairly symmetrical molecule there is an agreement between the value of a and the value, 1.33 $(M/d)^{1/3}$ wherein M is the molecular weight, d the density and the expression is the mean distance of the centers of two neighboring spherical molecules in the case of the densest packing. This interpretation of Eq. (5) should not be regarded seriously. That the apparent numerical agreement is not intrinsically noteworthy is seen if one realizes that such an agreement for the *second* diffraction peak is secured only by the omission of the theoretical *first* peak which occurs at 0° diffraction angle, and which is very much *greater* in magnitude. The disagreement is of greater magnitude than the agreement. Thus the Ehrenfest theory is inapplicable because both its assumptions and its predictions are contrary to the facts obtaining in liquids.

Debye's theory of scattering in gases. One of the ways of finding the interferences due to the interaction of the atoms constituting the molecule would be to perform experiments upon gases of different densities. The intermolecular interference could then be elminated and the interference within a molecule ascertained. The possibility in these experiments when aided by theoretical considerations led Debye[5] to discuss scattering in gases, both with single scattering particles and with pairs. The theory is strictly not applicable to liquids and is mentioned here merely because of an interesting point it presents. If the volume occupied by the gas particles is vanishing small in comparison with the free volume, the maximum intensity occurs at 0°. If the volume of the particles now becomes, for example, one half of the total volume of the gas, if $\lambda = 0.71$A, and if the particle diameter is 2.1×10^{-8} cm, then the maximum occurs at 16°. From this view point, the maximum at an angle other than zero may be regarded as caused by the limitation of the approach of scattering centers. To this extent it is

[3] Ehrenfest, Proc. Akad. Wet. Amsterdam, **27**, 1184 (1915).

[4] Keesom, Physica **2**, 118 (1922); Keesom and de Smedt, Proc. Amsterdam **25**, 118 (1922) and **26**, 112 (1923); Katz, Zeits. f. Physik **45**, 97 (1927).

[5] Debye, Jl. of Mathematics and Physics, **4**, p. 133 (1925) and in German in Phys. Zeits. **28**, 135 (1927)).

in agreement with the thought that the maximum depends upon the mean distance of separation of the molecules.

Theory of cybotaxis. The above theories do not assume any organization of molecules into a space array. The view point of this laboratory[6] is that every liquid contains a myriad of small groupings of molecules produced by forces acting between them, the groups being neither perfect in form nor permanent. The word cybotaxis means literally "space arrangement" and is adopted to designate this condition in a liquid. It is not a new state of matter, but a descriptive term applying to the physical state of a liquid. It is used for the sake of brevity and of emphasis. We have learned to recognize a crystal as being approximately perfect only in fragments. The liquid goes to a much greater extreme. Its semi-perfect small groups do not even retain their identity. Viscosity is that of groups and of unorganized molecular arrays between them and this does not depend directly upon the structure of a single molecule. The theory of diffraction in such a physical structure cannot be exactly that of crystal powders nor of unorganized molecules as in the foregoing theory of Raman and Ramanathan. But the crystal powder theory may be accepted as applicable to an idealized condition which the liquid state only roughly approximates at any instant. In such a theory Bragg's law holds for the maximum peak in the diffraction intensity curve, provided the beam is monochromatic. If it is not monochromatic, then, in general, the peak will be shifted in a direction dependent upon the shape of the frequency-intensity distribution curve. Moreover such a theory shows at once why the scattering is small near 0° and has a prominent peak in the first order according to Bragg's law, why the peak is broad and why higher orders are relatively weak. The first two are accounted for by the existence of the small groups, the third by the limited size of the groups and the fourth partly by the structure factor of the molecules. In regard to the breadth of the peak, preliminary observations in this laboratory show that it is proportional to wave-length as indicated by the powdered crystal theory of Laue,[7] and represented in the application to cubic crystals by,

$$B=\frac{2}{\cos\ (x_h/2)}\left(\frac{\log_e 2}{\pi}\right)^{1/2}\ \frac{\lambda}{ma}$$

wherein B is the breadth of peak at half-intensity, x_h is the angle of maximum intensity, λ is the wave-length of the radiation and ma is the total extension of the crystal in a direction perpendicular to the reflecting plane. This formula had been earlier used by other writers but without reference to a derivation.

The above shows that the assumption of the cybotactic condition and the adoption of the powdered crystal theory as an approximate one for

[6] See series of articles by Stewart and Morrow, Morrow, Stewart and Skinner and Stewart in Physical Review for 1927 and 1928.

[7] Laue, Zeits. f. Kristallographie, **46**, 115 (1926).

liquids, satisfies the principle phenomena herein discussed, viz., the small intensity near 0° and a maximum at an angle satisfying Bragg's law for a distance of separation of the molecules. But it goes further. It seems to account for the relative intensities of two peaks through estimates of the structure factor as in the case of the *n*-alcohols,[8] for the practically linear change of angular position of one of the maxima with content of carbon in straight chains while the other maximum remains unchanged, for the similarity of alteration of peaks in solid and liquid normal fatty acids[9] with change in carbon content, for the agreement of interpretation of diffraction measurements with experiments in monomolecular liquid layers, for the agreement of diffraction measurements on isomers[10] with current chemical views, for the comparison of diameters of the carbon chains with normal alcohols[9] saturated normal fatty acids[9] and normal paraffins,[11] and finally for the explanation of the three maxima[11] which apparently correspond to the three dimensions of the straight chain.[12] It should be mentioned that in the above view thermal vibration must appear in the form of elastic waves.

Conclusions. The general conclusion of the discussion is that the assumption of the molecular groupings in the liquid at any instant, or cybotaxis, with the acceptance of the crystal powder theory as an idealized one for the liquid, explains the phenomena found in the most simple manner.

PHYSICS LABORATORY
UNIVERSITY OF IOWA
June 1, 1918.

[8] Stewart and Morrow, Phys. Rev. **30**, 232 (1927).
[9] Morrow, Phys. Rev. **31**, 20 (1928).
[10] Stewart and Skinner, Phys. Rev. **31**, 1 (1928).
[11] Stewart, Phys. Rev. **32**, 153 (1928).
[12] The detailed discussion showing that these phenomena are accounted for adequately is omitted here not only because it would require a lengthy presentation of the experimental material but also because the reader who becomes acquainted with the experiments can readily supply this discussion.

THE DIRECTION OF EJECTION OF PHOTO-ELECTRONS BY POLARIZED X-RAYS

By C. J. Pietenpol

Abstract

Variation with angle from the plane of polarization of the number of photo-electrons ejected by x-rays in lateral directions.—Bubb and Kirchner have studied the lateral distribution of photo-electrons ejected by polarized x-rays by the Wilson cloud expansion method. This method is open to objections as pointed out by Bothe, and Watson has concluded that because of scattering by neighboring atoms it is impossible to determine the exact direction of ejection of the electron from the atom. It is thus difficult to determine the mechanism of electron ejection from such data. The writer has studied the lateral distribution by means of Geiger counters which could rotate about the polarized beam. The electrons were ejected from air at a low pressure in which the mean free path of the electron is many times the distance through which the electron must move to enter the counter. Allowing for the fact that completely polarized beams are impossible to obtain in practice, the data strongly favor the cosine squared relation of Auger and Perrin rather than the relation deduced by Bubb.

THEORIES to account for the lateral spreading of photo-electrons ejected by x-rays have in general been of three kinds. Bubb[1] and Bothe[2] have attempted to account for this space distribution by compounding the momentum of the quantum in the forward direction with a random momentum of the electron in its atomic orbit. Auger and Perrin[3] have deduced a probability relationship between the direction of the electron's velocity in its orbit and the direction of the electric field of the radiation by which the electron is ejected. Results similar to Auger and Perrin's have been obtained on the basis of the new quantum mechanics by Wentzel,[4] Oppenheimer,[5] and Beck.[6] Recently Watson[7] has shown that previous experimental results can be explained by the Rutherford theory of nuclear scattering.

Experimental tests of the lateral distribution have been made by Bubb[8] and Kirchner[9] by the use of the C.T.R. Wilson cloud expansion method. This method, although used by many experimenters, is open to a number of objections. As Watson has pointed out, the whole distribution of the photo-electrons can be explained by the scattering in neighboring atoms

[1] F. W. Bubb, Phil. Mag. **49**, 824 (1925).
[2] W. Bothe, Zeits. f. Physik **26**, 74 (1924).
[3] P. Auger and F. Perrin, Comptes Rendus **180**, 1742 (1925).
[4] G. Wentzel, Zeits. f. Physik **40**, 574 (1927).
[5] J. R. Oppenheimer, Zeits. f. Physik **41**, 291 (1927).
[6] G. Beck, Zeits. f. Physik **41**, 443 (1927).
[7] E. C. Watson, Phys. Rev. **31**, 728 (1928).
[8] F. W. Bubb, Phys. Rev. **23**, 137 (1924).
[9] F. Kirchner, Ann. d. Physik **83**, 521 (1927).

when this method is used. It is thus difficult to determine the mechanism of electron ejectiom from such data.

A method employed by Bothe[10] in investigating the longitudinal distribution was that of the Geiger point-counter. A similar method has been used by the writer to determine the lateral distribution. By this method it is possible to obtain a relatively large number of counts. Thus the writer has counted 1659 photo-electrons while the paper of Bubb's indicate a total of 156 counts.

Counters of various types and forms have been used and described by Hess and Lawson,[11] Kovarik and McKeehan,[12] Bothe and Geiger[13] and others. Counters of different types were constructed during preliminary trials by the author and tested by means of a string electrometer. Best results were obtained with an electrode made by fusing a small bead of about 0.1 mm diameter on a platinum wire of approximately one half this size. This small bead was placed within 2 mm of the front of the counter. About 25 small holes were drilled in the front of the counter. A thin sheet of mica was placed over these holes and the edges sealed with soft wax to make it air-tight. A thin sheet of brass with holes drilled to coincide exactly with those in the front of the counter was placed over the mica and held tightly against it by means of screws. The counter was filled with air at atmospheric pressure.

The amplifying device used was a four-stage, transformer coupled amplifier. The counter point was connected to the grid of a special high amplifying tube and also through a water resistance to earth. The second and third tubes were similar to the first having an amplification constant of about 30. A loud speaker was connected in the plate circuit of the last tube.

The cap of the counter was connected to the positive terminal of a high voltage battery. This could be adjusted by steps of two volts to a maximum value of about 3000 volts. The voltage required on the counter depended upon the individual point used, the dimensions of the counter, and the distance between the point and the front of the counter. For the type of counter with which best results were obtained the voltage was between 1800 and 2000. The voltage of the cells could be kept constant during a run by means of a high voltage kenetron rectifier which maintained a small charging current through the battery while observations were being made.

Each counter was tested by the use of β-rays from radium. The voltage on the counter was raised until the clicks in the loud speaker became clear and distinct. The radium was then removed and the counter tested for spontaneous discharges. If a counter showed more than two spontaneous discharges for a time of about three minutes, it was not used. Considerable trouble was found in the construction of counters which would count a large

[10] W. Bothe, Zeits. f. Physik **26,** 59 (1924).
[11] V. F. Hess and R. W. Lawson, Wiener Ber. **127,** 405 (1918).
[12] A. F. Kovarik and L. W. McKeehan, Phys. Rev. **8,** 574 (1916).
[13] W. Bothe and H. Geiger, Zeits. f. Physik **32,** 639 (1925).

number of β-rays and still not give spontaneous discharges. Points of different types were tried in an effort to obtain the best counter. It was found that steel needles ground to a sharp point by means of an oil stone gave fair results, provided the steel point was heated to a dull red in a gas flame. The spontaneous discharges were, however, more numerous with that type of point than with a small sphere fused on the end of a fine platinum wire. Sharp tungsten points or platinum spheres of considerable size were not found satisfactory.

The source of x-rays was a Coolidge 30-milliampere, 20-second tube. The voltage across the tube was supplied by a transformer of approximately 60,000 volts. The x-ray tube was placed in a box lined with 1/4″ lead and the transformers, placed below the tube, were completely surrounded by 1/32″ tin plate which was grounded. The lead box in which the tube was placed was also grounded. This was done to prevent stray fields which might affect the counter or amplifying system. A second lead box, closed on the top, bottom and three sides, was placed in contact with the first lead box. This contained the scattering block. The scattering block was placed at an angle of 45° with the direction of the primary rays. The rays scattered from this substance at 90° with the direction of the primary rays passed through an opening in the side of the box and then a brass cylinder holding the counter. The details of this cylinder are shown in Fig. 1. Inside the brass cylinder there was placed another coaxial cylinder of lead L held tightly in place by friction. Small circular apertures J, 5 mm in diameter and 6.8 cm apart, were made in the two ends. This served to constrict the beam of x-rays, thus rendering them more nearly parallel and also prevented in large measure any stray x-rays from entering the counter. Since the apertures J were accurately constructed to be along the axis of the tube H, any rotation of the tube H did not in any way alter the x-ray beam passing through it, and consequently the face of the counter was always at the same distance from the x-ray beam. This distance was 2.6 cm. The faces of the tube H were closed by sheets of mica I about 1/2 mm thick and were made air-tight by wax joints. A side tube M allowed a connection to be made to the vacuum pump. The whole tube could be rotated about its axis by being placed upon two semi-circular bearings near the two ends.

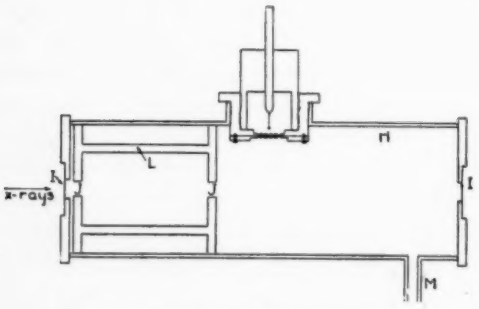

Fig. 1. Diagram of apparatus.

Compton and Hagenow[14] have shown that x-rays scattered at right angles are nearly completely polarized as the thickness of the scattering

[14] A. H. Compton and C. F. Hagenow, J.O.S.A. **8**, 487 (1924).

substance is decreased. For paper having a thickness of 0.25 cm there is almost complete polarization. This is the type of scattering block used in this experiment.

After counters had been tested by the β-rays of radium for constancy of number of discharges per minute, they were placed in the apparatus and the joints made air-tight by soft wax. The apparatus was then evacuated to about 0.004 mm of mercury. The filament rheostat was regulated for constant current through the tube. It was possible to run the tube for only 20 seconds at a time since it was not of the continuously operating type. It was necessary to wait for about one or two minutes between each interval that the tube was in use to allow cooling of the tube. The number of photo-electrons entering the counter during the 20 seconds of operation was counted by means of the loud speaker.

It was found that many counters which worked well for β-rays failed to register any photo-electrons. Some counters caused registrations which were either so weak or so few in number as to make them worthless. Each counter was repeatedly tested for spontaneous discharges. Unless a counter showed at least four counts per 20 seconds when in the plane of the electric vector and no spontaneous ones in a time of three minutes, it was not used. Although all counter points were constructed in the same way, there was a very marked difference in their behavior.

The cylindrical tube containing the counter was rotated until the counter was in the plane of the electric vector. Usually three sets of 20 second intervals were taken before the counter was rotated out of this plane. It was then set at 30° with the plane of the electric vector and another set of three counts taken. Similar observations were made then for 60°, 90°, 180°, and 270°. The counts at 180° and 270° were made simply to check the counts at 0° and 90°. Each run was continued as long as the apparatus operated properly. Ther terminations of the runs were due to the following reasons: (1) the ceasing of the counter to register photo-electrons, (2) the development of spontaneous discharges by the counter, (3) a defect in the x-ray apparatus which made it impossible to keep a steady current through the tube, (4) defects in the vacuum system which developed in rotating the cylinder containing the counter.

During one run a sheet of lead was placed over the slit in the x-ray box so as to cut off the x-ray beam. It was found that there was no indication of counts. This was done to make sure that the operation of the counter was not due to any external fields.

A counter which operated well for photo-electrons was taken out of the apparatus and a thick sheet of mica placed over the holes in the counter. When it was put back in the apparatus it showed no counts whatever although the counter continued to operate when the mica sheet was removed. This sheet was of such thickness that photo-electrons could not penetrate it. On the other hand it was not so great that x-rays were absorbed in it. This indicates that the number of stray x-rays which could enter the counter was exceedingly small.

Although many runs were started with counters which showed a relatively large number of photo-electrons, the actual number of runs which gave self-consistent results for any length of time were few. Those which showed that the counter was not behaving properly have been discarded only after a careful investigation which showed that there was something wrong with the apparatus. Those which were self-consistent for such a period that it was possible to obtain a good average result for the number ejected in the different directions are tabulated below. The corresponding times are given in seconds.

TABLE I. *Number of photo-electrons ejected at various angles with plane of polarization in plane perpendicular to x-ray beam.*

0°		30°		60°		90°		180°		270°	
No.	Time	No.	Time	No.	Time	No.	Time	No.	Time	No.	Time
98	340					15	340				
148	480					11	480				
14	120	12	120	9	120	2	120	8	60	0	60
61	300	64	420	30	420	8	360	30	120	5	120
241	600	229	720	93	720	40	600	42	120	6	120
65	180	31	120	11	120	1	120	42	120	5	120
98	420	70	420	28	420	10	420	112	420	20	240

If the number of counts is added for all runs and then reduced for equal times and expressed in terms of 100 in the 0° direction we get,

0°	30°	60°	90°	180°	270°
100	76.0	37.2	12.0	93.7	14.4

If the 0° and 180° directions and the 90° and 270° directions are combined and then reduced as before for equal times and expressed in terms of 100 in the plane of the electric vector (0−180) we get the following results.

0°-180°	30°	60°	90°-270°
100	76.7	32.5	12.8

The fact that for 100 counts in the plane of the electric vector there are 12.8 at right angles to this plane may have four causes other than the ejection of photoelectrons in a plane perpendicular to the electric vector. First, the scattering did not all occur at 90° because of the fact that a beam of rays was used instead of a line. Since the distances from the target to the scattering block and from the scattering block to the counter together with the size of the apertures are known, it is possible to calculate the greatest deviation of a scattered ray from 90°. This was found to be about 3°. Second, the beam is not completely polarized because of the fact that the scattering block has a thickness greater than one layer of molecules. Although Compton and Hagenow have shown that this effect is not greater for thin substances, there is nevertheless a certain amount of unpolarized radiation. A third reason for expecting some electrons to appear at this setting is that some are deflected from their original direction by collision. For the pressures used in this experiment a high speed electron should have

a theoretical mean path of about 12 cm. The face of the counter was 2.6 cm from the x-ray beam. The probability of collision is thus small, the more so as the experiments of Langmuir[15] have shown that the actual mean free path is considerably greater than that predicted by theory. A fourth reason lies in the fact that the effective area of the face of the counter covered about 4°. Thus with the counter set at the 90° position it actually covered the space between 88° and 92°.

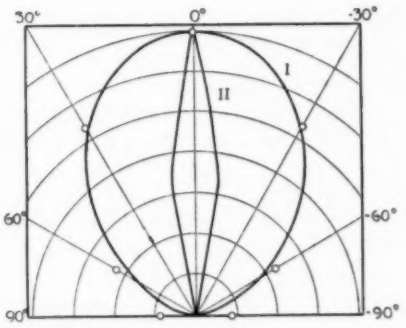

Fig. 2. Lateral distribution of photo-electrons. The points are experimental. Curve I is Auger and Perrin's theoretical curve: Curve II is Bubb's theoretical curve. The electric vector of the polarized x-rays is vertical.

The experimental points are plotted in Fig. 2 together with the theoretical curves of Bubb and Auger and Perrin. The curve of Bubb is based on an incident frequency of the $K\alpha$ line of tungsten and an ejected electron from the K shell of oxygen and nitrogen, averaged to give one value for computation. For this frequency there should, by Bubb's theory, be no photoelectrons ejected beyond 5° from the electric vector. It is to be noticed that the experimental points fit the curve of Auger and Perrin more closely than the curve of Bubb.

The writer wishes to express his sincere thanks to Professor J. C. Hubbard of the Johns Hopkins University for suggesting the problem and to Professors W. A. Lynch and R. T. Cox for their constant aid and interest during the investigation.

NEW YORK UNIVERSITY,
UNIVERSITY HEIGHTS, N. Y.
June 19, 1928.

[15] See Dushman, High Vacuum

THE PRINCIPLE OF UNCERTAINTY IN WEYL'S SYSTEM

By G. Breit

Abstract

Using Weyl's geometrical interpretation of quantum mechanics the fundamental relations of the transformation theory can be treated without making use of Dirac's δ function. The principle of uncertainty is particularly clear in this system. It is shown that in the discrete representation for a definite axis of the coordinate q all Eigenwerte of the conjugate momentum p are equally probable. It is also shown how in the limit of very fine subdivision the results of Heisenberg and Bohr are obtained. The whole treatment receives an easy interpretation by applying it to the problem of the diffraction of waves by a grating. Weyl's method of discussing quantities with continuous ranges of values is found to be equivalent to investigating diffraction phenomena in the limiting case of an infinitesimal grating space. The quantum condition $i(PQ-QP)=1$ is shown to be correct in a purely operational sense in spite of the fact that as a matrix equation it is untrue.

THE quantitative aspects of Heisenberg's principle of uncertainty have been discussed by Heisenberg[1] and by Bohr.[2] Bohr attacks the problem rom the point of view of waves, and Heisenberg's considerations are based on the Dirac-Jordan transformation-theory. Heisenberg himself brought out (reference 1, p. 181) a more visual representation of relations between quantum quantities which has since been developed by Weyl.[3] According to this formulation the clearest observable condition of a physical system is represented by a pure case—a mathematical ray. Physical quantities themselves are represented as in the Dirac-Jordan theory by quadratic forms or matrices. The fundamental postulate is that only the characteristic values of the matrices can be observed. If a ray is not directed in the direction of a principal axis of the quadratic form, no certain measurement of the corresponding physical quantity can be made. Hence the principle of uncertainty. However, no explicit derivation of the uncertainty for the momentum if the coordinate is known with a certain precision has been published from the point of view of Weyl's theory. It is of interest to work through such a derivation particularly because the fundamental postulates of Weyl's paper are more directly related to the principle of uncertainty than those of the usual transformation-theory. The probability of a physical quantity having a certain value is stated more concisely and is visualized geometrically by Weyl. Using his discrete representation we shall be able to discuss probability-relations for the continuous case by passing to the limit of a very dense Eigenwert spectrum. The result of the calculation will be essentially the same as that obtainable by the methods of Heisenberg or Bohr. However, the results will be found not to be entirely identical.

[1] Heisenberg, W., Zeits. f. Physik **43**, 172 (1927).
[2] Bohr, N., Nature, 580 (Apr. 14, 1928).
[3] Weyl, H., Zeits. f. Physik **46**, 1 (1927).

Namely, it will be found that the relative phases of the components of "experimentally good" pure cases must vary regularly. The difference between the phases of successive components of a pure case will be found to be constant for the "experimentally good" pure cases. It will also be found that the discrete representation given by Weyl on page 32 essentially reduces the problem to the consideration of the diffraction of a set of de Broglie waves or electromagnetic waves by a grating. The results of applying the quantum reasoning will turn out to be very similar to Duane's theory of diffraction. The experiment of photographing the diffraction-pattern of a monochromatically illuminated grating will be seen to be an illustration of observing a pure case.

1. We use Weyl's notation. Capital Roman letters denote matrices. Small Roman letters denote ordinary complex numbers. The complex conjugate of x is written $\bar{x}$. A vector in the fictitious, n-dimensional representative space with components $x_1, x_2, \cdots, x_n$ is written as $\mathbf{x}$. A quadratic form $\sum_{i,k=1}^{n} a_{ik} x_i \bar{x}_k$ is written as $A(\mathbf{x})$. The result of transforming a vector $\mathbf{x}$ by a matrix A is written as $\mathbf{x}A$. Explicitly if $\mathbf{y}=\mathbf{x}A$ the components $y_k=\Sigma_i a_{ik} x_i$. The units are chosen so that the quantum condition is

$$i(PQ-QP)=\mathbf{1} \tag{1}$$

where $\mathbf{1}$ is the unit matrix. We discuss a system with one degree of freedom. Weyl shows that the continuous group $\exp i(P\sigma+Q\tau)$ subject to (1) may be approximately covered by a finite group having for base two matrices A,B such that

$$A\colon\ x_k'=x_{k-1}(k>1),\ \ x_1'=x_n\ ;\ \ B\colon\ x_k'=\epsilon^{k+s}x_k,\ \ (\epsilon=\exp 2\pi i n^{-1})$$

The constant integer s we set arbitrarily $=0$. No generality is lost, because this amounts to interchanging the Eigenwerte of Q cyclically. We write $B=\exp iQ\delta\tau$, $A=\exp iP\delta\sigma$. Here $\delta\sigma$, $\delta\tau$ are small real numbers which must be chosen so that $AB=\epsilon BA$, the identical relation between A and B, be satisfied. As shown by Weyl, this leads on account of (1) to $\exp(i\delta\sigma\delta\tau)=\exp(2\pi i n^{-1})$. Hence $\delta\sigma\delta\tau=2\pi(n^{-1}+s)$, where s is any integer. We choose $s=0$ so as to deal with the smallest possible absolute values of $\delta\sigma$ and $\delta\tau$. We have

$$\delta\sigma\delta\tau=2\pi n^{-1} \tag{2}$$

It is very easy to find a Q such that $B=\exp(iQ\delta\tau)$ because B is diagonal. We make Q also diagonal. Let its kth element be q_k. Then the kth diagonal element $\exp(iQ\delta\tau)$ is $\exp(iq_k\delta\tau)=\exp(2\pi i k n^{-1})$. Hence $q_k=2\pi(\delta\tau)^{-1}(kn^{-1}+s)$ and for a fixed s we have $(q_k-q_{k-1})=2\pi(n\delta\tau)^{-1}=\delta\sigma$ by (2). The interval between two successive Eigenwerte of q is $\delta\sigma$ which will be in the future written as δq. We have, therefore, applying (2) again

$$q_k=k\delta q+s(n\delta q)\ ;\ s=(0,\pm 1,\pm 2,\cdots\pm\infty),\ (k=1,2,\cdots,n) \tag{3}$$

For a fixed s as δq decreases and n increases a given finite range $n\delta q$ of q is covered very densely. If s is varied the whole range of real values of q is covered. The interval $n\delta q$ then is a probability-period because the probabilities are determined by the axes which in their turn are determined by k. For most of the discussion it is immaterial whether the many-valuedness of the solution is taken into account. However, it will be shown in connection with the diffraction by a grating that it is important to take into account all the branches of the solution corresponding to different values of s.

In order to determine the matrix P we observe that the variables y_k determined by the unitary transformation

$$y_k = n^{-1/2} \sum_{s=1}^{n} \epsilon^{k(s-1)} x_s, \; x_{k+1} = n^{-1/2} \sum_{s=1}^{n} \epsilon^{-sk} y_s \tag{4}$$

are transformed by B if the x_k are transformed by A. Since $A = \exp(iP\delta\sigma)$ we obtain a solution for P as a matrix having the y_k for principal axes and having Eigenwerte:

$$p_k = k\delta p + t(n\delta p) \; ; \; t = (0, \pm 1, \pm 2, \cdots) \; ; \; (\delta p = \delta\tau) \cdots \tag{5}$$

Equation (2) now becomes

$$\delta p \delta q = 2\pi n^{-1} \tag{6}$$

Equation (4) shows at once that a pure case along any of the principal axes of P has equal probabilities for all the Eigenwerte of Q and vice versa. The square of the absolute value of any of these components is n^{-1}. In this *discrete* case it is the *equality* of the probability of all the values of p for a definitely determined axis of q that takes the place of uncertainty.

The meaning of the probability period for angle variables should be noted. If δq approaches zero but $n\delta q$ is kept constant, δp also remains fixed and finite. By passing to the limit we deal with a Q which represents an angle variable with a period $2\pi/\delta p$. The "conjugate" momentum is P which takes values differing from each other by the finite amount δp. The periodicity of Q is shown at once by expression (3) which using (1) becomes $q_k = k\delta q + 2\pi s/\delta p$. Since the axis corresponding to a given Eigenwert of Q is determined by k and not by s, the same probabilities correspond to different values of the angle variable, the differences between which are equal to the period $2\pi/\delta p$ or a multiple of it. Expanding the commutator relation $AB = \epsilon BA$ and taking into account only terms of the first order in δq we obtain $(1+iP\delta q)\exp(iQ\delta p) = (1+i\delta q\delta p)(\exp(iQ\delta p))(1+iP\delta q)$. On collecting terms in δq we obtain $P\exp(iQ\delta p) = (\exp(iQ\delta p))(P+\delta p)$. This relation in the form $Je^{2\pi iw} = e^{2\pi iw}(J+h)$ has been extensively used by Dirac. The only restriction on J in his treatment is that the successive Eigenwerte should differ by h. The absolute values of the Eigenwerte should not be determined by the commutator relation, therefore, but only their differences. In our treatment these Eigenwerte are given by (5). The probability period $n\delta p$ is infinite in the limit of $\delta q = 0$. In the finite region (5) determines the Eigenwerte completely

and contains no additive constant. It is clear, however, that we can always replace B by $B'=e^{ip_0\delta q_1}B$ without changing any of the relations.

2. We can now pass to the limit of having both δq and δp approach zero. By (6) this makes the probability-periods $n\delta q$ and $n\delta p$ both infinite and enables us to deal with arbitrary probability-distributions of q and p. We consider a given interval of q, say the interval a, and we pick out the pure cases giving the same probability for all the Eigenwerte of Q lying in a. Among these pure cases a certain class gives regularly varying probabilities for successive Eigenwerte of P. We consider these pure cases as representing the best conditions for measurement. We find that these "experimentally good" pure cases give such a probability-distribution among the Eigenwerte of P that its average width is related to the width of the interval a by Heisenberg's formula.

We call the axes belonging to the interval a: $1, 2, \cdots, m$ starting with 1 for simplicity of writing. We need the pure cases for which the probability along axes outside of the interval vanishes and for which the probabilities along all of the axes: $x_1, x_2, \cdots, x_m$ are equal. All such pure cases are

$$\begin{gathered} m^{1/2}x_k=\exp\,(i\theta_k)\ ;\ \theta_1=0(1\leqq k\leqq m) \\ x_k=0,\ \ (k<1\ \text{ or }\ k>m) \end{gathered} \tag{7}$$

Here the θ_k are a set of $m-1$, real, arbitrary, independent constants. The most interesting of these pure cases are those given by

$$m^{1/2}x_k=\exp\,(i(k-1)\theta) \tag{8}$$

By (4) the components of these along the principal axes of P are

$$y_k=\frac{1}{(mn)^{1/2}}\ \sum_{s=1}^{m}(\epsilon^k e^{i\theta})^{s-1}=\frac{1}{(mn)^{1/2}}\ \frac{1-\exp 2\pi im(kn^{-1}+\theta)}{1-\exp\ 2\pi i(kn^{-1}+\theta)} \tag{8.5}$$

This gives

$$|\ y_k\ |^2=m^{-1}n^{-1}\sin^2\pi m(kn^{-1}+\theta)\ \sin^{-2}\pi(kn^{-1}+\theta) \tag{9}$$

Writing p for the kth Eigenwert of P we have

$$p=k\delta p,\ \ a=m\delta q \tag{10}$$

We apply (6) to (9) expressing all quantities in terms of a, p, and δq. We obtain

$$|\ y_k\ |^2(\delta p)^{-1}=(\delta q)^2(2\pi a)^{-1}\sin^2\,(ap'/2)\ \sin^{-2}(p'\delta q/2)\ ;\ p'=p+2\pi\theta(\delta q)^{-1} \tag{11}$$

Keeping $2\pi\theta(\delta q)^{-1}$ constant say $-p_0$ and making δq very small we have

$$|\ y_k\ |^2/\delta p=(a/2\pi)(2/ap')^2\sin^2\,(ap'/2)\ ;\ p'=p-p_0 \tag{12}$$

This is the probability of a unit interval at p. To within an additive constant p' is the same as p. The distance of the central maximum of the probability-

UNIVERSITY OF MICHIGAN LIBRARIES

distribution (12) from the first minimum (Rayleigh's criterion) is Δp given by

$$a\,\Delta p = 2\pi \tag{13}$$

If the units were chosen so that $i(PQ-QP)=1h/(2\pi)$ this would be $a\Delta p = h$. In the limit of δq, $\delta p = 0$ for the special class of rays defined by (8) we obtain therefore Heisenberg's relation. It is easily verified that the probability-distribution (12) is in agreement with Bohr's analysis of p into frequencies. The function to be analyzed is then a "square" wave in q vanishing outside the interval a and having the constant value a^{-1} inside a.

We note the following points: (I) In order to obtain a probability-distribution (12) we must deal with a special type of a pure case, namely, that determined by (8). The general type of pure case (7) giving the same probability-distribution for q gives much more complicated probability-distributions than (12). These do not correspond to Bohr's analysis and are not to be considered as "experimentally good" for a simultaneous measurement of q and p. Their essential feature is a permutation of the probabilities of different values of p and a scattering of the large probabilities corresponding to the central maximum of (12). (II) The result of averaging over the θ_k in (7) gives entirely equal probabilities of all values of p. Simultaneous good experimental determinations of q and p correspond, therefore, definitely to observations of single pure cases not their averages—even in the limiting continuous case. (III) The process used by Weyl to derive Schroedinger's equation involves the use of a limiting process in which in accordance with (3) and (5) both q and p have probability-periods $n\delta q$ and $n\delta p$. As the limit, δq, $\delta p = 0$ is approached the probability-periods become infinite by (6). Weyl's process is, therefore, equivalent to analyzing the probability-distributions into Fourier series and passing to the limit for the Fourier integral.

3. Equation (12) is of the same form as the expression for the intensity in the problem of the diffraction of light or de Broglie waves by a slit. Its derivation does not involve the concept of waves and reminds us particularly of Duane's treatment of diffraction.[4] The immediately important thing above is not the transfer of momentum to the slit but the fact that the limitation introduced by the slit in the coordinate q gives the particular distribution (12) for p. We can picture these relations in the discrete case as well. The inclusion of all values of s and t in (3) and (5) is seen to be important, because a grating of finite width has only a finite resolving power. The pure case given by $y_k=1$, $y_\sigma=0$, $(\sigma\neq k)$ and (4) cannot correspond to the Eigenwerte of q for $s=0$ alone; it must correspond to the Eigenwerte of q for all of the possible values of $s=0$, ± 1, etc. Similarly for p, any pure case must be interpreted as giving with equal probabilities all the Eigenwerte with the same k and different t in (5). The pure case (7) we interpret as a wave having complex amplitudes defined by the x_k of (7) at very narrow grating-slits with positions q_k defined by (3). The meaning of the probability-period for q is that the

[4] Jordan, P., Zeits. f. Physik, **37**, 376 (1926).

phase of the wave for the same k and different s is the same. All slits separated by the distance $n\delta q$ emit with the same phase. A pure case having a component only along the axis x_k is interpreted as the diffraction-pattern due to a number of equidistant slits with vibrations of equal phase separated by $n\delta q$. The different possible directions of diffraction are separated by intervals δp given by (6) as $\delta p = 2\pi/(n\delta q)$ or in ordinary units as $\delta p = h/(n\delta q)$. The picture corresponding to a pure case along an axis of Q is therefore given by a grating with a wide spacing $n\delta q$ and a closely spaced diffraction-pattern with the small separation δp. Conversely a pure case along an axis of P, i.e., along a y_k is pictured by a grating with the narrow spacing of slits given by δq, the vibrations between successive slits differing by a factor ϵ, and a wide diffraction-pattern corresponding to one value of k and all values of t in (5). Now the spacing between successive diffraction-lines is $(n\delta p)$ given by $(n\delta p) = 2\pi/\delta q$. The relation between the grating space and the possible diffraction-pattern is the same in both cases. In general the specification of the x_k component of a pure case is pictured as the assignment of the relative complex amplitude to the vibration at the kth slit within the period $n\delta q$ and the specification of the y_k component of the pure case means the assignment of the relative complex amplitude to the kth diffraction-line within the period $n\delta p$. The assignment of all the x_k components at once means the complete specification of the diffraction-pattern and determines the components along y_k, therefore, as well. In Eq. (7) the quantities θ_k mean the relative phases of vibrations at different slits. The special class of pure cases (8) corresponds to a plane wave incident on the grating. It is clear now why $2\pi\theta/\delta q$ had to be kept constant. It is also clear in what respect the rays (7) can give different results from (8). If, for example, by changing the thickness of the transmission-grating periodically we should superpose a periodic variation in θ_k on that given by (7), we would get a periodic variation in the intensities of the diffraction-lines. In the limiting case of a single slit for which we derived (12) periodic phase-changes within the slit produce the effect of superposing on (12) a periodic curve. Thus it is clear why (12) is not the only type of probability-distribution possible. Whether q is confined to a definite interval a or spread with an error-curve probability as in Heisenberg's treatment, we do not obtain only a pure case of the type corresponding to (12). Heisenberg's assignment of probabilities to p and q is, therefore, not the only one possible. We can always vary it by changing the θ_k in a manner different from (8). We thus see that Weyl's theory gives results similar but not identical with those of Heisenberg and Bohr.

We are now in a position to obtain the physical meaning of the operations A and B. According to the definition applying A to a pure case $\mathbf{x}$ means to form such a new pure case $\mathbf{x}' = \mathbf{x}A$ that the components in the new pure case x' are given by $x_k' = x_{k-1}$ for $k > 1$ and $x_1' = x_n$. For the grating this means a simple displacement through one grating space with respect to the incident wave. This is entirely clear for $k > 1$ and it is also true for $k = 1$ on account of the period $n\delta q$. The components along x_n, x_0, x_{-n}, etc., are the same. Writing $x_1' = x_n$ is equivalent to writing $x_1' = x_0 = x_{-n} = \cdots$. Similarly the

UNIVERSITY OF MICHIGAN LIBRARIES

operation B can be pictured by the components of the pure case along y_k. If B is applied to the x_k the components y_k change into $y_k' = n^{-1/2}\sum_{s=1}^{n}\epsilon^{k(s-1)+s}x_s$ $=\epsilon y_{k+1}$. The ϵ being common to all y_k' it does not affect the pure case. The operation B is, therefore, equivalent to a displacement in the domain of diffraction-lines by one diffraction-line. [In a sense it is equivalent to a displacement of the photographic plate.] We have also $x_k' = \epsilon^k x_k$ which means a change of the phases of all of the incident vibrations. Over the whole probability-period the path-difference changes by one wave-length due to B. Since the determinant of (4) does not vanish we can describe B either by the y_k or by the x_k completely. By stating the relative phases of vibrations arriving at the photograph plate we can describe the pure case just as well as by stating them at the slits of the grating. Just as A simply shifts all the probability-amplitudes for q by one and produces only a phase-change in the probability-amplitudes of p, so B shifts the probability-amplitudes of p by one and produces only a phase-change in the probability-amplitudes of q. If B^t and A^s are applied in any order we obtain a shift in q and in p; however, the shapes of the probability-curves are unchanged. Only the phases of the probability-amplitudes are altered.

Now if in equations (4) we know all the $|x_s|$ and the $|y_k|$, i.e., the total probabilities, we can also determine the relative phases of all of the components though not the absolute phases. Knowing the intensity-distribution at the grating and the intensity-distribution in the diffraction-pattern determines the pure case. We see why the group should be Abelian. If it were not we would be getting different pure cases for the same final result in the q and p probability-distributions depending on the order in which the different powers of A and B are applied.

4. In discussing this subject with the writer Dr. G. Y. Rainich pointed out that Eq. (1) is not literally correct since the elements of $i(PQ-QP)$ in the system of principal axes of Q are $ip_{lm}(q_m-q_l)$ and therefore can by no means represent a unit matrix. This apparent paradox offers no real difficulty, however. The meaning of $i(PQ-QP)=1$ should be made clear. Using our representation of Q and P we can derive definite expressions for them. They will not satisfy (1). In fact, there is no proof in Weyl's paper that they should. It is only proved there that $\exp(iP\delta q)\ \exp(iQ\delta p)=\epsilon\ \exp(iQ\delta p)$ $\exp(iP\delta q)$ and that for continuous Abelian groups, if they exist for the body of rays, (1) is true. A direct calculation for the elements of the matrix $i(PQ-QP)$ does *not* give numbers approaching elements of a unit matrix. Eq. (1) is true only in the sense that $i(PQ-QP)$ considered as an operator on ψ changes ψ into itself provided certain conditions are satisfied by ψ and provided the matrices Q, P are properly interpreted. It is of interest to write down the calculations because they represent exactly the step which is most easily taken by the use of Dirac's δ function and omitting them may appear as covering up a weak point of the theory. The Hermitean form $P(x)$ $=\sum_1^n P_k y_k \bar{y}_k = \sum_{k=1}^{n}(p_k/n)\exp(2\pi i n^{-1}(l-m)k)x_l\bar{x}_m$ by (4). This determines the

matrix elements of P. They are $P_{lm}=\sum_{k=1}^{n} p_k n^{-1}\exp 2\pi i n^{-1}(l-m)k$ or substituting for n from (6) $p_{lm}=\sum_{k=1}^{n}(2\pi)^{-1}p_k\delta q\delta p\,\exp(iq_l-q_m)p_k)$. We verify, in the first place, that for ψ the operation P is equivalent to $i(d/dq)$. This is proved by Weyl by expanding $\exp(iP\delta q)$. Since the same expansion is involved in proving (1) it is safest to verify the result directly. We consider a pure case defined by its x_k components given by $x_k=\psi(q_k)(\delta q)^{1/2}$. We operate on this pure case by P and obtain a new pure case $\Psi(q_m)=\sum_{l=1}^{n} p_{lm}\psi(q_l)$. Substituting the above value of p_{lm} we can represent the result by an integral in the limit of $\delta q=0$, $\delta p=0$ in the form

$$(P\psi(q))_m=\Psi(q_m)=\int_{-\infty}^{+\infty}\int_{-\infty}^{+\infty}(2\pi)^{-1}pe^{i(q-q_m)p}\psi(q)dqdp=i(d\psi(q)/dq)_{q=q_m} \quad (14)$$

by Fourier's Integral. This is true only provided we can replace $\sum_{k=1}^{n}$ and $\sum_{l=1}^{n}$ by $\int_{-\infty}^{+\infty}$. Thus the direct solutions (3) and (5) are not applicable without introducing an additive constant of the type mentioned at the end of §1 so as to keep the point 0 both of the q and p spectrum in the middle of the first probability period. The additive constant varies, therefore with n and is infinite if n is infinite. Passing to the limit in this special way the integral representation is justified provided the integral has a meaning. The passage from the integral to $i(d\psi(q)/dq)$ is justified provided the Fourier expression for

$$\psi(q_m)=(2\pi)^{-1}\int_{-\infty}^{+\infty}\int_{-\infty}^{+\infty}\psi(q)\,\exp\,(i(q-q_m)p)dqdp$$

holds and provided this result may be differentiated with respect to q_m under the integral sign.

Under similar restrictions the operation $C=i(PQ-QP)$ may be shown to be in the limit equivalent to unity. In fact $c_{lm}=ip_{lm}(q_m-q_l)$. The transformed pure case is now

$$F(q_m)\ =\sum c_{lm}\psi(q_l)=(i/2\pi)\int_{-\infty}^{+\infty}\int_{-\infty}^{+\infty}(q_m-q)p\,\exp\,(i(q-q_m)p)dqdp$$

$$=i\left[iq_m\left(\frac{d\psi(q)}{dq}\right)_{q=q_m}-i\left(\frac{d(q\psi(q))}{dq}\right)_{q=q_m}\right]=\psi(q_m)$$

where in addition to the restrictions just mentioned we require that $q_m\psi(q_m)$ should be expressible as a Fourier Integral and that this expression should be differentiable with respect to q_m.

We see, therefore, that (1) is not true in the geometrical sense of Weyl. The differentiability of $\psi(q)$ and $q\psi(q)$ is essential in the above derivation.

UNIVERSITY OF MICHIGAN LIBRARIES

Geometrically, however, there is no reason why $\psi(q)$ should be differentiable, and (1) is, therefore, to be understood only as an operation and not as a matrix, *i.e.*, it is to be understood in the sense that for a pure case represented by a differentiable ψ in the limit of εq, $\varepsilon p = 0$ the operation $i(PQ-QP)$ is equivalent to multiplication by unity. It is also essential that the limit should be approached in such a way as to make the probability periods corresponding to $s=0$, $t=0$ in (3) and (5) fill ultimately the whole finite region of the q and p spectra. Since A and B leave the spectra of p and q undetermined to within an arbitrary additive constant, this can always be arranged and in fact must be arranged just that way for otherwise the finite region of q would have an added restriction since two probability periods would join in the finite region. If they should join at a point q_0 the probability amplitude just to the left of q_0 would always have to be the same as the probability amplitude at an infinite distance to the right of q_0. This would represent a very special condition.

Although the formulation of Weyl's theory is apparently different from that of Dirac, we may note here that the expressions for the result of operating on $\psi(q)$ by Q or by P are practically identical in form for the two. Thus taking Dirac's expressions in the beginning of his §5 in "The Physical Interpretation of Quantum Dynamics" and writing them for one degree of freedom we have

$$\xi(\xi'\alpha') = \int \xi''\delta(\xi'-\xi'')d\xi''(\xi''/\alpha') = \xi'(\xi'/\alpha') \ ;$$

$$\eta(\xi'\alpha') = \int \eta(\xi'\xi'')d\xi''(\xi'')\alpha') = \int (-ih)\delta'(\xi'-\xi'')d\xi''(\xi''/\alpha') = -ih\frac{d(\xi'/\alpha')}{d\xi'}$$

Here $\xi(\xi'\alpha')$, $\eta(\xi'\alpha')$ are according to Dirac matrices written down in a mixed reference system ξ', α'. In Weyl's language they are pure cases obtained respectively by operating on the pure case $\psi=(\xi'/\alpha')$ by the matrices Q and P. The index α is not necessary for Weyl because it is implied in the choice of a definite initial pure case $\psi(q)$. If, for instance, all the pure cases $\psi(q)$ are directed along the principal axes of a matrix H, the Eigenwert spectrum of H supplies the index α by specifying which particular ψ we are considering. We thus identify ξ'' with q, ξ' with q_m. The component along the q_m axis of $Q\psi(q)$ is in Weyl's theory obtained directly as $q_m\psi(q_m)$. However, it may also be written as

$$(Q\psi(q))_m = \int_{-\infty}^{+\infty}\int_{-\infty}^{+\infty}(2\pi)^{-1}q\psi(q)\exp\left(i(q-q_m)p\right)dqdp = q_m\psi(q_m)$$

by Fourier's Integral. Writing *symbolically*

$$\delta(q-q_m) = (2\pi)^{-1}\int_{-\infty}^{+\infty}\exp\left(i(q-q_m)p\right)dp$$

this is exactly the form of Dirac in the expression for $\xi(\xi'\alpha')$ because with this symbolism

$$(Q\psi(q))_m = \int_{-\infty}^{+\infty} q\psi(q)\delta(q-q_m)dq$$

With the same symbolism expression (14) becomes

$$(P\psi(q))_m = -i\int_{-\infty}^{+\infty} \delta'(q-q_m)\psi(q)dq$$

where

$$\delta'(q-q_m) = (2\pi)^{-1}\int_{-\infty}^{+\infty} ip \exp\,(i(q-q_m)p)dp$$

so that δ' is formally the derivative of δ. This expression for $(P\psi(q))_m$ differs from Dirac's only by the factor h as it should, since this h of Dirac is the ordinary $h/2\pi$, and since Weyl's units differ from Dirac's by that factor.

The essential feature of the symbolism employed above in order to make Weyl's theory identical with Dirac's is the order of the integrations over q and p. When our expression for δ is substituted in Dirac's formulas it is always to be understood that the integration over p entering into the expression for δ is to be performed after the integration over q. This particular order is determined by the fact that a Fourier Integral has no meaning for the opposite order of integrations.

DEPARTMENT OF TERRESTRIAL MAGNETISM,
CARNEGIE INSTITUTION OF WASHINGTON,
July, 1928.

UNIVERSITY OF MICHIGAN LIBRARIES

THE SPARK SPECTRUM OF NEON

By A. S. Ganesan

Abstract

A list of lines in the spark spectrum of neon between λ2300 and λ1850 is given. Many of the lines seem to belong to Ne III.

Introduction

THE spark spectrum of neon has been studied recently by several investigators. L. Bloch, E. Bloch and G. Dejardin[1] have tabulated a list of lines in neon at successive stages of ionization. Their method essentially consisted in applying an oscillatory discharge to an electrodeless tube and studying the production of the lines as the potential of the discharge was systematically increased. T. L. de Bruin[2] has succeeded in classifying several lines in the second spectrum of neon (Ne II) into multiplets of the quartet system. The wave-length measurements in these cases extend only to λ2300. Russell, Compton and Boyce[3] have studied the spark spectrum in the extreme ultra-violet by the use of a vacuum spectrograph. They have classified many of the lines into doublet and quartet systems. The presence of terms of even multiplicity in the second spectrum of neon is in conformity with the spectroscopic alternation law. In the present paper the wave-lengths in the spark spectrum of neon in the hitherto uninvestigated region λ2350−λ1850 are given.

Experimental Details

The spectroscope used was a small quartz one made by Bellingham and Stanely. This gave a dispersion of about 10A per millimeter at λ2300, and 5A per millimeter at λ1900. The gas was contained in a vacuum tube of the H-type fitted with aluminum electrodes. The capillary tube was about 10 cm long and 1.5 mm bore. The tube was viewed "end-on" through quartz windows. To the discharge tube were permanently attached the necessary accessories, namely, bulbs of phosphorous pentoxide which removed all traces of water vapor, tubes containing caustic potash to absorb carbon dioxide and charcoal tubes for liquid-air cooling.

The neon gas was commerically obtained in 2-litre cylinders and was found to be fairly pure, though not spectroscopically pure—the chief impurities being hydrogen and the more volatile gases of the atmosphere. The apparatus was exhausted by means of a "Hyvac" rotary pump and the charcoal tubes were strongly heated during the process of exhaustion. The

[1] L. Bloch, E. Bloch and G. Dejardin, Journal de Physique **7**, 129, (1926).
[2] T. L. de Bruin, Zeits. f. Physik **46**, 856 (1928).
[3] Russell, Compton and Boyce, Proc. Nat. Acad. Sci. **14**, 281 (1928).

gas was admitted into the tube in small quantities. Nitrogen and the more volatile impurities were removed by cooling the charcoal tubes to the temperature of liquid air. The last traces of hydrogen were removed by a palladium tube attached to the apparatus, and which was electrically heated. By repeated exhaustion and passing a heavy and continuous current at intervals, and by the above precautions to remove impurities, the

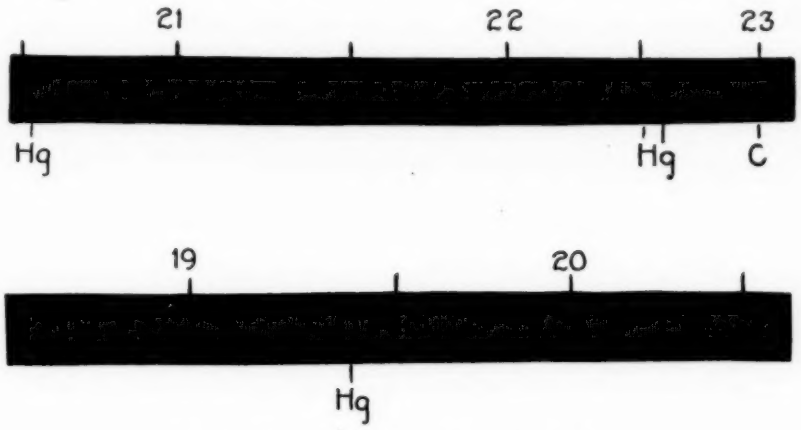

Fig. 1. Photograph of spark spectrum of neon.

tube was filled with pure gas. Yet in all plates the strong and persistent lines due to mercury and carbon always made their appearance; also the lines due to silicon at various stages of ionization. But these lines due to impurities could easily be identified and eliminated, and their presence afforded a check on the accuracy of the measurement and an estimation of the probable error. The silver spark was used as comparison. The plates were

TABLE I. *Wave-lengths in spectrum of neon.*

Int.	λ, I.A.	ν, vac.	Int.	λ, I.A.	ν, vac.	Int.	λ, I.A.	ν, vac.
0	2279.12	43863.0	3	2180.97	45836.8	1	2078.91	48086.7
5	2273.68	43967.9	1	2178.69	45884.7	3	2065.20	48405.9
2	2266.14	44114.2	2	2177.75	45904.5	0?	2062.7	48464.6
2	2264.94	44137.6	1	2176.70	45926.7	0	2061.9	48483.4
2n	2263.22	44171.1	6	2163.80	46200.4	0	2057.93	48576.9
1	2262.23	44190.5	5	2161.14	46257.3	1	2025.40	49357.0
1	2216.75	45097.0	5	2159.48	46292.8	0	1988.37	50276.3
3	2216.05	45111.2	0?	2153.14	46429.1	2	1973.06	50666.0
3	2213.75	45158.1	0	2151.68	46460.6	0?	1956.8	51087.0
3	2211.88	45196.3	1	2151.23	46470.4	0?	1948.9	51293.9
1	2211.08	45212.6	2	2150.65	46482.9	1	1945.25	51390.4
3	2209.39	45247.2	2	2149.94	46498.2	1	1944.74	51403.8
0n	2208.3	45269.5	1	2138.59	46745.0	1	1938.07	51580.7
2	2207.32	45289.6	0	2099.21	47621.8	2	1929.27	51816.2
0	2206.5	45306.5	1	2096.11	47692.2	0	1928.10	51847.6
2	2205.05	45336.3	1	2095.44	47707.4	3	1915.33	52193.1
0?	2204.9	45339.3	0	2089.38	47845.8	1	1906.74	52428.3
0?	2202.2	45394.9	0?	2086.82	47904.5	0	1879.49	53188.1
1	2182.28	45809.2	0	2085.43	47936.4	1	1868.47	53502.0

UNIVERSITY OF MICHIGAN LIBRARIES

measured with a photo-measuring micrometer reading to a thousandth of a millimeter.

Table I gives the list of wave-lengths expressed in International Angstroms. In the third column are given the corresponding wave-numbers reduced to vacuum. The estimated error in the wave-lengths is 0.05A.

Many of the lines in the spectrum seem to belong to Ne III. The same potential that excites the lines of Ne II in the near ultra-violet is not sufficient to being out these lines. Moreover the unmistakable presence of triplets and isolated single lines seem to show that the terms are of odd multiplicity. The most prominent triplet is the one at λ2163.

	λ	ν	Δν
(6)	2163.80	46200.4	56.9
(5)	2161.14	46257.3	35.5
(5)	2159.48	46292.8	

The separations 56.9 and 35.5 are approximately in the ratio 3:2.

The group of six lines at λ2216 is very striking. The wave-numbers and separations of this group are given below:

	ν	Δν		ν	Δν
(3)	45111.2	46.9	(3)	45247.2	42.4
(3)	45158.1	38.2	(2)	45289.6	46.7
(3)	45196.3	50.9	(2)	45336.3	

Interfused with this multiplet is a fainter group of four lines

	ν	Δν
(1)	45097.0	115.6
(1)	45212.6	56.9
(0)	45269.5	37.0
(0)	45306.5	

It may be noted that in this group the last two separations are approximately the same as the triplet separations mentioned above.

Another regularity that may be noted is the constant separation in the following pairs of lines:

(1)	49357.0	2836.1	(3)	52193.1
	(1309.0)			(1308.9)
(2)	50666.0	2836.0	(1)	53502.0

The above work was done in the Spectroscopy laboratory of the Imperial College under Professor A. Fowler, to whom the author wishes to express his thanks.

SPECTROSCOPY LABORATORY,
IMPERIAL COLLEGE, LONDON.
June, 1928.

THE 29 AND 30—ELECTRON-SYSTEM SPECTRA OF ARSENIC AND SELENIUM

By R. A. Sawyer and C. J. Humphreys

Abstract

New vacuum-spark data in the extreme ultra-violet have been obtained for arsenic and selenium. By aid of previous classifications in the 29 and 30—electron-system spectra of copper, zinc, gallium and germanium, it has been possible by extrapolation of the Moseley diagram, the irregular doublet law, screening constant data and the triplet interval ratios to predict the location of and to identify the lines arising from transitions between the lowest levels in the spectra of As IV, As V, Se V and Se VI. The *ionization potential* of As V is determined as 62.4 volts, that of Se VI as 81.4 volts.

The $(4P^2)\ ^3P$ separation of the 30—electron-system spectra is observed to show a rapid increase with respect to the separation both of $(4s\ 4p)^3P$ term and $(4p)^2P$ term of the next ion. The theoretical significance of this effect, which is observed here for the first time, and which does not appear in the corresponding iso-electronic spectra of the lighter elements, is discussed. The effect is believed to be due to a change of coupling of the quantum vectors with increasing nuclear charge.

I. Apparatus and Procedure

THE vacuum-spark spectra of arsenic and selenium have been photographed with a one-meter vacuum spectrograph identical with that described by Sawyer.[1] A glass spark-box, similar to that described by Sawyer and Smith[2] was provided with a ground bearing fitting the conical end of the side-arm which carried the spectrograph slit. The only important modification of the spark box was the replacing with brass cones of the glass cones which carried the electrodes in the previous investigation. This gives a spark-box which is simple, convenient and almost entirely free from insulation or vacuum difficulties. The spark-box and spectrograph were evacuated separately—the spark-box by a two-stage glass Kurth pump, the spectrograph by a large three-stage Leybold steel pump. The vacuum attained was so good that discharge fog on the spectrograms was completely eliminated.

The arsenic was used in the form of pure metallic arsenic—small pieces being held in the clamps in which the brass cones mentioned above terminated. Pure selenium electrodes were used similarly but because of the high resistivity of selenium better results were obtained by melting selenium into a hole in the end of an aluminum electrode. In some cases one carbon electrode was used to give the carbon lines with greater intensity than that with which they normally appear on all vacuum spark plates. Hydrogen 1215.68 and the carbon lines were used as standards, together with, in the case of aluminum electrodes, the aluminum and oxygen lines.

[1] Sawyer, J.O.S.A. **15**, 305 (1927).

[2] Sawyer and Smith, J.O.S.A. **14**, 287 (1927).

UNIVERSITY OF MICHIGAN LIBRARIES

The spectrograph allows a range of nearly 3000A to be photographed at once and in this work the range 0−2900A was always on the plates. The actual spectra extended to somewhat below 400A. Thus the stronger lines below 1450A could be measured in the second order and those below 950A in the third. As few lines of any intensity were found in either spectrum above 1500A practically all lines were measured in two or three orders. The definition of the grating was exceedingly good and the lines could be measured closely. It is believed an absolute accuracy of at least 0.05A and a relative accuracy in multiplet separations of 0.03A has been attained.

II. The 29-Electron-System Spectra

The 29-electron-system spectra of gallium and germanium, Ga III and Ge IV, were first analyzed by Carroll[3] and remeasured and extended slightly by Lang.[4] In the present work the corresponding spectra of arsenic and selenium, As V and Se VI, have been identified by the aid of the regular and irregular doublet laws and the Moseley diagram. The classified lines in these spectra together with the approximate term values determined are given in Table I. In most cases there was no ambiguity in the identification of the

Table I. *29-electron-system spectra*

Comb.	λ	*I*	ν	Δν	Terms	
			As V			
$(4d)^2D_3-(4f)^2F_{3,4}$	1056.71	5	94633			
$(4d)^2D_2-(4f)^2F_3$	1051.64	4	95090	457		
					$(4s)^2S_1$	505136
$(4s)^2S_1-(4p)^2P_1$	1029.50	10	97135		$(5s)^2S_1$	241540
$(4s)^2S_1-(4p)^2P_2$	987.69	10	101246	4111	$(4p)^2P_1$	408001
					$(4p)^2P_2$	403891
$(4p)^2P_2-(4d)^2D_2$	737.18	5	135652		$(4d)^2D_2$	268239
$(4p)^2P_2-(4d)^2D_3$	734.77	8	136097	445	$(4d)^2D_3$	267794
$(4p)^2P_1-(4d)^2D_2$	715.50	7	139762	4110	$(4f)^2F_{3,4}$	173149
$(4p)^2P_2-(5s)^2S_1$	615.95	4	162351			
$(4p)^2P_1-(5s)^2S_1$	600.74	3	166461	4110		
			Se VI			
$(4s)^2S_1-(4p)^2P_1$	886.82	5	112762			
$(4s)^2S_1-(4p)^2P_2$	844.15	5	118462	5700	$(4s)^2S_1$	658994
					$(5s)^2S_1$	325400
$(4p)^2P_2-(4d)^2D_2$	608.39	3	164368		$(4p)^2P_1$	546232
$(4p)^2P_2-(4d)^2D_3$	605.89	4	165047	679	$(4p)^2P_2$	540532
$(4p)^2P_1-(4d)^2D_2$	588.01	4	170065	5697	$(4d)^2D_2$	376164
					$(4d)^2D_3$	375485
$(4p)^2P_2-(5s)^2S_1$	464.83	2	215132			
$(4p)^2P_1-(5s)^2S_1$	452.83	2	220833	5701		

lines, the lines chosen being the only choices in the region predicted by the application of the x-ray laws. The $\Delta\nu$ values for the $(4p)^2P$ doublet separations in each spectrum agree among themselves well within our assumed limit of error. The two $\Delta\nu$ separations for $(4d)^2D$ in As V show a disagreement

[3] Carroll, Phil. Trans. **225**, 357 (1925).
[4] Lang, Phys. Rev. **30**, 762 (1927).

which is certainly larger than the probable error of measurement. There is however no other choice for the DF combination on our plates and we have therefore included these lines tentatively. In the selenium spectrum two lines are found (λλ814.77, 898.71; $\nu\nu$122734, 123654) which have the correct separation and occur in the expected position. These lines however are definitely a part of the Se V spectrum and so are not here classified. The $(4d)^2D-(4f)^2F$ pair of Se V is either not excited in our source or there is an error in the selection of this doublet in one of the earlier spectra which makes the prediction of the expected location of the doublet incorrect. It is well known that the irregular doublet law does not hold so exactly in the case of this combination, doubtless, as has been pointed out by Bowen, and Millikan[5] because of the change of the $(4d)$ orbit to a penetrating orbit with increasing nuclear charge.

The application of the regular and irregular doublet laws to these spectra is shown in Table II and constitutes of course the chief evidence for the

TABLE II. *Application of the x-ray laws to 29-electron spectra.*

Term	Element	Regular doublet law $\Delta\nu$	σ	$\Delta\sigma_1$	$\Delta\sigma_2$
	Cu I	248	20.19		
	Zn II	873	18.23	1.96	
$(3d^{10}4p)^2P$	Ga III	1718	17.06	1.17	0.79
	Ge IV	2790	16.27	0.79	0.38
	As V	4110	15.67	0.60	0.19
	Se VI	5700	15.19	0.48	0.12
					1.51
	Cu I	6.4	24.47	2.07	−0.66
	Zn II	40.8	22.40	0.56	0.45
$(3d^{10}4d)^2D$	Ga III	107	21.84	1.22	0.38
	Ge IV	255	20.62	0.77	
	As V	454	19.85	0.39	
	Se VI	679	19.46		

Comb.	Element	Irregular doublet law ν	$\Delta\nu_1$	$\Delta\nu_2$
	Cu I	30535		
	Zn II	48483	17949	1264
$(4s)^2S_1-(4p)^2P_1$	Ga III	65167	16684	544
	Ge IV	81307	16140	312
	As V	97135	15828	201
	Se VI	112762	15627	
	Cu I	19150		
	Zn II	47554	28404	1235
$(4p)^2P_2-(4d)^2D_2$	Ga III	77193	29639	341
	Ge IV	106491	29298	137
	As V	135652	29161	445
	Se VI	164368	28716	
	Cu I	5484		
	Zn II	20303	14819	6124
$(4d)^2D_3-(4f)^2F_3$	Ga III	41246	20943	4451
	Ge IV	66640	25394	2594
	As V	92633	27988	

[5] Bowen and Millikan, Phys. Rev. **28**, 923 (1926).

correctness of the classifications. The screening constants are computed from the usual formula

$$\Delta\nu=\frac{\alpha^2R(Z-\sigma)^4}{n^3l(l+1)}$$

The regular decrease of the second difference of the screening constant for the $(4p)^2P$ terms is notable. There is an irregularity in the second differences of the screening constant for the $(4d)^2D$ terms. An even greater irregularity occurs in the case of the 47-electron-system (silver-like) spectra classified by Lang[6] and there may be some perturbing effect in these terms. The second differences of wave-number also show an irregularity in the application of the irregular doublet law to $(4p)^2P_2-(4d)^2D_2$. All these irregularities may be connected with the change of the $4d$ orbit to a penetrating orbit.

Term values in these spectra may be obtained either by applying a Rydberg formula to the two S terms or by extrapolating the $(\nu/R)^{1/2}$ values for the preceding spectra. The result in either case is nearly the same. The values have been chosen so the $(\nu/R)^{1/2}$ values for $(4s)^2S$ and $(4p)^2P$ will form a smooth sequence with those of the preceding spectra. Table III

TABLE III. *Values of $(\nu/R)^{1/2}$ for 29-electron spectra together with their differences.*

	Cu I	Zu II	Ga III	Ge IV	As V	Se VI
$(4s)^2S_1$	0.7535	1.1490	1.5021	1.8300	2.1450	2.4506
Δ_1		0.3955	0.3531	0.3279	0.3150	0.3056
Δ_2		0.0424	0.0252	0.0129	0.0094	
$(4p)^2P_2$	0.5359	0.9311	1.2840	1.6103	1.9185	2.2194
Δ_1		0.3952	0.3529	0.3263	0.3082	0.3009
Δ_2		0.0423	0.0266	0.0181	0.0073	
$(4d)^2D_3$	0.3357	0.6609	0.9716	1.2730	1.5623	1.8498
Δ_1		0.3252	0.3107	0.3014	0.2893	0.2875
Δ_2		0.0145	0.0093	0.0121	0.0018	
$(5s)^2S_1$	0.4180	0.7172	0.9877	1.2400	1.4836	1.7200
Δ_1		0.2992	0.2705	0.2523	0.2436	0.2364
Δ_2		0.0287	0.0182	0.0087	0.0072	

gives the values of $(\nu/R)^{1/2}$ for the 29-electron spectra together with their first and second differences and shows how smoothly the so-called Moseley diagram lines for these spectra run. The actual term values cannot be in error by more than 1000 or 2000 cm^{-1}. The values of the $(4s)^2S$ term correspond to an ionization potential of 62.4 volts for As V and of 81.4 volts for Se VI.

III. THE 30-ELECTRON-SYSTEM SPECTRA

The 30-electron-system spectra of gallium and germanium have been analyzed by Lang[4] who has given several of the triplets arising from the

[6] Lang. Proc. Nat. Acad. Sci. **13**, 341 (1927).

lowest levels and the singlet resonance lines in each spectrum. The homologous lines in the spectra of As IV and Se V have been identified in our data by the aid of extrapolation of the x-ray laws and the triplet intervals. The classified lines in the two spectra and approximate term values are given in Table IV. The $\Delta\nu$ values for the various intervals will all be seen to agree well within the limits of error. The *PD* and *PS* triplets are especially unmistakable in arsenic where these groups stand out by themselves.

TABLE IV. *30-electron-system spectra.*

Comb.	λ	*I*	ν		Δν	Terms	
			As IV				
$(4s4p)^3P_2-(4p^2)^3P_1$	980.58	8	101981		2526	$(4s4p)^3P_0$	343400
$(4s4p)^3P_1-(4p^2)^3P_0$	971.13	8	102973			$(4s4p)^3P_1$	342250
$(4s4p)^3P_1-(4p^2)^3P_1$	956.87	8	104507		1151	$(4s4p)^3P_2$	339720
$(4s4p)^3P_2-(4p^2)^3P_2$	953.25	8	104904				
$(4s4p)^3P_0-(4p^2)^3P_1$	946.45	8	105658		2531		
$(4s4p)^3P_1-(4p^2)^3P_2$	930.80	8	107435				
$(4s^2)^1S_0-(4s4p)^1P_1$	892.68	10	112022				
$(4s4p)^3P_2-(4s4d)^3D_1$	762.75	2	131105—			$(4s4d)^3D_1$	208615
$(4s4p)^3P_2-(4s4d)^3D_2$	761.99	4	131235—	130	2526	$(4s4d)^3D_2$	208485
$(4s4p)^3P_2-(4s4d)^3D_3$	760.80	5	131441—	206		$(4s4d)^3D_3$	208279
$(4s4p)^3P_1-(4s4d)^3D_1$	748.33	5	133631—		2532		
$(4s4p)^3P_1-(4s4d)^3D_2$	747.57	5	133767—	136			
$(4s4p)^3P_0-(4s4d)^3D_1$	741.93	5	134784		1153		
$(4s4p)^3P_2-(4s5s)^3S_1$	711.07	7	140633			$(4s5s)^3S_1$	199087
$(4s4p)^3P_1-(4s5s)^3S_1$	698.50	6	143164		2531		
$(4s4p)^3P_0-(4s5s)^3S_1$	692.94	4	144313		1149		
			Se V				
$(4s4p)^3P_2-(4p^2)^3P_1$	839.49	8	119120		3614	$(4s4p)^3P_0$	500025
$(4s4p)^3P_1-(4p^2)^3P_0$	830.30	6	120438			$(4s4p)^3P_1$	498430
$(4s4p)^3P_1-(4p^2)^3P_1$	814.77	6	122734			$(4s4p)^3P_2$	494820
$(4s4p)^3P_2-(4p^2)^3P_2$	808.71	7	123654		1596		
$(4s4p)^3P_0-(4p^2)^3P_1$	804.31	5	124330		3608		
$(4s4p)^3P_1-(4p^2)^3P_2$	785.78	5	127262				
$(4s^2)^1S_0-(4s4p)^1P_1$	759.07	8	131740				
$(4s4p)^3P_2-(4s4d)^3D_1$	615.10	1	162575—	212		$(4s4d)^3D_1$	332247
$(4s4p)^3P_2-(4s4d)^3D_2$	614.30	4	162787—	335	3613	$(4s4d)^3D_2$	332033
$(4s4p)^3P_2-(4s4d)^3D_3$	613.04	5	163122—		3616	$(4s4d)^3D_3$	331698
$(4s4p)^3P_1-(4s4d)^3D_1$	601.73	4	166188—	215			
$(4s4p)^3P_1-(4s4d)^3D_2$	600.95	4	166403—		1594		
$(4s4p)^3P_0-(4s4d)^3D_1$	596.01	5	167782				
$(4s4p)^3P_2-(4s5s)^3S_1$	519.58	4	192463		3608	$(4s5s)^3S_1$	302355
$(4s4p)^3P_1-(4s5s)^3S_1$	510.02	3	196071		1593		
$(4s4p)^3P_0-(4s5s)^3S_1$	505.91	2	197664				

The regular and irregular doublet laws are obeyed by the triplets in these 30-electron spectra in an unimpeachable manner as will be seen from Table V. In all cases the smooth run of the second differences is unbroken.

The only choice in these triplet spectra which presents any ambiguity is that of the line $(4s4p)^3P_1-(4p^2)^3P_0$ since $(4p^2)^3P_0$ has only this one combination. The identification was made from the two or three possibilities

TABLE V. *Application of the x-ray laws to 30-electron spectra.*

Term	Element	Regular doublet law $\Delta\nu$	σ	Δ_1	Δ_2
	Zn I	579.2	19.38		
				1.58	
$(4s4p)^3P$	Ga II	1382	17.80		0.63
				0.95	
	Ge III	2403	16.85		0.25
				0.70	
	As IV	3677	16.15		0.16
				0.54	
	Se V	5210	15.61		
	Zn I	7.95	25.22		
				2.31	
$(4s4d)^3D$	Ga II	65	22.91		0.98
				1.33	
	Ge III	179	21.58		0.55
				0.78	
	As IV	336	20.80		0.18
				0.60	
	Se V	550	20.20		

Comb.	Irregular doublet law Element	ν	$\Delta\nu$	$\Delta_2\nu$
	Zn I	30267		
			35732	
$(4s4p)^3P_1-(4s4d)^3D_1$	Ga II	65999		1394
			34338	
	Ge III	100337		1044
			33294	
	As IV	133631		737
			32557	
	Se V	166188		
	Zn I	47890		
			19520	
$(4s4p)^3P_1-(4p^2)^3P_1$	Ga II	67410		780
			18740	
	Ge III	86150		383
			18357	
	As IV	104507		130
			18227	
	Se V	122734		

by a consideration of the ratio of $(4p^2)^3P_0-(4p^2)^3P_1$ to $(4p^2)^3P_1-(4p^2)^3P_2$ in these spectra and the choice was made so that this ratio should show a smooth progression with nuclear charge. This progression is seen in the fifth column of Table VI and is believed to be a sufficient justification for the

TABLE VI. *Triplet intervals*

Element	$\Delta P^0_{01}/\Delta P^0_{02}$	$\Delta D_{12}/\Delta D_{13}$	$\Delta P^0_{12}/\Delta P_{12}$	$\Delta P_{01}/\Delta P_{02}$
Zn I	0.328	0.428	———	———
Ga II	0.324	0.354	1.023	0.365
Ge III	0.318	0.402	0.950	0.355
As IV	0.313	0.389	0.864	0.344
Se V	0.307	0.391	0.796	0.336

choice made. No other choice would give a reasonable progression of these intervals. The $^3P^0P$ group[7] in Zn I was first identified by Sawyer and Beese[8] who found four lines corresponding to the combinations of $(4s4p)^3P_{0,1,2}$ with $(4p^2)^3P_0$ and $(4p^2)^3P_1$. In the position of the combinations with $(4p^2)^3P_2$

[7] In accordance with a new system of notation recently suggested by a committee of spectroscopists we replace PP' by P^0P. According to this system terms arising from configurations of electrons, for which the sum of the l values is odd, are called odd terms and designated by a superscript 0. If the sum of the l values of the electrons is even, the term is said to be even. Thus $(sp)^3P$ is odd whereas $(p^2)^3P$ is even.

[8] Sawyer and Beese, Nature **116**, p. 936 (1925).

are two diffuse lines whose reversal in the heavy arc and diffuse character led to their classification as $(4s4p)^3P_2-(4p^2)^1D_2$ and $(4s4p)^3P_1-(4p^2)^1D_2$.[9] If in spite of their appearance these two lines are classified as the combinations with $(4p^2)^3P_2$ we obtain as the ratio of $(4p^2)^3P_0-(4p^2)^3P_1$ to $(4p^2)^3P_1-(4p^2)^3P_2$, the value of 0.355. This seems to depart from the smooth progression of this ratio by an amount larger than can be accounted for by the accuracy of measurement. We are still forced to assume that the combinations with $(4p^2)^3P_2$ are masked by this diffuse pair.

Table VI also shows the perfectly smooth progression of the $(4s4p)^3P$ interval ratio (column one) and a slight irregularity in the $(4s4d)^3D$ interval ratio (column two) which may however be due to a relatively greater inaccuracy of measurement of the D intervals which are about one-tenth those of the P. Column four of Table V shows a very interesting effect pointed out here for the first time; in this type of spectra viz, the steady and rapid increase of the $(4p^2)^3P$ separation with respect to the $(4s4p)^3P$ separation. The theoretical importance of this phenomenon will be discussed in a later section of this paper.

TABLE VII. *Values of $(\nu/R)^{1/2}$ for 30-electron spectra together with their differences.*

	Zn I	Ga II	Ge III	As IV	Se V
$(4s4p)^3P$	0.6178	1.0100	1.3895	1.7595	2.1235
Δ_1		0.3922	0.3795	0.3700	0.3640
Δ_2		0.0127	0.0095	0.0060	
$(4s5s)^3S$	0.4487	0.7255	1.0355	1.3469	1.6599
Δ_1		0.2768	0.3100	0.3114	0.3130
Δ_2		0.0332	0.0014	0.0026	
$(4s4d)^3D$	0.3440	0.6532	1.0152	1.3777	1.7386
Δ_1		0.3092	0.3620	0.3625	0.3609
Δ_2		0.0528	0.0005	−0.0016	

The 30-electron-system spectra should have a singlet system as well as a triplet, but the singlets are much harder to locate because of the lack of characteristic separations and, in the vacuum spark, of higher series members. The approximate location of the $(4s^2)^1S-(4s4p)^1P$ line may however be predicted by the rule first given by Sawyer and Beese.[7] and discussed more fully by Sawyer.[8] This prediction may be checked by the application of the irregular doublet law. The classifications of the line $(4s^2)^1S-(4s4p)^1P$ given in Table IV were obtained in this way. The choices made in each case were practically the only possibilities. The application of the irregular doublet law and of the rule given by Sawyer and Beese is shown in Table VIII.

The triplet term values in the spectra of As IV and Se V could be determined only by extrapolation of the Moseley diagrams since no second term members were found. The term values so determined are given in Table IV

[9] Sawyer, J.O.S.A. **13**, 431 (1926).

TABLE VIII. *Application of the rule of Sawyer and Beese and of the irregular doublet law in the location of singlet combinations.*

	^1SP	$^3P^0{}_1P_1$	^2SP	$^1SP-{}^2SP$
Zn	46744	47900	48480	− 1740
Ga	70700	67400	65170	+ 5530
Ge	91876	86150	81300	+10580
As	112022	104500	97130	+14900
Se	131740	122730	112760	+19000

and Table VIII gives the values of $(\nu/R)^{1/2}$, for the terms of the 30-electron sequence showing the first and second differences of the values.

Dr. R. J. Lang has kindly informed us that the lines which we have classified as As IV and As V appear faintly or not at all on his plates taken with a less violent vacuum spark in the course of his unpublished work on the As III spectrum. This is good evidence that the lines in question belong to a higher stage of ionization than As III. The location of As VI lines may be predicted from the data given by Mack, Laporte and Lang[10] but they do not appear on our plates. It may thus be inferred that our classified lines belong to the As IV and As V spectra without doubt.

IV. THE $(4p^2)^3P$ SEPARATIONS

The observed relative increase in the $(4p^2)^3P$ separation with respect to the $(4s4p)^3P$ separation has been mentioned. The former also shows a similar increase with respect to the $(4p)^2P$ separation in the spectrum of the ion of next higher degree. These features require some special consideration. Table IX contains a complete list of these separations in the iso-

TABLE IX. *Multiplet separations together with the relative separation of $(p^2)^3P$ and ^2P*

	Zn	Ga	Ge	As	Se
$(p)\Delta^3P$	874	1718	2790	4110	5700
$(sp)\Delta^3P$	579	1382	2403	3677	5210
$(p^2)\Delta^3P$		1437	2684	4460	6824
$(p^2)\Delta^3P/(p)\Delta^2P$		0.8365	0.9620	1.0852	1.1972

electronic spectra we are considering with the exception of $(4p^2)^3P$ in Zn I.[11] The $(4s4p)^3P$ separations are observed to be smaller in all cases than the corresponding $(4p)^2P$ or $(4p^2)^3P$ separations, and for higher ionizations become nearly equal to $(4p)^2P$ which, as we shall point out, is to be expected. The $(4p^2)^3P$ separations range from somewhat smaller to considerably larger than $(4p)^2P$ as we proceed through the series of elements. In the case of the pure Russell-Saunders coupling both the $(4p^2)^3P$ and the $(4s4p)^3P$ should be slightly smaller than $(4p)^2P$ according to a recent theore-

[10] Mack, Laporte and Lang, Phys. Rev. **31**, 748 (1928).

[11] This separation is omitted because, as mentioned above, the complete measurement of the P^0P group was impossible owing to the presence of a pair of diffuse lines which masked a part of the group.

tical investigation by Goudsmit and Humphreys.[12] Although the theory predicts that to a first approximation these separations should all be the same, the screening effect of the second valence electron would be expected to reduce the triplet separations with respect to the doublet.

We can show that the total $(4s4p)^3P$ separation will not be thus affected As is known from other spectra higher nuclear charge is favorable to a change of coupling. The (sp) configuration with Russell-Saunders coupling gives ^1P and ^3P terms. When we go over to the limiting (jj) coupling we still have four levels characterized by the same inner quantum numbers but two of them having values 0, 1, lie relatively close together and are separated by the $(4p)^2P$ interval of the next ion from two others of values, 2 and 1. Fig. 1 will make this arrangement clear. Without going into the rules of correlation at this point, it may be stated the levels of corresponding j values in the Russell-Saunders case go over to the new levels in such a way that the connecting lines do not cross. Consequently, while the triplet intervals may change, we no not expect achange in the total $(4s4p)^3P$ separation with respect to $(4p)^2P$ but rather expect the former to approach the latter as a limit.

Fig. 1.

The increase in the relative $(p^2)^3P$ separations has been observed for the first time in the spectra we have investigated. Spectra of lighter elements, found in the first two rows of the periodic table and studied by Millikan and Bowen[13], do not show this effect. The P^0P groups are quite symmetrical showing that the $(sp)^3P$ and $(p^2)^3P$ separations are the same. They are also somewhat smaller than the corresponding $(p)^2P$ separation of the next ion. These features are of course to be expected since, as we have pointed out, any departure from the Russell-Saunders coupling should occur only with relatively high nuclear charge.

Although a change of coupling does not affect the total $(4s4p)^3P$ separation, the results are quite different for $(4p^2)^3P$. The correlation of levels must be considered in detail in order to explain the observed features of the spectra. The ^1S, ^1D, and ^3P multiplets no longer appear in the case of the limiting (jj) coupling, but we expect instead the following arrangement: a lowest level characterized by a j value 0; above that, at a distance equal to the doublet of the ion, two relatively close levels, of j values 1 and 2; and, at again the same distance higher, two levels with j values 2 and 0. The lowest levels of lead seem to show a configuration approximating this ideal arrangement.

The rearrangement of levels in changing over to another coupling is quite analogous to what happens in going to series limits in complicated spectra. Consequently it would seem promising to try Hund's method, for the correlation of series limits to our problem of change of coupling.

[12] S Goudsmit and C. J. Humphreys. Multiplet separations. Phys. Rev. **31**, 960 (1928).

[13] I. S. Bowen and R. A. Millikan, PP' groups in atoms of the same electronic structure, Phys. Rev. **26**, 150 (1925).

But we arrive by this method at very strange results. In order to use Hund's scheme we must first consider the result of applying a weak magnetic field. The remarkable result is that a part of the magnetic levels of $(4p^2)^3P_2$ will go to one and the other part to the other of the two levels having j equal to 2, occurring in the extreme case of the (jj) coupling. A similar behavior is predicted for the $^1D_2$ levels. As we cannot expect the levels to split up when we gradually change the coupling, we must assume that the two levels, having j equal to 2, cross over and interchange their magnetic levels at the point of intersection. The point where the levels intersect might be considered as a certain type of degeneration where either coupling is equally probable. This seems to be the most satisfactory explanation of the increase of the $(4p^2)^3P$ separations. Fig. 2 illustrates the scheme of correlation. It is assumed in these spectra that the point of intersection has not yet been reached.[14]

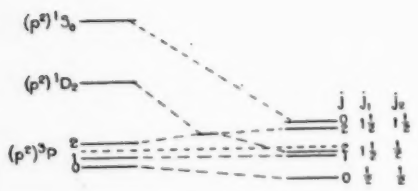

Fig. 2.

The authors take pleasure in expressing indebtedness to Dr. S. Goudsmit for valuable suggestions and discussions regarding the theoretical interpretation of the $(p^2)^3P$ separations.

DEPARTMENT OF PHYSICS
UNIVERSITY OF MICHIGAN
June 2, 1928.

[14] The explanation given above of the remarkable increase of the $(4p^2)^3P$ separation with respect to the doublet of the next ion is necessarily based on the applicability of the rules given by Hund. According to Hund's reasoning, near the series limit the emitting electron is so loosely coupled with the other electrons, that its influence may be neglected. Hund derives his rules, using this assumption, by a consideration of the magnetic energy in an outer field. The magnetic energy is however of the same order of magnitude for each electron, independent of strong or weak interaction between electrons. In other words, the magnetic behaviour of the levels near the series limit is not at all like that of the state of the ion, in which one electron is completely removed. Such considerations lead to some uncertainty as to the applicability of Hund's rules, and may possibly affect the explanation given here. Quite recently Shenstone has shown, Nature **121**, 619 (1928), that in certain cases spectroscopic data are in disagreement with the results of these rules, it being observed that the levels converge to other series limits than those predicted by Hund.

THE INTENSITIES OF THE LINES IN THE SPECTRUM OF MERCURY

By E. O. Hulburt

Abstract

Number of quanta emitted per atom.—The total radiation, measured with a thermocouple, in the spectral region 6000 to 2300A from a small quartz mercury lamp of known size filled with mercury vapor at a known pressure was 1.85×10^{-10} ergs per atom per sec. From this and the intensities of the lines it came out that each atom on the average emitted each second 11.4, 8.9, 5.0, 2.3, etc., quanta of yellow, green, blue, violet, etc., light, respectively.

The intensities of the lines.—The intensities of twenty-four lines of the spectrum were measured with a quartz spectrograph, a thermocouple and a photoelectric cell, all calibrated, and in some cases with a photographic densitometer. Plotting the logarithm of the intensity against the frequency for the lines of a series gave roughly straight lines of about the same slope for the sharp series ($2^3P_n - m^3S_1$) and for the diffuse series ($2^3P_n - m^3D_{123}$). The temperatures of the excited atoms derived from the slopes were 3900° and 2600° Kelvin for the sharp and diffuse series, respectively.

THE intensities of twenty-four lines of the mercury spectrum in the region λ6000 to 2300A have been measured in order to find the intensity relationship among the lines of a series. Earlier measurements[1] were not sufficiently extensive for this purpose. The present experiments have led to the conclusion that the distribution of energy among the lines was as if the temperatures of the excited atoms were several thousand degrees.

A quartz mercury lamp, Fig. 1, was filled with mercury and maintained at a pressure of 1.3 atmospheres. Current was introduced by means of the electrodes *A* and *D*. The section *BC*, 4.5 cm in length and of internal diameter 0.4 cm was heated by a flame or a hot wire until the mercury vaporized and

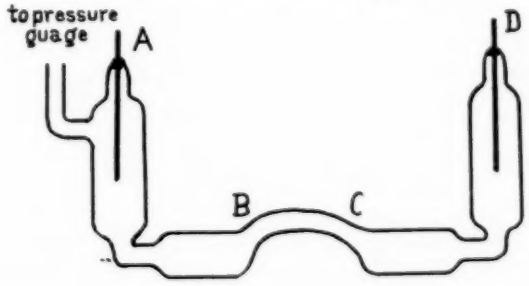

Fig. 1. Quartz mercury lamp.

the arc started. Once started, the heating element was removed and the arc burned steadily and brightly. With 5 amperes direct current and 130 volts in the lamp the surface brightness was 500 times or more that of the "Lab Arc."

[1] See Harrison and Forbes, Journ. Opt. Soc. of Amer. **10**, 1 (1925), and references *infra*.

The number of quanta emitted per atom. The energy radiated from the mercury lamp was measured with a thermopile and galvanometer which had been calibrated with a tungsten lamp in a manner described in a former paper.[2] A galvanometer deflection of 1 mm meant an energy flux of 9.7 erg cm^{-2} falling on the thermopile. By means of a diaphragm with a hole in it the radiation from a section of the mercury arc 4 mm in length was allowed to fall upon the thermopile, which was 240 cm away and in a box with a quartz window to protect it from air currents. The galvanometer deflection was 80 mm when the pressure in the arc was 1.3 atmospheres and the power was 650 watts (5 amperes and 130 volts). By the use of calibrated absorbing screens it was found that 0.275 of the energy radiated from the arc and received by the thermopile with the quartz window was in the spectral region 2300 to 6500A. Assuming that the 4 mm section of the mercury lamp was a point source the total energy in this spectral region radiated in all directions from the section of the lamp was

$$4\pi\times240^2\times80\times9.7\times0.275=1.54\times10^8 \text{ erg sec}^{-1}.$$

Taking the temperature of the mercury vapor to be 546° Kelvin the number of atoms in the lamp section was 8.33×10^{17}. Therefore the energy in the spectral region 2300 to 6500A radiated per atom per second was $1.54\times10^8 \div 8.33\times10^{17}=1.85\times10^{-10}$ erg. When the pressure was increased to 2, 2.5 and 3.5 atmospheres, maintaining the power always at the constant value 650 watts, the ergs radiated per atom per sec. were 1.8, 1.6 and 1.3×10^{-10}, respectively (assuming the temperature to be 546° Kelvin at all times). Thus the energy radiated per atom was roughly constant as the pressure was increased over a small range, other factors remaining constant, and the energy radiated from the section of the lamp increased linearly with the pressure.

Since the relative intensities of the lines in the spectrum from 2500 to 6500A were known (as described in later paragraphs) the energy 1.85×10^{-10} erg sec^{-1} $atom^{-1}$ may be divided among the various spectrum lines according to their intensities in order to determine the number of quanta emitted per atom per second. It came out that on the average each atom emitted each second 11.4 quanta of yellow light (5790 and 5770A), 8.9 quanta of green light (5461A), 5.0 quanta of blue light (4358A), 2.3 quanta of violet light (4077 and 4047A), 6.8 quanta in the group of ultra-violet line at 3660A, etc. It may be recalled that the number of quanta per atom per second emitted in the stronger Balmer lines of hydrogen was found to be of unit order.[2] It is perhaps not at all surprising that the numbers of quanta of the more intense mercury lines were again roughly of unit order, because the densities of the atoms in the mercury discharge were an order of magnitude or so greater than in the hydrogen discharge and spectroscopic experience showed that the prominent mercury lines were somewhat more intense than the prominent hydrogen lines.

The intensities of the lines. Spectrograms of the mercury arc are given in Fig. 2. The diffuse series lines were broadened by the high pressure and

[2] Crew and Hulburt, Phys. Rev. **29**, 843 (1927).

current conditions in the mercury vapor, and a fairly strong continuous spectrum appeared in the region 2800 to 2500A. The exposure in the second strip of Fig. 2 was not long enough to show the continuous background

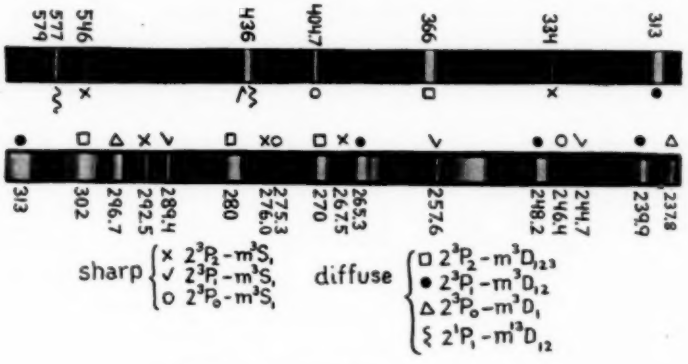

Fig. 2. Spectra of quartz mercury arc.

clearly. The light of the mercury arc was focussed by a concave mirror, of platinum cathodically deposited on glass, on to the slit of a quartz spectrograph (Hilger, Type D33). The spectral energy curve, given in Fig. 3, was measured with a thermocouple and galvanometer, the thermocouple being placed behind the second slit of the spectrograph. The curve of Fig. 3, which gives the true spectral energy distribution, was obtained by correcting the galvanometer deflections for the reflecting power of platinum and the calculated transmission of the spectrograph at each wave-length. The

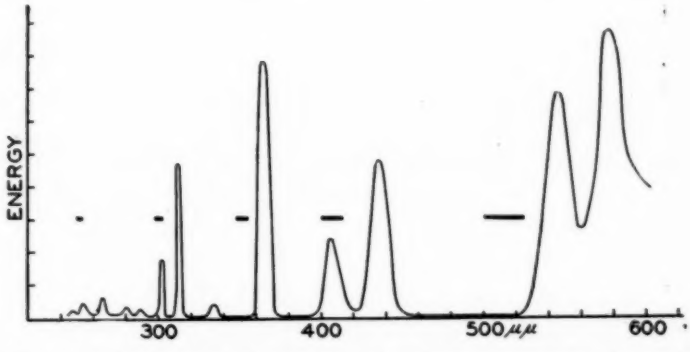

Fig. 3. The true distribution of energy in the mercury spectrum determined with the thermopile. The black marks give the spectral impurity due to the finite width of the slits of the spectrograph.

impurity of the spectrum, obtained by adding together the widths of the two slits in angstrom units, for various wave-lengths is shown by the heavy black marks in Fig. 3. It is seen that the curves of the mercury lines, or line groups, are as wide as these black marks. This is as it should be for slits which are wider than the lines, and hence no slit-width correction was necessary.

A sodium hydride quartz photoelectric cell, connected to a quadrant electrometer, was placed behind the second slit of the spectrograph. Either the cell or the thermocouple could be moved into position behind the slit. Readings with the cell and the thermocouple in turn for the strong mercury lines gave the sensitivity curve of the photoelectric cell, Fig. 4: again, as in Fig. 3, the heavy black marks in Fig. 4 give the spectrum impurity due to the finite width of the slits. This curve was used thenceforth in reducing the electrometer readings to relative energy values. Because of the relatively low values of the sensitivity of the cell and of the intensities of the mercury lines in the wave-length region below 3000A there was an appreciable effect of scattered light in this region. This was carefully determined by observations with a glass absorbing screen which was opaque to wave-lengths below 3000A.

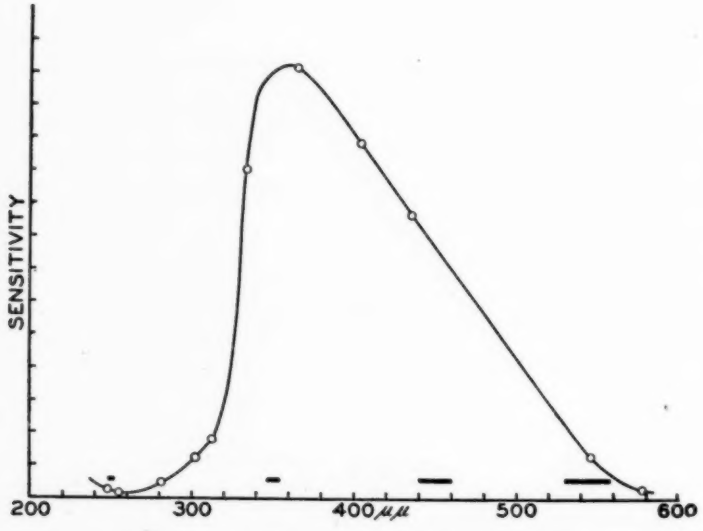

Fig. 4. The sensitivity curve of the sodium hydride quartz photoelectric cell.

In Fig. 5 is given the true energy spectrum of the mercury light for the shorter wave-lengths obtained with the photoelectric cell. The portion of the energy due to scattered light is in the area below the straight dotted line. The curved dotted line which is drawn touching the valleys of the energy curve was taken to represent the energy of the continuous spectrum. The energy in each line was obtained from the area of each peak above the continuous spectrum curve. The two black marks give the impurity of the spectrum. The lines were for the most part narrower than the spectral impurity due to the width of the slits, and no slit-width correction was made. For the lines varied greatly in their characteristics, being narrow, diffuse, complex, etc., as seen in Fig. 2, and it was thought that a slit correction might perhaps have introduced as many errors as it eliminated. As a matter of fact the valleys between the peaks should perhaps be deeper, they are too shallow

because of the effect of the slit width. Therefore too much energy has been ascribed to the continuous spectrum and not enough to the peaks. This systematic error is probably, compensated, partially at least by the method of using the area under the peak to give the relative intensity of the line, a method which becomes erroneous in the case for which the line is narrower than the slits.

In Table I are given the intensities in ergs emitted per atom per second of twenty-four lines or line groups. Seventeen of these came directly from Figs. 3 and 5, the seven others required special treatment. The line 4046 was resolved from its neighbor 4077 by means of the photoelectric cell and spectrograph with narrowed slits. The intensities of the lines 2752, 2759, 2464, 2446 and 2675 were determined by means of calibrated recording densitometer curves of photographic spectrograms. The combined

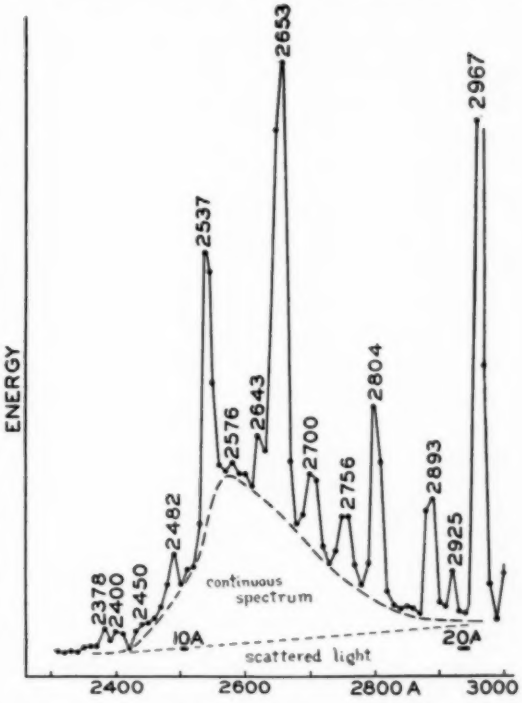

Fig. 5. The true distribution of energy in the shorter wave-length region of the mercury spectrum determined with the photoelectric cell.

TABLE I. *Intensities of mercury lines.*

Series	m	Wave-length (angstroms)	Energy (ergs atom^{-1} sec^{-1})	Series	m	Wave-length (angstroms)	Energy (ergs atom^{-1} sec^{-1})
					3,4	5790	40.9
	2	4046	9.80×10^{-12}	$2^1P_1-m^1D_1$		5770	
$2^3P_0-m^3S_1$	3	2752	0.146		4,5	4347	
	4	2464	0.024	$2^1P_1-m^3D_2$		4339	2.0
	2	4358	20.3				
$2^3P_1-m^3S_1$	3	2893	0.244		3	2967	2.1
	4	2576	0.023	$2^3P_0-m^3D_1$	4	2534	—
	5	2446	0.016		5	2378	0.032
	2	5460	32.2				
	3	3341	1.86		3	3131	22.0
$2^3P_2-m^3S_1$	4	2925	0.68	$2^3P_1-m^3D_{12}$	4	2653	1.16
	5	2759	0.056		5	2482	0.086
	6	2675	0.007		6	2399	0.054
					3	3663	36.4
				$2^3P_2-m^3D_{1,2,3}$	4	3025	6.3
					5	2805	0.45
					6	2699	0.20

intensity of the two yellow lines is given in the table, their separate intensities were not determined (they seemed to be of about equal intensity). The combined intensity of the second members (4347 and 4339) of their respective series was determined with the recording densitometer; the two lines were much weaker than their companion 4358. The values, given in Table I as ergs emitted per atom per second, were obtained by dividing up the total emitted energy 1.85×10^{-10} erg atom^{-1} sec^{-1} among the lines and the continuous spectrum according to their relative energies.

Temperatures of the excited atoms. If there is a sort of temperature equilibrium in the mercury arc the number of atoms excited from an energy E_0 to an energy E will be proportional to the Boltzmann factor $\epsilon^{-(E-E_0)/KT}$, where K is the molecular gas constant and T is the temperature of the excited atoms. Writing $h\nu$ for $E-E_0$, the intensity i of radiation of wave-number ν (frequency $c\nu$) is

$$i=a\epsilon^{-h\nu/KT}, \tag{1}$$

where a represents the various probabilities of state and of transition. If a is a constant for the lines of a series the logarithm of the intensity of a line plotted against the wave-number should be a straight line for the series.

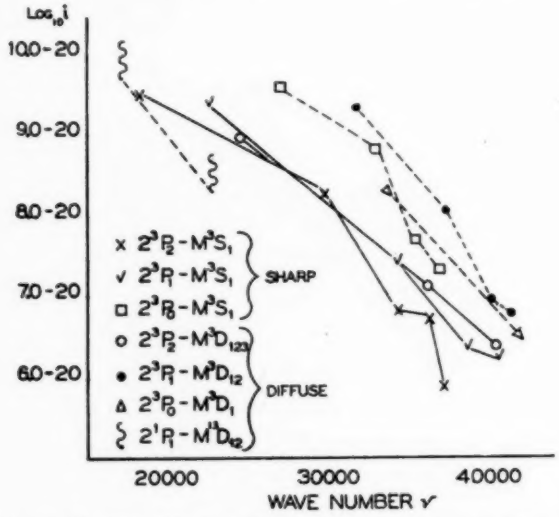

Fig. 6. The logarithm to the base 10 of the line intensity i plotted against the wave-number ν for the lines of the various series of the mercury spectrum.

This is done in Fig. 6, using the intensities of Table I, and it is seen that the points lie roughly on straight lines. This indicates that the Boltzmann term was the important one and that the variation in the probability function a with the march of the series was relatively small; although it is possible, of course, that a is not constant but varies with ν in some regular manner.

The slopes of the lines of Fig. 6 were approximately the same for the three sharp series and for the four diffuse series. From the slopes the temperatures of the excited atoms of the sharp and diffuse series were calculated to be

3900 and 2600° Kelvin, respectively. These values seem to be in accord with general notions of the effects in an electric discharge. The average temperatures of the gas molecules are probably lower. It may be recalled that measurements of the widths of spectrum lines of discharges at pressures below 1 mm of mercury gave, on the theory of Doppler broadening,[3] temperatures for the emitting particles sometimes of several hundred and sometimes of several thousand degrees.

If instead of comparing the intensities of the lines of a series, we examine lines which arise from transitions from the same upper level to differing lower levels, things are not so simple. For example the three lines 5460, 4358 and 4045A have the upper level 2^3S_1 in common and their respective lower levels are 2^3P_2, 2^3P_1 and 2^3P_0. Their relative intensities are 32.2, 20.3 and 9.8 and the log i,ν curve is not at all a straight line. Similarly for the diffuse levels. In this case, therefore, the intensities depend upon other probabilities in addition to the Boltzmann term. Assigning weights in accordance with the numbers of Zeeman sub-levels gave no better agreement. Apparently theory is hardly able yet to describe completely the complicated actions in a mercury arc at atmospheric pressure. Slack[4] found similar discrepancies between the calculated and the observed intensities of the Balmer lines of hydrogen.

Brief discussion of the measurement of the intensity of spectrum lines. An extended investigation of the intensities of spectral lines over wide ranges of wave-length is a step-by-step process at the present time. The energies in large blocks of the spectrum must first be determined by absorption screen methods. Detailed mapping of the lines in each block may then be carried out with a spectrograph and suitable measuring devices, such as the thermocouple and the photoelectric cell. These devices may be supplemented by photographic methods, such as the densitometer and the neutral wedge. The photographic methods give high resolution but require independent calibration; the spectra of Fig. 2 and the data of Table I could be used conveniently for calibration purposes. The neutral wedge method, due to Merton,[5] is very elegant, but a wedge which is accurately neutral over wide intervals of the spectrum is difficult to find. It might be possible to make by photographic methods an optical wedge, so adjusted for use with a particular photographic plate, that the intensities of all the lines could be read directly from the spectrogram.

NAVAL RESEARCH LABORATORY,
BELLEVUE, ANACOSTIA, D. C.,
June 14, 1928.

[3] Merton, Proc. Roy. Soc. **A91**, 421 (1915): Schönrock Ann. d. Physik **20**, 995 (1906).
[4] Slack, Phys. Rev. **31**, 527 (1928).
[5] Merton, Proc. Roy. Soc. **92**, 322 (1915).

BERYLLIUM HYDRIDE BAND SPECTRA[1]

By William W. Watson

Abstract

Two new band systems appear in a Be arc in hydrogen, one in the green from 4800A to 5120A, the other from 3700A to beyond 2200A in the ultra-violet. Measurements of the bands of both systems at high dispersion are reported, and the quantum analysis is given. The green band group belongs probably to the $^2P \rightarrow {}^2S$ class due to BeH molecules. It consists of the 0–0, 1–1, 2–2, etc., bands, degrading to the violet, but all branches exhibit a marked shift to the red for $j>30$. The analysis gives $I_0' = 2.6833\times10^{-40}$ gm cm^2 and $I_0'' = 2.7212\times10^{-40}$ gm cm^2 for the moments of inertia, $r_0'' = 1.35\times10^{-8}$ cm, $\omega_0' = 2053.4$, $\omega_0'' = 2025.7$. The ultra-violet system consists of singlet P, R branch bands degrading to the red, the equation for the zero-points being $\nu = 39059+1460.5n'-14.5n'^2-2182.0n''+41.0n''^2$. For this system, $I_0' = 3.85\times10^{-40}$ gm cm^2 and $I_0'' = 2.50\times10^{-40}$ gm cm^2, $r_0'' = 1.29\times10^{-8}$ cm. A discussion of the probable electronic transition for the ultra-violet bands is included.

WITH an arc between beryllium electrodes in an atmosphere of hydrogen at about 4 cm pressure as a source, two new band systems arising undoubtedly from a beryllium-hydrogen compound are observed. One system consists of numerous strong series of lines in the region 4800–5120A, with a prominent head at 4991A, and with a marked convergence of the branches at both ends of the group. This spectrum has also been reported recently by Peterson.[2] The other system includes a considerable number of interlacing branches in the ultra-violet from 3700A to beyond the 2200A photographic limit of the 21-foot grating. Spectrograms of the green group have been obtained in both the first and second orders of the 21-foot grating, but the ultra-violet region has been photographed in the first order only.

Green Beryllium Hydride Bands

The green bands have been analyzed into a number of apparently singlet P, Q, and R series, with five P, five R, and three Q branches of measurable intensity. Fig. 1 indicates the course of the stronger branches, the origin of the most intense set of branches corresponding to the 4991 head. The lines of the three strongest branches, which constitute in our assignment the 0-0 band of the system, are given in Table I, together with the $2\Delta F'$ and $2\Delta F''$ values as obtained from the $P-R$ combination differences. It is to be noted that for $j<30$, the branches degrade to the violet, but that for values of $j>30$, all of the branches shift markedly to the red. A similar reversal in the direction of the degrading has been reported by Hulthèn[3] in the case of the CaH bands. This phenomenon must be an

[1] This paper gives the details of the investigation reported to the American Physical Society at the Washington meeting April, 1928.

[2] M. Peterson, Phys. Rev. **31**, 1130 (1928), (Abstract).

[3] E. Hulthèn, Phys. Rev. **29**, 97 (1927).

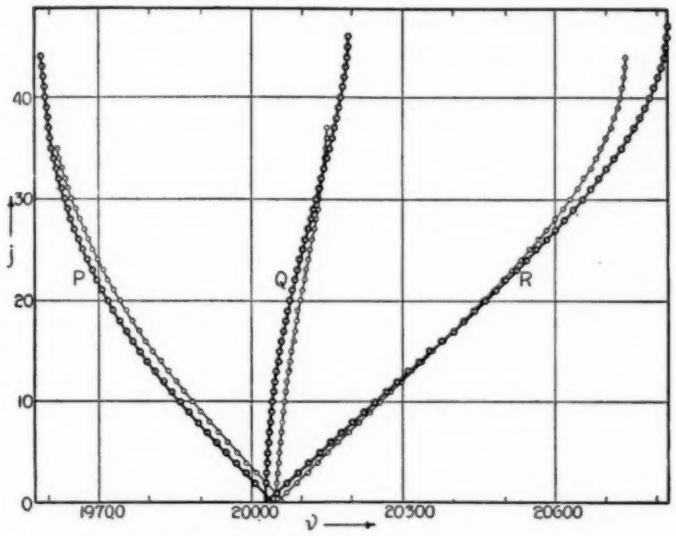

Fig. 1. Fortrat diagram of λ4991 BeH band group. Strong set of branches is the 0–0 band. Weaker branches are the 1–1 band. In order not to complicate the diagram the 2–2 and 3–3 bands are not shown.

indication of a rather high degree of molecular instability, to be represented in the equation

$$\nu_j = \alpha j^2 + \beta j^4 + \gamma j^6 + \delta j^8 + \cdots \tag{1}$$

for the frequencies of the lines in any branch by the relatively increased effectiveness of the higher powered terms in j for large values of j. The fact that the branches all apparently end just when the first difference between successive lines becomes zero is probably just a coincidence.

Both the initial and final state ΔF's of Table I can be represented quite closely by

$$2\Delta F = 4BT + 8DT^3 + 12FT^5 + 16HT^7 \tag{2}$$

where $T = j - 1/2$. The average values of these coefficients determined by using several sets of distributed $\Delta F/T$ values are:

$$B_0' = 10.3046 \text{ cm}^{-1} \qquad B_0'' = 10.1622 \text{ cm}^{-1}$$
$$D_0' = -1.03762 \times 10^{-3} \qquad D_0'' = -1.02306 \times 10^{-3}$$
$$F_0' = +8.451912 \times 10^{-8} \qquad F_0'' = +9.64116 \times 10^{-8}$$
$$H_0' = -7.06581 \times 10^{-12} \qquad H_0'' = -9.50282 \times 10^{-12}$$

From these coefficients, the exact equation (1) for the lines of one of the branches can be obtained.

The small percentage change in B is indicative of a very narrow Condon parabola in the $n'\ n''$ array of bands; in fact, only the $\Delta n = 0$ sequence is to be expected. Therefore it is logical to assign the other sets of branches in this group to transitions $1-1$, $2-2$, etc. Furthermore, a rather natural

TABLE I.[4] *Rotational data for λ4991, 0—0 band of BeH.*

j_k	$R(j_k)$	$P(j_k)$	$Q(j_k)$	$2\Delta F'$	$2\Delta F''$
1½	20050.78				
2½	72.00	20011.15		60.85	59.68
3½	93.63	19991.10		102.53	100.74
4½	114.97	71.26		143.71	141.81
5½	36.37	51.82	20033.50	184.55	182.21
6½	58.21	32.76	34.74	225.45	222.20
7½	79.94	14.17	36.28	265.77	262.11
8½	201.76	896.10	38.06	305.66	301.48
9½	23.81	78.46	40.16	345.35	340.56
10½	45.75	61.20	42.46	384.55	379.34
11½	67.85	44.47	45.06	423.38	417.51
12½	89.92	28.24	47.82	461.68	455.34
13½	311.91	12.51	50.78	499.40	492.53
14½	33.92	797.39	54.18	536.53	529.20
15½	55.78	82.71	57.47	573.07	565.26
16½	77.63	68.66	61.08	608.97	600.63
17½	99.26	55.15	65.14	644.11	635.47
18½	420.67	42.16	69.12	678.51	669.54
19½	41.94	29.72	73.31	712.22	702.70
20½	62.82	17.97	77.79	744.85	735.26
21½	83.61	06.68	82.45	776.93	766.79
22½	504.05	696.03	87.18	808.02	797.68
23½	24.25	85.93	92.09	838.32	827.63
24½	43.98	76.42	97.03	867.56	856.69
25½	63.50	67.56	102.21	895.94	884.88
26½	82.66	59.10	07.38	923.56	912.21
27½	601.24	51.29	12.68	949.95	938.52
28½	19.57	44.14	18.18	975.43	963.88
29½	37.34	37.36	23.49	999.98	988.38
30½	54.49	31.19	29.04	1023.30	1011.98
31½	71.13	25.36	34.35	1045.77	1034.37
32½	87.15	20.12	39.70	1067.03	1055.68
33½	702.69	15.45	44.97	1087.24	1076.14
34½	17.44	11.01	50.27	1106.43	1095.55
35½	31.65	07.14	55.46	1124.51	1113.78
36½	44.99	03.66	60.51	1141.33	1131.20
37½	57.55	00.45	65.36	1157.10	1147.44
38½	69.16	597.55	69.99	1171.61	1162.32
39½	80.05	95.23	73.96	1184.82	1176.29
40½	89.31	92.87	78.45	1196.44	1189.29
41½	98.81	90.76	82.18	1208.05	1200.60
42½	806.39	88.71	85.40	1217.68	1212.17
43½	12.93	86.64	87.83	1226.29	1221.41
44½	18.28	84.98	90.13	1233.30	1229.89
45½	22.27	83.04	91.84	1239.23	1235.77
46½	24.51	82.51	92.79	1242.00	
47½	25.44				

prediction would be that these bands belong to the $^2P \rightarrow {}^2S$ class due to BeH molecules, so that there should be some similarity with the green

[4] Each line we suppose to be an unresolved doublet (see text). Thus the line $R(j_k)$ for $j_k = \frac{1}{2}$ would correspond to the j transitions $1-0$ and $2-1$, while the line $P(j_k)$ for $j_k = 1\frac{1}{2}$ would correspond to the j transitions $0-1$ and $1-2$.

MgH bands and the A bands of CaH which also belong to this class. Now the MgH and CaH bands consist of electronic doublets with separations of the same magnitude as the separation of the $^2P_1$ and $^2P_2$ levels of the corresponding atoms (K atom for CaH and Na atom for MgH). One would predict, then, that the doublet separation at the origin in these BeH bands should be about 0.3 cm^{-1} as for the ^2P levels in the corresponding Li atom. This is just beyond the limit of resolution on our second order plates, but there is nevertheless a suspicion of doubling of the first lines of the strongest R branches. The magnetic interaction between the electronic spin angular momentum s and σ_k, the component of the electronic orbital angular momentum along the nuclear axis of the molecule, is therefore in this case very small, and even for quite low speeds of nuclear rotation, the s tends to set itself along the axis of j (Hund's case b).

Owing to the incomplete resolution of the fine-structure of the band, and the consequent lack of exact knowledge of the missing lines and relative intensities at the beginnings of the branches, we cannot be quite sure about the electronic transition involved. The order of intensity of the branches for low values of j is distinctly $Q>R>P$, however, as it should be for a $^2P\rightarrow{}^2S$ transition.[5] If the transition were $^2S\rightarrow{}^2P$, the order of intensity should be $Q>P>R$. For a case $b^2P\rightarrow{}^2S$ transition, the rotational term formulas should be

$$F'_{1,2}(j_k)=B'(j_k^2-\sigma_k^2)+\cdots\ ;\qquad F''_{1,2}(j_k)=B''j_k^2 \tag{3}$$

with $j=j_k\pm 1/2$. And we then assume that the term separation is too small to be detected and that the lines due to transtions between F_2 substates are coincident with lines for F_1 substates having j_k larger by one unit. It is thus clear why the observed ΔF's can be represented by Eq. (2).

The values of ω_0, the vibrational frequency of the molecule for vibrations of infinitesimal amplitude, can be computed from the B and D constants, using the relation $\omega_0=(-4B^3_0/D_0)^{1/2}$. This calculation gives $\omega'_0=2053.4$ and $\omega''_0=2025.7$, the small change in ω_0 corresponding to the small change in B. Since the difference between the ω'_0x' and ω''_0x'' factors in the vibrational energy formula is necessarily quite small, the origins of the $0-0$, $1-1$, $2-2$, etc., bands must be rather close together. This is in agreement with the interpretation of the several weaker branches as being other $\Delta n=0$ transitions. The origin of the next to the strongest set of branches, no doubt the $1-1$ band, is at 20050.5, as is indicated in Fig. 1. And since ν_e (the head of the strongest Q branch) is 20031.3, we can write $20050.5=20031.3+2053.4(1-x')-2025.7(1-x'')$, which gives $\omega'_0x'-\omega''_0x''=-8.5$, an altogether probable value. The two values of B yield for the moments of inertia, $I'_0=2.6833\times10^{-40}$ gm cm^2 and $I''_0=2.7212\times10^{-40}$ gm cm^2 respectively. Therefore, the internuclear distance of the BeH emitter in the ^2S state is 1.35×10^{-8} cm.

[5] The relative intensities of the branches for bands representing transitions between various doublet states can be computed from the equations given by Mulliken, Phys. Rev. **30**. 787 (1927).

Ultra-violet Beryllium Hydride Bands

The ultra-violet many-lined spectrum has been analyzed in part, in the region from 2700A to 3200A, into a number of bands degrading to the red, and consisting of singlet P and R branches only. Several of these bands are very prominent, and the series of strong lines can be traced for considerable distances among the numerous weaker lines. Table II gives the

Table II. *Lines in the ultra-violet BeH bands.*

j	0−1		0−3		1−3		1−4	
	R	P	R	P	R	P	R	P
½	36925.04		32889.96				32439.68	
1½	933.96	36891.30	894.91	32855.69		34305.05	448.80	32409.37
2½	933.96	863.81	902.05	831.47	34343.62	277.77	454.23	386.21
3½	929.30	829.89	902.05	803.09	343.62	246.40	454.23	356.47
4½	918.54	789.92	894.91	767.92	336.15	210.00	448.80	324.28
5½	900.76	741.76	883.81	727.62	322.60	170.00	439.68	285.75
6½	875.75	690.60	867.85	683.44	305.05	123.89	424.33	243.90
7½	845.57	633.08	845.44	633.24	279.87	071.90	405.17	197.57
8½	808.21	569.12	818.93	579.33	250.74	015.80	381.06	146.64
9½	766.15	498.06	787.14	520.25	216.50	33954.46	352.57	091.36
10½	714.83	421.36	751.42	456.45	176.74	888.32	319.51	032.00
11½	659.35	339.77	709.00	388.26	131.85	817.77	281.69	——
12½	598.06	251.13	662.69	315.92	082.03	742.31	239.68	31900.01
13½	530.23	157.19	612.02	239.68	026.76	663.26	193.39	828.36
14½	456.70	058.24	556.00	157.82	33966.78	577.12	142.96	752.81
15½	376.77	35953.15	495.77	072.57	902.52	487.74	088.26	672.95
16½	291.54	843.91	431.23	——	823.72	394.54	030.24	590.16
17½	201.11	729.44	362.41	——	759.08	296.42		
18½	104.48	609.79	289.07	31793.33	680.79	195.51		
19½	003.35	484.00	211.78	692.17	598.08	090.62		
20½	35896.06	354.59	129.45	588.74	511.14	32980.57		
21½	784.72	220.55			420.27	876.85		
22½	668.52	081.97			325.07	751.42		
23½	546.47	34939.93			227.13	633.24		
24½	420.06	793.22			125.10	511.81		
25½	289.74	642.50			019.48	386.21		
26½	155.44	488.38			32911.43	258.57		
27½	016.71	330.64			799.60	129.45		
28½	34874.76	170.00			683.44	31995.43		
29½	728.36	006.26						
30½	578.53	33839.20						
31½	425.86	670.29						
32½	269.83	498.89						
33½	111.06	325.07						
34½	33950.09	149.60						
35½	787.63	32972.04						

frequencies of the lines in the 0−1, 0−3, 1−3, and 1−4 bands, and in Table III are given the combination differences which justify the vibrational assignments. These differences for the same states in the several bands are in general equal throughout to within the possible experimental error of the measurements. Table IV gives the zero-points of all the bands measured, together with measurements on three heads (those given in brackets)

TABLE III. *Combination differencies in the ultra-violet BeH bands*

j	0−1 $2\Delta F'$	0−3 $2\Delta F'$	0−3 $2\Delta F''$	1−3 $2\Delta F''$	1−3 $2\Delta F'$	1−4 $2\Delta F'$
1½	42.66		58.49			39.43
2½	70.15	70.58	——		65.85	68.02
3½	99.44	98.96	134.13	133.62	97.22	97.76
4½	128.62	126.99	174.43	173.62	126.15	124.52
5½	159.00	156.19	211.47	212.26	152.60	153.93
6½	185.15	184.41	250.57	250.70	181.16	180.43
7½	212.49	212.20	288.52	289.25	207.97	207.60
8½	239.09	239.60	325.19	325.41	234.94	234.42
9½	268.09	266.89	362.48	362.42	262.04	261.21
10½	293.47	294.97	398.88	398.73	288.42	287.51
11½	319.58	320.74	435.50	434.43	314.48	——
12½	346.93	346.77	469.32	468.59	339.72	339.67
13½	373.04	372.34	504.87	504.91	363.50	365.03
14½	398.46	399.18	539.45	539.02	389.66	390.15
15½	423.62	423.20	——	572.24	414.78	415.31
16½	447.63	——	——	606.10	438.18	440.08
17½	471.67	——	637.90	637.21	462.66	
18½	494.69	495.74	670.24	668.46	485.28	
19½	519.35	519.61	700.33	700.22	507.46	
20½	541.47	540.71		730.23	530.57	

TABLE IV. *Vibrational assignments of ultra-violet BeH bands.*

$\nu = 39059 + 1460.5n' - 14.5n'^2 - 2182.0n'' + 41.0n''^2$

n'	$n''=0$	1	2	3	4	5
0	(39059)	36918	34859	32882		
1	(40505)			34328	32433	
2	(41922)				33850	32037

which are clearly visible on low dispersion plates, but which were not measured at high dispersion. The vibrational equation connecting these zero points is

$$\nu = 39059 + 1460.5n' - 14.5n'^2 - 2182.0n'' + 41.0n''^2 \qquad (4)$$

There are of course other bands in this system which have not been measured and which are consequently not shown in Table IV. The general course of the intensity distribution of the bands is evident, however. The intense bands are grouped along a rather wide Condon parabola, a fact which is to be correlated with a large change in the moment of inertia between initial and final electronic states. We find that the values of $2\Delta F'$ and $2\Delta F''$ can be accurately represented for all except the three or four lowest j values by the formula $2\Delta F = 4Bj + 8Dj^3$, with j having half-integral values. The values of the constants B and D have been obtained by application of this equation to the data, using a semi-graphical method recommended by Birge.[6] The results of these computations are:

[6] R. T. Birge, National Research Council Bulletin No. 57, page 172.
[7] R. T. Birge, Phys. Rev. 31, 919, 1928.

$B_0' = 7.1328\ \text{cm}^{-1}$ $B_1'' = 10.3275\ \text{cm}^{-1}$

$D_0' = -6.80\times10^{-4}$ $B_2'' = 10.0200\ \text{cm}^{-1}$

$B_1' = 6.9968\ \text{cm}^{-1}$ $\alpha'' = B_1'' - B_2'' = 0.3075$

$\alpha' = B_0' - B_1' = 0.1360$ $B_0'' = B_1'' + \alpha'' = 10.6350\ \text{cm}^{-1}$

Therefore, the moments of inertia are $I'_0 = 3.85\times10^{-40}$ gm cm^2 and $I''_0 = 2.50\times10^{-40}$ gm cm^2, the percentage change in I being rather large. This value of I''_0 corresponds to an internuclear distance of 1.29×10^{-8} cm for a BeH dipole as the emitter.

It has been pointed out recently by Birge[7] that the quantity $R = 2xB_0/\alpha$, where x is the coefficient of the n^2 term in the vibrational formula (4) divided by ω_0, has an average value of 1.4 ± 0.2, when a number of molecules are considered. For this final vibrationless state, $R = 2\times0.0188\times10.635/0.3075 = 1.3$, which is a satisfactory agreement. Also, the D constants as computed from the $D = -4B^3/\omega^2_0$ relation agree well with the values given above.

The $\Delta F''$ differences for these ultra-violet bands and for the green BeH bands are so nearly alike that it may be that these two band systems have a common final ^2S state, although since no ultra-violet band involving the $n'' = 0$ state has been measured, a direct comparison of the $\Delta F''$ values with those for the green bands is impossible. Because of their simple P, R branch structure, the ultra-violet bands would then be assigned to the transition $^2S \rightarrow {}^2S$. The fact that there is no evident doubling in these bands is no argument against the $^2S \rightarrow {}^2S$ assignment, since the lines may be unresolved doublets as in the visible BeH bands. It should be pointed out, however, that the branches of the ultra-violet bands do not exhibit any rotational perturbation for high j values, whereas in the CaH spectrum the B bands ($^2S \rightarrow {}^2S$) have the same "red shift" near the end of the branches as do the A bands ($^2P \rightarrow {}^2S$), and the C bands of CaH (also $^2S \rightarrow {}^2S$) give evidence too of the unstable condition of the molecule for high rotational velocities. Furthermore, if one extrapolates the $\Delta F''$ values for $n'' = 1, 2, 3,$ and 4 to $n'' = 0$, the expected equality of the resulting $\Delta F''$ values with those for $n'' = 0$ in the green bands does not appear.

It is just possible, then, that these two band systems have no state in common, and that the ultra-violet system is indeed a $^1S \rightarrow {}^1S$ transition, the carrier being perhaps a BeH^+ molecular ion formed in the arc. The $\Delta F''$ values for the $n'' = 0$ state in the ultra-violet bands must be obtained, however, for one thing, for comparison with the green bands, in order to definitely decide on the electronic transition involved. At present the ultra-violet bands are perhaps best tentatively assigned as $^2S \rightarrow {}^2S$, the final state being the same as that for the green bands.

RYERSON PHYSICAL LABORATORY,
UNIVERSITY OF CHICAGO,
June, 1928.

THE LESS REFRANGIBLE BANDS IN THE SPECTRUM OF TIN MONOCHLORIDE

By W. F. C. Ferguson

Abstract

Four groups of bands previously obtained by Jevons in a discharge through $SnCl_4$ vapor are now found also in streaming active nitrogen. Two groups, α and β, were previously classified as a $^2S \rightarrow {}^2P$ transition in SnCl; with the help of new measurements, and from an examination of the band structure, it is concluded that the other two groups, λ3500 and λ3800, are a $^2D \rightarrow {}^2P$ transition with the same ^2P state as the α and β bands. The chlorine isotope effect confirms the identity of the emitter as SnCl and confirms the vibrational quantum number assignments. The vibrational intensity distribution (intensity concentrated in $\Delta n = 0$ sequence) is in qualitative agreement with theory, for the ratio of ω_e'' to ω_e'. An attempt was made to obtain analogous bands by introducing SnI_4 vapor into active nitrogen, but no new bands were obtained.

Introduction and Experimental Procedure

IN AN uncondensed discharge through the vapor of $SnCl_4$ Jevons[1] has found four groups of bands, and two continuous bands. He obtained equations representing the α and β groups and found the isotope effect of chlorine for SnCl. These groups were later classified by Mulliken[2] as a $^2S \rightarrow {}^2P$ electronic transition. Two groups, near λ3800 and λ3500, shaded toward the red, were unidentified by Jevons; these are the object of the present paper. Strutt and Fowler[3] describe the spectrum of chlorides of tin in streaming active nitrogen, mentioning only a continuous band and a band group in the region λ4768 − λ4430. The present work is a continuation of that last mentioned, but evidently with a more intense exposure. The band group, however, does not appear in the region λ4768 − λ4430. The present spectrum corresponds with that obtained by Jevons (Plate 2)[1] in the uncondensed discharge, except in particulars to be discussed below. The measured spectrum was obtained with a quartz spectrograph giving a dispersion of from 8A per mm to 11A per mm in the region investigated. An Eastman 40 plate was used with an exposure of three hours. The pressure in the afterglow tube was about 15 mm. At high pressure the continuous band of the region λ3300 − λ3600 was found to be weaker relative to the λ3500 group.

Structure and Interpretation

No rotational lines were resolved in any of the less refrangible bands. An intensity minimum is observed near the head of each in a few of the most intense bands, apparently giving two heads. The obvious interpretation, however, is that each band has an R head and a Q head, the intensity mini-

[1] W. Jevons, Proc. Roy. Soc. **A110**, 365 (1926).
[2] R. S. Mulliken, Phys. Rev. **28**, 481 (1925).
[3] R. J. Strutt and A. Fowler, Proc. Roy. Soc. **A86**, 105 (1912).

mum being around the zero line. (Also an isotope effect sometimes appears; see below). In the λ3500 group R branches appear of nearly uniform intensity from the zero lines to the band heads. The intensity of an R branch is much less than that of a Q branch. Measurements made in this group on Q heads, which should be very close to the origins, are recorded in Table I. In the λ3800 group the bands present a similar appearance but with R branches more intense than Q branches. The distance from Q heads to R heads was measured where possible. Using these few measured values the positions of Q heads were calculated, by extrapolation, for bands where R heads only could be measured. These values are given in Table I. Measured wave-numbers of R heads in both groups are given below the table.

TABLE I. *Less refrangible bands of tin chloride. Column n' n'' gives the vibrational quantum numbers; O − C, observed minus calculated values of wave-number, calculated values being obtained from formulas given below. Relative intensities in the λ3800 group are given for R heads.*

		λ3500 group $SnCl^{35}$ − Q heads				λ3800 group $SnCl^{35}$ − Q heads			
n'	n''	Int.(Q)	λ(I.A.)	Wave-no.	O−C	Int.(R)	λ(I.A.)	Wave-no.	O−C
2	1					0	3728.9	26810.	.8
3	2					0	38.4	742.	2.3
4	3	0	3478.4	28741.	0.3	0	49.0	666.	2.0
0	0	5	87.54	665.3	0	5	61.29	579.1	0
1	1	4	94.59	607.5	−.2	5	69.17	523.5	−.5
2	2	3	3502.30	544.5	.6	4	77.71	463.6	.9
3	3	2	11.04	473.5	−.4	3	87.47	395.4	.2
4	4	1d	20.5	397.	−.7	2	98.17	321.0	−.5
0	1	1	30.60	315.7	0	1	3811.31	230.3	−.3
1	2	1	37.45	260.9	.6	2*	19.53	173.8	−3.7
2	3	1d	45.24	198.8	.1	2	27.69	118.0	−.2
3	4	1d	53.67	131.9	1.0	2	37.36	052.2	−.5
4	5	0	63.3	056.	.9	2	47.7	25982.	1.0
0	2					}			
1	3					}	masked by CN		
2	4					}			
3	5					0	88.3	711.	−1.2
4	6					1	98.9	641.	−1.5
5	7					1	3910.5	565.	−1.6
0	3					0	14.6	538.	−1.6

d = diffuse *masked by NO band structure

R. heads. λ3500 group: (0,0) 28676.1, (1,1) 28615.7, (2,2) 28551.0, (3,3) 28478.8.
R. heads. λ3800 group: (2,1) 26825, (3,2) 26754, (4,3) 26676, (0,0) 26597.9, (1,1) 26537.8, (2,2) 26475.3, (3,3) 26405.2, (4,4) 26329.5, (0,1) 26244.3, (1,2) 26185.2, (2,3) 26127.6, (3,4) 26060.5 (4,5) 25989, (3,5) 25718, (4,6) 25647, (5,7) 25571, (0,3) 25547.

The existence of a strong Q branch shows that $\Delta\sigma_k = \pm 1$. The λ3500−λ3800 group separation is near but less than the $\alpha-\beta$ separation. The latter is $^2P_{1\frac{1}{2}}-{}^2P_{\frac{1}{2}}$. The condition $\Delta\sigma_k = \pm 1$, and also the λ3500−λ3800 separation can be accounted for by assuming the transition $^2D \rightarrow {}^2P$, with $\Delta\nu = 273.9$ for the ^2D states, see Fig. 1. These bands (Table I) are represented within experimental error by the following equations:

$$SnCl^{35}\begin{cases}\lambda 3500\text{ group: } \nu = 28665.3+296.2n'-4.2n'^2-350.7n''+1.1n''^2\\ \lambda 3800\text{ group: } \nu = 26579.1+297.5n'-4.1n'^2-349.5n''+1.0n''^2\end{cases}$$

These completely agree with a $^2D\rightarrow{}^2P$ transition. The initial state coefficients in both groups are very nearly the same, indicating states closely related, like $^2D_{1\frac{1}{2},2\frac{1}{2}}$. The final state coefficients indicate final levels in common with Jevons' β and α groups, respectively, equations for which are:

$$SnCl^{35}\begin{cases}\beta\text{: } \nu = 33622.6+431.3n'-1.2n'^2-351.4n''+1.2n''^2\\ \alpha\text{: } \nu = 31262.5+431.3n'-1.2n'^2-353.5n''+1.0n''^2\end{cases}$$

(Agreement in case of the $\lambda 3800$ group is much closer if R branch heads are used. This may be due to the present method of ascertaining Q heads for that group). Further confirmation of vibrational quantum number assignments is given by the isotope effect (see below).

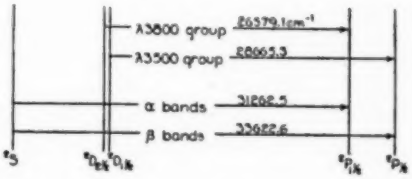

Fig. 1. Electronic energy levels and transitions in SnCl. To scale, except $^2P-{}^2D$ separation is shown half size.

The distribution of intensity in a single band from a $^2D\rightarrow{}^2P$ transition can be estimated theoretically from formulas given by Mulliken.[4] With a reasonable assumption as to the temperature (of active nitrogen) and as to the size of the SnCl molecule, this distribution was calculated; and the relative intensity of P, Q, and R branches agrees with that observed as well as could be expected. Calculations show that the Q branch reaches high intensity very close to the origin. (Intensity of the P branch is very small compared to the Q branch). The R branch for $^2D_{1\frac{1}{2}}\rightarrow{}^2P_{\frac{1}{2}}$ is less intense than the Q branch; and for $^2D_{2\frac{1}{2}}\rightarrow{}^2P_{1\frac{1}{2}}$ the R branch intensity is greater—possibly greater than the Q branch. In either case the R branch near the origin shows an intensity minimum, leaving an open region. The different appearance of these same bands as photographed by Jevons in a discharge can be satisfactorily accounted for also. For a higher temperature (as in a discharge) the R branch will have a strong maximum at its head ("line-like"); and the Q branch will be weaker relative to the R branch; (the Q branch in the $\lambda 3800$ group is barely visible in Jevons' reproduction).

The intensity in each group is concentrated in the $\Delta n=0$ sequence, falling off rapidly toward the $+1$ and $+2$ sequences. Only one minus sequence in each group is observed,—for very few and weak bands. In view of the ratio of final to initial vibrational frequencies this distribution is compatible with Condon's[5] theory, resembling the case of SiN; but the asymmetry about the zero sequence is striking and indicates peculiar $V(r)$ curves.

[4] R. S. Mulliken, Phys. Rev. **29**, 391 (1927).
[5] E. U. Condon, Phys. Rev. **28**, 1182 (1926).

Isotope Effect

In several instances weak band heads were associated with the stronger heads recorded above. The displacements of these weaker heads from the stronger were measured and are recorded in Table II. The isotopic coefficient[6] ρ for $SnCl^{37}$ compared to $SnCl^{35}$ is 0.9791. The theoretical displacement of a $SnCl^{37}$ band head from a $SnCl^{35}$ band head is therefore 0.0209 of the distance of the latter from the group origin. Measured and theoretical isotopic displacements are recorded in Table II. (For the λ3800 group, displacements of R heads were observed).

Table II. *Measured and theoretical isotopic displacements.*

		λ3500 group ($\nu_0 = 28665.3$)			λ3800 group ($\nu_0 = 26579.1$)		
n'	n''	$\nu(SnCl^{35})$	$\Delta\nu$ obs. $SnCl^{37} - SnCl^{35}$	$\Delta\nu$ calc. $.0209(\nu_0 - \nu)$ $SnCl^{35}$	$\nu(SnCl^{35})$	$\Delta\nu$ obs. $SnCl^{37} - SnCl^{35}$	$\Delta\nu$ calc. $.0209(\nu_0 - \nu)$ $SnCl^{35}$
3	3				26395.4	4.6	3.8
4	4	28397.	6.	5.6	321.0	8.2	5.4
0	1	315.7	7.1	7.3	230.3	7.6	7.3
1	2	260.9	8.8	8.4		*	
2	3	198.8	11.1	9.7	118.0	12.7	9.6
3	4	131.9	11.1	11.1	052.2	12.0	11.0
4	5	056.	14.	12.7	25982.	14.	12.5

* masked by NO band structure

The measured displacements agree within experimental error with the calculated values. This agreement proves the identity of the emitter as SnCl. It also proves the correctness of the assignment of vibrational quantum numbers. The tin isotope effect, discussed fully by Jevons, was not resolved with the dispersion here employed.

Experiment with Tin Iodide

The above experiment was repeated using stannic iodide (SnI_4) in active nitrogen. It produces no characteristic spectrum in the region λ7000–λ1900A. The tin and iodine line spectra and bands of iodine appear rather strong, iodine lines being photographed at λλ1844 and 1830 in 30 minutes.

The writer wishes to express his thanks to Professor R. S. Mulliken for suggesting this problem, and also for his generous advice in the progress of the work.

Washington Square College,
New York University,
June, 1928.

[6] R. S. Mulliken, Phys. Rev. 25, 119 (1925).

ABSORPTION BAND SPECTRUM OF IODINE MONOCHLORIDE

By Earl D. Wilson

Abstract

Wave-lengths and series relations in the visible absorption spectrum of ICl.—The visible absorption spectrum of ICl has been photographed and measured. Eight new members have been located in the two series described by Gibson and Ramsperger as corresponding to $n''=1$ and $n''=2$. The limit of convergence of the former series is at $\nu=17430\pm5$ cm^{-1}, which makes the heat of dissociation equal to 49650 ± 15 calories per mol. Four members of a new series for which $n''=3$ have been found, so that it has been possible to compute the fundamental vibratory frequency of the molecule as 381.9 cm^{-1}. Still another series of five members is recorded, whose presence may be due to the existence of a close electronic doublet having a separation of about 36 cm^{-1}. The *ratio of the two specific heats* of gaseous ICl has been calculated to be 1.30 in agreement with empirical results. The *fine structure* of three consecutive bands has been measured, and the corresponding values of the parabolic parameter C have been computed to be in agreement with the theory of change of moment of inertia, I, with ω, the frequency of vibration of the molecule. By combining both sets of data for band heads and fine structure, the following approximate values for the *moment of inertia* have been computed: $I''=575\pm100\times10^{-40}$ g·cm^2; $I'=995\pm200\times10^{-40}$ g·cm^2.

Introduction

SINCE the experimental researches of Wood on the fluorescence spectrum of iodine and the interpretation of his results by Lenz in terms of quantum theory, attention has been focused upon the band spectra of molecules from the halogen group of elements. Further investigations of the molecular spectra of I_2 and also of Br_2 and Cl_2, notably by Mecke and Kuhn, has led logically to new research upon the corresponding spectra of IBr and ICl. Because of its unsusually high state of dissociation at ordinary temperatures, the absorption spectrum of IBr vapor has not yet been measured; but the more favorable monochloride has yielded definite results, its spectrum—in common with those of all the other halogen molecules—being situated in the red-to-green part of the visible spectrum and possessing one series which obviously converges to a definite limit.

Aside from preliminary work by Roscoe and Thorpe,[1] iodine monochloride has been investigated recently by Gibson and Ramsperger[2] and independently by the writer. It is felt that the present interest in the band spectrum of ICl warrants the presentation of somewhat more accurate measurements, which in addition to extending the series recorded by Gibson and Ramsperger and adding two new series, also include measurements of fine structure not made heretofore. The writer's investigation is therefore briefly outlined in the following.

[1] Roscoe and Thorpe, Phil. Trans. **167**, 207 (1876).

[2] Gibson and Ramsperger, Phys. Rev. **30**, 598 (1927).

TABLE I. *Absorption band heads of ICl*

λ(I. A.)	ν(vac.)	λ(I. A.)	ν(vac.)	λ(I. A.)	ν(vac.)	λ(I. A.)	ν(vac.)
5730.13	17446.9	5891.06	16970.2	6229.5	16048.2	6516.14	15342.3
69.4	328.0	5915.10	901.2	67.1	15951.9	44.36	276.1
73.23	316.6	41.31	826.9	68.8	947.6	88.00	174.9
78.7	300.1	70.62	744.0	82.78	912.1	6610.8	122.6
85.1	281.0	6002.97	16653.8	6315.0	830.9	63.96	002.0
92.90	257.7	38.7	555.3	24.92	806.1	82.3	14960.8
5801.8	232.7	78.12	447.9	38.83	771.4	6709.9	899.2
11.88	201.3	6120.63	333.7	6366.74	15702.3	57.6	794.1
23.72	166.5	34.9	295.7	85.06	657.3	81.3	742.4
37.5	125.9	66.33	212.6	6422.44	566.1	6836.80	622.7
53.04	080.4	80.66	175.0	48.57	503.0	56.35	581.0
70.82	028.7	6215.59	084.1	81.43	424.4	6920.8	445.2
		22.25	066.9			35.8	414.0

TABLE II. *Fine structure of ICl bands at* λ6325, λ6385 and λ6449.

m*	λ(I. A.)	ν(vac.)	m	λ(I. A.)	ν(vac.)	m	λ(I. A.)	ν(vac.)
0	6324.92	15806.1	?	6371.17	15691.4	55	6435.10	15535.5
15	29.04	795.8	53	72.16	88.9	?	40.39	22.7
16	29.58	94.5	54	73.94	84.6	?	41.53	20.0
17	30.04	93.3	55	75.72	80.2	58	42.67	17.2
18	30.67	91.7	56	77.42	76.0	60	46.40	08.2
19	31.27	90.2	57	79.34	71.3	?	49.04	01.9
20	31.88	88.7	0	85.06	57.2	0	48.57	03.0
21	32.64	86.8	?	89.67	45.9	19	54.83	488.0
22	33.27	85.3	?	90.40	44.1	20	55.48	86.4
23	34.08	83.2	23	93.93	35.5	21	56.13	84.9
24	34.91	81.2	24	94.70	33.6	22	56.78	83.3
25	35.61	79.4	25	95.52	31.6	23	57.55	81.4
26	36.42	77.4	26	96.34	29.6	24	58.28	79.7
27	37.43	74.9	27	97.17	27.6	25	59.12	77.7
28	38.19	73.0	28	98.13	25.3	26	59.89	75.8
29	39.23	70.4	29	98.99	23.1	27	60.85	73.6
30	40.18	68.1	30	99.93	20.9	28	61.68	71.6
31	41.24	65.4	31	6400.92	18.4	29	62.65	69.3
32	42.20	63.0	32	02.01	15.8	30	63.54	67.1
33	43.67	59.4	33	03.09	13.1	31	64.53	64.8
34	44.43	57.5	34	04.15	10.6	32	65.57	62.3
35	45.70	54.3	35	05.25	07.4	33	66.54	59.9
36	46.74	51.8	36	06.48	04.9	34	67.75	57.1
37	47.96	48.7	37	07.65	02.1	35	68.85	54.4
38	49.25	45.5	38	08.85	599.1	36	69.93	51.9
39	50.54	42.3	39	10.18	95.9	37	71.11	49.0
40	51.94	38.9	40	11.44	92.8	38	72.40	45.9
?	52.75	36.9	41	12.92	89.2	39	73.56	43.2
41	53.43	35.2	42	14.14	86.2	40	74.96	39.8
42	54.57	32.3	43	15.62	82.7	?	75.12	39.5
43	56.05	28.7	44	16.85	79.7	42	77.59	33.6
44	57.59	24.9	45	18.32	76.1	43	78.92	30.4
?	58.79	21.9	46	19.88	72.3	44	80.36	27.0
?	59.77	19.5	47	21.45	68.5	45	81.81	23.5
?	60.52	17.6	48	22.89	65.0	46	83.29	20.0
47	62.14	13.6	49	24.81	60.4	47	84.73	16.7
48	63.49	10.3	50	26.31	56.7	48	86.38	12.7
49	65.19	06.1	51	27.97	52.7	?	95.19	391.7
50	66.76	02.2	52	29.73	48.5	?	98.14	84.8
51	68.43	698.1	53	31.48	44.2			
52	70.13	93.9	54	33.38	39.6			

* Values of m assume $m=0$ at head and have no theoretical significance.

The wave-lengths of all observed band heads were measured from the plates by means of a low-power comparator. These measurements together with corresponding frequencies are recorded in Table I. The fine structure of three consecutive bands in the red was measured under much higher magnification. The resulting data are arranged in Table II.

Arrangement of Band Series

No attempt is made here to assign independently quantum values of n'' to the Deslandres' series, but the plausible assignments by Gibson and Ramsperger are adopted. However, their arbitrary assignments of n' are shifted one unit to admit a new member on the long wave-length end of the series $n''=2$. Table III shows specifically that six new members have been added to the converging series $n''=1$ and two new members to the weaker series $n''=2$. The series $n''=3$, consisting of four members is entirely new. Thus a value of 379.8 cm^{-1} is obtained for the second frequency interval in the normal group of energy levels in addition to the value of 381.2 cm^{-1} for the first interval.

Experimental Procedure

Photographs were made in the first order on panchromatic plates with a 10-foot Rowland concave grating mounted in Eagle fashion. Continuous radiation, supplied by a 400-watt stereopticon bulb, was projected through ICl vapor contained in a tube of Pyrex glass, 60 cm long, with fused-on end plates of the same material. The vapor from pure ICl was admitted into the evacuated chamber at the center and was caused to progress slowly toward exhaust outlets near each end by proper adjustment of the pump. By this means the absorption spectrum of iodine as a dissociation product was reduced to a minimum. Exposures varied from 5 to 60 minutes. The iron arc was used for a comparison spectrum.

Table III. *Series in band system of ICl*

n'	$n''=1$ Writer	G&R	$\Delta\nu'$ Writer	G&R	$n''=2$ Writer	G&R	$\Delta\nu'$ Writer	G&R	$n''=3$ Writer	$\Delta\nu'$ Writer	$\Delta\nu''(1,2)$ Writer	G&R	$\Delta\nu''(2,3)$ Writer	n'
0	(14825.4)				14445.2		177.5							0
1	15002.0		172.9		622.7	627	171.4	171			379.3			1
2	174.9		167.4		794.1	798	166.7	167	14414.0	167.0	380.8		380.1	2
3	342.3	347	160.7	162	960.8	965	161.8	160	581.0	161.4	381.5	382	379.8	3
4	503.0	509	154.3	152	15122.6	125	153.5	155	742.4	156.8	380.4	384	380.2	4
5	657.3	661	148.8	149	276.1	280	148.3	150	899.2		381.2	381	376.9	5
6	806.1	810	141.5	143	424.4	430	141.7	140			381.7	380	——	6
7	947.6	953	135.7	135	566.1	570	136.2	136			381.5	383	379.8	7
8	16084.1	088	128.5	127	702.3	706	128.6	128			381.8	382	Weighted	8
9	212.6	215	121.1	123	830.9	834	121.0	119			381.7	380	mean	9
10	333.7	338	114.2	113	951.9	953	115.0	120			381.8	385		10
11	447.9	451	107.4	106	16066.9	073	108.1	106			381.0	378		11
12	555.3	557	98.5	100	175.0	179	96.5				380.3	378		12
13	653.8	657	90.2	90	271.5						382.3			13
14	744.0	747	82.9	84							——	——		
15	826.9	831	74.3	74							381.2	382	: mean	
16	901.2	905	69.0	67										
17	970.2	972	58.5	60										
18	17028.7	032	51.7	52										
19	080.4	084	45.5	45										
20	125.9	129	40.6	41										
21	166.5	170	34.8	35										
22	209.3	205	31.4	32										
23	232.7	237	25.0	24										
24	257.7	261	23.3											
25	287.0		19.3											
26	300.1		16.5											
27	316.6		11.4											
28	328.0													
29														
30														
31														
32	17430±5		17410±30 : limit of convergence											

Fig. 1 is an energy level diagram including the new levels and showing the disposition of one of the new series.

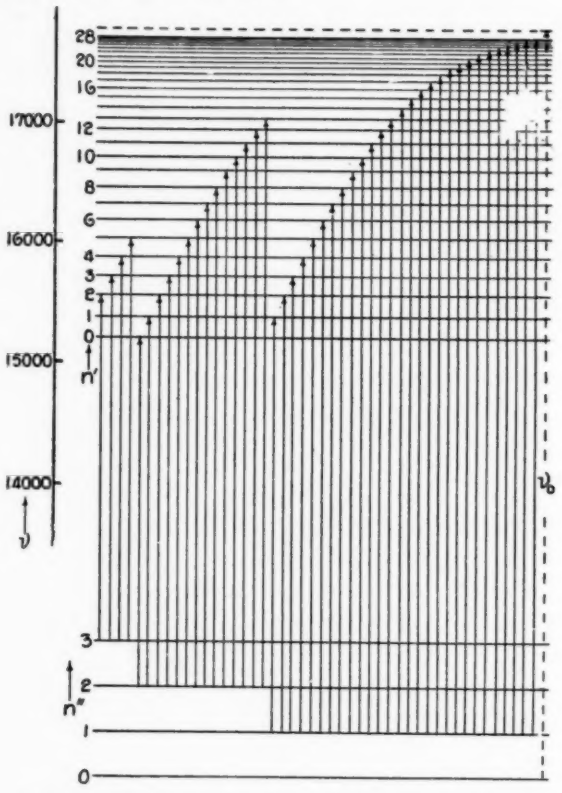

Fig. 1. Energy level diagram for the visible absorption spectrum of ICl.

Besides the heads classified in Table III, there remain out of Table I four additional ones which may be tabulated as follows:

ν	$\Delta\nu'$	$\nu(n''=1)$	$\Delta\nu'$	$\Delta\nu''$
15771.4	140.7	15806.1	141.5	34.7
15912.1	136.1	15947.6	135.7	35.5
16048.2	126.8	16084.1	128.5	35.9
16175.0	120.7	16212.6	121.1	37.6
16295.7		16333.7		38.0

wherein is included a member of the series $n''=2$. By comparison of $\Delta\nu''$s it is seen that there is a rather good agreement between these and a similar group in Table III. There seems to be a real increase in the values of $\Delta\nu''$ together with the increase in ν. This would suggest an isotope effect, but the calculated displacement for this effect corresponding to $\nu=15806$ is 332 cm^{-1}, which is about ten times larger than the above values of $\Delta\nu''$.

This extra series may be due to the existence of an electronic doublet with a separation of about 36.3 cm^{-1}.

Heat of Dissociation of ICl

According to a method developed by Birge and Sponer,[3] the frequency

[3] Birge and Sponer, Phys. Rev. **28**, 259 (1926).

at the limit of a convergent series for a non-polar molecule is given by

$$\nu_D = \nu_{n'} + \int_{n'}^{n_0'} \omega^{n'} dn',$$

where $\omega^{n'}$ is the frequency interval between $\nu_{n'}$ and $\nu_{n'-1}$, and n'_0 is the value of n' for which ω becomes zero. If $\omega^{n'}$ is plotted against corresponding values of n' (in which process $\omega^{n'}$ is to be considered as corresponding to n' rather than to $n'-1$ or the average of the two), the area under the curve

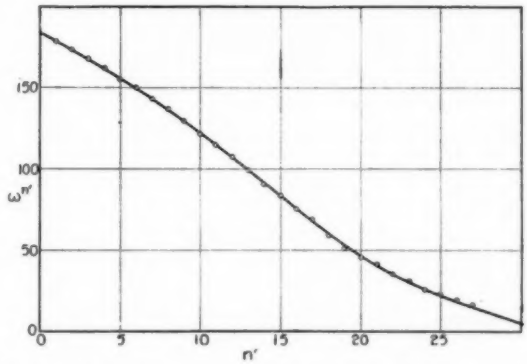

Fig. 2. Curve showing variation of $\omega^{n'}$ with n'.

is a numerical measure of the integral. Fig. 2 is such a curve plotted from Table III. The computed area is 2604.6 units when n' begins at zero. The extrapolated value of ν corresponding to $n'=0$ is 14825.4. Hence,

$$\nu_D = 14825.4 + 2604.6 = 17430.0.$$

The estimated error is about $\pm$ 5 units.
The heat of dissociation becomes

$$D = 2.152 \pm 0.001 \text{ volt} = 49650 \pm 15 \text{ calories per mol.}$$

The new frequency interval furnished by the series for $n''=3$ gives a means of computing ω_0'', the fundamental frequency of the molecule in the normal state. For by fundamental theory,

$$\omega_0''(1-x'') = 381.2; \quad 2\omega_0''(1-2x'') = 381.2 + 379.8 = 761.0.$$

Hence, solving $\omega_0'' = 381.9$ and $x'' = 0.0018$. Finally also, $\omega_0'' x'' = 0.69$. Assuming that this law of convergence holds to the limit, it is easy to compute that the normal series of levels would converge at about the 278th level or about 82100 cm^{-1} from the zero state.

Ratio of Specific Heats

It has been shown by Planck[4] that if ν is the fundamental frequency of vibration of a diatomic molecule, the specific heat at constant volume is given by the equation

$$\frac{C_v}{R} = \frac{5}{2} + \frac{x^2 e^x}{(e^x-1)^2},$$

[4] Planck, La Theorie du Rayonnement et les Quanta, p. 112 (1911).

in which x has been used as an abbreviation for $h\nu/RT$. For a temperature of 100°C, $x=1.466$.

Hence, $C_v/R=3.33$, and $C_p/R=1+C_v/R=4.33$. Therefore, $C_p/C_v=\gamma=1.30$. This value is in close agreement with the mean value 1.31 determined experimentally by Strecker[5] for γ at the same temperature.

Discussion of Fine Structure

Even a casual glance at Table II reveals that the fine structure must be of a simple nature. Aside from an occasional extra line, the measurements consist of three parabolic series corresponding to the three bands heading respectively at 6325, 6385 and 6449A. Fig. 3 is a curve plotted from the data

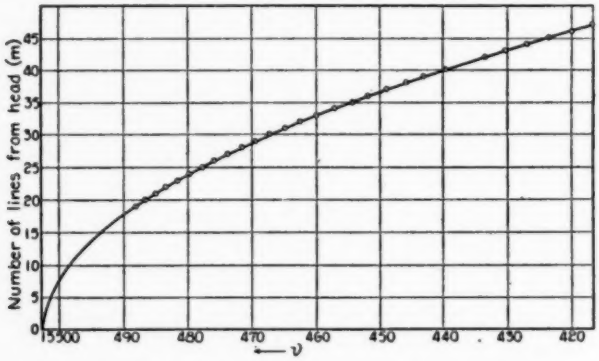

Fig. 3. Typical parabolic curve for fine structure.

for the latter band. The curve has been extended to tangency at the head according to a parabolic law. The data for the other two bands yield exactly similar curves. Unfortunately there is no definite indication of the presence of the null lines, and hence it is impossible to evaluate the frequency interval at the origin, which is necessary to a computation of moment of inertia. However, certain quantitative results may be definitely secured.

In evaluating the constant C of the general band formula, it is immaterial whether the measured lines belong to a P, Q, or R branch, for C is nearly identical for all three types.

For sake of definiteness, let us set for the frequency of any line of the branch in a band $\nu_1=A-2Bm_1-Cm_1^2$. Any other line in the same branch will be given approximately by $\nu_2=A-2Bm_2-Cm_2^2$. Subtracting, $\nu_1-\nu_2=(m_2-m_1)\ [2B+C(m_2+m_1)]$. Let $m_2-m_1=10$. Then, $\nu_1-\nu_2=20[B+C(m_1+5)]$. Similarly, if we set $m_3-m_1=20$, $\nu_1-\nu_3=40[B+C(m_1+10)]$. Both B and m_1 may be readily eliminated so that one obtains $100C=\nu_2-(\nu_1+\nu_3)/2$ where ν_1, ν_2 and ν_3 are the frequencies of lines ten intervals apart in order. This is a very convenient equation for determination of C, and shows that analytically C is a measure of the difference between any frequency and the average value of two frequencies symmetrically situated on either

[5] Strecker, Wied. Ann. 17, 93 (1882).

side. Applying this equation to all possible sets of lines in the three bands, the mean values of C obtained for each band were:

Band Head	15503.0	15657.2	15806.1
C	0.0388	0.0398	0.0412

The physical significance of C as taken here is given by the identity

$$C \equiv \frac{h}{8\pi^2 c}\left[\frac{1}{I''} - \frac{1}{I'}\right],$$

where I' is the moment of inertia in the excited state, and I'' that in the normal state. Comparing values of C for the different bands, it can be readily observed that the value of I' increases as one proceeds toward the limit of the series. This is in agreement with the established correlation between I and ω (the vibrational frequency) which are consistently found to be roughly in inverse proportion. By approximate extrapolation, C becomes 0.035 for $n'=0$ as assigned.

Moment of Inertia

An approximation to the value of the moment of inertia of ICl can be obtained if it is assumed that the assignments of n' are nearly correct. For Mecke[6] has pointed out that the product of the mean value of ω by the mean value of the moment of inertia is nearly equal to the product $\omega'' I''$. Or, $(178+382)(I'+I'')/2 = 382\, I''$; whence, $I' = 1.73\, I''$. Also

$$C = \frac{h}{8\pi^2 c}\left[\frac{1}{I''} - \frac{1}{I'}\right] = 0.035.$$

Solving these two equations simultaneously,

$$I'' = (575 \pm 100)10^{-40}\ \text{g}\cdot\text{cm}^2;$$
$$I' = (995 \pm 200)10^{-40}\ \text{g}\cdot\text{cm}^2.$$

As indicated, these results may be in error by as much as twenty percent.[7]

In conclusion, the writer wishes to express his thanks to Professor Alpheus W. Smith who originally suggested the problem and whose personal interest has been a strong incentive throughout the investigation.

Mendenhall Physical Laboratory,
Ohio State University.
May, 1928.

[6] Mecke, Zeits. f. Physik **32**, 823 (1925).

[7] If we assume momentarily that the extra series tabulated below Table III might be the heads of Q branches belonging to the nearest strong band, a position for the null line of the band at $\nu = 15806$ would be determined. Under this assumption, the value of the constant B turns out to be 1.195; whence, $I' = 23.1 \cdot 10^{-40}\ \text{g}\cdot\text{cm}^2$. This result is only two or three percent. of the approximate value obtained above by another method, and hence we dismiss the possibility of the extra series, being accounted for by Q branches.

THE ABSORPTION SPECTRUM OF LIQUID BENZENE

By James Barnes and W. H. Fulweiler

Abstract

A precision method is described for measuring the wave-lengths of radiation in the near infra-red region of the spectrum using a six-foot Rowland concave grating with a Thalofide cell. The results obtained are believed to be accurate within 0.001μ. With this method the wave-length of an outstanding absorption band of liquid benzene was determined. The frequency of this band together with those of other bands previously measured by the authors substantiate the theory that the absorber of these radiations is a linear anharmonic oscillator, whose energy states are represented by odd multiples of half quanta.

THE wave-lengths of the outstanding absorption bands of liquid benzene in the near infra-red region of the spectrum have been measured in recent years by Ellis,[1] Driesch[2] and Márton.[3] They used prism spectroscopes with thermopiles and their results, which are generally recorded to 0.01μ, are far from being in good agreement. In recent papers the authors[4] have reported their results which were obtained with gratings and by photography in the region less than 1μ in wave-length. With a recording densitometer[5] the wave-lengths of the centers of two outstanding bands of benzene were measured. The values obtained were 0.8744μ and 0.7133μ. Since this was published another band at 0.6060μ was observed and measured. To obtain a satisfactory photograph of this band a column of liquid 4.3 meters in length was used. The above values are believed to be accurate within 0.001μ.

On account of some theoretical considerations we were anxious to extend our measurements into the region greater than 1μ in wave-length and still retain the same degree of accuracy by using the same concave grating which had a radius of six feet and a dispersion of 0.000933μ per millimeter in the first order. Eastman's "Infra-red Sensitive" plates were found to be unsatisfactory in this region. A Hilger thermopile having ten bismuth-silver couples in air was next tried with a sensitive Coblentz galvanometer and a slit width of 1 mm. No measurable deflections of the galvanometer were obtained between 1 and 1.5μ. The work of Case[6] and of Kaplan[7] with the "Thalofide cell" suggested that this detector might be sufficiently susceptible to radiations in this region to use with the grating. It proved to be most satisfactory and the results described below were obtained with

[1] Ellis, Phys. Rev. **23**, 48 (1924).
[2] Driesch, Zeits. f. Physik, **30**, 200 (1924).
[3] Márton, Zeits. f. Phys. Chem. **117**, 97 (1925).
[4] Barnes and Fulweiler, Journ. Am. Chem. Soc. **49**, 2034 (1927), and **50**, 1033 (1928).
[5] Barnes and Fulweiler, J.O.S.A. and R.S.I. **15**, 331 (1927).
[6] Case, Phys. Rev. **15**, 289 (1920).
[7] Kaplan, J.O.S.A. and R.S.I. **14**, 251 (1927).

one of these cells which was kindly loaned to us by Captain H. B. Ely of the Frankford Arsenal, to whom we wish to express our thanks.

Apparatus and Methods

The source of continuous radiation was a 100 C.P. "Pointolite" lamp. The absorption cells, screens and lenses, as well as their disposition in front of the slit of the spectroscope were the same as described in an earlier paper.[4]

The Thalofide cell was rigidly mounted behind an adjustable slit on the camera stand of the Rowland grating mounting. As the stand was moved along its linear track its position was read on a fixed scale. This was calibrated in terms of wave-lengths by means of the second order arc lines of copper and mercury. The linear relationship obtained indicated the accuracy of the adjustments. The whole mounting with slit, grating and cell was enclosed in a large light-proof box. By adjusting the sizes of the holes in the screens in front of the slit the entering beam was limited so that it just covered the ruled portion (5×3.5 cm) of the grating.

The Wheatstone bridge method for observing the change in the resistance of the cell when radiation fell upon it was employed. The circuit which is shown in Fig. 1 was earthed at A. T is the Thalofide cell which had a resistance of 210 megohms in the dark at room temperature. R_1, R_2, and R_3 are resistances comparable in value with that of T. They were made in the usual way by drawing thin lines with india ink on paper between metal clips. E is a Dolezalek electrometer. With 100 volts on the needle the sensitivity was 620 mm per volt at a scale distance of 2 meters—the distance used. With slit widths of 1 mm on the spectroscope and on the cell a battery potential, B, of 45 volts was sufficient to give deflections from 50 to 450 mm in the region between 1.11 and 1.17μ. The results recorded below were obtained in this region as a preliminary run showed that it contained a strong absorption band.

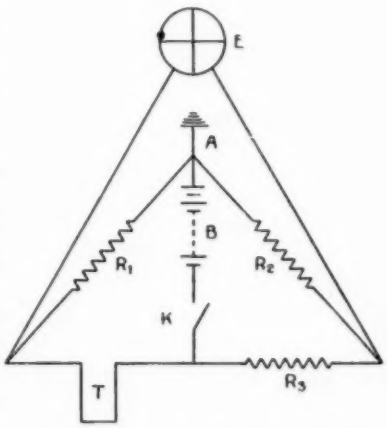

Fig. 1. Diagram of circuit used with Thalofide cell.

When the battery key, K, was closed there was always a small deflection of the needle because of the fact that it was impossible to make the ratio of the resistances T/R_1 exactly equal to R_3/R_2 and also on account of the resistance of the Thalofide cell being slightly lowered when a small current is passed through it. However, within fifteen minutes a position of equilibrium was reached and then the cell worked remarkably satisfactorily under the influence of the small intensities of radiation used. It responded quickly, the zero point remained surprisingly constant and the deflections

produced by radiation of a definite wave-length agreed with one another within one percent.

Preliminary observations with red and infra-red filters placed in front of the spectroscopic slit showed that the influence of second order radiation on the cell was negligible compared to that of the first order in the region investigated. No filters were, therefore, used. It was also observed that the glass windows of the absorption cells had no selective absorption bands but because of reflection and general absorption the transmitted radiation was uniformly cut down about twenty percent for all wave-lengths.

The method of taking observations was to close the key, K, and leave it closed throughout a run, then to set the pointer connected with the cell T on a scale division corresponding to a definite wave-length falling on the cell. A shutter was then raised allowing the radiation to pass through the spectroscopic slit and the maximum deflection read. Dropping the shutter the absorption cell was lowered into place between the screens, the shutter raised and the deflection noted. This observation was repeated. Then the absorption cell was removed and the first observation repeated. The mount was then moved along the scale a few millimeters or less and another set of readings taken and so on throughout the range investigated.

The ratio of the mean of the two middle readings to the mean of the first and last readings gives what we shall call the "transmission ratio" rather than the "transmission percentage" of the liquid in the cell. To calculate the latter it would be necessary to know the amount of radiation lost and gained by internal and external reflection produced by the cell when empty and full. The transmission ratio is, however, sufficient for the determination of the wave-length of the center of an absorption band.

The benzene was purified by washing it ten times with 95% sulphuric acid and once with a caustic soda solution. Then it was steam distilled and fractionated and the middle 70% shaken with mercury. It was then fractionated by freezing until the freezing point was constant which was 5.483°C.

Results and Discussion

The results obtained are recorded by small circles on the curves of Fig. 2. These curves show the variation in the transmission ratio with wave-length for three lengths of benzene with different slit widths as given in Table I.

Table I. *Slit widths and absorption lengths used in obtaining the curves in Fig. 2.*

Curve	Width of slits of Spectroscope and Thalofide cell	Absorption length
A	1 mm	1 mm
B	0.5 mm	11 mm
C	1 mm	20 mm

The broad absorption band shown by these curves has its center at 1.1409μ within $\pm 0.001\mu$. The small rise in the curves at the bottom of these graphs indicates that the band is a doublet. Although the shape and intensity of the components are not known a rough estimate gives 0.008μ as

their separation. This corresponds to a frequency difference of 2×10^{12} sec^{-1} which agrees within the limits of measurement with the frequency difference of the components of the absorption band[8] at 0.8744μ. It is also interesting to note that the shorter wave-length component appears to have the greater intensity. The curves also indicate a very weak absorption band at 1.164μ.

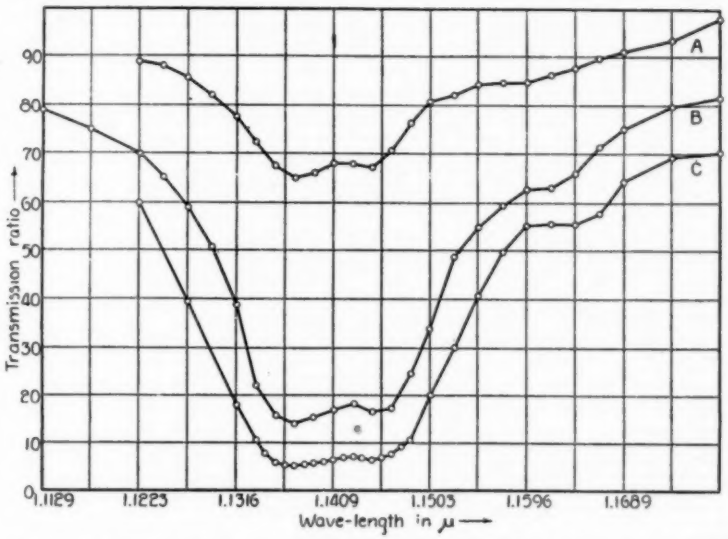

Fig. 2. Variation of transmission ratio with wave-length for three lengths of liquid benzene.

In Table II, the first column, λ, contains the authors' values of the wave-length of the outstanding absorption bands of benzene in the region so far investigated. The second column, $1/\lambda$, gives their wave-numbers reduced to vacuum as obtained from Kayser's "Tabelle der Schwingungszahlen" and by extrapolation for the longest wave-length. The third column gives the differences of the successive wave-numbers. These differences decrease as the wave-numbers increase and, therefore, as the frequencies increase. This is characteristic of radiations emitted or absorbed by an anharmonic oscillator.

TABLE II. *Wave-lengths and wave-numbers of absorption bands of liquid benzene.*

$\lambda(\mu)$	$1/\lambda(cm^{-1})$	Consecutive difference
1.1409	8762	
.8744	11433	2671
.7133	14015	2582
.6060	16497	2482

Extending, by inspection, this approximately harmonic series into the longer wave-length region we get two more bands near 1.7μ and 3.2μ where the series appears to stop. Assuming that 3.2μ is the wave-length of the radiation associated with the fundamental frequency of the oscillator then the

[8] Barnes and Fulweiler, Journ. Am. Chem. Soc. 50, 1035 (1928).

orders, m, of the harmonics are those given in the first column of Table III. Now the formula[9] for an anharmonic oscillator is

$$\omega_m = m\omega_0(1-mx)$$

where ω_m is the wave-number of the radiation absorbed by the oscillator, ω_0 and x are constants. Applying this expression to the four observations given in Table II we get by the method of least squares the following values for the constants.

$$\omega_0 = 3085.8 \text{ cm}^{-1}, \quad x = 0.01823$$

Columns three and four of Table III give the values of the wave-numbers and of the wave-lengths calculated by the above equation. The last column shows the differences between the calculated and the observed values. The agreement is very satisfactory. The wave-lengths of the first two bands as measured by Coblentz[10] (C), Ellis (E), Driesch (D), and Márton (M) and our measurements of the last four bands are given in the fifth column.

TABLE III. *Calculated and observed bands of liquid benzene.*

Order m	Transition quanta	Calculated wave-numbers $\omega_m = 1/\lambda(\text{cm}^{-1})$	Calculated wave-lengths $\lambda(\mu)$	Observed wave-lengths $\lambda(\mu)$	Calc.-Obs. wave-lengths
1	1/2→ 3/2	3030	3.300	3.25 (C) 3.30 (M)	
2	3/2→ 5/2	5947	1.682	1.68 (C) 1.66 (E) 1.688 (F) 1.70 (M)	
3	5/2→ 7/2	8751	1.1422	1.1409	+0.0013
4	7/2→ 9/2	11443	0.8736	0.8744	−0.0008
5	9/2→11/2	14023	0.7129	0.7133	−0.0004
6	11/2→13/2	16490	0.6062	0.6060	+0.0002

If we assume that there exists an absorption band further out in the infra-red than the one at 3.3μ and thereby increase by unity each value of the m's assigned above to the bands we get a negative value for x. This seems unreasonable so we believe that the band with a wave-length approximately 3.3μ, corresponding to a frequency of 90.9×10^{12} sec^{-1}, is the fundamental of this outstanding absorption series of liquid benzene.

Attributing this series to a linear oscillator which may be the molecule as a whole or better a CH group and applying the quantum theory we get for the phase integral over a complete vibration

$$\oint pdq = \oint mvdx = \pi m v_0 x_0 = nh \tag{1}$$

where m, v_0 and x_0 are the mass, maximum linear velocity and maximum linear displacement respectively of the oscillator and n an integer.

The total energy (kinetic and potential) of the oscillator is given by

$$E = mv_0^2/2$$

[9] Cf. Page "Molecular Spectra in Gases" Bulletin National Research Council, pp. 42–45 (1926).

[10] Coblentz, Carnegie Inst. Pub. 35, pp. 76 and 231 (1905).

Hence from Eq. (1)

$$E=n^2h^2/2\pi^2mx_0^2 \tag{2}$$

Now by Bohr's frequency condition

$$E_1-E_0=h\nu \tag{3}$$

If x_0 be considered constant, *whatever the linear velocity*, we get from Eqs. (2) and (3) that

$$\nu=(n_1^2-n_0^2)h/2\pi^2mx_0^2 \tag{4}$$

where ν is the frequency of the radiation absorbed and n_0 and n_1 the quantum numbers associated with the energy levels E_0 and E_1. If only energy changes of one unit at a time are permitted, that is $n_1=n_0+1$, $n_2=n_1+1$, etc, then Eq. (4) becomes

$$\nu=(2n_0+1)h/2\pi^2mx_0^2 \tag{5}$$

which shows that the frequencies absorbed should be proportional to certain integers. That this is almost true is shown by the results given in Table II. If the zero energy state is designated by $n_0=0$ and the next state by $n_1=1$, then by Eq. (5) the fundamental frequency, ν_1, absorbed in the transition $0\rightarrow1$ is equal to $h/2\pi^2mx_0^2$. Let us call this quantity A. The second harmonic which is given by the transition $1\rightarrow2$ where $n_1=1$ and $n_2=2$ has by Eq. (5) a frequency, ν_2 equal to $3A$, and so on for the higher harmonics. We, thus, obtain the relation that

$$\nu_1:\nu_2:\nu_3:\cdots::1:3:5:\cdots$$

which certainly is not the sequence of frequencies and, therefore, of wave-numbers as given in the third column of Table III. If, however, we assign, to the quantum numbers, n, odd multiples of $1/2$ as in the "new" wave-mechanics, then Eq. (5) for the transition $(1/2\rightarrow3/2)$ from zero energy state where now $n_0=1/2$ to state where $n_1=3/2$, gives for the fundamental frequency, ν_1, the value of $2A$. For the second harmonic, $(3/2\rightarrow5/2)$, $\nu_2=4A$, and so on for the higher harmonics. Then we get the relation that

$$\nu_1:\nu_2:\nu_3:\cdots::1:2:3:\cdots$$

which agrees with the observations above except for the small correction term on account of the oscillator vibrating anharmonically. The transition quanta for the various frequencies are given in the second column of Table III.

In conclusion, it may be of interest to calculate the maximum amplitude, x_0 of the oscillator, which is assumed to be approximately constant for the various harmonics. Taking, for example, the fundamental $(1/2\rightarrow3/2)$ where $\nu_1=90.9\times10^{12}$ sec^{-1} and for h, 6.55×10^{-27} erg·sec and assuming that the oscillator is the CH group, then $m=21.58\times10^{-24}$ g, we get for x_0 from Eq. (5) the value $5.8.\times10^{-10}$ cm which is of the order of 1/100 of the average dimension of the molecule of solid benzene as determined by Bragg.

BRYN MAWR COLLEGE, BRYN MAWR, PA. (J. B.)
UNITED GAS IMPROVEMENT CO., PHILADELPHIA, PA. (W.H.F.).
July, 1928.

THE RECOMBINATION OF ARGON IONS AND ELECTRONS

By Carl Kenty

Abstract

Afterglow spectrum in argon due to recombination.—The arc spectrum of argon is found to persist approximately 0.001 sec. after an arc of 0.4 amp. in pure argon at 0.5 mm pressure is cut off. Lines involving jumps from high energy levels are relatively much stronger in the afterglow than in the arc. When sodium vapor is present the *D* lines are strong in the arc but absent in the afterglow showing that the electron speeds in the afterglow are too low to excite the spectrum of argon by direct electron impact. The highly excited argon atoms must therefore be produced by the recombination of ions and electrons. The presence of 0.001 mm of hydrogen does not affect the intensity of the afterglow so that the persistence of metastable atoms is not involved in the production of the afterglow.

Effect of applied potentials on the afterglow.—Accelerating voltages of 3 to 10 volts quench the afterglow during the period of application of 0.001 sec. Retarding after-voltages up to 90 volts have practically no effect. Measurements with an intermittently connected exploring electrode show that the velocities of the electrons are increased by the applied accelerating voltage but unaffected by the retarding voltage. The quenching is apparently the result of the decreased probability of recombination because of the higher velocities of the electrons. When low accelerating voltages have been applied for 0.001 sec. the intensity of the afterglow and the conductivity of the arc space in the period immediately following this application are both greater than they would be had the voltage not been applied. The intensity of the afterglow is thus directly related to the concentration of positive ions and the quenching of the afterglow shown to be connected with a saving up of ions as it should be if the effect of the after-voltages is to prevent recombination.

Ordinary arc spectra are obtained under conditions which are here most unfavorable to the occurrence of recombination. They are presumaly primarily excitation spectra. The use of intermittent discharges for obtaining recombination spectra and strong high series members is suggested.

The measurements show positive ion concentrations in the afterglow of the order of 10^{12} per cc. The mean energy of the electrons is 0.4 volt. From the measured rate of change of the concentration of ions, there results a value of 2×10^{-10} for the coefficient of recombination. This value may be in error by a factor of 5 because of several unavoidable errors.

WHILE experimenting with a rapidly interrupted low voltage arc in argon and using a synchronously rotating sectored disc and a spectroscope, the writer noticed a striking afterglow. This afterglow persisted several thousandths of a second after the arc was cut off, as was shown by varying the time between the cut-off of the arc and the exposure of the slit of the spectroscope.

The argon at a pressure of 0.5 mm was purified and kept pure by circulating it over a misch-metal arc. The mercury diffusion pump used for circulating the gas was placed between two liquid-air traps so that no mercury vapor reached the experimental tube. The arc took place in a bulb 8 cm in diameter, between a hot oxide-coated platinum filament and

a plane tungsten anode, about 1 cm square, mounted 0.5 cm away. The arc current was about 0.4 amp. and the arc voltage 15.5, nearly the ionizing potential of argon.

The afterglow became brighter with the purification of the argon and was found to consist of a large number of bright lines distributed throughout the visible spectrum, and of especial brilliancy in the green. Detailed spectroscopic examination showed that all these lines were arc lines of argon, but with an intensity distribution markedly different from the distribution obtained in the ordinary arc spectrum, the high series members being relatively enhanced in the afterglow.

Spectroscopic Study of Afterglow

The afterglow was photographed with a Hilger glass, constant deviation, spectrograph and with a small Hilger quartz spectrograph. The bulb containing the arc was provided with a quartz window, and the arc space was focussed, by means of a quartz lens, on the slit of the spectrograph. The sectored disc of 10 cm radius revolved a few millimeters in front of this slit, and was so adjusted on the commutator shaft that at the point of cut-off of the arc, the distance yet to be traversed by the edge of the sector before exposure of the slit was about 4 mm. There was thus no possibility of light from the arc itself getting into the spectrograph. The commutator and sectored disc were run at about 1800 r.p.m. and there were two interruptions of current per revolution. The distance of 4 mm thus corresponded to about 0.0002 sec. which was therefore the time between the arc cut-off and the exposure of the slit. Exposures of from 1 to 44 hours were made, some very good photographs being obtained at 12 hours. Eastman Astronomical Green Sensitive plates were used for the green, Cramer Contrast plates for the violet and ultra-violet, Ilford Panchromatic plates for the red and Eastman Extreme Red Sensitive plates for the extreme red. In all about 160 lines were measured on photographs of the afterglow and identified with argon arc lines listed in Meissner's[1] classification of the arc spectrum of argon. Comparison photographs of the afterglow and of the arc showed that, in the afterglow, lines involving jumps from high s and d states to the $2p$ states were very much stronger with respect to $1s-3p$ and $1s-2p$ lines than in the arc. This difference was very striking, and made the two spectra look entirely different at first sight. On arranging the $2p-md$ and $2p-ms$ lines in their respective series and comparing the intensities in the afterglow and in the arc it was found that within each individual series, the high series members were relatively enhanced in the afterglow. Table I shows two such comparisons which are typical of all. This relative enhancement of high series members and the fact that the $2p-md$ lines are relatively so much stronger than the $1s-3p$ lines, indicates that the excited gas producing the afterglow is relatively much richer in atoms in the high excited states than the excited gas in the ordinary arc.

[1] Meissner, Zeits. f. Physik, **37**, 238 (1926); **39**, 172 (1926); **40**, 839 (1926–27).

TABLE I. *Illustrations of relative enhancement of high series members in afterglow. Comparison of direct arc and afterglow intensity of $2p_{10}-md$. Arc exposure = 5 sec; afterglow exposure = 12 hours.*

m	Afterglow Intensity	Direct Arc Intensity	m	Afterglow Intensity	Direct Arc Intensity
5	6	10	5	15	20
6	4	2	6	14	8
7	2	0	7	10	1
8	3	—	8	8	0
9	1	—	9	2	—
10	3	—	10	3	—

Two simple explanations of the production of this afterglow can be offered. (1) The atoms are excited by electrons of high velocity present after the applied voltage is cut off because of a persistence of space charge effects. The different distribution of intensities would indicate a different distribution of velocities from that of the arc. (2) The excited atoms result from the recombination of positive ions and electrons. That (1) is incorrect and (2) is the true explanation is strongly suggested by the observed facts concerning the emission of the D lines of Na.

BEHAVIOR OF THE D LINES OF SODIUM

Quite accidentally, sodium had been introduced along with the oxides used in coating the filament. This sodium was dislodged from the filament fast enough to give a small trace of sodium vapor in the arc space, so that in the arc itself the D lines were the brightest lines in the field of view. In the afterglow the D lines were entirely absent. They could be induced in the afterglow however by the application of arc accelerating voltage of 4–11 volts in the after period. An experiment with an auxiliary arc, having a clean hot tungsten wire for a cathode, and placed about 2 cm away from the main arc, showed that the D lines were emitted strongly in the auxiliary arc provided only that the main oxide filament was lighted. Sodium vapor must therefore have always been present in the arc space.

The argon lines emitted in the afterglow showed the presence of argon atoms in excited states which were only 0.084 volt below ionization, the spectroscopic term values for which were as low as 684 wave-number units ($13\ d_4 = 684\ \text{cm}^{-1}$). Therefore argon atoms were present in the afterglow having energy of excitation of 15.6 volts with respect to the normal argon atoms and of 3.9 volts with respect to the metastable $1s_3$ state of argon, but the absence of the D lines showed that there was no appreciable number of electrons present having energies as great as 2 volts. These excited argon atoms could not therefore have been produced by direct electron impact. The excitation of the D lines by the application of small accelerating voltages is in agreement with this point of view.

The argument is greatly strengthened by the results of the following experiment which was suggested by Professor J. Franck. Hydrogen at a pressure of several thousandths of a millimeter was admitted with no ap-

preciable diminution of the afterglow. This would presumably have precluded the possibility of metastable argon atoms persisting so long. The afterglow is therefore definitely not connected with the presence of metastable atoms. The excited atoms which emit the observed lines could not be produced, therefore, by the excitation of mestastable excited atoms by impact with 3.9 volt electrons but would necessitate the presence of 15.6 volt electrons for their production by single impact. The production of the excited argon atoms by recombination of positive ions and electrons would, however, lead to the emission of the argon arc spectrum, without the emission of the *D* lines, provided the concentration of sodium ions was of a smaller order of magnitude than that of the argon ions.

Discussion of Spectroscopic Results

Miss Hayner[2], using an interrupted arc in mercury vapor, found just such an afterglow as occurs in the present experiment, the high series lines being relatively enhanced in the same way. She also ascribed this afterglow to emission by excited atoms resulting from recombination. Her conclusion that the electron speeds in the afterglow were too low to cause direct excitation was based mainly on the relative weakness of the 2537 line. The argument is somewhat similar to that presented here with respect to the behavior of the *D* lines. It seems to be somewhat more certain in the present case because of the much greater disparity of the voltages concerned.

Mohler[3] has obtained spectra of Cs and K under conditions favorable to the recombination of ions and electrons which he ascribes to recombination. In these spectra there is just such a relative enhancement of the high series lines as is found in the present experiment, and the *F* and *D* series are enhanced relatively to the *S* and *P* series. Mohler also finds continuous spectra in these cases extending beyond the series limits, and a broadening of the lines near the limits. The fact that continuous spectra have not been detected in the present experiment may be connected with the much greater complexity of the argon term system, each continuous region of Mohler's spectra being analogous to a set of ten or a dozen continuous regions in argon spread over a considerable range of wave-lengths. These many overlapping continuous regions would be much harder to detect. Other observers have also found spectra which they ascribed to recombination.[4]

Stroboscopic Study of the Effects of After-voltages

In order to be able to view the afterglow at any point in the cycle, and to study the effects of after-voltages, a stroboscopic device was arranged. This consisted simply of a disc with sectors 2 mm wide cut out to

[2] Hayner, Zeits f. Physik, **35,** 365 (1925).

[3] Mohler, Phys. Rev., **31,** 187 (1928).

[4] Rayleigh, Proc. Roy. Soc., **A108,** 262 (1925) and **A112,** 14 (1926); Paschen, Sitzungsber. d. Pr. Akad., p. 135, 1926; Stark, Ann. d. Physik **52,** 255 (1917); Belasse, Comptes Rendus, **184,** 1002 (1927).

correspond with the commutator segments, mounted on the same shaft as the commutator, and placed about 15 cm in front of the arc. By placing the eye close to the disc and following it around slowly in the direction of its motion, all the different stages of the arc and of the afterglow could be viewed in succession. First the arc itself was a relatively small red ball of light about 1 cm in diameter surrounding the cathode. After the cut-off of the arc, the afterglow could be seen as an intense yellowish green ball of light starting from a diameter of a centimeter or so and very rapidly expanding to fill uniformly a space several centimeters in diameter, and then gradually diminishing in intensity until just before the next cycle it had practically disappeared.

If the disc were viewed from the distance of several feet, the appearance was somewhat as shown in Fig. 1. The area A appears reddish in color and is the area from which light from the arc comes to the eye. Thus A corresponds to the "on" period of the arc. A' is a narrow dark transition

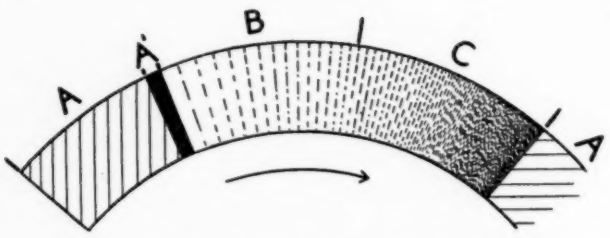

Fig. 1. Appearance of sectored disc rotating synchronously in front of interrupted arc; eye several feet from disc. Period A (0.001 sec) represents direct arc and is red in color. Period A' (0.00025 sec) is a dark transition region. Periods B and C represent the afterglow and are yellow-green in color.

region to be mentioned later. The area represented by B and C together is yellowish green, being illuminated by the afterglow, and is bright at the left side of B, gradually becoming fainter until at the right side of C it is dark. The arrow indicates the direction of motion of the disc. The distance represented by the width of area A corresponds to a time of about 0.001 sec., which is therefore the time of duration of the arc.

The commutator had extra segments which made it possible to apply any desired voltage in period B. With positive voltages, the afterglow was quenched in period B. This effect, beginning at about +2 volts was quite marked at +4 volts and amounted to a complete extinction at +8 volts. With positive voltages greater than 11, the "abnormal" low voltage arc in argon began to appear, so that B was illuminated with reddish light. Negative voltages up to 90 volts, applied in period B had no effect on the afterglow except a very slight weakening in the neighborhood of the cold electrode. This latter result agrees with the results of Miss Hayner.[2]

When the arc space was observed in period C, with the eye close to the disc, it could be seen that the luminosity in this period was increased by

applying positive potentials of 3 or 4 volts in period *B*, but was quenched by applying positive potentials as large as 8 or 9 volts in period *B*.

Reverse potentials up to 90 volts during *B* had no effect on the luminosity in *C*. An auxiliary commutator was now arranged so that a third arbitrary voltage could be applied during period *C*. The currents which could be passed during *C*, with either a small accelerating voltage (3 or 4 volts), or a large negative voltage, were found to increase by as much as 20% when accelerating potentials of 3 or 4 volts were applied in period *B*. On the other hand these currents would decrease from the normal value by about this percentage if a positive voltage of 8 or 9 volts were applied during *B*. Reverse voltages in period *B* up to 90 volts had no effect on the current in *C*.[5] The current which can be passed in period *C* is presumably proportional to the average concentration of ions in the space during that period, so that luminosity and ion concentration are found to go hand in hand, being increased and decreased by the same agency. This is rather striking evidence that the afterglow is connected with recombination, probably more striking, for instance, than if the ion concentration and luminosity were found merely to decay in a way roughly compatible with recombination, in which case the agreement might be fortuitous since obviously both must be falling off with the time.

The afterglow described by Miss Hayner[2] did not appear immediately upon the cut-off of the arc, but appeared only after an intermediate period of about 0.00024 sec., during which time the line 2537, the only line present, fell away in intensity. This intermediate period she explained as a time during which the electron speeds were decreasing, at the end of which they became low enough for recombination to set in. Then followed the afterglow with the high series lines strongly developed. That the same intermediate period exists in the present experiment is evidenced by the narrow dark transition area *A'* between *A* and *B* of Fig. 1. It was found possible to increase the intermediate period to several times its ordinary value by connecting a condenser of 8 mf capacity across the arc. This is, however, nothing more than a method for applying a temporary, changing, positive after-voltage which produces a quenching effect as the steady after-voltages do.

The experiments described below indicate that the positive after-voltages do raise the average velocity of the electrons so that Miss Hayner's explanation of the effect seems to be correct. The width of the normal transition dark space in the present experiment, indicates that certainly within a few ten thousandths of a second after the arc cut-off the electron speeds have fallen to a value low enough to permit recombination. Miss Hayner[2] does not specifically mention any effect of accelerating voltages on the afterglow but does explain the lack of effect[6] of reverse voltages as resulting from a shielding by space charge sheaths.

[5] Eckart, Phys. Rev. **26**, 454 (1925).

[6] See also Compton and Eckart, Phys. Rev., **25**, 139 (1925).

Probe Wire Measurements

Since the probability of recombination presumably decreases with increase of the speed of the combining electrons,[7] the quenching effect of the accelerating voltages applied in the after period can be ascribed to a decrease of the probability of recombination resulting from the speeding up of electrons. The ineffectiveness of large retarding voltages would have to be ascribed to the formation of a space-charge sheath around the negative electrode, outside of which the conditions would be unchanged.

Professor K. T. Compton suggested the use of Langmuir's exploring electrode method to get direct experimental evidence as to the velocities of the electrons. Accordingly a 5 mil probe wire about 3 mm long was placed 1.5 cm from the oxide cathode. Connection to this probe was made through an auxiliary commutator, the brushes of which could be rotated around the shaft as axis to any desired position. The width of the segments and brushes were such that the probe remained in circuit for a time corresponding to a rotation of the shaft of 15.5°. The total angle corresponding to the after-period of the arc was about 60°, so that within the limits defined by a rotation of about 45°, the probe could be put in circuit at any desired time after the arc had been cut off. Probe potentials were measured with respect to the arc electrodes which except in special cases were short circuited during the after period.

Langmuir and Mott-Smith[8] showed that where a single group of electrons is present having a Maxwellian distribution of velocities, and in the case of steady currents, the logarithm of the electron current if plotted against the applied voltage should give a straight line over the range of voltages at which the probe is negative with respect to the space around it. The slope of this straight line gives a measure of the mean speed of the electrons. The method is believed to give reliable measurements of electron speeds also in the present case, where the probe is used intermittently, because experiments with steady arcs using the probe first continuously and then intermittently gave the same type of curves and the same values of electron speeds in each case.

Fig. 2 shows a typical example of a large number of curves obtained with this intermittent use of the probe in the afterglow. In this case the probe was in circuit from 0.00064 sec. to 0.0026 sec. after the arc was shut off. The pressure was 1.6 mm and the arc current 0.4 amp. The curve, although not a straight line, can be compounded fairly well of two straight lines, each one representing a group of electrons having a Maxwellian distribution of velocities. Straight line *I* was drawn first, and from this and the experimental curve, straight line *II* was obtained by subtracting the currents represented by corresponding ordinates. The mean energies of the two groups of electrons as calculated from the slopes of the two straight

[7] Milne, Phil. Mag., **47**, 209 (1924), Mohler.[3]

[8] Langmuir and Mott-Smith, Gen. Elec. Rev., **27**, pp. 449, 538 (1924). A short summary of the method is given by Compton and Eckart,[6] Phys. Rev., **25**, 139 (1925).

lines were 0.9 volt for the high speed and 0.40 volt for the low speed group. It is evident that the choice of straight line *I*, and hence the determination of the mean speed of the fast group is somewhat uncertain. A relatively large change in the slope of this line, however, is necessary to cause an appreciable change in the slope of line *II*, so that the mean speed of the low speed group is probably determined within 10%. The space potential, chosen at 3.6 volts is subject to a probable error of several tenths of a volt.

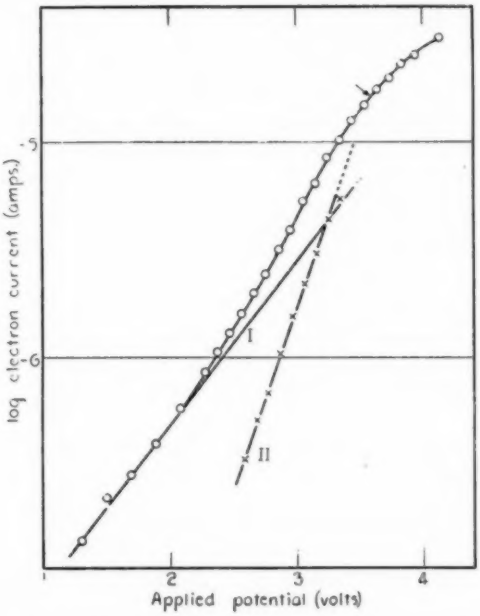

Fig. 2. Current-voltage characteristic of probe, used intermittently in afterglow.

Similar curves taken at various times after the cut-off of the arc, showed that the mean electron speed and the space potential, both being presumably kept up by a positive ion space charge, remained sensibly constant for several thousandths of a second after comparative equilibrium had been reached a few ten-thousandths of a second after the arc cut-off. After this time the currents to the probe became too small for convenient measurement. Currents could usually be measured with a microammeter, a galvanometer being used for currents as small as 10^{-7} amp. More sensitive instruments were not employed, to follow the decay of ionization further, on account of a small transient current, of about 1×10^{-7} amp., which seemed to be caused by capacity or inductance effects accompanying the interruption of the main arc.

Effect of After Voltages on Electron Speeds

With the arrangement of commutators it was possible to take probe measurements in the afterglow superposing any desired after-voltage on

the arc electrodes. These after-voltages were applied during period B (see Fig. 1) which lasted from 0 to 0.003 sec. after the arc was shut off. Connection was made with the probe wire between 0.0006 and 0.0024 sec. after the arc cut-off. Pure argon at 1.6 mm was used in these experiments. The arc current during period A was 400 ma. The results are summarized in Fig. 3. Curve I shows the mean speed of the slow group of electrons plotted against the after-voltage. The slow speed group is presumably the group taking part in the recombination. It is seen from the curve that positive after-voltages above 2 volts increase the electron speeds, while reverse voltages up to 90 volts have no appreciable effect. That the increase in electron speeds sets in only at +2 volts is believed to be due to contact difference of potential between the tungsten anode and oxide coated filament. As the positive after-voltage is increased from 2 to 7.5 volts, the mean speed of the slow group of electrons increases by a factor of 5. The mean

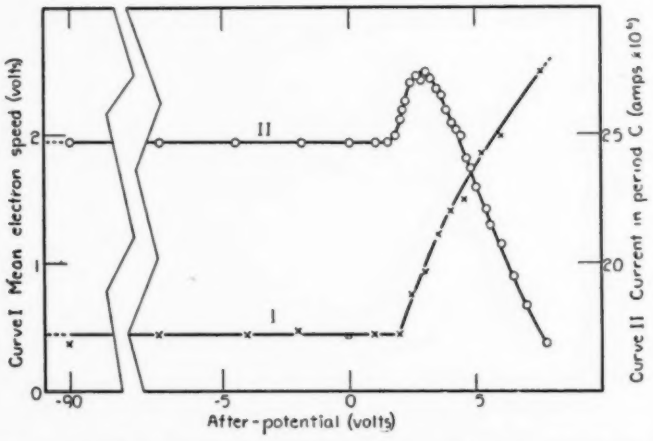

Fig. 3. Effect of after-voltages on electron speeds and subsequent conductivity. I. Variation of mean speed of electrons in afterglow with applied voltage. II. Variation of current in period C with voltage applied in period B. Current is between arc electrodes with accelerating potential of 4 volts.

speed of the fast group was also found to increase from 1 to 6 volts approximately over this range. The quenching of the afterglow by positive after-voltages is now perfectly explained on the theory of recombination since it is certain that the probability of recombination decreases rapidly as the electron speeds increase.[7] The failure of even large reverse voltages to affect the afterglow is thus also perfectly explained, inasmuch as the velocities of the slow electrons and the space potential in the region of the probe are unchanged.

If the ions have been prevented from recombining during period B, there should be more of them left over in period C, provided that they have not been swept out of the space by the same field which speeded up the electrons and provided that the rate of disappearance of ions from the space by recombination is not normally negligible compared with the rate

of disappearance by diffusion to the walls. Curve *II* (Fig. 3) shows the current which could be passed between the arc electrode in Period *C*, with a positive voltage of 4 volts, plotted against after-voltages in period *B*. Large negative voltages were also used in period *C* and quite similar curves were obtained. Such currents are presumably proportional to the average ion concentration in period *C*. It is seen from the curve that negative voltages during period *B* have no effect on the current during period *C*. This agrees with the results of Eckart[5] in a similar experiment with helium. On the other hand, with positive voltages during *B* the currents during *C* are first increased and then decreased, as the voltage is made higher. Moreover, the intensity of the light in period *C* first increased and then decreased in exactly this way. Both phenomena, which are undoubtedly a manifestation of the same thing, are in accord with expectations, the increase in current and light intensity in period *C* being ascribed to a saving-up of the ions during period *B* because of the decreased rate of recombination, the decrease with higher voltages resulting from a sweeping out of the ions by the larger fields. The first of these effects must eventually be outweighed by the second since there are only a limited number of electrons present in the first place. The saving-up effect would be expected to appear before the sweeping-out effect because the rate of recombination decreases rapidly, probably with the fourth power[3] of the electron speeds, or square of the electron energies. The electron energies, however, have been found to increase roughly in proportion to the applied after-voltage over the small range of voltage here considered, so that the rate of recombination should decrease as the square of the after-voltage. On the other hand the rate at which ions are swept out by the field probably increases only in proportion to the applied after-voltage.

The increase of current in period *C* occurs with the application of positive voltages in period *B* which are between 2 and 4 volts. In view of the contact difference of potential, these applied voltages probably correspond to an actual potential drop across the arc space of between 0 and 2 volts. These voltages are too low for the ionization of impurities, or of metastable argon even if present. The increase of current in period *C* must therefore be due to a saving up of ions in period *B* and not to the formation of new ions.

The space potential with regard to the oxide coated electrode was not affected by the application of negative potentials up to 90 volts, but remained at about 3.6 volts above it. A positive ion space charge sheath must in these cases exist around the cold electrode in such a way as practically completely to shield the space from it. The whole applied potential drop must exist between this sheath and the cold electrode. On the other hand when accelerating after-voltages were applied, the space potential did not change with respect to the anode remaining about 3.6 volts above it. Thus in this case there is a shielding space charge of positive ions around the hot cathode. But in this case, however, a large current (10^{-2} amp.) of relatively fast electrons is being shot into the arc space, and since presumably both fast and slow electrons are leaving the arc space the mean speed

of the electrons is raised. With reverse potentials applied in period B, the currents obtained were less than 10^{-4} amp.

In connection with the quenching of the afterglow by positive after-voltages it is interesting to note that Miss Hayner[2] apparently did not make spectroscopic observations with positive after-voltages, and that Eckart,[5] in his account of an experiment with an interrupted arc in helium mentions only one case where he looked for an afterglow and that was with a positive voltage superposed. That he failed to observe a recombination spectrum of helium, similar to the present one in argon, is thus sufficiently in accord with our observations.

The present experiment explains in general why recombination spectra have so seldom been observed. The reason is, evidently, that in most gaseous discharges just such accelerating potentials exist as are found in this experiment greatly to reduce recombination. For instance, in the present experiment, the arc, when run continuously, appeared as a small bright ball of light around the cathode. This ball of light was reddish in color because of the relatively great intensity of the low series members. The space around this ball was nearly dark. Probe wire measurements showed, however, that there was a sufficient concentration of electrons and positive ions in this dark outer space to have made it brilliantly luminous with the light resulting from recombination had the mean speed of the electrons been 0.4 volts instead of 2.5, as measured. This light would moreover have been yellowish green in color because of the relative enhancement of the high series members. The spectrum of the arc itself is emitted from a region where the average velocity of the electrons is high, and where therefore the rate of recombination will be low. The spectrum of the arc must, therefore, be primarily an excitation spectrum, and it is thus easy to understand why, in it, lines corresponding to transitions between low levels are relatively so extremely intense.

The present intermittent method of obtaining spectra resulting from recombination is of advantage because in such experiments these are emitted under circumstances in which the electron speeds are far too low to cause any direct excitation by collision. The resulting spectra must therefore be characteristic only of the recombination process.

The Coefficient of Recombination

The saving-up effect, above mentioned, which is caused by small accelerating after-voltages, shows that the rate of disappearance of ions by recombination is at least of the same order of magnitude as the rate of disappearance by diffusion. It should therefore be possible to obtain an estimate of the coefficient of recombination, α, from measurements of the ion concentration at various times after the arc is cut off. The rate at which ions recombine[9] is given by $dn/dt = -\alpha n^2$, assuming that the concentrations of positive ions and electrons are equal. Integration gives $1/n = \alpha t + 1/n_0$

[9] Townsend, "Electricity in Gases," pp. 188–220.

where n_0 is the concentration at zero time. If $1/n$ is plotted against time a straight line should therefore result, the slope of which will be equal to the coefficient of recombination. A set of measurements of electron concentration was accordingly made by the probe method using Langmuir's expression relating the electron current to the probe at space potential and the electron concentration. The positive ion concentration must have been very closely equal to the electron concentration in these experiments because otherwise a large resultant space charge would have been present which would have been detected by its effect on the space potential. The pressure in this case was 0.8 mm and the arc current was 0.4 amp. The electron concentration decreased from 7×10^{12}/cc to 2×10^{12}/cc in the interval from 0.00025 to 0.0025 sec. after the arc was shut off. The mean electron speed of the slow group of electrons, which was the most important group, remained sensibly constant over this interval, at 0.4 volts. Plotting $1/n$ against t, an approximately straight line was obtained, from the slope of which, α, for electrons of this mean speed, was calculated to be 2×10^{-10}/sec. This value, which, since diffusion has been neglected, represents the upper limit for the coefficient of recombination, may be in error by a factor of 2 because of the uncertainty already mentioned in connection with Fig. 1 in locating the space potential. It may be in error by another factor of 2 because of an uncertainty inherent in the intermittent use of the probe, which although not affecting the measurements of the electron speeds, would affect the measurements of the ion concentration. This uncertainty is evidenced by the fact that currents obtained with the probe used intermittently in a steady arc were about twice as large as those obtained with the probe used continuously in the same arc, considering the ratio of the times during which the probe was connected. The measurements as made however should be consistent among themselves. It is hoped that the present method can be refined so as to give a more accurate determination of the coefficient of recombination, and also by applying suitable after-voltages, to yield quantitative information on the variation of this coefficient with electron speeds.

My best thanks are due to Professor L. A. Turner for his very inspiring guidance throughout the course of this work.

PALMER PHYSICAL LABORATORY
PRINCETON UNIVERSITY
June 29, 1928

THE DIFFUSION OF METASTABLE ATOMS IN MERCURY VAPOR

By J. Horace Coulliette

Abstract

The diffusion of metastable atoms in mercury vapor was studied with a four-electrode tube of special construction, and with short voltage pulses separated by variable time intervals actuating the accelerating and photo-electric gauzes. The change in the rate of arrival of metastable atoms at the outer boundary of a spherical volume of gas was determined as a function of the time elapsed after a number of atoms had been formed at the center. Observations were made at vapor pressures ranging from 3×10^{-9}mm to 0.33 mm. A comparison of the experimental results with the theoretical values for normal mercury atoms under the same conditions shows that the assumptions made by Webb and Messenger that metastable mercury atoms travel across the experimental tube and produce a direct action upon the "photo-electric" plate is correct. It is also found that the effective radius of the metastable mercury atom is about 1.5 times as large as that of the normal atom, and that metastable and normal mercury atoms obey the same general laws of diffusion. Evidence of the loss of energy of excitation as the result of collision between normal and metastable mercury atoms was found.

THE existence of metastable energy levels of the atom was first suggested for helium by Franck and Reiche[1] and is now well established. Several workers[2,3,4] have attempted measurements of the average life of the metastable state for mercury. Webb[5] found, by his alternating current method, that the average time of existence of the mercury atom in the metastable state for any temperature was proportional to the dimensions of the tube, i.e. to the distance through which the metastable atom would have to travel to reach the walls of the tube. He did not find, however, the expected increase in this time with the increase in the vapor pressure of the mercury. In his experiments advantage was taken of the fact that metastable mercury atoms free electrons from a nickel surface. Messenger[6] has confirmed this, and her results show that practically all the "photo-electric" current in a tube of the Lenard type with untreated nickel "photo-electric" plate is due to the metastable atoms or some other material body coming in direct contact with the "photo-electric" surface. The investigation described in this paper was undertaken to clear up the difficulty found in Webb's work, and to get more accurate information in regard to these bodies. The results confirm the assumption that these bodies are metastable atoms; for the sake of clearness they will be referred to as such throughout the discussion. A new method of studying the motion of these metastable

[1] Franck and Reiche, Zeits. f. Physik **1**, p. 154 (1920).
[2] Turner, Phys. Rev. **23**, p. 464 (1924).
[3] Marshall, Astrophys. J., **60**, p. 243 (1924).
[4] Gerlach and Schutz, Phys. Zeits., **26**, p. 33 (1925).
[5] Webb, Phys. Rev., **24**, p. 113 (1924).
[6] H. A. Messenger, Phys. Rev., **28**. p. 962 (1926).

atoms in mercury vapor was developed, which eliminated many of the complicated summations of effects which were necessary in Webb's work.

METHOD

The metastable atoms were produced and studied in a four-electrode tube, a cross-sectional diagram of which, drawn to scale, is shown in Fig. 1. Electrons emitted from a uni-potential hot cathode, F, were accelerated

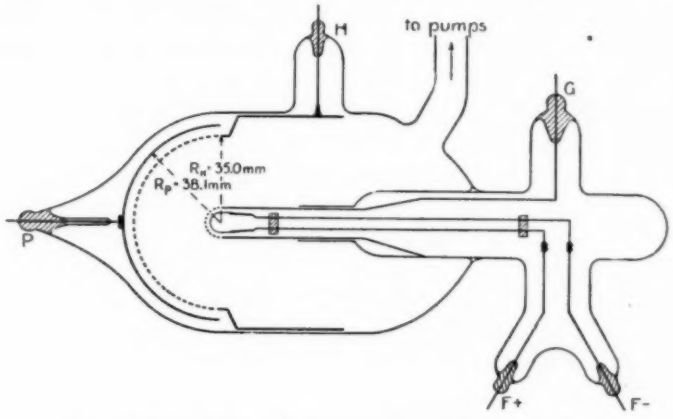

Fig. 1. Cross-sectional diagram of experimental tube.

by a potential difference applied between a hemispherical gauze, G, and the hot cathode. This G-F voltage consists of two parts: first, a constant potential difference just insufficient to produce metastable atoms; second, a voltage pulse of short duration, which we shall designate as the G-F pulse, superposed periodically on the constant potential difference. The metastable atoms were produced during the application of this G-F voltage pulse in the immediate vicinity of the gauze, G, and diffused through the volume of the gas to the detecting system, referred to as the "photo-electric" system, consisting of a nickel gauze, H, and a nickel plate, P. This "photo-electric" system has been shown by Messenger[6] to respond primarily to metastable atoms in a tube of this type with nickel surfaces. No electrons from the hot cathode could reach this system because of the voltage distribution on the electrodes. Between H and P a constant voltage was applied which, acting alone, gave no electrometer current; i.e. the average current to and from the plate due to electrons freed from the plate and the gauze by metastable

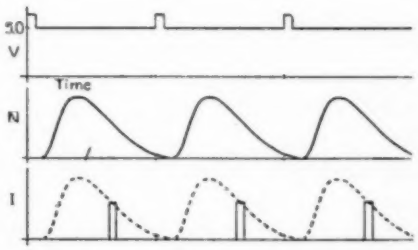

Fig. 2. Metastable atoms are produced during the G-F voltage pulse indicated in Graph V vs Time. The curve N vs Time indicates the rate of arrival of metastable atoms at the plate. The "photo-electric" current indicated in the curve I vs Time is a rectangular pulse, the peak value of which follows the dotted curve as the time interval between the G-F and H-P voltage pulses is varied.

atoms and radiation and due to currents resulting from leakage, etc., was zero. Therefore, when a voltage pulse of short duration was superposed on this constant *H-P* voltage, there resulted a current to the electrometer proportional to the quantity of metastable atoms reaching the "photo-electric" system during this pulse. It should be noted that some part of this current was due to the photo-electric effect of the radiation produced in the tube, but this was usually of negligible amount. By varying the time interval between the *G-H* voltage pulse and the *H-P* voltage pulse the rate of arrival of the metastable atoms at the wall formed by the "photo-electric" surface was determined as a function of the time elapsing since their production at the center of the tube. Fig. 2 illustrates graphically this method and shows the relation between the time of the production of the metastable atoms, their time of arrival at the wall, and the "photo-electric" current produced by them.

Apparatus

The experimental tube was designed to approximate spherical symmetry. The small oxide-coated platinum filament of the uni-potential type described by Webb[5] was located at the center of the sphere. The accelerating gauze, *G*, was a hemisphere of very fine platinum gauze welded over the end of a tube of sheet nickel, diameter 10 mm. The "photo-electric" gauze was a hemisphere of nickel gauze, 35.0 mm radius, mounted on a cylinder of sheet nickel which lined the walls of the glass tube. The "photo-electric" plate was a hemisphere, radius 38.0 mm, spun from a sheet of nickel. This plate was mounted rigidly on a nickel rod sealed into the end of the tube. The entire tube was enclosed in a box which could be maintained at the desired temperature. The system was evacuated by a mercury diffusion pump, pumping continually during observations. The pressure of residual gas was read with a McLeod gauge. Liquid mercury was present in the tube in order to keep the vapor pressure at saturation. The electrical circuits used to produce and apply the *G-F* and *H-P* voltage pulses are shown diagrammatically in Fig. 3. When the frequency of the voltage pulse was greater than 1000 per second a vacuum tube oscillator of the Hartley type, using a 7.5-watt Radiotron, UX-210, supplied the initial excitation wave for the pluse sets; for frequencies less than 1000 per second the oscillator was replaced by a specially constructed commutator. The excitation wave was applied across (see Fig. 3) two non-inductive resistances, R_1 and R_2, and a variable inductance, L_1, connected in series. By properly choosing the values of inductance and resistance in this combination, two voltage waves, differing in phase by 160°, were obtained. These two voltage waves were applied to the grids of the vacuum tubes 1 and 2, respectively. The grids of these tubes were biased so that plate current could flow only during the positive half cycle of the excitation wave. Consequently, the plate currents from the tubes 1 and 2 were half waves roughly rectangular in form. The plate currents from tubes 1 and 2 passed through the resistances, R_3 and R_4, respectively, and the resulting *IR* drops con-

trolled the grids of tubes 3 and 4 respectively. These two tubes gave plate currents more nearly rectangular in form, and differing in phase by 160°. The outputs of both tubes 3 and 4 were put through the resistance R_5, and the resulting IR drop blocked tube 5 completely except for the 20° interval during which no current was flowing through resistance R_5. The plate current from tube 5 was, therefore, a rectangular pulse existing during this 20° of the cycle. This 20° interval was sufficiently short to give the needed resolution. The plate current pulse from tube 5 passed through a non-inductive potentiometer, R_6, and the desired fraction of the resulting IR drop was applied to the experimental tube. The maximum value of L_1 was about 140 mh. The values of the non-inductive resistances R_1 and R_2 were 1500 ohms each, and the values of resistances R_3, R_4, R_5, and R_6 were 20,000 ohms each. The resistances R_7, R_8, and R_9, were 1/2 megohm grid

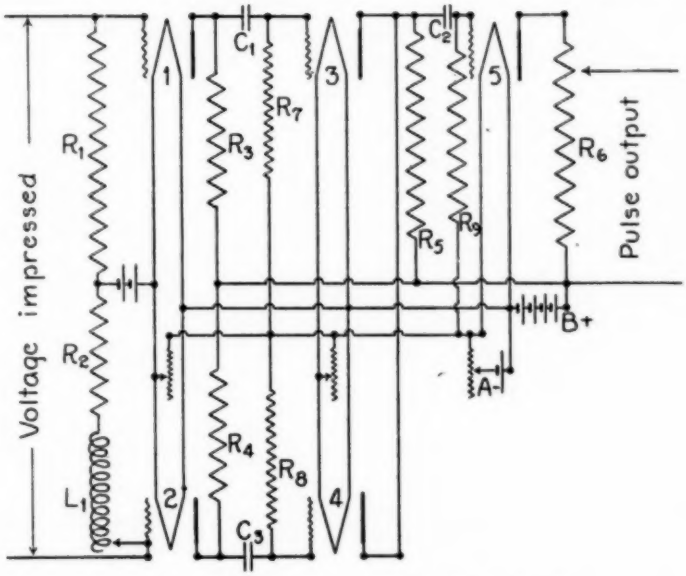

Fig. 3. Diagram of voltage pulse circuit.

leaks. The capacities C_1, C_2 and C_3 were 0.02 microfarad. The tubes 1, 2, 3 and 4 were Radiotrons, type 201-A, and tube 5 was a Western Electric 102-D.

Since all the resistances used were non-inductive the apparatus performed equally well for all frequencies used, when the proper adjustment of the inductance L_1 was made. The circuits diagrammed in Fig. 3 will hereafter be referred to as a voltage pulse set.

Two such voltage pulse sets were used, one for the production of the *G-F* voltage pulse, and another for the *H-P* voltage pulse. The two sets were exactly similar except that in the set for the *H-P* pulse the resistances R_1 and R_2 were 100,000 ohms each, and the inductance L_1 was replaced by a variable condenser. The variation of time interval between the application of the *G-H* pulse and *H-P* pulse was obtained by means of a phase shifting device placed between the exciting source and the *H-P* pulse set.

This phase shifting device consisted of a combination of inductance and resistance connected as shown in Fig. 4. The input wave passed through the inductance L_2 and the resistance R_p. L_2 and L_3 were "Duo-Lateral" coils of 1500 turns each, and R_p was chosen to make $2\pi Mf = R_p$, where f is frequency and M the mutual inductance between L_2 and L_3. The resistance of the output circuit i.e. R_1 and R_2 of the *H-P* pulse set, was made large (more than 200,000 ohms) so that the output e.m.f. consisted approximately of the two components—the IR drop in the resistance R_s and the induced e.m.f. in the coil L_3. By varying the mutual inductance and the resistance R_s simultaneously, it was possible to vary the phase of the output e.m.f. with respect to the input through 90° and the proper adjustment of the two reversing switches extended the possible variation through the full 360° of the cycle. It should be noted that R_p was adjusted for each frequency in order to make the maximum drop in the resistance equal to the maximum induced e.m.f. in the coil L_3. The device was readily calibrated by simple computation of the magnitudes of the values of RI and MdI/dt necessary to give the desired phase angles. These phase angles, as well as the wave form, were checked on a cathode ray oscillograph.

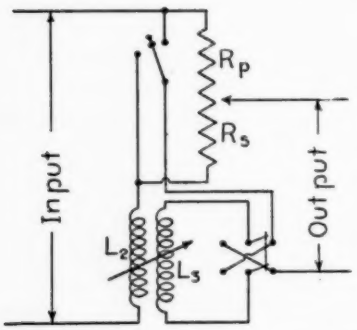

Fig. 4. Diagram of phase shifting circuit.

The special commutator was used to give the exciting voltage for the low frequencies where the values of inductance required by the Hartley circuit became inconveniently large. This commutator was run by a synchronous motor, and was arranged to control both the *G-F* and *H-P* pulse

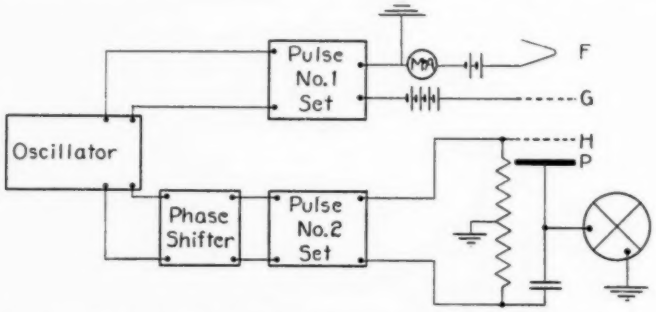

Fig. 5. Schematic diagram of connections to experimental tube.

sets. The two sets were controlled by identically constructed commutator discs mounted on a common axle. Each commutator disc was a bakelite wheel carrying on its periphery twenty-four carefully insulated brass segments. The alternate segments of the commutator disc were connected to a battery through a pair of slip rings in such a way that the device formed a high speed reversing switch. Hence, the voltage impressed on the pulse

sets was rectangular in wave form. The desired phase angle between the waves for the two pulse sets was obtained by rotating one commutator brush with respect to the other about the common axis.

Since the "photo-electric" gauze and plate of the experimental tube form a condenser in series with the electrometer, the application of a pulsating voltage to the gauze, *H*, resulted in a large deflection of the electrometer due to the induced charge. This was eliminated by making the "photo-electric" system one branch of a balanced capacity bridge, as shown in Fig. 5. When balanced, the electrometer deflected only for a current between the "photo-electric" gauze and plate. Fig. 5 shows schematically the complete set of circuits.

Procedure and Results

The procedure for making a set of observations consisted in adjusting the Hartley oscillator or the commutator to give a wave of known frequency, and observing the electrometer readings for various values of time interval between the *G-F* and the *H-P* pulses. A series of observations was made using various values of amplitude of the *G-F* pulse. The apparatus was not sufficiently sensitive to give satisfactory resolution in curves taken when using peak values of less than 5.6 volts (4.9 volts d.c and 0.7 volt pulse) for the *G-F* voltage pulse. Various values of this peak voltage gave curves that were identical in form. Hence measurements were made using values of peak voltage chosen to give electrometer readings within a convenient range. The curves obtained by plotting the time intervals versus the electrometer readings showed the variations in the rate of arrival of metastable atoms at the "photo-electric" plate with the time which had elapsed since their production.

The experimental results are illustrated by typical curves given in Figs. 6 to 9. Figure 6 gives the results for a mercury-vapor pressure in the experimental tube of 3×10^{-9} mm, mean free path 50,000 cm, temperature of the walls of the tube $-80°$C. Figure 7 gives results for vapor pressure of 5.4×10^{-4} mm, mean free path 13.5 cm, temperature of walls 10°C. Figure 8, Curve *B*, gives the results for vapor pressure 0.0013 mm, mean free path 5.7 cm, temperature of walls 20°C. Figure 8, Curve *C*, gives results for vapor pressure 0.0051 mm, mean free path 1.5 cm, temperature 37°C. Figure 9 gives results for vapor pressure 0.036 mm, mean free path 0.25 cm, temperature 65°C.

Discussion of Results

In studying these curves we must divide them into three groups: (a) those made at low temperatures at which the metastable atoms made a negligible number of collisions in traversing the tube: (b) those made at intermediate temperatures, at which the number of collisions made by any metastable atom in crossing the tube is small, a considerable number making no collisions: (c) those made at high temperatures, at which practically all metastable atoms made a number of collisions, and the laws of gaseous diffusion are expected to apply.

For Group (a), the dimensions of the vessel are very small in comparison with the mean free path, and the greater portion of the metastable atoms starting from the center of the vessel reached the walls without collision with other mercury atoms. When the metastable atoms start at the center of the spherical walls, their arrival is determined simply by the radius of the sphere and their speeds. With a Maxwellian distribution of velocities, the number having velocities between c and $c+dc$ is given by

$$4\pi N_0(hm/\pi)^{3/2}e^{-hmc^2}c^2dc$$

where N_0 is the total number starting, h a constant of kinetic theory, m the mass of atom. Hence the number N_t arriving during the interval between t and $t+dt$ is proportional to $(1/t^4)e^{-hmL^2/t^2}$, where D is the radius of the spherical wall.

When the mean free path of an atom is small in comparison with the dimensions of the sphere, (Group (c)), each metastable atom makes a large number of collisions with normal mercury atoms, and the rate of arrival at the wall is computed by the ordinary laws of diffusion of one gas in a second gas. For an approximate solution we consider the walls to form a closed sphere, near the center of which the metastable atoms are released during a negligibly short time interval. Assume the metastable atoms to be formed uniformly throughout a small sphere of radius a, and let the walls be a concentric sphere of radius b. The diffusion equation for the case of spherical symmetry is, if K be written for the diffusion constant of the metastable atoms in mercury vapor:

$$K\frac{\partial N}{\partial t}=\frac{\partial^2 N}{\partial r^2}+\frac{2}{r}\frac{\partial N}{\partial r}.$$

and assuming that metastable atoms become normal atoms on striking a metal wall (as shown by the results of Group (a), to be discussed later) the boundary conditions are: when $r=0$, N is finite, when $r=b$, $N=0$; when $t=0$, $N=f(r)=C$ (constant) for $r=0$ to $r=a$; and $N=f(r)=0$ for $r=a$ to $r=b$.

The solution is

$$\begin{aligned}N&=(\alpha r)^{-1/2}J_{1/2}(\alpha r)e^{-\alpha^2 t/K}\\&=(2/\pi)^{1/2}\sum A_\alpha(\alpha r)^{-1}\sin(\alpha r)e^{-\alpha^2 t/K}\\&=\sum(A_p/r)\sin(\alpha r)e^{-\alpha^2 t/K}\end{aligned}$$

where $A_p=(2/b)\int_0^a r\sin(p\pi r/b)\,dr$

Evaluating this integral we find

$$N=\frac{1}{r}\sum\frac{2b}{p^2\pi^2}\left\{\sin\frac{(p\pi a)}{b}-\frac{p\pi a}{b}\cos\frac{(p\pi a)}{b}\right\}\sin\frac{(p\pi r)}{b}e^{-Kp^2t\pi^2/b^2}$$

The rate of arrival of metastable atoms at the spherical boundary, C, is proportional to dN/dr for $r=b$.

Therefore

$$C=[\text{const}\ dN/dr]_{r=b}$$

and

$$C=(\text{const})\frac{1}{b}\sum\frac{2b}{p^2\pi^2}\left\{\sin\frac{(p\pi a)}{b}-\frac{p\pi a}{b}\cos\frac{(p\pi a)}{b}\right\}\frac{p\pi(-1)^p}{b}e^{-Kp^2\pi^2t/b}$$

The dimensions of the experimental apparatus are such that $a=0.63$ cm, and $b=3.80$ cm. Substituting these values we find the required relationship between the time interval between the G-F and H-P voltage pulses and the arrival of metastable atoms at the walls.

When the mean free path of the diffusing metastable atoms is of the same order of magnitude as the minimum possible path in the experimental tube (Group (b)) the theoretical treatment becomes very complicated. Some of the atoms cross the tube without making any collisions, while others make one or more collisions while travelling to the "photo-electric" plate. The fraction of the total number of atoms which have travelled a

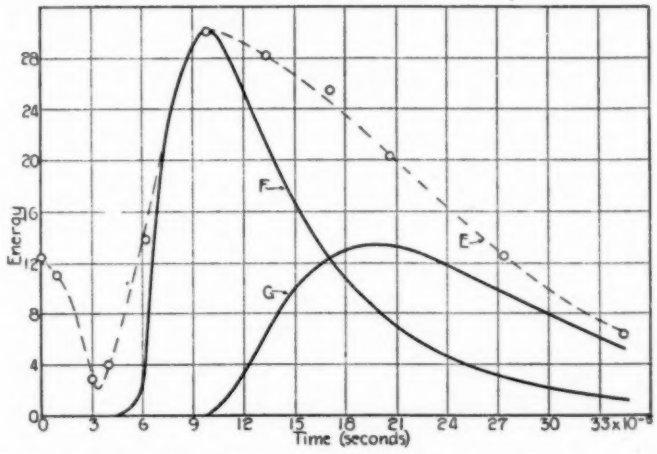

Fig. 6. Curve F gives theoretical arrival of metastable atoms travelling with Maxwellian velocity distribution for $T=770°$K. Curve G gives arrival of atoms travelling with Maxwellian velocity distribution for $T=193°$K. Curve E is the summation of Curves F and G.

distance greater than r since their last collision[7] is approximately e^{-r/λ_c} where λ_c is the mean free path of the metastable atoms. From this we may make an estimate of the percentage of the metastable atoms crossing without collisions. In the above relationship, two atoms are said to collide when they approach so that the distance between their centers is equal to the sum of their radii. This definition of a collision permits a very wide variation in the resulting path deflections.

The points plotted in Fig. 6 show how the metastable atoms arrived at the "photo-electric" plate with respect to time, when the walls of the tube were kept at the temperature of solid carbon dioxide (193°K). The small maximum in the curve at $t=0$ is due to radiation, probably λ2537 as the "photo-electric" surface is slightly sensitive to this radiation. The persistance of this radiation is, however, in all cases so short that it has ceased to produce appreciable effect before the metastable atoms begin to reach the surface in appreciable number. The breadth of this radiation maximum in Fig. 6 is due, not to great persistance, but to the resolution

[7] Jeans, Dynamical Theory of Gases, p. 158.

of the apparatus. (The persistance of λ2537 at this temperature is of the order of 10^{-7} seconds as determined by direct tests made in this laboratory but not yet published.) This maximum was present in all the experimental curves, but, since our primary interest is in the metastable atoms, it has been omitted from all other curves to avoid complication. The remainder of the curve is readily explained by assuming that 60% of the metastable atoms have a mean velocity corresponding to the temperature of the hot cathode, while 40% have a mean velocity corresponding to the temperature of the walls of the tube; the velocity of the metastable atoms being taken the same as for normal mercury atoms at the corresponding temperature. The temperature of the hot cathode was estimated from a rough comparison with an optical pyrometer to be about 770°K. Curve *F* shows the computed arrival of those atoms travelling with velocities having a Maxwellian distribution determined by the temperature of this hot cathode. Curve *G* shows the computed curve for the arrival of those atoms travelling with velocities determined by the temperature of the walls of the tube. The curve *E* is the summation of the curves *G* and *F*. It will be noted that the experimental points, shown by circles, fall very closely on the summation curve *E*. The close agreement here seems to show, first, that the metastable atoms and the normal mercury atoms have the same velocity distribution for a given temperature; second, that the metastable and the normal mercury atom have the same mass; and third, that the metastable atom changes to a normal atom immediately upon striking the metal walls of the vessel. The possibility of any considerable number of metastable atoms reflecting from the walls without losing their energy of excitation is eliminated, because such reflection at this vapor pressure would increase the average time interval between excitation and the delivery of the energy of excitation at the "photo-electric" plate by at least 1.5 times, and the curve indicates no considerable number of atoms arriving after such a lengthened time. Foote and Mohler[8] have suggested that an excited atom may combine with a normal atom to form an Hg_2 molecule. If the excited bodies arriving at the "photo-electric" plate were Hg_2 molecules, which dissociated upon arrival and delivered the excitation energy to the plate, the abscissae of the curve would be multiplied by the factor 1.4. We conclude, therefore, that we are dealing with metastable atoms at least in the case of this low pressure.

The experimental curve obtained when the walls of the tube were kept at 10°C is shown in Fig. 7. Curve *D* represents the computation for the time of arrival of those metastable atoms which cross the tube without making any collisions, assuming that 60% of these atoms have the same temperature as the hot cathode, and 40% have the same temperature as the walls of the tube. The ordinates of this curve are adjusted to fit the early part of the experimental curve as closely as possible. The difference between the experimental curve and Curve *D* is shown by Curve *C*. This curve, *C*, is approximately a Maxwellian velocity distribution, and is interpreted to represent the arrival of those metastable atoms which have undergone

[8] Foote and Mohler, Origin of Spectra, p. 106.

large deflections in crossing the tube. The number of collisions indicated by the area under Curve C is less than the number which would be predicted by the kinetic theory, because it does not include those atoms which were only slightly delayed in reaching the plate, as for example those atoms

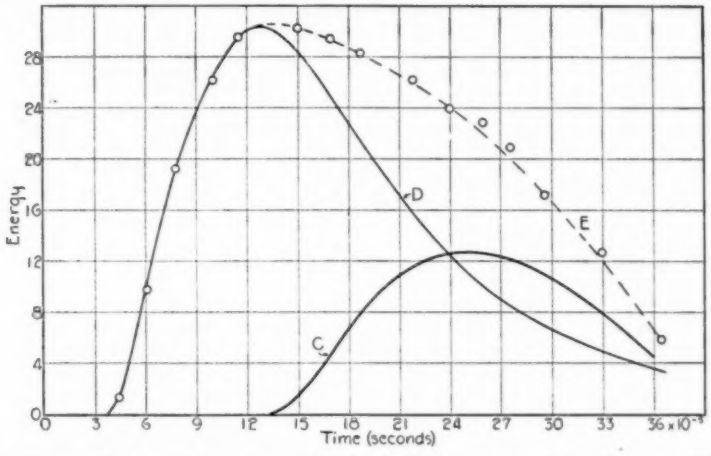

Fig. 7. Curve D gives the computed arrival of atoms crossing without collisions in gas at $T=283°K$. Curve E gives the experimental curve for gas at $T=283°K$. Curve C is the difference between Curves E and D.

which underwent only a small change in direction. The area under Curve D is 72% of the total area under the experimental curve. This gives us an upper limit for the number of metastable atoms crossing the tube without collision. The corresponding mean free path, λ_c, calculated from e^{-r/λ_c} fixes

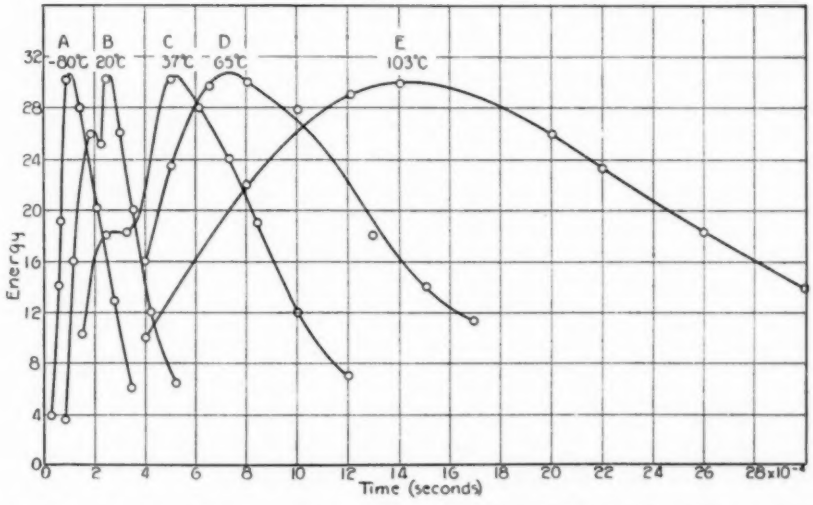

Fig. 8. Experimental curves for temperatures −80°C, 20°C, 37°C, 65°C and 103°C.

a lower limit for the effective diameter of the metastable atom which is 1.3 times the diameter of the normal mercury atom.

The curves B and C in Fig. 8 give the observations at 20°C and 37°C, and are typical of the range of pressure denoted as Group (b). The curves

A to E show graphically the transition from the range of low pressure represented by the curve for $-80°C$, Curve A, to the range of high pressure represented by the curves for 65°C, and 103°C, Curves D and E. No attempt has been made to compare the curves of Group (b) with theory quantitatively, because we do not understand the mechanism of the collisions sufficiently well. The general form of these curves indicates that the behavior is somewhat as we would expect, since the increase in the average time of arrival of the metastable atoms at the walls follows the increase in vapor pressure. The curves of this group indicate, in general, that some atoms cross the tube without making collision, while others make several collisions and are greatly delayed in arriving at the walls of the tube. Other curves taken in this intermediate range show even more marked complexity.

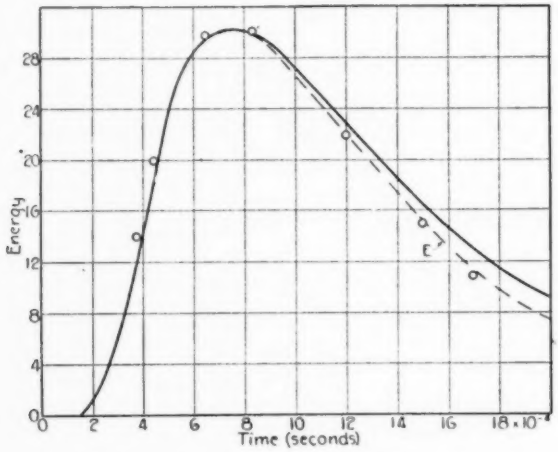

Fig. 9. Continuous line gives the computed curve for the arrival of diffusing metastable atoms when Diffusion Constant = 1700. Circles indicate observed values for temperature of gas 65°C.

For vapor pressures at which the diffusion process is the determining factor we get curves such as that shown in Fig. 9. The experimental curve E, (dotted) taken at 65°C, is in good agreement with the curve (solid line) computed from the diffusion equation given above. The value of the diffusion constant used in plotting the computed curve was chosen to give the best possible agreement with the experimental data.

Table I gives certain data for the curves discussed above. The temperatures used are listed in Column 1, and the corresponding number of atoms per cubic centimeter appears in Column 2. Column 3 shows the radius of the tube divided by the mean free path of the normal mercury atom, and Column 4 shows the same quantity for the metastable atom, assuming its diameter to be 1.5 times as large as that of the normal atom. For Groups (a) and (b), Columns 5 and 6 show the value of the quantity e^{-r/λ_c} (the fraction of the number of atoms crossing without collision) for the normal and metastable atoms, respectively. For Group (c), Column 5 shows the value of the diffusion constant D calculated from $D = 0.152/\nu\sigma^2(hm)^{1/2}$

TABLE I. *Data for curves of Figs. 6, 7, 8, 9.*

Temp.	Number of atoms per cc.	Radius of Tube ÷ mean free path: Normal Atom	Radius of Tube ÷ mean free path: Metastable Atom	$e^{-r/\lambda c}$: Normal Atom	$e^{-r/\lambda c}$: Metastable Atom	Diffusion Constant: Normal atom	Diffusion Constant: Metastable atom	Diffusion Constant: Experimental
	Low temperature range. Group (a).							
−80°C	1.50×10^{18}	7×10^{-5}	1.6×10^{-4}	1.00	1.00			
10°C	1.84×10^{13}	.26	.58	.79	.56			
20°C	4.33×10^{13}	.61	1.37	.56	.26			
	Intermediate temperature range. Group (b).							
27°C	7.6×10^{13}	1.07	2.4	.35	.09			
37°C	1.6×10^{14}	2.30	5.2	.11	.005			
	High temperature range. Group (c).							
65°C	1.05×10^{15}	15.2	34.2			2660	1930	1700
71°C	1.60×10^{15}	23.3	52.5			1760	1275	1190
103°C	8.43×10^{15}	121.	272.			351	253	750

given by Jeans[9] as the best value. Here ν is the number of atoms per cubic centimeter, σ is the diameter of the normal mercury atom, m is the mass of the atom, and h is a constant. Column 6 gives the values of the constant calculated for the interdiffusion of normal and metastable mercury atoms, when the diameter of the metastable atom is assumed to be 1.5 times as large as that of the normal atom, using the relationship $D_{12}=(c^2_1+c^2_2)^{1/2}/3\pi\nu S^2_{12}$. Here c_1 and c_2 are the mean velocities of the normal and metastable atoms, respectively, and S_{12} is the average of the diameters of the normal and metastable mercury atoms. Column 7 gives the values of the diffusion constant which were found by trial as best fitting the experimental curves, assuming only the processes of pure diffusion to be acting.

The value of the diffusion constant which best fits the experimental curve for 65°C is 1700. Substituting this value in the equation for D_{12} given above, the value of the effective diameter of the metastable atom is found to be 1.6 times that of the normal atom. The value of the diffusion constant which is best fitted to the experimental curve may, however, be too small, since the "photo-electric" plate was a hemisphere placed at the end of a cylindrical tube while the computation of the theoretical curve was made for a closed spherical volume. It is estimated that the error due to this fact is not more than 10%, which would accordingly reduce the estimated diameter. Taking 1.6 as the upper limit, and the value 1.3, determined from the 10°C curve, as the lower limit of the ratio of the diameters of the metastable and normal mercury atoms, we would estimate this ratio to be 1.5, which gives the effective diameter of the metastable mercury atom, 4.5×10^{-8} cm $\pm 0.5\times10^{-8}$ cm.

It is of interest to compare this estimate of the diameter of the metastable atom with the diameter of the excited mercury atom as determined

[9] Jeans, Dynamical Theory of Gases, p. 318.

from the quenching of resonance radiation and other methods. Stuart[10] estimates the diameter of the 2^3P_1 excited atom to be about three times as large as the normal atom, while Foote[11] estimates it to be 1.3 times as large. The experimental values of the diffusion constant, found above, again require the rejection of the idea that the excited body transferring energy to the "photo-electric" plate is an Hg_2 molecule, since the molecule having a mass and a radius each twice that of the normal atom would require a diffusion constant about 1/5 as large as the experimental values.

The experimental value of the diffusion constant for 103°C is 750. A comparison of this with the value 253 computed for the metastable atom having a diameter 1.5 times as large as that of the normal atom indicates that some process other than diffusion must be involved. Such a process may be collision of the second kind between the normal and metastable atoms, resulting in the destruction of the metastable state. An approximate calculation shows that a decay factor corresponding to one dissipative collision in 1300 will bring the computed curve into fair agreement with the experimental observations. This value of the dissipative factor is of the same order of magnitude as that found by Zemansky[12] in his work on the quenching of resonance radiation. Another possible process of dissipation of the energy of the metastable atoms is the formation, as the result of collisions, of Hg_2 molecules which strike the "photo-electric" plate without dissociation and without giving up their excitation energy to the plate. That this dissipation is not due to the presence of foreign gases seems certain, since throughout the experiment the tube was connected to the pumping system and the gauge showed less than 0.0001 mm residual gas pressure.

It appears that the failure of Webb[5] to find the expected variation in the time of diffusion with pressure was due to the form of the tube used (and perhaps in some degree to the dissipative action of foreign vapors arising from the greased joints in his experimental tube).

Summarizing the results discussed above we find that the metastable carrier of energy is a metastable mercury atom having a radius 1.5 ± 0.2 as large as that of the normal mercury atom. The velocity distribution at a given temperature is the same for the metastable atoms and the normal mercury atoms. A metastable atom loses its excitation energy immediately upon striking the metal walls of the tube. There is a strong indication of a dissipative process in which one collision in thirteen-hundred with normal mercury atoms results in the metastable atom losing its excitation energy.

In conclusion I wish to express my indebtedness to Professor H. W. Webb, at whose suggestion and under whose guidance this work was done. Thanks are also due to Dr. F. G. Slack and Dr. D. R. White for their assistance in checking the computations.

COLUMBIA UNIVERSITY
July, 1928.

[10] Stuart, Zeits. f. Physik **32**, 262 (1925).
[11] Foote, Phys. Rev. **30**, 288 (1927).
[12] Zemansky, Phys. Rev. **29**. 521 (1927).

TEMPERATURE OF THE CATHODE AS A FACTOR IN THE SPUTTERING PROCESS

By L. R. Ingersoll and L. O. Sordahl

Abstract

Effect of high cathode temperatures on the rate of sputtering of metals.—Gold, platinum and nickel show an increase in the rate of sputtering in argon with increase in cathode temperature. The lower the sputtering voltage the more pronounced the effect. Films sputtered from a hot cathode show considerable initial aging, i.e., suffer less change in resistance on baking and show a more definite crystal structure than those from a cold cathode. While evidence is presented to show that the "explosion theory" of sputtering may have a certain basis of fact, especially as regards starting conditions, the results are, on the whole, consistent with the explanation of sputtering as essentially a vaporization process. The indications are, however, that ordinary evaporated films, even when produced under the same pressure as sputtered films, contain less gas, pointing to the excitation accompanying the discharge as an important factor in the process of gas occlusion in the films.

Introduction

A SURVEY of present day theories[1] of the process of cathodic sputtering readily leads one to the conclusion that the temperature of the cathode ought to be a factor in the rate of sputtering. Previous experimental evidence, however, does not support this conclusion. Grandquist,[2] sputtering from platinum cathodes in air at temperatures up to "red heat," found substantially the same amount of metal lost by the cathode at the higher temperatures as at the lower ones. Blechschmidt,[3] sputtering silver in hydrogen at 1500 to 2000 volts got the same deposit with the cathode at 500°C as at room temperatures. Feeling that this could hardly represent the general law and that a more thorough study of the problem was called for, we carried out the following experiments.

Experimental

A large series of films, over four hundred in number, were sputtered from cathodes of nickel, platinum and gold in a residual atmosphere of argon. A few nickel films were also made in hydrogen. The cathode C, Fig. 1, was in the form of a hairpin strip which could be heated by battery current to 1000°C or higher. The anode A was a square hollow copper block, cooled by circulating water. On its four sides were fastened the $22\times36\times0.25$ mm pieces of microscope coverglass F on which the films were deposited. The anode was carried by a ground joint which allowed

[1] For good summaries and references see A. Güntherschulze, Zeits. f. Tech. Physik **8**, 169 (1927); Zeits. f. Physik **36**, 563; **37**, 868; **38**. 575 (1926): A. v. Hippel, Ann. d. Physik. **80**, 672; **81**, 1043 (1926): E. Blechschmidt, Ann. d. Physik **81**, 999 (1926): T. Baum, Zeits. f. Physik **40**, 686 (1927). For a resume of earlier work see V. Kohlschütter, Jahrb. d. Radioakt. u. Elekt. **9**, 355 (1912).

[2] See Kohlschütter, reference 1, p. 384.

[3] See Blechschmidt, reference 1, p. 1015.

each glass in succession to be turned towards the cathode and at a distance of 9 mm.

Sputtering chamber. This was a cylindrical glass jar large enough (14×24 cm) to avoid the complications due to surface charges. The joint at the top was sealed with gasket and wax, allowing the vessel to be withdrawn readily for the removal of a set of films. The metal and glass tubes were sealed in with De Khotinsky cement. The whole was frequently baked at 300°C with a fair vacuum inside, the joint and brass top-plate on such occasions being water-cooled.

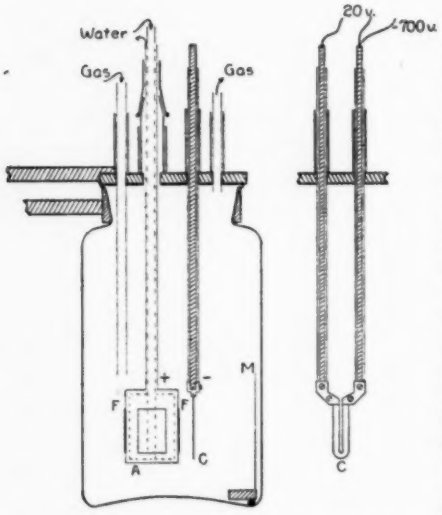

Fig. 1. Diagram of sputtering chamber.

During sputtering the residual gas, argon, was allowed to flow slowly through the chamber, being drawn off by a Hyvac pump. The argon was very good (A 98.2%, N_2 1.4%, O_2 0.4%) but was further purified by passage over magnesium turnings at about 600°C, and in most cases also through a copper and copper-oxide purifying system. These precautions, while perhaps not absolutely necessary, seemed desirable as we had previously found that a small percentage of impurity in the residual gas may produce a marked effect on the deposit. The chamber further had liquid-air traps on both inflow and outflow sides, and in view of the continual flow of gas—inflow tube almost down to the film— and the relatively high pressure (about 1/3 mm) it was not considered that wax vapors from the joint could produce any contamination.

Cathodes. These were 99.5% nickel, Baker furnace platinum and very pure gold, respectively. The nickel cathode was of 0.1 mm strip in the form of a hairpin about 12×46 mm overall with 1 mm between the inside edges of the strip. The platinum and gold were somewhat thinner.

Temperatures were measured with an optical pyrometer. To keep a small area of the side wall of the chamber free of deposit for this purpose, a small mica shield *M*, magnetically operated, was arranged. The "cold" temperatures of the cathode, i.e. no heat input save that due to the discharge, were calculated from radiation considerations and from measurements on the increase of the dark space as the strip heated with the discharge. The two methods gave concordant results of from 150 to 360°C according to circumstances. The unheated parts of the cathode, i.e., aluminum leads, nickel clamp, etc., were sheathed with glass or mica and were specially designed to give a minimum of exposed area.

Films. The sputtering was all done with the aid of a small d.c. dynamo, the potential, for reasons which will appear later, being relatively low,—

from 500 to 800 volts. The films were all deposited in sets of three, the fourth being a blank used in connection with the adjustment of discharge conditions. In general the first and third films were made under identical conditions, cathode cool, say, the second film then being with cathode hot. To secure uniformity of results it was found best to precede each film by several minutes of sputtering on the blank under exactly the same conditions as were to be used in making the film.

All films were sputtered with cathode dark space as nearly as possible 7 mm, or about three-quarters of the distance cathode to film. This necessitated a somewhat higher pressure, about 0.40 mm at the high-temperature sputtering, than the 0.24 mm used with the cathode cool. When correction was made for the fraction of the cathode not subject to heating, it was found that the "net" sputtering current (around 6 milliamp.) was, for a given voltage, almost exactly the same in the hot and cold cases. The time of deposition varied greatly but was usually from 15 to 30 minutes.

While in the preliminary results the film thickness measurements were on the basis of optical density determinations, all the final data depend on direct weighings of the deposits. As the mass of the piece of film under test was usually only a few tenths of a milligram, careful micro-balance weighings were necessary, and for these we are indebted to Mr. Rex Robinson of the Department of Chemistry of this University. The glass on which the film was to be deposited was acid-washed and, generally, baked at 600°C. After sputtering, a small section, one or two sq. cm in area and of nearly uniform density, was cut from the film and then baked (so that the hot- and cold-sputtered films might be on the same basis as regards gas content) at 475°C for a few minutes in 2 mm of argon. The film-on-glass was then weighed, the film removed with acid and the glass alone weighed. All weighings were repeated, the two determinations usually checking to 0.002 mg.

Evaporation. It is obvious that if the cathode is heated to a sufficiently high temperature ordinary vaporization will begin to play an important part. This effect in connection with sputtering has been noted by many observers, particularly with the more volatile metals. In the present work the temperature, save in a few cases, was kept below the point where this phenomenon entered as a factor.

Vaporization was tested for by running the cathode at the desired temperature, without the accompanying electrical discharge and with the gas pressure at its normal value (about 0.40 mm for A) for hot sputtering. The deposit was negligible in all cases save for the highest temperature at which each metal was sputtered. At the highest temperature for platinum (1350°C), however, evaporation accounted for about 11% of the sputtered deposit, and a correction of this magnitude was accordingly made, while for gold at 960°C the correction was 22%. In the case of nickel a correction of 1% was subtracted from the deposit at 1100°C.

It may be remarked as a matter of theoretical interest that the extent of the deposit, i.e. breadth of deposit on glass plate for a given cathode,

was very nearly the same for evaporation as for sputtering at the same pressure, indicating that each process involves substantially the same considerations, i.e. diffusion.

Results

Table I gives a synopsis of the results. While the results show some scattering the consistency is quite satisfactory in view of the irregularities inherent in all sputtering operations. The rate of deposition of metal is

Table I. *Rates of sputtering in argon.*

Metal	Potential (volts)	Net current (ma.)	Cathode temperature (°C)	Deposit (mg/cm²min.)	Deposit (hot) / Deposit (cold)
Gold	500	3.9	150	0.00353	
			960	0.00481	1.36
Platinum	500	3.9	150	0.00165	
			1120	0.00240	1.45
			1350	0.00352	2.13
Platinum	700	about 7	about 250	0.0123	
				0.0120	
			1185	0.0144	1.17
				0.0141	
			1200	0.0134	
Nickel	800	—	about 360	0.00427	
				0.00413	
			1100	0.00597	1.42
Nickel	700	7.3–7.5	330	0.00248	
				0.00261	
				0.00252	
				0.00219	
			700	0.00279	
			850	0.00302	
			980	0.00365	
			1050	0.00361	
			1100	0.00418	
				0.00460	1.73
				0.00416	
				0.00402	

decidedly larger at higher cathode temperatures, the curves, plotted in Fig. 2, being exponential in form. This fact, together with the rather striking one, shown in the last column of the table, that the increase for higher temperatures is greater for lower voltages, explains why previous observers have not found this temperature effect. For Blechschmidt, for example worked only up to 500°C and at 1500 to 2000 volts.

Although the curves show a decidedly upward trend this is by no means as rapid as that of the vapor pressure curve, plotted (the actual ordinates are not given) for the case of nickel from the results of Jones, Langmuir and Mackay.[4] The rate of rise of the sputtering curve undoubtedly varies

[4] H. A. Jones, I. Langmuir and G. M. J. Mackay, Phys. Rev. **30**, 201 (1927).

with the gas. From the few films of nickel sputtered in hydrogen it was concluded that the increase of sputtering with temperature is not as great in this gas as in argon.

Theory. The most complete theory of the process of cathodic sputtering is that of v. Hippel,[5] who has developed quantitative formulae in a fairly successful manner. The positive ion impinging on the cathode is supposed to expend its energy in heating a little area of surface ΔF so that it remains for a time Δt at a high average temperature, causing rapid localized evaporation. Most of this vapor is condensed on the cathode, but a fraction diffuses over and deposits as the sputtered film. v. Hippel's final expression for the amount of this deposit is a somewhat complicated one, involving $\Delta F \cdot \Delta t$ as a factor and an exponential term in T, the momentary temperature of the bombarded element of area.

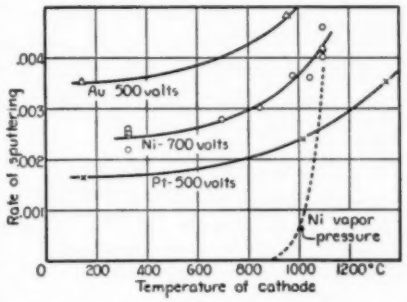

Fig. 2. Rate of sputtering of gold, nickel and platinum in argon as dependent on the temperature of the cathode. (Ordinates are milligrams of metal per square cm per min.)

In attempting to fit this theory with the facts, particularly as regards the form of the temperature-sputtering curve for nickel, two separate assumptions have been tried. The first is that the temperature T of the momentary hot spots on the cathode is independent of the actual cathode temperature—being in any case very much higher than this—and that heating the cathode increases the sputtering through an increase in ΔF and Δt. This reduces the problem to one of heat conduction, involving an instantaneous point source, for which, with certain simplifying assumptions, the theory is readily available.[6] Calculations on this basis give a curve of the same general form as those of Fig. 2, but flatter.

The second assumption is to the effect that $\Delta F \cdot \Delta t$ is to be considered the same at the higher cathode temperature as at the lower, and that T is increased by just the amount of the cathode rise. This does not lead to very satisfactory results. It may be observed that neither of these assumptions fits the actual case, which undoubtedly involves increases in T, ΔF and Δt on heating the cathode. Dr. v. Hippel (letter) also suggests that surface layers of adsorbed gases on the cold cathode may cause reflection of the positive ions and also serve to increase the atomic emission-work, causing less sputtering than at higher temperatures when the gas layer is largely driven off.

The fact that the increase of sputtering at high cathode temperatures is less at higher voltages is perhaps to be accounted for by supposing that the greater the energy of the impinging ion the less important as a factor is the molecular energy, i.e., temperature, of the cathode.

[5] A. v. Hippel, Ann. d. Physik **81**, 1043, (1926). Dr. v. Hippel has also kindly let us see the manuscipt of a forthcoming paper in the Annalen involving an extension of this theory.

[6] See, e.g., Ingersoll and Zobel, "Mathematical Theory of Heat Conduction" (Ginn and Co.) p. 129.

Physical properties of the films. Hot and cold-sputtered films show a slight difference of color, the latter being generally somewhat brownish and the former dark gray, sometimes with a bluish color. Baking for a few minutes at 475°C usually brings them to substantially the same color, i.e., that of the hot-sputtered film.

As is well known, sputtered films suffer a rapid and irreversible change in resistance on heating, known as aging. Many measurements of resistance at various temperatures were made in the present case and typical curves are shown in Fig. 3. While these tests were carried out in high vacuum, substantially similar results, at slightly higher temperatures however, occur under one atmosphere of argon. The straight lines are essentially cooling curves, although actually made by cooling down to room temperature from the highest point and then measuring the resistance on heating up again. Platinum gives curves of the same type. It is evident from the figure that the hot-sputtered film is largely aged as deposited, and this is undoubtedly due to the heating of the film surface, in spite of its water-cooled backing, due to the neighboring hot cathode and to the discharge. The curves for the cold-sputtered films are quite similar to those given by Bartlett.[7]

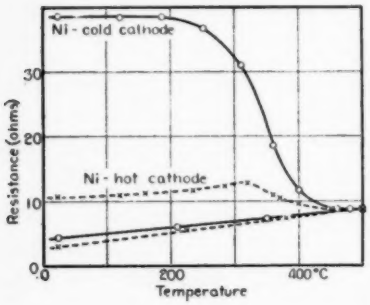

Fig. 3. Effect of heat treatment on hot and cold-sputtered films of nickel.

While the crystal structure of these films has been studied at length in some cases, only a preliminary statement will be made here as the matter is somewhat complicated and is being further investigated. In general it may be said that hot-sputtered nickel films resemble the massive metal while cold ones may initially be amorphous or else show a crystal structure with a somewhat swollen lattice, indicating a not impossible nickel-argon compound. In line with this is the fact that cold-sputtered nickel films are generally non-magnetic and hot ones magnetic. Aging by heat treatment, i.e. baking, drives out the gas[8] in the film and brings about more complete crystallization. As already remarked, hot-sputtered films show large initial aging.

Other effects. It has been recognized for a long time that a gas-filled metal evaporates much more readily than one which is out-gassed. Berliner,[9] who first studied this effect, suggested that the gas may likewise influence cathodic sputtering. As further developed by Bush and Smith[10] this has given rise to the "explosion" theory of sputtering, whereby the positive

[7] R. S. Bartlett, Phil. Mag. **5**, 848 (1928).

[8] While there is every reason to believe this statement it must be admitted that this gas has not actually been found and measured, save in some special cases such as palladium-hydrogen. The matter is to be studied further.

[9] A. Berliner, Wied. Ann. **33**, 289 (1888).

[10] V. Bush and G. C. Smith, Jour. Am. Inst. of Elect. Eng. **41**, 627 (1922).

ions are imagined as developing, on being shot into the cathode, such pressures that miniature explosions of the metal take place.

Our apparatus seemed to offer opportunity to make a quasi-test of this theory and accordingly the following experiment was tried: The nickel strip cathode was first "filled" with gas (on the above hypothesis) by cold-sputtering for several minutes, the cathode temperature being kept down by placing an interrupter in the circuit so that the current was flowing effectively for only half the time. A film was then sputtered (continuously) for two minutes, say. The cathode was then outgassed by heating to 1200°C for several minutes, allowed to cool, and the second film then sputtered. The third film was made like the first.

This gave three films, all deposited for the same time, same gas pressure and at the same cathode temperature—"cold" sputtering, i.e., around 300°C. For the first and third, however, the cathode was supposed to be initially gas-filled, while for the second it was reasonably gas-free. A great many tests were made in this way, with the order reversed in many cases. For cathodes of nickel strip only 0.1 mm thick no systematic difference could be detected, but for 0.25 mm strip the rate of sputtering from the gas-filled cathode was appreciably greater, possibly because the thicker strip retained more gas. The initial current from the gas-filled cathode was almost always higher than the other (correction was of course made for this factor), indicating the outrush of the imprisoned gas, which would not occur, initially, when the cathode had been previously heated.

If it be admitted that this experiment gives what amounts to an exaggeration of the gas effect it must be allowed that there is some basis of fact in the explosion theory. It need not, however, cause any essential change in the fundamental sputtering theory. For whether the positive ion produces its "vaporizing" effect through the medium of a gas cushion or by more direct transference of its energy to the metal of the cathode, the phenomenon is essentially the same.[11]

Another secondary experiment which was tried serves to add a little evidence on the question of the charge on metal vapor atoms from a charged electrode. Vaporization tests, as already described, were made in a large number of cases and in many of these a potential of two or three hundred volts—just short of sufficient to produce a discharge—was applied between cathode and anode. In no case was the amount of deposit changed by this potential. While a little evidence has been obtained in this laboratory to the effect that metal vapors contain a small percentage of ionized atoms, this fraction must, as usually supposed, be very small.

[11] This statement perhaps requires modification in the light of v. Hippel's experiments indicating the essentially *atomic* character of the sputtering process. We are inclined to agree with v. Hippel's suggestion (loc. cit. p. 1045) that the explosion process is probably no more than an auxiliary effect, and, we should add, one more likely to come into account at the beginning of the process. He also makes the suggestion that our results might be accounted for on the basis of the decreased thermal conductivity which undoubtedly accompanies absorption of gas by a metal, and hence the longer duration of the element of time Δt during which the localized evaporation takes place.

Lastly, a start has been made on the task of comparing carefully the properties of sputtered films and of films produced by evaporation from the same cathode and under the same gas pressure. It is hoped that in this way there may be gained some further insight into the sputtering mechanism. As already remarked, the extent of distribution of the deposit was about the same in each of the two cases, indicating a fundamental similarity in the two processes. The deposits, too, were similar in appearance and the resistance curve for the single specimen (nickel) tested was not unlike that for hot-sputtered nickel as shown in Fig. 3. The evaporated film, however, although made with the same pressure of argon, seemed to be more completely initially aged, i.e. probably contained less gas, than even the hot-sputtered films.* This might be taken to indicate that the ionization or excitation incidental to the electrical discharge is an essential feature of the sputtering process and results in a greater occlusion of gas. That ionization or other "activation" increases the adsorption of gas at a surface is in line with the findings of others.[12]

PHYSICAL LABORATORY
UNIVERSITY OF WISCONSIN
June 28, 1928.

* (Note added in proof). Experiments since the above was written on (hot) sputtered and vaporized films of nickel and platinum produced in hydrogen, argon and helium (the latter furnished through the kindness of the Helium Division, U. S. Bureau of Mines), indicate clearly that this is a general law. The matter is, however, dependent on film thickness.

[12] See, e.g., R. E Burk, Proc. Nat. Acad. Sci. **13**, 67 (1927), who concludes from experiments on the thermal decomposition of ammonia at a molybdenum surface that only activated molecules of nitrogen are condensed on such a surface so as to form a "poisoning" film.

PHOTO-ELECTRIC THRESHOLDS AND FATIGUE

By George B. Welch*

Abstract

Photo-electric fatigue.—Using elements of the highest purity, clean surfaces were prepared, in a vacuum of the order of 10^{-6} mm of Hg, by means of an electromagnetic filing device. A linear relation was found between the logarithm of the photo-electric current and the logarithm of the time elapsed since polishing the specimen. The rate of fatigue depends upon the element used and the factors which produce fatigue and, for a given substance, increases numerically as the threshold is approached. Increasing the pressure increases the rate of fatigue. The action of light has a negligible effect.

Photo-electric thresholds.—The values for Ca, Fe, Co, Ni, Cu, Zn, and Ge are, respectively, 4475, 3155, 3165, 3040, 2955, 3180, and 2880A. Within a period of several hours at least photo-electric fatigue causes no change in these values when a high vacuum is used. Evidence for a shift towards shorter wave-lengths is obtained for lower vacua.

The "patch" theory.—A theory in which contamination takes place at discrete areas of the surface of the element is proposed to account for the experimental facts obtained.

IF RADIATION of certain frequencies is allowed to fall upon material substances, electrons are emitted from the latter, a phenomenon known as the photo-electric effect. If, however, the radiation frequency falls below a minimum value, depending upon the substance used, the effect ceases. The wave-length corresponding to this minimum frequency is called the photo-electric threshold. Much conflicting evidence has been offered on the question as to whether this threshold is an intrinsic property of the element under consideration or depends upon the condition of the surface upon which the radiation falls. If our present ideas regarding the structure of matter have any claim of representing even approximately its actual state, the probablity of obtaining a surface which is *absolutely* homogeneous seems very small. If we can produce conditions by which a fresh surface is prepared in a high—but not necessarily the highest—vacuum, any contamination which may take place, from any probable cause whatever, will probably take place slowly enough and at discrete areas of the surface so that, for a considerable time, certain portions of the original surface will continue to exist and to eject electrons corresponding to an incident radiation frequency which need not increase so long as any portion of the original surface continues to exist. A theory of this sort, along the lines of which Woodruff,[1] and Richardson and Young[2] have made suggestions, will be considered more in detail in connection with the data of this investigation. Before presenting the evidence the statement is made that, so far as these

* The writer wishes to express his thanks to Professor Ernest Merritt, Professor J. R. Collins, and Mr. H. W. Banta for their helpful suggestions during the progress of the work.

[1] Woodruff, Phys. Rev. **26**, 655 (1925).

[2] Richardson and Young, Proc. Roy. Soc. **A107**, 377 (1925).

experiments are concerned, a "patch" theory seems adequate for an explanation of the facts.

In this paper a report of photo-electric measurements, involving threshold determinations and fatigue effects, for a series of elements of the highest purity is made. The results are then discussed in connection with the patch theory. To determine the thresholds the photo-electric currents per unit intensity were plotted against the wave-lengths used and the curves extended until they intercepted the latter axis. This method involves the measurements of the intensity distribution of the incident radiation and the saturation currents corresponding to given monochromatic illuminations.

Measurement of the Intensity Distribution of the Incident Radiation

A Gallois quartz mercury-arc lamp[3] was used as a source of illumination, and monochromatic radiation was secured by passing the light through a Bausch and Lomb monochromator fitted with a constant deviation quartz prism. This monochromatic radiation was directed upon a sensitive linear thermopile connected to a Coblentz galvanometer.[4] The monochromator slit width used in the intensity measurements, as well as throughout the entire work, was 0.10 mm, a value which, in the spectral region used, was found to be effective in preventing overlapping of the lines. With a 120-volt storage battery as source, the lamp was operated with a potential difference of 84 volts across its terminals and a current of 2.60 amperes. With the aid of an inductance in series with the lamp, constant operating conditions could be maintained. In order to eliminate the disturbing effects from electromagnetic machinery in and around the laboratory upon the galvanometer all readings were taken very late at night or early in the morning.

The following table gives the average relative intensities of the lines measured, that of 2537A being taken arbitrarily as 100.

Table I. *Relative intensities of incident radiation.*

Wave-length	Intensity	Wave-length	Intensity
4259A	418.	2967A	70.0
4050	352.	2894	21.4
3650	479.	2804	34.8
3330	38.9	2650	76.3
3130	300.	2537	100.
3022	130.	2400	15.5

Measurement of Photo-electric Currents

The principle involved in measuring the photo-electric currents consists of placing the specimen at the axis of an evacuated cell which contains a metal cylinder, and charging this cylinder to a sufficiently high potential so that the electrons emitted from the specimen under the influence of the

[3] George, Rev. d'Optique **4**, 88 (1925).
[4] Coblentz, Bull. Bur. Stand. **9**, 56 (1913).

incident radiation will be drawn to the walls of the tube. The rate at which the specimen becomes positively charged, which can be determined by means of an electrometer, will be a measure of the current. As fresh surfaces of the element must be prepared in vacuum, the cell must also contain a device for the performance of this task.

The plan of the photo-electric cell is shown in Fig. 1. The specimen S is attached to a brass rod and insulated from the soft iron cylinder A by means of a fused quartz tube Q. The collar C contains a small hole and set screw for the purpose of connecting a wire, leading from the electrometer, to the specimen. B is another soft iron cylinder to which is attached a brass rod R and a file F. By means of electromagnets which may be slipped over the glass tubing the iron cylinders with their attachments may easily be moved back and forth. In order to prepare a fresh surface of the specimen A was moved backward and B forward until the file was in contact with the specimen and the rod R was in the guide tube R'. The electromagnet coaxial with A was then moved forward so that the specimen pressed firmly against the file. The latter could then be moved to and fro, and the filing easily accomplished When t' is was done t'e fi'e could be moved out of the way into the position shown in the diagram. The specimen was then moved forward until it was within the cylinder of oxidized copper, O. This was connected by means of the wire L to the positive terminal of a 45-volt battery, the negative terminal being grounded. Monochromatic radiation passed through the quartz window W and impinged upon the specimen.

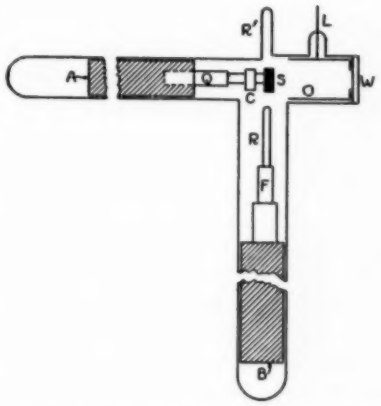

Fig. 1. Diagram of photo-electric cell.

When it was necessary to put a new specimen into the apparatus, the file was carefully cleaned and washed with alcohol. Great care was taken to see that no particles from the specimen previously used remained on this part of the apparatus.

The vacuum was produced by means of a two-stage, water cooled, mercury diffusion pump, backed by a Cenco Hyvac oil pump. There were also inserted in the system between the diffusion pump and the cell the customary liquid-air trap and a trap containing cocoanut charcoal. The latter could be heated and then cooled in order to adsorb residual gases in the system. A MacLeod gauge was used to measure pressures. On this instrument it was possible to estimate pressures of the order of 10^{-6} mm of mercury, and in the investigations here reported the minimum reading was obtained in every case.[5]

[5] Some investigators have reported the measurement of pressures of the order of 10^{-7} mm of mercury with a MacLeod gauge. The use of this instrument depends upon the applicability of Boyle's law at low pressures, which throws some doubt upon the validity of these measurements.

All the glass used was of Pyrex and on the high vacuum side of the apparatus there were no stopcocks or wax joints, with the following exceptions. The quartz plate (*W* in Fig. 1) was sealed to the cell with deKhotinsky cement. The wires, which were sealed into the glass, from the specimen and the oxidized copper cylinder, were of platinum. This metal does not make an absolutely tight seal into Pyrex, and a drop of deKhotinsky cement was used on the outside of the tubing at the two places where the wires were sealed into the glass.

The photo-electric currents were measured by the rate of drift method, using a Compton electrometer with a sensitivity of about 2000 mm per volt.

A special effort was made to secure elements of the highest purity for this work. The calcium and cobalt were obtained from Kahlbaum; the zinc was furnished by the New Jersey Zinc Company; the Bureau of Standards supplied samples of copper, iron, and nickel; and the Cornell University Department of Chemistry purified the germanium.

Variation of Current with Time: Photo-electric Fatigue

Although the photo-electric current was steady during the time required to take a set of readings for a given spectral line, all the elements showed fatigue during the course of the observational period. In order to make use of the readings in threshold determinations it was necessary that some method be devised to reduce the photo-electric current corresponding to each spectral line to a common time basis. This can be done conveniently and accurately, since the results of this investigation show that a linear relation exists between the logarithm of the photo-electric current and the

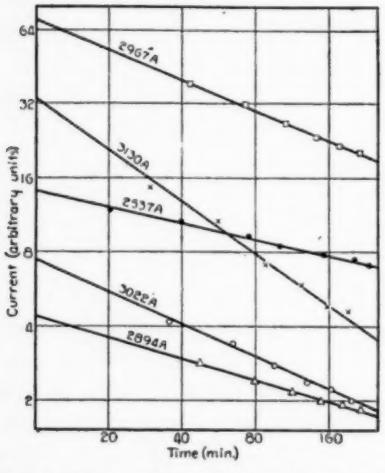

Fig. 2. Photo-electric fatigue in cobalt.

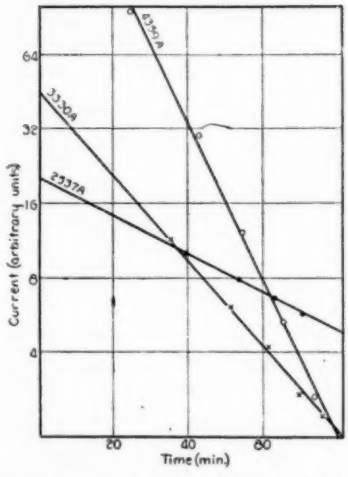

Fig. 3. Photo-electric fatigue in calcium.

logarithm of the time elapsed since polishing the specimen. Because of the static charges developed during the course of the polishing it was rarely possible to take accurate readings until at least ten minutes after the process was completed; but from this time until, in some cases, up to seven hours after polishing, this linear relation was found to hold consistently.

A number of typical curves showing the above relation will be found in Figs. 2 to 4. The ordinates are the reciprocal times for the spot of light on the electrometer scale to drift 10 cm, which are, of course, proportional to the currents; the abscissas represent the time after polishing, in minutes. Logarithmic paper has been used for the plotting of the curves. The order of magnitude of the ordinate scale is not necessarily the same throughout a single diagram; it was desired merely to exhibit conveniently the results corresponding to a number of monochromatic radiations for a given element.

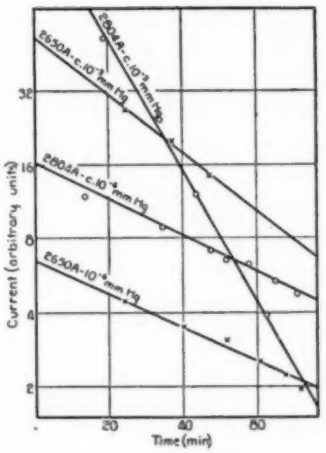

Fig. 4. Photo-electric fatigue in copper, showing effects of high and low vacua.

It will be noticed in the case of each element that the slope of the curve is greatest for the radiation from the spectral line of the longest wave-length from which it was possible to obtain an effect. It will also be noticed that the slopes of the curves become progressively less as radiation of shorter wave-lengths is used. This fact is perhaps most strikingly shown in the case of calcium. (See Fig. 3.) The range of wave-lengths covered is more than 1800A. The slope of the curve corresponding to 4259A, which is near the threshold, is -2.08; for 3330A, it is -1.15; and for 2537A, -0.51. The occurrence of this type of phenomenon is characteristic of all the elements investigated and indicates that the rate of fatigue increases as the threshold is approached. So far as these results show a greater decrease in the photo-electric activity in the regions of longer wave-lengths they are in agreement with those of Suhrmann,[6] although he makes no mention of having found a systematic relation between current and time.

It should be mentioned that, in the case of zinc, some observations were obtained in which the photo-electric current remained practically constant, or showed a slight increase, for about half an hour after the surface was scraped. Then fatigue set in, following the relation found in the cases of the other elements. There were observations, however, in which the zinc showed what may be called the "normal" behavior, and in view of the general consistency of this behavior in the cases of the other metals it has seemed reasonable for the present to attribute the above mentioned results to spurious effects, which have not yet been located.

It is interesting to notice that the rate of fatigue seems to be the greatest for calcium, an element upon which the gases in the atmosphere rapidly produce surface changes. For elements upon which the air seems to have less effect the decrease in photo-electric activity was much smaller, e.g. germanium showed the smallest fatigue effects of all the substances. In connection with this point, experiments made with copper in high and low

[6] Suhrmann, Ann. d. Physik **67**, 43 (1922).

vacua contribute some interesting information. Typical results are shown in Fig. 4. There it is easily seen that the rate of fatigue increases greatly with increase of pressure. In the case of the 2804 line the slope of the curve, under the best possible vacuum conditions, is -0.49; when the pressure is increased to the order of 10^{-3} mm of mercury, the value of the slope increases numerically to -1.76. In the case of the 2650 line the difference is not so great, although the effect is perfectly definite. These results indicate that the interaction between the residual gases in the apparatus and the surface of the element is a factor in producing fatigue. It must be stated, however, that these observations are not extensive enough to warrant the statement that gaseous contamination is the sole cause, or even the primary factor, in producing fatigue. This statement is offered as a precautionary one, although it should at the same time be borne in mind that much of the evidence obtained in this series of experiments may be offered in support of a gaseous contamination theory of fatigue.

Later in this paper a theory will be proposed which will account for the above facts, as well as those to be mentioned below. These experiments, however, show fairly definitely that the variation of photo-electric sensibility is not caused primarily by the action of light. This is in keeping with the findings of Hallwachs[7] and Allen.[8] The principal experiment on this point consisted of two series of observations on nickel, each lasting over a period of seven hours. In one case the specimen was illuminated continuously by light from the quartz mercury-arc lamp; in the second case, it was carefully shielded from the light except during the brief periods required for readings. The current-time linear relation was found in both cases and the slopes of the curves were identical within the limits of experimental error. These results indicate that the effect of light in producing fatigue is negligible. Other less extensive experiments conducted throughout this investigation are entirely confirmatory.

Photo-electric Thresholds

The general method for determining the photo-electric thresholds was as follows: The values for the currents corresponding to a given time after polishing were found from the fatigue curves already mentioned. From these values and the energy distribution of the incident radiation the currents per unit intensity were computed and plotted against the respective wave-lengths. The point where the curve cuts the latter axis will be the threshold.

In Figs. 5 to 8 characteristic curves are shown. In Figs. 5 and 6 are plotted a series of curves showing the currents per unit intensity for different times after polishing the specimen. One very important characteristic may be pointed out at once: Although there is a large variation in the currents per unit intensity with time, the curves for a given element inter-

[7] Hallwachs, Phys. Zeits. **5**, 489 (1904).

[8] Allen, Ann. d. Physik **32**, 1111 (1910); Phil. Mag. **20**, 565 (1910).

sect at a common point on the wave-length axis, which indicates that, within the limits of experimental error, *there is no change in the threshold value.*

It is realized that in extrapolating a curve which is not linear, objections may be offered to the accuracy of the results. Every effort, however, has been made to draw each curve independently of the others. Check observations taken with an intervening period of from two to six months

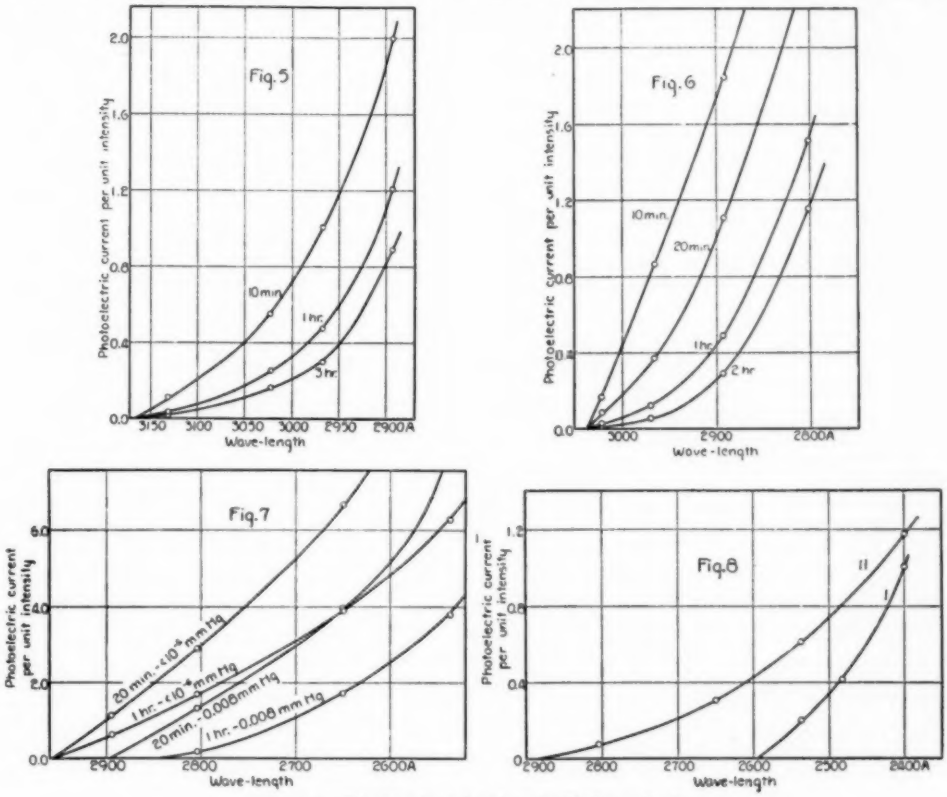

Fig. 5. Photo-electric threshold for cobalt.
Fig. 6. Photo-electric threshold for nickel.
Fig. 7. Photo-electric thresholds for copper with high and low vacua.
Fig. 8. Photo-electric thresholds for germanium: (I) prepared in air (II) prepared in high vacuum.

give values, the extremes of which do not differ (except in the case of calcium) by more than 20A. In the necessary cases filters were used to cut out any possible stray radiation from shorter wave-lengths. An analysis of the results indicates that the maximum error in determining the threshold probably does not exceed 10A. (In the case of calcium this value may be 20 or 25A.)

In Table II is given a list of the photo-electric thresholds determined in this investigation.[9] These photo-electric thresholds have also been con-

[9] The values for iron, cobalt, and nickel differ only slightly from those given in a preliminary report at the New York meeting of the American Physical Society, February, 1928. See Phys. Rev. **31**, 709 (1928).

verted into the equivalent values in volts of the energy required to release the photo-electrons from the element under the specified conditions.

TABLE II. *Results of threshold measurements.*

Element	Threshold	Work Function	Element	Threshold	Work Function
Calcium	4475A	2.76volts	Copper	2955A	4.18 volts
Iron	3155	3.91	Zinc	3180	3.89
Cobalt	3165	3.90	Germanium	2880	4.29
Nickel	3040	4.06			

For the purpose of comparison there are also given in Table III some of the threshold values obtained by other workers. It can easily be seen that there is considerable variation in the results taken as a whole. In making a general comparison of the results of this investigation with those of other workers, there seems to be no definite relation between the threshold values and the vacuum conditions of the experiments.

TABLE III. *Threshold values of other workers.*

Element	Hamer[10]	Hughes[11]	Richardson and Compton[12]	Werner[13]
Calcium	4000A	3700A		
Iron	2870			
Nickel	3050			2850A
Copper	2665		3090A	2750
Zinc	3425	3016	3570	

In the case of germanium it is interesting to compare the value given here with that found by the writer in a previous investigation using much poorer vacuum conditions.[14] (See Fig. 8.) The latter result was 2590A compared with 2880A in the former. The lower value indicates a shift which may, perhaps, be attributed to contamination by the atmosphere of the specimen before it was placed in a vacuum of the order of 10^{-3} mm of mercury.

That a shift in the threshold towards the shorter wave-lengths may take place in a moderate vacuum is shown in Fig. 7. The curves here show clearly that when a high order of vacuum is maintained there is no observable change in the threshold, but that there is a displacement towards the shorter wave-lengths coincident with an increase in pressure.

THE "PATCH" THEORY

In order to explain the fatigue phenomena and the constancy of the photo-electric thresholds, reference is made to the "patch" theory suggested

[10] Hamer, Jour. Opt. Soc. Amer. **9**, 251 (1924).
[11] Hughes, Phil. Trans. Roy. Soc. London, **A212**, 205 (1912).
[12] Richardson and Compton, Phil. Mag. **24**, 575 (1912).
[13] Werner, Upsala Universitets Årsskrift (1914).
[14] Welch, Jour. Opt. Soc. Amer. **14**, 233 (1927).

by Richardson and Young. The theory proposed here was suggested by that of Richardson and Young, but it has been developed along lines which will account for the results obtained in this investigation.

Let us suppose that the filing process produces a surface which is nearly, but not absolutely homogeneous. Or, if we assume a perfectly homogeneous surface, it is reasonable to suppose that within a short time it may become contaminated in spots. At present there is insufficient evidence for making any statement regarding the precise nature of this contamination or of the non-homogeneity of the surface. This, however, is unnecessary for the development of the theory up to its present state. Now, it may further be assumed that these patches increase in area and in "thickness." The term "increase in thickness" is used advisedly: it means nothing more than an increased retarding effect on the escape of electrons from the element.

Let us postulate a light quantum with energy $h\nu_0$. If the interaction between radiation and matter takes place in the region of the uncontaminated surface, an electron will be ejected. But if the interaction takes place at one of the patches, the retarding effect of this patch will not permit the ejection of the electron. If the light quantum has energy somewhat greater than $h\nu_0$ it will be effective not only in the uncontaminated areas, but also in the places where the patches are the thinnest. As the frequency of the incident radiation increases the area from which the electron emission can take place becomes greater.

If there is an increase in the size of the patches the area over which the light quantum $h\nu_0$ is effective is diminished. Radiation of frequency ν_0 will still be able to cause the ejection of electrons, but there will be fewer of them, and the current will be correspondingly diminished. If the thickness of the patches is also increasing there will be diminutions in the number of emitted electrons corresponding to higher frequencies. It by no means follows, however, that the thickness of the patches will increase at the same rate as their area.

Since the experimental results show a linear relation between the logarithm of the photo-electric current and the logarithm of the time, this relation may be expressed by the equation

$$i = Ct^{-\alpha}$$

where i is the photo-electric current, C is a constant depending upon the units, t is the time, and α is a quantity which is a function of the element used and the factors which produce fatigue and, for a given substance, increases numerically as the threshold is approached. Probably this relation is not strictly true, especially during the first few minutes after filing. When, under favorable circumstances, it was possible to obtain readings very soon after preparing the surfaces, the values were smaller than are required by the equation, which demands that the current be very large immediately after polishing.

It seems that a theory of patches, such as that outlined here, is adequate for the explanation of the results of this investigation. The increase

in area and in thickness of the patches will account for fatigue and also for the differences in the rate of fatigue when the frequency of the incident radiation is varied. If the contamination of the surface takes place slowly there will occur for a long time the emission of the electrons with radiation of the "true" threshold frequency. This is verified by the fact that the threshold values do not change, within the limits of experimental error, for a period of several hours, at least. If the experiments were carried on over a period of several days, the threshold would perhaps be shifted towards the shorter wave-lengths. At any rate, the electron emission from the specimen would, for radiation near the threshold frequency, probably be so small that it could be detected only with an electrometer of very high sensitivity, if at all.

If the patches are produced, wholly or partly, by gaseous contamination, as the experiments on copper and germanium suggest, it should be possible to obtain further information by introducing known gases at different pressures into the photo-electric cell. An investigation of this type, however, would necessitate an extensive study of the surface chemistry involved.

There is, of course, the possiblity that contamination at the surface of a metal may produce an increase in its photo-electric activity. These experiments have given no definite evidence for the existence of such a phenomenon, although at present there seems to be no reason for its being inconsistent with the "patch" theory.

The details of the theory and their experimental verification have not been carried to the point where, in the mind of the writer, their application to existing data may satisfactorily be made. In particular, one possible cause of contamination remains be to investigated: the effect of vapors from the deKhotinsky cement where the quartz window was sealed to the apparatus. Up to the time of this paper it was not possible to secure a satisfactory quartz to Pyrex seal in order to eliminate these possible vapors. Plans for the carrying out of a series of experiments with this type of apparatus are under way and it is hoped that it will soon be possible to publish the results.

CORNELL UNIVERSITY,
June, 1928.

THE POTENTIAL OF PHOTOACTIVE CELLS CONTAINING FLUORESCENT ELECTROLYTES

By H. W. Russell

Abstract

Variation with time of illumination of the potential of a cell containing rhodamin B dissolved in absolute alcohol.—A theory of the variation of potential with time has been developed for the photoactive cell. It is assumed that the exciting light produces a chemical change in the electrolyte. Allowing for the effects of diffusion the expression

$$E=K \log (T^{1/2}-t^{1/2}+t/2T^{1/2}-t^2/8T^{3/2}+B/I)-K \log (B/I)$$

where E is the e.m.f., T is time of illumination, t is time after illumination ceases, I is the intensity of illumination, and K and B are constants, has been derived. By the use of a cell with platinum electrodes containing Rhodamin B in absolute alcohol and illuminated with monochromatic light, results in good agreement with the theory are secured. Diffusion is shown to play an important part. Goldmann's theory is shown to be inadequate. No "limiting potential," independent of the intensity of illumination, was found. No evidence was found which indicated the presence of the Hallwachs photo-electric effect.

Introduction

IN 1839 Edmund Bequerel[1] noted that if two similar electrodes were immersed in a suitable solution and the region around one was illuminated a difference of electrical potential between the electrodes was produced. Much later Rigollot[2] noted this effect with fluorescent electrolytes. Hodge[3] showed that the apparent change in resistance found by Nichols and Merritt[4] on illumination of fluorescent electrolytes was due to the setting up of an electromotive force. Goldmann,[5] in a very thorough investigation, independently found the e.m.f. and studied its variation with time of illumination.

Goldmann found what he called the "photo-electric potential." The magnitude of this "photo-electric potential" was independent of the intensity of the exciting light. This led him to believe that the potential had its origin in the Hallwachs photo-electric effect. However, E. Bauer[6] and others[7] [8] believe that the important process is a photochemical modification of the sensitive substance and that these material compounds give their oxidation or reduction potential to the electrode. Using this theory of the origin of the e.m.f. and taking account of the effect of diffusion, a theory

[1] Bequerel, Comptes Rendus **9**, 144, 561 (1839).
[2] Rigollot, Comptes Rendus **66**, 878 (1893); Jour. d. Physique **6**, 520 (1897).
[3] Hodge, Phys. Rev. **28**, 25 (1908).
[4] Nichols and Merritt, Phys. Rev. **19**, 415 (1904).
[5] Goldmann, Ann. d. Physik **27**, 449 (1908).
[6] Bauer, Zeits. f. Physik. Chemie **63**, 683 (1908).
[7] Staechelin, Zeits. f. Physik. Chemie **94**, 542 (1920).
[8] Murdoch, Proc. Nat. Acad. Sci. **12**, 504 (1926); Faraday Soc. Trans. **23**, 593 (1927).

of the variation of the e.m.f. with time has been developed which involves no unusual assumptions.

Theory

Consider a straight glass tube of great length containing a suitable dye solution as electrolyte. Let the ends be closed by similar semi-transparent electrodes and have the concentration and temperature of the electrolyte uniform. Except for the effect of outside forces there should be no difference of electrical potential between the electrodes. Now admit light to the electrolyte through one of the transparent electrodes. Assume that the dye is changed chemically by oxidation or reduction into a new material. Because of absorption this change takes place largely at the end where the light is admitted and the concentrations of the substance formed will be different at the two electrodes; hence a difference of potential, dependent upon the relative concentrations, is to be expected. If the new substance is produced in a very thin layer near the electrode, the concentration at this electrode should increase quite rapidly during illumination, and the e.m.f. should increase. If the light source is removed diffusion away from the electrode should diminsh the concentration of the new substance, and the e.m.f. should decrease.

To determine the effect of diffusion consider a tube of infinite length in which diffusion may occur. At the end let there be a source of material which will diffuse, and let the strength of this source be Q grams of material per unit time. Now it can be shown that the concentration C at any time T and distance x is given by

$$C=(Q/h\pi^{1/2})\int_0^T e^{-x^2/4h^2(T-\tau)}(T-\tau)^{-1/2}d\tau$$

where h depends on the diffusivity.
To solve this make the following substitutions:

$$\alpha=x/2h;\ A=Q/h\pi^{1/2};\ \alpha^2/w^2=T-\tau;$$

and we get

$$C=2A\int_{\alpha/T^{1/2}}^{\infty} e^{-w^2}w^{-2}dw.$$

Integrating by parts

$$C=2AT^{1/2}e^{-\alpha^2/T}-4A\alpha^2\int_{\alpha/T^{1/2}}^{\infty} e^{-w^2}dw,$$

giving as the solution

$$C=2A\left\{T^{1/2}e^{-\alpha^2/T}-\alpha\pi^{1/2}[1-\Theta(\alpha/T^{1/2})]\right\}$$

where $\Theta(\alpha/T^{1/2})$ stands for $(2/\pi^{1/2})\int_0^{\alpha/T^{1/2}} e^{-w^2}dw$—the probability integral.

Expressing this in series

$$C=2AT^{1/2}\left(1-\frac{\alpha^2}{T}+\frac{\alpha^4}{2!T^2}\cdots\right)-\alpha\pi^{1/2}\left(1-\frac{2}{\pi^{1/2}}\left[\frac{\alpha}{T^{1/2}}-\frac{\alpha^3}{3T^{3/2}}+\cdots\right]\right)$$

and approximately

$$C=2A\left(T^{1/2}+\frac{\alpha^2}{T^{1/2}}-\frac{\alpha^4}{6T^{3/2}}-\alpha\pi^{1/2}\right)$$

This approximation is quite good to $\alpha=T^{1/2}$.

After a time T the source is stopped. The future condition of an infinite tube initially with a concentration $C=f(x)$ is given by

$$C=(1/\pi^{1/2})\int_{-\infty}^{+\infty}f(x-2ht^{1/2}\beta)e^{-\beta^2}d\beta$$

Integrating, for $x=0$ this gives

$$C=2A\left(T^{1/2}-t^{1/2}+\frac{t}{2T^{1/2}}-\frac{t^2}{8T^{3/2}}\right)$$

Now assume that the action of light on the dye produces a new material at a rate proportional to the intensity of the light. The concentration of material produced by illumination, assuming that the light penetrates a short distance, is C. Now further assume that before illumination the substance which is to be produced is present at a concentration c_1, the old substance at a concentration c_2. If these substances give rise to an oxidation-reduction potential obeying the Nernst theory, the electrode potential at the unilluminated end will be

$$E_1=E_0+K\log(c_1/c_2)$$

where

$$K=(RT/nF)\log_e 10$$

while at the illuminated end, if we assume that no appreciable fraction of the original material is changed

$$E_2=E_0+K\log[(c_1+C)/c_2]$$

The e.m.f. of the cell is

$$E=E_2-E_1=K\log\left(\frac{C}{2A}+\frac{c_1}{2A}\right)-K\log\frac{c_1}{2A}$$

Now assume that the strength of the source $Q=kI$, where I is the intensity of the light and k is a constant, depending on the wave-length of the light used. Hence, $c_1/2A=B/I$ where B is a constant. Putting in the value of C at the electrode at any time

$$E = K \log \left(T^{1/2} - t^{1/2} + \frac{t}{2T^{1/2}} - \frac{t^2}{8T^{3/2}} + \frac{B}{I} \right) - K \log (B/I)$$

In this T is the time during illumination and is constant after the illumination ceases, while t is the time in the dark; $t=0$ at the instant illumination ceases and at all times before.

Experimental Conditions

The experimental conditions consistant with the assumptions of the theory are as follows: The cell should permit diffusion similar to that which would take place in an infinitely long tube; the electrodes should be alike, and should be kept at the same temperature; the exciting light should be absorbed in a thin layer of the dye near the electrode; the concentration of the original dye solution should be constant; the light used should be of known quality and intensity; the potential change should be followed with an instrument of short period, drawing no current.

An inverted U type of cell of the form shown in Fig. 1 was used. Because of the very slow diffusion of the electrolyte and the short time involved, the length of the tube may be considered infinite. The electrodes were

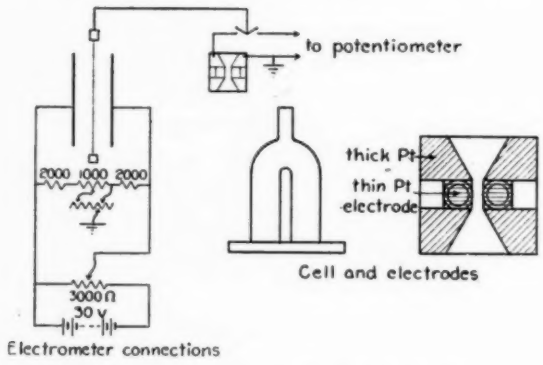

Fig. 1. Electrometer, cell, and electrodes.

of platinum, sputtered in the form shown in the figure, on a single piece of glass. The middle transparent portions had a transmission of greater than 50 percent for all wave-lengths in the visible; the outer portions were thick, almost opaque films of platinum. Copper lead wires were soldered to these thick films. The tube forming the cell was fastened to the base with an alcohol resisting cement: "Gumsol" proved most satisfactory. There was no cement connecting the electrodes so that the resistance between them was very high. Illumination was secured by placing the cell on a reflecting prism, one electrode being covered with black paper.

Rhodamin B in absolute alcohol was chosen as the fluorescent solution. Numerous workers have found it to give a large effect. Goldmann used it for his work. On the basis of Mrs. Jenkins'[9] results a three percent solution was chosen.

[9] Jenkins, Phys. Rev. 18, 402 (1921).

The light source was a Heraeus quartz mercury arc. Nearly monochromatic light was secured by means of filters. Wratten filter No. 77A isolated the green (λ5461) and No. 22 isolated the yellow (λλ5791, 5769). A solution of copper sulphate and ammonium carbonate in a 1 cm glass cell was used to isolate the blue (λλ4358, 4046, 4078). A 1 cm cell containing a three percent solution of cupric chloride in water was used at all times to absorb the infra-red radiation. Temperature differences between the electrodes should have been small.

The intensity of the illumination was measured with a sensitive Coblentz linear thermopile and a low resistance galvanometer having an all copper circuit. The thermopile was placed in the box with the photoactive cell and could be raised out of the path of the light by a cord. Calibration with a radiation standard showed the system, with the galvanometer scale at 2 meters, to have a sensitivity of 5.5×10^{-8} watt sper sq. mm per cm deflection. The intensity will be expressed in centimeters deflection. The intensity of illumination was changed by varying the resistance in series with the mercury arc. About half an hour was allowed for the lamp to reach a steady state, and the intensity was measured with the thermopile before and after each run.

The difference in potential between the electrodes was measured by means of a string electrometer of the Stebbins'[10] type. The displacement of the fiber could be made proportional to its change in potential in the range covered by the eyepiece of the observing microscope. A sensitivity of 200 divisions of the eyepiece scale per volt was generally used. To increase stability and to decrease the damping, the entire electrometer was placed under a bell jar and evacuated to a pressure of about 0.1 mm of mercury. The eyepiece was placed outside of the bell jar. The period of the fiber was so short that the electrometer would assume a steady reading in less than a second after the application of the potential causing a deflection of 40 divisions. The calibration was checked before and after each run by means of a potentiometer.

Sulphur was used for insulating the electrical system from ground. The resistance to ground was greater than 20,000 megohms, and the resistance between the electrodes of a cell when empty was of the same order. When filled with the dye solution, the resistance of the cell as measured by an alternating current bridge was a few thousand ohms. The electrical circuit is shown in Fig. 1.

Time was measured with a chronograph. The key was closed the instant the fiber of the electrometer crossed each scale division. Times were read from the record to the nearest tenth of a second.

Results

Fig. 2 shows curves of the potential-time relation. The light was yellow of intensity 60. Two runs taken under the same conditions are shown. That the effect is reproducable is apparent. Curves for the same cell with

[10] Swann, J.O.S.A. and R.S.I. **11**, 375 (1925).

light of intensity 30 and 15 are shown in Fig. 3. Fig. 4 shows curves taken with green light of intensities 100, 50, and 3.3. Fig. 5 shows curves for yellow, green, and blue light, all at the same intensity.

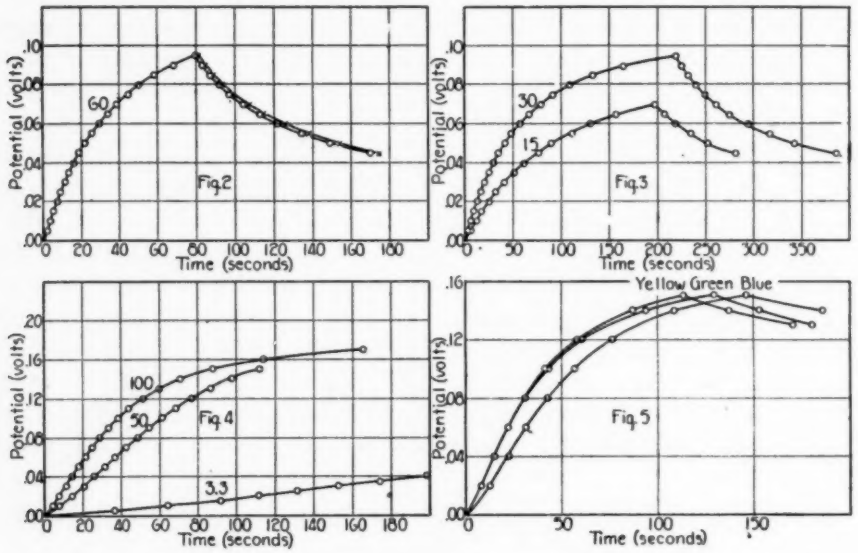

Fig. 2. Potential-time curve. Light off at peak of curve. Yellow light, $I=60$. Two runs, second indicated by crosses.

Fig. 3. Potential-time curves. Yellow light, $I=30$, 15.

Fig. 4. Potential-time curves. Green light, $I=100$, 50, 3.3.

Fig. 5. Potential-time curves. Yellow λλ5791, 5769; Green λ5461; Blue λλ4358, 4046, 4078; $I=100$

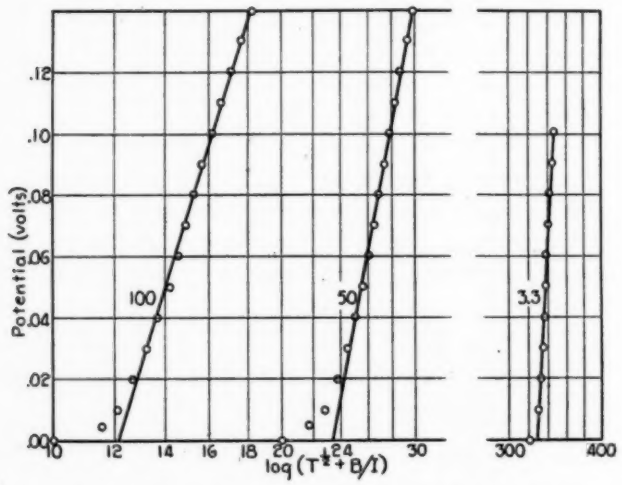

Fig. 6. Potential-log $(T^{1/2}+B/I)$. Green light, $I=100$, 50, 3.3. Data of Fig. 4.

Value of B in the theoretical equation developed cannot be found from our knowledge of the properties of Rhodamin B. By trial 1000 was chosen

as the value of B. Taking the data used in the curves of Fig. 4, the lines of Fig. 6 result. Here values of E are plotted as ordinates against the logarithm of $T^{1/2}+B/I$. These are straight lines as called for by the theory, and are in a rough way parallel. The failure of the points to fall on the line for small

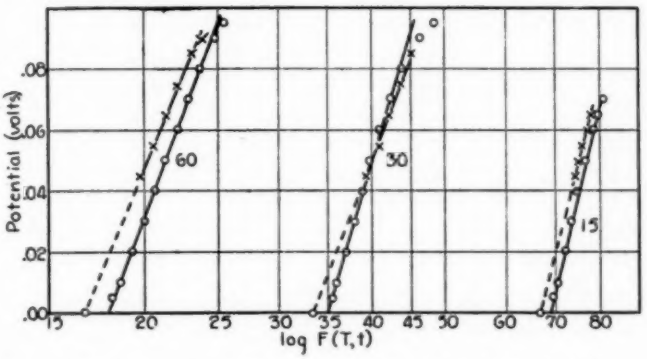

Fig. 7. Potential-log $F(T, t)$ curves. Yellow light, $I=60$, 30, 15. Circles-growth of e.m.f. Crosses decay in dark. Data of Figs. 2 and 3.

values of E can be accounted for by assuming a small constant negative e.m.f. to be built up in the first moments of illumination. Such an initial e.m.f. has been noted by Wilderman,[11] Grumbach,[12] Rule,[13] and others. Its

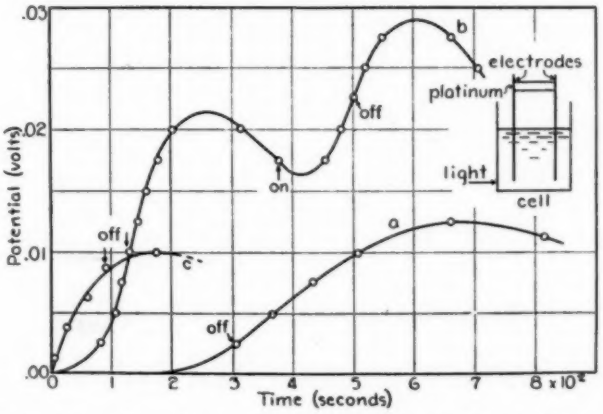

Fig. 8. Potential-time for cell as shown. Curve *a*—electrode 0.7 mm from cell wall; Curve *b*—electrode 0.1 mm from cell wall; Curve *c*—electrode reversed. Light through electrode, then into dye.

explanation may lie in an intermediate compound indicated by the work of Wood.[14]

The decay of the e.m.f. in the dark is shown by Fig. 7 where E is plotted against the logarithm of $T^{1/2}-t^{1/2}+t/2T^{1/2}-t^2/8T^{3/2}+B/I$. The growth

[11] Wilderman, Proc. Roy. Soc. **A77.** 274 (1906).
[12] Grumbach, Comptes Rendus, **176,** 88 (1923); **179,** 626 (1924); **180,** 1102 (1925).
[13] Rule, Phil. Mag. **1,** 532 (1926).; Proc. Nat. Acad. Sci. **14,** 272 (1928).
[14] Wood, Phil. Mag. **43,** 757 (1922).

curves are also shown. These data are the same as those of Figs. 2 and 3. The results for decay are in better agreement with the theory than the results for growth. This again indicates that during illumination there is present some source of e.m.f. which is not allowed for in the theory.

As a further test of the importance of diffusion, experiments were made with a different type of cell. Two strips of glass bearing sputtered platinum electrodes were immersed in a rectangular glass cell containing a six percent solution of Rhodamin B. First, one electrode was placed 0.7 mm from the wall, and the other electrode was placed 2 cm behind it. Green light of intensity 100 was allowed to fall upon this cell. The results are shown in Fig. 8, curve *a*. Illumination ceased at the time marked "off." Then, placing the electrode closer so that only a thin layer of dye was between the cell wall and the electrode, the curve *b* was obtained. Here, after stopping illumination, it was started again. Curve *c* shows the effect when the electrodes were reversed so that the light passed first through the transparent electrode then into the dye.

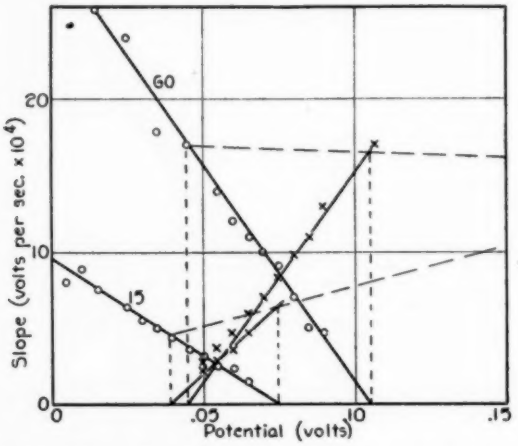

Fig. 9. Goldmann plot; dE/dt against E. Circles—growth in light; crosses—decay in dark.

Curves *a* and *b* show a lag between the illumination and the change in potential. This indicates that material formed by the light at the cell wall must diffuse to the electrode before it produces its effect. When the electrode is closer to the wall the time of the lag is, of course, shorter. Curve *c* indicates, however, that this cell when used under a condition similar to that used with the cells previously discussed gives the effect found with those cells. Because the new material is formed at the electrode, it immediately produces its effect. Stirring the cell during the decay caused E to return to zero.

This experiment indicates that the material which causes the e.m.f. is formed at or near the place where the light enters the dye and that diffusion is an important factor in controlling the potential-time relation.

Fig. 9 shows a check of Goldmann's theory by his method of plotting, using the data of Figs. 2 and 3. The circles indicate the rate of growth of E plotted against the corresponding E. The crosses give the same relation for the decay of E. The dashed lines are the rate of growth corrected for the effects which cause decay. According to Goldmann's theory these dashed lines should intersect the E axis at the same point. The value of E at this intercept Goldmann called the "photo-electric potential." Obviously for these data the "photo-electric potential" is not independent of the intensity of the exciting light. Furthermore the points of the growth curve do not show a very good agreement with Goldmann's equation.

A photo-electric limiting potential should increase with increasing frequency of the exciting light. Fig. 5 shows that the blue is far less effective than the yellow. It is probable that only a fraction, dependent upon the wave length, of the absorbed energy is used to produce the chemical change upon which the photo-voltaic effect depends.

The writer wishes to express his indebtedness to Professor C. C. Murdock, who suggested this problem, and to Professor R. C. Gibbs and Professor Ernest Merritt, who gave valuable aid during its progress.

CORNELL UNIVERSITY,
June 18, 1928.

THE REFRACTIVE INDEX OF SODIUM VAPOR AND THE WIDTH OF THE *D* LINES IN ABSORPTION

By John Q. Stewart and Serge A. Korff

Abstract

Employing classical methods, a theoretical relation is developed between the refractivity of sodium vapor near the *D* lines and their observed width in absorption. A preliminary experimental test of this relation is described. The method involved observation of the wave-lengths of interference fringes produced by sodium vapor when a Michelson interferometer was used in conjunction with a spectroscope and a source of white light. This is a convenient means of determining refractivity in cases where it varies rapidly with wave-length. The approximate observations verify the classical theory, and serve to give a determination of e^2/mc^2 which is correct in order of magnitude. As regards the scattering of radiation, therefore, sodium atoms *may* be considered as behaving in a manner analogous to Hertzian oscillators. Further experimental study is planned.

1. Apparatus

IN ORDER to determine the refractive index of sodium vapor near the *D* lines, light from a strong tungsten lamp was fed into a Michelson interferometer and then into a spectroscope. The direction of dispersion of the latter was in the plane of the interferometer-arms. An electrical resistance furnace, which contained the sodium in a Pyrex tube with an optically flat quartz plate hermetically sealed to each end, was placed in one arm of the interferometer. Two compensating plates were inserted in the other arm, and the interferometer was set for the condition of white light fringes, the two arms being then optically equivalent. (This adjustment was made with no current in the furnace, and, consequently, with altogether negligible vapor pressure of sodium in the tube.) When this condition was exactly realized, the entire range of the spectrum was clear of fringes; since with zero path difference reinforcement takes place at all wave-lengths.

If now the crank of the interferometer was slowly turned, so that the path-difference became x, interference took place at all wave-lengths λ for which $2x/\lambda$ was an odd integer. Thus, as x increased, dark fringes moved into the field of view of the spectroscope from the violet side, and passed along toward the red. These fringes stood at right angles to the direction of dispersion, like broad, hazy absorption lines against the continuous background of the light from the hot filament. As x was increased they came closer together, in accordance with obvious theory.

If the interferometer arms were kept equal and the furnace was heated, the dark *D* lines appeared when a sufficient amount of sodium had evaporated into the tube. The intense dispersion near the *D* lines[1] was now exhibited by the formation of dark fringes which moved out from them—

[1] R. W. Wood, Physical Optics, p. 421.

towards the red from D_1, towards the violet from D_2—as the temperature of the sodium was increased.

Obviously the formation of such fringes resulted from the variation of refractive index with wave-length. Close to the D lines the variation was rapid, with moderate vapor density, and the fringes were narrow. Farther away the variation was slow, and the fringes were broad and diffuse.

If the number of a fringe is known—whether it was the first or ζ'th dark or bright fringe that had "split off" as the temperature increased, and moved out from D_1 or D_2—elementary considerations yield the value of the refractive index for its central wave-length. Thus, with ideal apparatus of this sort, micrometer settings on fringes yield the index of refraction across the spectrum, without the necessity of employing various monochromatic sources of light.

The only Michelson interferometer available was too short to permit of introducing a long tube of sodium vapor. Because of the difficulty of sealing optically flat plates at the ends, only the central part of the tube was heated in the preliminary study herein described. The ends were cooled by a few turns of lead tubing through which cold water ran. The flats were sealed to the Pyrex glass tube with white wax. The whole tube, however, had to be less than 10 cm in length. The natural result was that the wax always melted before many observations could be taken. Consequently, only crude observations have as yet been made.

A longer interferometer is being constructed, and Mr. Korff plans to continue the study. The chief purpose of the present paper is to describe the theory and method involved.

2. Theory

Classical methods, due largely to Lorentz, give the following approximate dispersion formula for frequencies near the "resonance frequency" of an atom, considered as a simple harmonic oscillator.[2]

$$\mu-1=-3na\lambda_0^2/8\pi\beta, \tag{1}$$

where λ_0 is the wave-length of "resonance," 5895.9×10^{-8} cm for D_1, 5890.0 for D_2; $\beta=(\lambda_0-\lambda)/\lambda_0$, where λ is the wave-length of the dispersed radiation and β is supposed small; n is the number of *active* atoms per unit volume; and a is the "radius" of the electron, given by $2e^2/3mc^2$ (e being electronic charge, m electronic mass, c the speed of light), or 1.88×10^{-13} cm.

Equation (1) is invalid for high vapor densities, where $n\lambda^3$ is large compared with unity, because its derivation neglects the reinforcement of the field of the primary radiation by "polarization." Nor does it hold for β as small as a/λ.

Integrating (2) through unit column of the sodium vapor in the line of sight,

$$\int(\mu-1)dz=-3a\lambda_0^2\int ndz/8\pi\beta$$

[2] *Eg.*, J. Q. Stewart, Astrophysical Journal, **59**. 32 (1924).

But $\int n dz = N$, the number of active molecules in this column of unit cross-section; and $2\int(\mu-1)dz/\lambda = \zeta$, the phase-shift in half periods. Thus (1) becomes

$$\zeta = -3Na\lambda_0/4\pi\beta \tag{2}$$

In the present experiment ζ is ± 1 for the first dark fringe that, with rising temperature, moves out from the D lines, 3 for the second dark fringe, 5 for the third, and so on. Thus (2) predicts that $\zeta\beta$ is constant for all the fringes produced, by each D line separately, with a given N, that is, at a given temperature and vapor pressure of the sodium.

The opacity of the vapor likewise can be calculated from classical electron theory, as

$$K = 3\pi n a^2/2\beta^2, \tag{3}$$

where K is the volume opacity coefficient, such that initial intensity I_0 of the primary radiation is reduced in distance z through the vapor to $I_0 e^{-Kz}$. Equation (3) is subject to the same restrictions as (1).

Employing theory previously published,[2] and recently confirmed, in a preliminary way, by observations of Fairley,[3] the "observed width," of a D line is, from equation (3), derived as

$$w = (6\pi)^{1/2} a\lambda_0 (N/k)^{1/2}, \tag{4}$$

where w is the wave-length difference in cm between the observed edges of the dark line, where the corresponding contrast is given by the number k. This number is such that the ratio to the brightness of the continuous background of the light in the line at the observed edge is e^{-k}. Thus k expresses the sensitivity of the method of detecting the edge of the line, and is smaller if a smaller contrast can be observed—corresponding to the measurement of the dark line as broader.

Eliminating N from (2) by means of (4),

$$\zeta\beta = -kw^2/8\pi^2 a\lambda_0 \tag{5}$$

A more complex formula than (5) must, however, here be employed, because of the presumed simultaneous and superposed scattering by D_1 and D_2. Minkowski's measurements[4] showed that twice as many atoms are active in scattering D_2 as D_1. Consequently it is readily shown that (5) must be replaced by

$$\zeta\beta_1\beta_2/(\beta_2+2\beta_1) = -kw_2^2/16\pi^2 a\lambda_0 = -A, \tag{6}$$

where w_2 is the width of D_2, and A is a function of w_2 only.

The question of the ratio of active atoms to total atoms is not dealt with by the classical premises. Minkowski's measurements showed that a minimum of 0.97 of all sodium atoms, at low vapor densities, are active in

[3] A. S. Fairley, Astrophysical Journal, **67**, 114 (1928).

[4] Minkowski, Ann. der Phys. **66**, 206 (1921); Zeits. f. Physik **36**, 839 (1926).

producing D_1 and D_2 together—very closely 1/3 for D_1 and 2/3 for D_2. Equation (6) is dependent only on the ratio of atoms active in D_2 to D_1, regardless of what fraction each bears to the total number of sodium atoms present.

3. Results

Only preliminary results have yet been obtained, for the reason already stated. The interference fringes theoretically expected have been observed for three different sodium tubes; and, qualitatively they behaved as expected as the temperature was increased. No fringes were observed, however, between the D lines—but it is hoped to find these later.

Quantitatively, equation (6) has been crudely verified. Keeping the temperature fixed at a certain value (about 300°C) the width w_2 was measured visually by the micrometer of the spectroscope employed, as in Fairley's work. (The measurements were made in the first order, with a theoretical resolving power of 40,000, employing a grating spectroscope). Settings were also made on the centers of the dark fringes caused by the sodium vapor.

As an example of the results, with w_2 about 0.75A, rough settings were made on the centers of six dark fringes, three to the red of the D lines ($\zeta>0$, $\beta<0$), and three to the violet ($\zeta<0$, $\beta>0$). These measurements, together with the corresponding values of A computed thereby from the left hand member of (6), are recorded in Table I.

Table I. *Illustrative observations of fringes.*

ζ	$5896\beta_1$	$5890\beta_2$	A
5	−9.9	−15.9	0.0037
7	−5.7	−11.7	34
9	−4.2	−10.2	35
−7	12.6	6.6	31
−5	17.7	11.7	37
−3	24.9	18.9	35

The computed value of A should, by theory, be constant. The observed degree of constancy is fair, in view of the lack of time for measurements before the tube gave out. (Especially, the count of ζ may have been wrong by one dark fringe, as the farther fringes were difficult to see, being broad and diffuse. However, the computed constancy of A makes this seem unlikely.)

Taking, as the average of all six settings, $A=0.0035$; and substituting it in the right hand term of (6), with $w_2=7.5\times10^{-9}$ leads to $k=0.11$. This is of the expected order of magnitude, and corresponds to a contrast of 10/11 at the "edge" of the line. If in future work k can be determined by photometric methods, the electronic radius, a, will be computable directly from (6).

4. Conclusions

Obviously, the experimental test of the above equations must be continued with precision. The rough agreement of theory and prediction already established illustrates the usefulness of the classical idea that, in scattering radiation, the sodium atom behaves as if it were a simple harmonic oscillator, having "resonant" wave-lengths at D_1 and D_2.

Equations (1) and (3) are based on this idea. In deriving these, the equation of motion of the vibrating electron in the atom is taken as

$$m\frac{d^2q}{dt^2}-\frac{ma}{c}\frac{d^3q}{dt^3}+4\pi^2 m\nu_0 q=eE \tag{7}$$

where q is the small displacement from the assumed equilibrium position, due to the impressed field E of the primary radiation, and ν_0 is the "resonant" frequency. The second term expresses the classical radiation damping. The third term, expressing an assumed restoring force proportional to displacement, has the justification that its introduction explains observations of Rayleigh opacity and refractive index. (This paper does not enter into a discussion of the relation of the classical premises to those of modern quantum theory.)

The theory and methods of this paper were worked out by Stewart; the observations were made by Korff.

Princeton, N. J.
May 5, 1928.

ANOMALOUS MAGNETIC ROTATION IN EXCITED NEON

By R. N. Jones

Abstract

The anomalous magnetic rotation of the plane of polarization was observed near twenty lines belonging to the transition, s_3-p_k, s_4-p_k, and s_5-p_k. Quantitative measurements were made of the angle of rotation for different frequencies near sixteen lines. The effect is the normal effect, symmetrical on both sides of the line, the direction of rotation being negative.

Dispersion constants for excited neon.—From the angle of rotation the dispersion constants were determined, using the formula derived by Kuhn. This formula requires a knowledge of the relative intensities in the longitudinal Zeeman effect. These were calculated from the theoretical rules of Hönl, and were found to give good results. The relative transition probabilities, for absorption lines having the same lower state, were calculated from the ratios of the dispersion constants, using Ladenburg's formula. The values so found are, in general, in good agreement with the values determined by Kopferman and Ladenburg directly from the anomalous dispersion.

IT is known that most of the strong lines in the yellow-red region of the neon spectrum are, more or less, absorbed by the gas, when excited by an electric discharge.[1] That these lines show anomalous dispersion has been shown by Ladenburg and others.[2] The present paper deals with the results of some investigations of the rotation of the plane of polarization of light near these same lines. The effect was observed for all lines belonging to the transitions, s_3-p_k, s_4-p_k and s_5-p_k, except for s_4-p_1 (5400A). From a measure of the angle through which the plane of polarization is rotated, the dispersion constant may be evaluated, and from its value for absorption lines arising from the same initial state the relative transition probabilities for the lines in question may be calculated.

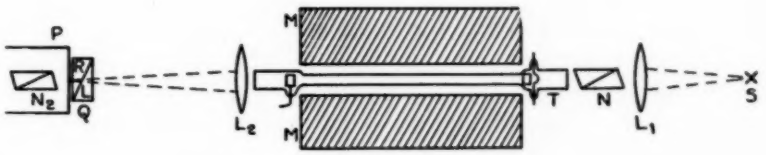

Fig. 1. Arrangement of apparatus.

Figure 1 shows the arrangement of the apparatus for photographing the effect. The light from the source S, (in this case a 500-watt straight filament projection lamp) is rendered parallel by the lens L_1 and polarized by the nicol N. It then passes through the tube T containing neon, and is focussed by the lens L_2 so as to form an image of the lamp filament on the

[1] See K. W. Meissner, Ann. d. Physik (4) 76, 124 (1925).

[2] Ladenburg Kopferman and Carst. Sitz. Ber. der Preuss. Akad der. Wiss, 1926. Also R. Ladenburg, Naturwissenschaften, p. 1208, Dec. 1926.

slit of a stigmatic spectrograph. Immediately before the slit is placed a quartz block Q, made up of two sections, one R, of right handed, and the other L, of left handed, quartz. The quartz block used was made from a Cornu prism by inverting one of the sections and placing them together so as to form a rectangular block. The action of this block is to cause the light entering different parts of the slit to be polarized at different angles. That is, starting from one end of the slit there is a uniform rotation of the plane of polarization of the light entering the slit, as one proceeds to the other end. Now, if a second nicol N_2 be placed immediately behind the slit, there will appear on the photographic plate a system of horizontal bands, due to the fact that the second nicol will cut out the light from those parts of the slit which are illuminated by light polarized at an angle perpendicular to its plane of transmission. The width of these bands varies with the wave-length. For the block used they varied from about 7 mm at 5800A to about 9 mm at 6500A. If in any way the plane of polarization for any frequency is changed, that part of the bands corresponding to this frequency will be shifted upward, or downward, depending on the direction of rotation. A measurement of the amount of this displacement of the bands gives at once the angle through which the plane of polarization has been rotated, for the frequency at which the displacement occurs. A displacement equal to the width of a band corresponds to 180° rotation. Also, the direction of the displacement gives the direction of the rotation.

The magnetic field was produced by the large solenoidal magnet M. The magnet is 46 cm in length and produces an average field of 1180 gauss, at 10 amperes. All the work was done with this field. The magnet is provided with a cooling system, and can be run continuously at 10 amperes, without overheating. The average value of the field was determined by measuring the rotation produced by a tube of water when placed in the field.

The tube T was constructed of Pyrex and provided with aluminum electrodes. The narrow part, within the magnet, had an inside diameter of 16 mm. To aid in starting the tube into operation, a hot filament was provided, but was necessary only in starting. A large aluminum electrode was used as soon as the current began to flow. Some trouble was, at first, experienced in freeing the tube of impurities, and as this is very necessary, it seemed desirable to be able to bake the tube out at rather high temperature. To do this with cemented windows was impossible, so Pyrex windows of the correct size were cut, and polished, and sealed into the ends of the tube. It was found that if they were well annealed, they did not crack and the tube could be repeatedly heated to 500°C, without any trouble. In this way the only impurity in evidence, after filling with pure neon, was a small trace of carbon monoxide which usually disappeared when the tube had been in operation a few minutes. The pressure was in all cases 4 mm.

The exciting current was provied by rectifying and filtering alternating current. Throughout the work the exciting current was maintained at

10 ma.[3] The exciting current was not perfectly uniform due to the lack of sufficient capacity in the filtering circuit, since a variation in the intensity of the light from the tube could be observed, if the tube was viewed stroboscopically, indicating a fluctuating current. No test was made to determine the amount of the variation.

The effect to be observed takes place over an exceedingly narrow region of frequencies on either side of the absorption line. High dispersion is therefore necessary if quantitative measurements are to be made of it. With ordinary dispersion the regions rotated appear as sharp as the emission lines themselves. They may be observed in a small spectroscope by removing the quartz block and setting the analyzing nicol for transmission. Then, when the field is excited, they appear as narrow dark lines on the bright background. It is difficult to observe them as bright lines on a dark background, as can be done in the case of the sodium bands,[4] because they are masked by the emission lines from the tube, due to the excitation. What is observed is an apparent brightening of these lines. The direct observation of the absorption lines themselves is also difficult for the same reason, but they can be observed, at least in the case of the stronger lines.

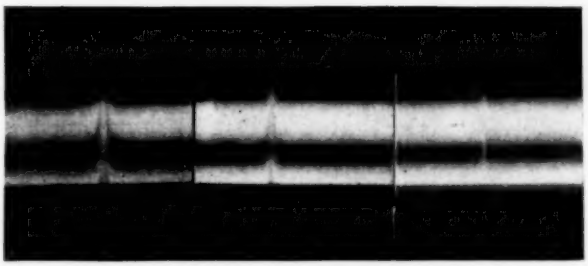

Fig. 2. Effect produced at 6402, 6334 and 6304A.

The spectrograph used was a 30-foot focus Littrow instrument, equipped with a Michelson grating with an 8 inch ruled surface with 15000 lines to the inch. For most of the work the 5th order was used, which gave a dispersion of 0.27A per mm at 5800A, and 0.22A per mm at 6500A. Because of the high dispersion, and the rather complicated optical system through which the light has to pass, the light is extremely faint when falling upon the plate, and long exposures are therefore necessary. The exposure-time was in all cases from 40 to 50 hours. Wratten and Wainwright panchromatic plates were used.

Figure 2 shows the effect produced at 6402, 6334 and 6304A.[5] 6402

[3] This current, at a pressure of 4 mm, does not give a maximum effect. However, in view of the long exposures, and the fact that the pressure decreases as the tube is operated, it was thought advisable to keep the pressure relatively high and the current low. Refilling the tube was troublesome and time consuming, and this pressure and current gave readily measurable effects.

[4] R. W. Wood, Physical Optics, page 536.

[5] The negatives are rather flat, and do not reproduce clearly. The upturned bands can be seen quite clearly for 6304 on the original negative.

shows the largest effect, and 6304 is one of the lines showing the least. These reproductions are natural size, and show the extreme narrowness of the effect. In the case of 6304, the total rotation takes place within a tenth of an Angstrom unit, on each side of the center of the line.

Because of the long exposure required, the rotations at the infra-red lines were not measured, but first-order photographs showed that the effect was present for all lines arising from the states s_3, s_4, and s_5, and was particularly marked for 7032A.

To measure the rotation produced, and its change with the frequency, a carriage was arranged on the measuring machine, so that the plate could be measured both perpendicular and parallel to its length. Measurements were then made of the course of the center of a band as the absorption line was aproached. Since the band turns up very suddenly, it is almost as narrow as a spectrum line, and little diffiuclty was experienced in setting on the center of the steep part. At the place where the rotation sets in it is easier to follow the edge of the band. However, as this part of the band was not used for measurements, its exact determination is not important. From the measurements so made, a curve was plotted for each line. Fig. 3 shows such a curve for 6334A.[6] The dots are from one plate, and the crosses from another. These plates were taken at widely different times, and the curve shows how well the results can be duplicated. In general two, and in some cases three, plates were secured for each line, and the results plotted together, on one curve. Since the curves are almost vertical, a small variation in the position of the curve means a large variation in the measured angle. For this reason the curves must be accurately determined. For the stronger lines the curves from different plates agreed as well as for the one illustrated but for the weaker lines, where the measured angle is smaller, variations of as much as 10 or 12 percent from the mean value of the measured angle for different plates, occurred. It seems, though, that the method of plotting the measurements for several plates on one curve should give a value for the measured angle that differs by much less than this from the true value.

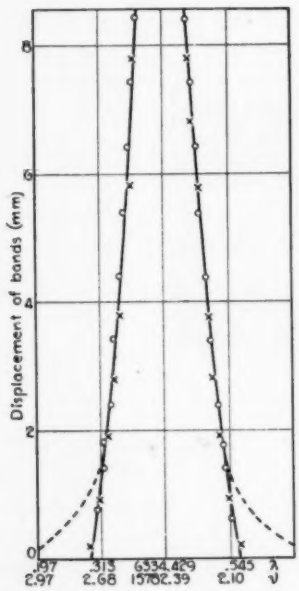

Fig. 3. Curve for λ6334A.

The effect was observable for twenty lines in all, but was too weak to be measured for λ6128. It is to be noted that the three states, for which the effect is observable, are the three components of a triplet P term i.e. $^3P_0$, $^3P_1$, and $^3P_2$ and of these $^3P_0$ and $^3P_2$ are metastable states. The other term of the s group, s_2, is the term $^1P_1$, and shows no rotatory effect that

[6] The vertical scale is plotted in millimeters but this distance is proportional to the rotation. This print is about one tenth the size of the original graph.

could be observed, although no attempt was made to bring it about by exceptionally strong excitation. The effect is the normal effect symmetrical on both sides of the line. The direction of rotation is negative for all lines measured.

To determine the dispersion constant η_k from the measured angle of rotation, the formula given by Kuhn[7] was used. Starting from the classical dispersion formula,

$$n^2-1=\frac{e^2}{\pi m}\sum\frac{\eta_k}{\nu_k^2-\nu^2+i\nu\nu_k'} \tag{1}$$

Kuhn shows, that for an isolated absorption line showing an anomalous Zeeman effect, the rotation per unit length of field traversed should be given by;

$$\phi=\frac{\eta_k e^2\alpha}{2mc}\sum\frac{\alpha_s\beta_s}{\delta^2-\alpha^2\alpha_s^2} \tag{2}$$

at least to a first order of approximation. Where α is the normal Zeeman separation, for the field used, δ is the frequency difference between the unresolved line and the frequency for which the rotation is measured, and e, m and c have their usual designations. The summation is to be extended over the right, or left, circular components in the longitudinal Zeeman effect. α_s is the splitting factor for the s^{th} component, and β_s the intensity of the s^{th} right, or left, circular component, relative to the total intensity for all right, or left, circular components. It is to be noted that the formula (2) is only valid provided δ is not too small.

If $\delta=\rho\alpha$, and if θ_k is the total rotation near the line k then

$$\phi_k=\frac{\theta_k}{l}=\frac{\eta_k e^2}{2mc\alpha}\sum\frac{\alpha_s\beta_s}{\rho^2-\alpha_s^2} \tag{3}$$

Introducing the values of e, m, c, α and l, putting $\sum\alpha_s\beta_s/(\rho^2-\alpha_s^2)=\sigma_k$, and solving for η_k there results;

$$\eta_k=8.1\times10^9\theta_k/\sigma_k \tag{4}$$

In the classical theory η_k is proportional to the number of atoms per unit volume, that is $\eta_k=Nf_k$. f_k is a characteristic constant of the dispersing atom and is connected with the strength of the dispersion i.e. with the intensity of the absorption. In the case of dispersion by atoms in excited states, we must write $\eta_k=N_kf_k$, where N_k is now not the total number of atoms per unit volume, but the number in the excited state giving rise to the absorption line k. η_k will then depend on the conditions which govern the production of excited states, and will depend on the conditions of excitation. But for absorption lines arising from the same excited state, the ratio of the η_k values should be constant and independent of the conditions of excitation.

[7] W. Kuhn, Det. Kgl. Dansk. Vid. Selsk **7**, 12. 1926.

Formulae showing the significance of η_k in terms of the quantities characteristic of the quantum theory have been given by Ladenburg[8] and Kramers.[9] The formula, first derived by Ladenburg from considerations of the emission and absorption of energy in the classical and quantum theories, is;[10]

$$\eta_{kj} = N_k A_{kj} g_k \tau_{kj}/3g_j \tag{5}$$

where A_{kj} is the probability of transition from state k to state j. The g's are the statistical weights of the states in question,[11] and τ_{kj} has the significance $\tau_{kj}=3mc^3/8\pi^2e^2\nu_{kj}^2$, where ν_{kj} is the frequency of the absorption line corresponding to the transition $k\rightarrow j$. It is seen that, if N_k is the same for two lines, the ratio of the A's, for the two lines, can be calculated from the ratio of the η's.

The evaluation of the quantities σ_k requires a knowledge of the splitting factors and the intensity distribution in the Zeeman effect. The Zeeman effect in neon has been worked out by Bach, [12] but the intensity ratios have not been measured experimentally. To get values for the relative intensities of the Zeeman components recourse was had to the theoretical rules given by Hönl.[13]

The results of the investigations are brought together in Table I. Measurements were made on sixteen lines, which are arranged in three groups, according to their common s term, and set down in order of intensity. The intensities are those given by Dorgelo and de Groot.[14] The Zeeman effects are taken from Bach's paper. The relative intensities as calculated from Hönl's rules are given by the numbers beneath the perpendicular components. The bars over the numbers indicate the strongest components, and it is seen that the rules give in each case the correct ones as the strongest components. The angle of rotation was measured first for $\delta=0.15$ wave number. The reason for choosing this value was that it brought the point of measurement on to the most accurately determined part of the curves.

To determine whether the value of η_k remained constant for each curve, a second determination was made for as large a value of δ as could be used. For the s_3 and s_4 groups it was found that η_k was the same, within the limits of error, for the two measurements as is shown by the table. This was not true however for the s_5 groups, there being a large difference between the η_k values for the two measurements. Further determinations for different

[8] R. Ladenbrg, Zeits. f. Physik **4,** 451 (1921); Also Zeits. f. Physik **48,** 15 (1928).

[9] Kramers, Nature **113,** 673 **114,** 310 (1924).

[10] Kramers theory adds a factor $(1-N_kg_j/N_jg_k)$ to take care of the effect due to transitions to states of lower energy, the so-called negative dispersion, but Ladenburg shows reasons for believing that, under ordinary conditions of excitation, this factor is to be looked upon as a small correction factor only. It is therefore neglected here.

[11] $g_k=2gj_k-1$, j_k Sommerfeld's inner quantum number for state k.

[12] E. Bach, Ann. d. Physik (4) **76,** 317 (1925).

[13] H. Hönl, Zeits. f. Physik **31,** 340 (1925).

[14] Dorgelo and W. de Groot, Zeits. f. Physik **36,** 897 (1926).

TABLE I. *Values of magnetic rotation of neon lines*

λ	Comb.	I	Zeeman Effect $R=30$	δ	σ_k	θ_k	η_k	Mean η_k	A/A	Kopferman Ladenburg η_k	A/A
6266	s_3-p_3	16	(0) 30 1	.15	.1590	62	3.16×10^{13}	3.13×10^{13}	1	2.15×10^{11}	1
				.23	.0600	23	3.10				
6532	$-p_7$	15	(0) 20 1	.1	.2320	58	2.02	1.96	.57	1.36	.55
				.15	.0963	23	1.90				
6163	$-p_2$	10.5	(0) 40 1	.15	.2414	56	1.88	1.78	.59	1.32	.62
				.2	.1153	24	1.69				
6506	s_4-p_3	39.5	(0) (10) $\overline{24}$ 34 44 6 3 1	.15	.1574	83	4.27	4.29	1	3.38	1
				.23	.0619	33	4.32				
6382	$-p_7$	32.5	20 (24) 44 1 1	.15	.1912	84	3.56	3.44	1.39	2.45	1.44
				.23	.0707	29	3.32				
6096	$-p_4$	20.5	(0) (5) $\overline{34}$ 39 44 6 3 1	.15	.2113	65	2.49	2.50	.66	2.15	.69
				.23	.0800	25	2.53				
6074	$-p_3$	15	(0) 44 1	.15	.2860	58	1.64	1.66	2.22	1.40	2.28
				.23	.1008	21	1.69				
6304	$1-p_5$	10	(0) (7) $\overline{30}$ 37 44 6 3 1	.15	.1881	29	1.25	1.25	.31	.9	.3
6029	$-p_2$	4	(4) 40 44 1 1	.15	.2632	45	1.38	1.38	.62	~.6	~.3
6402	s_3-p_3	100	(0) (6) (10) $\overline{30}$ 35 40 45 50 15 10 6 3 1	.15	.1920	239	10.08	17.55	1	7.25	1
				.23	.0763	153	16.24				
				.30	.0413	90	17.65				
				.35	.0297	64	17.45				
6143	$-p_8$	34	(11) (22) 23 $\overline{37}$ $\overline{45}$ 53 2 3 3 2	.15	.2683	128	3.86	6.57	.57	2.16	.66
				.23	.0907	76	6.57				
				.30	.0495	40	6.56				
6334	$-p_9$	34	(8?) (16) 29 $\overline{34}$ $\overline{45}$ 56 2 3 3 2	.15	.2666	127	3.86	5.59	.45	3.26	.41
				.23	.0937	63	5.62				
				.26	.0648	44	5.55				
5944	$-p_5$	17.5	(6) (12) 33 $\overline{39}$ $\overline{45}$ 51 2 3 3 2	.15	.2724	72	2.14	3.30	.31	1.59	.33
				.23	.0957	39	3.30				
6217	$-p_7$	10	(0) 20 (25) 45 $\overline{70}$ 1 3 6	.15	.8555	77	.73	1.95	.27	.9	.27
				.23	.1592	39	1.98				
				.25	.1184	28	1.92				
5881	$-p_2$	9	(0) (5) 40 45 $\overline{50}$ 1 3 6	.15	.3350	57	1.38	2.03	.32	1.0	.40
				.23	.1116	28	2.03				
5975	$-p_3$	3	(10) (15) 30 45 $\overline{60}$ 1 3 6	.15	.4699	68	1.17	1.60	.24	~.5	~.2
				.23	.1318	26	1.60				

values of δ indicated that as δ was increased η_k increased but finally approached a constant maximum value.

The explanation seems to be due to the fact that, for this group, the Zeeman types are in general much more complicated than in the other groups, and also are broader. It will be noticed, besides, that, in general, they have their strongest components near the outside of the pattern. This means that, for small values of δ, the frequencies at which the measurements are made are, in fact, much closer to the strong components of the absorption line, than in the case of the other groups. Formula (2) then breaks down and does not give the correct value of η_k.

In the column headed "mean η_k" are listed the average values of the constant maximum values of η_k, for each line, and from these the relative A values are calculated using formula (5).

Just as this work was completed, the work of Kopferman and Ladenburg[15]

[15] H. Kopferman and R. Ladenburg, Zeits. f. Physik **48**, 26 (1928).

on the anomalous dispersion in neon came to hand. Their values for η_k, and for the relative A values determined directly from the anomalous dispersion, are included in the last two columns. The η_k values listed are the saturation values for increasing exciting current, measured for a pressure of 3.5 mm. As is to be expected, their η_k values are quite different from the author's. For the relative A values there is in general good agreement, particularly in the s_3 and s_4 groups. The result supports the validity of Kuhn's formula (2) and also Hönl's rules for the intensities in the Zeeman effect, at least for the simpler Zeeman types.

In conclusion the author wishes to express his thanks to Dr. G. S. Monk for his assistance in connection with this work.

RYERSON PHYSICAL LABORATORY
UNIVERSITY OF CHICAGO
June, 1928.

NOTE ON MAGNETIC PROPERTIES OF EVAPORATED FILMS OF NICKEL

By K. J. Miller

Abstract

Films of nickel produced by evaporation on aluminum foil were tested in fields up to 167 gauss. The coercive force reached a value approximately three times that for hard drawn wire and retentivity was observed as high as 65 percent. Coercive force decreased with decreasing deposit temperature and increasing thickness. No critical thickness was observed. Films were of uniform thickness and were uninfluenced in their properties by distortion after deposit.

THE work described here is presented to supplement the papers already published from this laboratory on the general subject of magnetism in thin ferromagnetic films by Sorenson[1] and Edwards.[2] The apparatus and material used were the same in their essential characteristics as described in the papers mentioned above and the reader is referred to them for the descriptions. In this investigation the vacuum system was altered to permit deposit at pressures less than 4×10^{-4} mm of mercury. Aluminum foil 0.0005 inches (0.0013 cm) thick was used as the base for deposit. Demagnetization of the films was accomplished by the use of a special coil in series with a water rheostat giving a maximum field of approximately 500 gauss. The search coil of the testing apparatus was replaced during part of the investigation by a larger one than ordinarily used to permit the test of specimens without the necessity of distorting them to fit the inside of the coil.

The films were tested for uniformity of thickness by comparing the intensity of light transmitted through them. The variation in thickness over the whole expanse of film did not exceed 10 percent.

The accompanying table is a list of all the films tested. They fall into two general classes viz., (1) heated films—deposited at not less than 250°C—and (2) unheated films—deposited at not more than 100°C. Of the films listed in the group of undistorted films numbers 1 and 20 fall into the former class and number 2 in the latter. Film number 5 in each class received a heat treatment after deposit which accounts for their variation from others in each class. The films 1 and 2 listed under the undistorted films are those tested in the larger search coil without first being rolled into a small cylinder as the others were. Number 20 of the undistorted films is identical with the number 20 of the heated films. The results show it as tested in both coils. The films tested without distortion conform to others of their class except in the matter of induction. This effect was traceable to the geometry of the search coil used for these films. The values given for nickel wire are for hard drawn wire from which the films were made.

In the graph the coercive force is plotted as ordinate and the thickness as abscissa. Probably two straight lines drawn among these points, one for each of the two classes would properly represent the variation. The

[1] A. J. Sorenson, Phys. Rev. **24**, 658 (1924).
[2] R. L. Edwards, Phys. Rev. **29**, 321 (1927).

TABLE I. *List of all films tested. t—thickness in millimicrons; B—induction at 167 gauss; I_r—retentivity in percent; H_c—coercive force in gauss.*

Heated Films					*Unheated Films*				
No.	t	B	I_r	H_c	No.	t	B	I_r	H_c
8	34	3200	60	84	8	42	2450	28	40
10	57	2500	50	90	10	51	1850	31	40
9	58	2900	36	80	9	59	2100	30	46
12	85	3600	51	84	12	68	3400	25	40
5	113	2350	66	68	15	70	4150	37	46
4	119	3000	65	80	5	91	1750	55	54
15	132	3450	57	82	16	118	2350	36	42
16	156	3600	62	72	19	139	1900	51	46
19	178	3000	65	80	13	156	2450	43	43
13	227	2150	65	72	18	174	2500	28	40
18	244	4000	56	62	17	178	2900	35	50
20	302	3200	60	68	14	196	2450	39	47
7	331	2100	59	55	20	221	2250	46	42
Ni	wire*	3600	68	30	7	304	1400	48	47

Undistorted Films				
No.	t	B	I_r	H_c
1	175	2350	54	66
2	112	1370	33	48
20	302	2600	66	67

*Due to Edwards

gradual decrease of coercive force with thickness increase in the heated films should be noted. There is no point of critical thickness apparent. This checks the conclusions of Edwards[2] rather than those of Sorenson.[1] The fact that the films deposited at higher temperatures show a greater deviation from the normal value for the nickel wire than do those much less heated is also worthy of note.

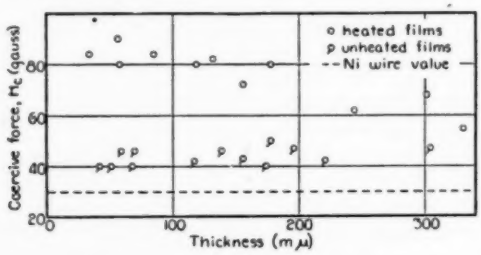

Fig. 1. Variation of coercive force with thickness and heat treatment.

Computation of the force exerted by the base on the nickel film due to differences in contraction when the whole was cooled from deposit temperature to room temperature showed it to be a compressive force of the order of 10kg/mm². This is within the elastic limit of bulk nickel and should have resulted in a marked increase in induction over bulk nickel. No such increase is observed, and no explanation for this anomaly is apparent.

The writer appreciates the cooperation of the staff of the Department of Physics of the State University of Iowa in this work and especially that of Professor G. W. Stewart who suggested the investigation.

PHYSICS LABORATORY,
STATE UNIVERSITY OF IOWA,
December, 1927.*

* Received June 26, 1928. Ed.

THE ENTROPY AND THERMODYNAMIC POTENTIALS OF REAL GASES AND MIXTURES OF REAL GASES AND A MASS ACTION LAW FOR CHEMICAL REACTION BETWEEN REAL GASES: II. INTEGRATED EQUATIONS*

By James A. Beattie

Abstract

The general thermodynamic equations derived in the first paper are integrated by means of a new equation of state for gas mixtures. Thus the energy, heat content, entropy and thermodynamic potentials $F_{V,T}$ and $F_{p,T}$ of a mixture of real gases, and the chemical potential and fugacity of a gas in a mixture are expressed as integrated functions of V, T, n_1, n_2, $\cdots$, and the constants of the equation of state of the pure gases composing the mixture. The expression for the thermodynamic potential $F_{V,T}$ is a fundamental equation in the Gibbs sense. A mass action law for reactions between real gases is given, the "mass action constant" K_p being expressed in terms of the variables V, T, x_1, x_2, $\cdots$, ν_1, ν_2, $\cdots$, and the equation of state constants of the pure gases composing the equilibrium mixture. The determination of the values of the various integration constants are discussed for the following cases: (a) non-isothermal and (b) isothermal variations in the state of a system composed of gases which react chemically, (c) non-isothermal and (d) isothermal variations in the state of a system composed of nonreacting gases.

1. Introduction

In THE first paper[1] there were derived general thermodynamic equations for the energy U, entropy S, heat content H, and thermodynamic potentials $F_{V,T}$ and $F_{p,T}$, of a mixture of real gases, also for the chemical potential μ_1 of a gas in a mixture and for the variation of the "mass action constant" K_p. Whenever possible these quantities were expressed in terms of both sets of independent variables V, T, n_1, n_2, $\cdots$ and p, T, n_1, n_2, $\cdots$. All of the general equations were derived from two assumptions regarding the limiting conditions of mixtures of real gases: (a) at infinitely low total pressure, the equilibrium pressure of a gas in a mixture is equal to the product of its mole fraction times the total pressure, and (b) at infinitely low total pressure, the energy of a mixture of gases is equal to the sum of the energies of the component gases when each is at the same temperature and occupies the total volume of the mixture.

Each of the general equations contains a definite integral which requires an equation of state for gas mixtures for its evaluation. Recently a new equation of state[2] has been proposed, and it has been compared with the compressibility data on twelve gases. The equation reproduces the experi-

* Contribution from the Research Laboratory of Physical Chemistry, Massachusetts Institute of Technology, No. 210.

[1] Beattie, Phys. Rev. **31**, 680 (1928).

[2] Beattie and Bridgeman, Jour. Amer. Chem. Soc. **49**, 1665 (1927); other papers to appear shortly.

mentally determined pressures over the measured temperature field, and for a wide range of densities in a very satisfactory manner. In this comparison the data of several investigators were correlated, and it was found that in general the equation reproduces the measurements of one experimenter somewhat better than the overall agreement between the data of different observers. The equation is

$$p=\frac{RT(1-\epsilon)}{V^2}[V+B]-\frac{A}{V^2} \tag{1}$$

$$A=A_0(1-a/V)\ ;\quad B=B_0(1-b/V);\ \epsilon=c/VT^3$$

in which R is the gas constant and A_0, a, B_0, b and c are constants which depend upon the kind of gas.

This equation of state has been applied[3] to mixtures of gases by use of a simple rule for the calculation of the values of the constants of the mixture from the composition and the values of the constants of the pure component gases: the rule being that each of the parameters $A_0^{1/2}$, a, B_0, b and c are combined linearly with the composition. Thus for a mixture in which the molal composition is n_1, n_2, $\cdots$ the rule of combination is

$$\begin{aligned} A_{0m}&=[\textstyle\sum(n_1A_{01}^{1/2})]^2\ ; & a_m&=\textstyle\sum(n_1a_1)\ , & B_{0m}&=\textstyle\sum(n_1B_{01})\ ; \\ b_m&=\textstyle\sum(n_1b_1)\ ; & c_m&=\textstyle\sum(n_1c_1) & R_m&=\textstyle\sum(n_1)R \end{aligned} \tag{2}$$

where the subscript m refers to the value of the constant of the mixture, the subscript 1 to Gas 1, and the summation is taken over all of the gases composing the mixture. This rule of combination has been applied to the extensive data of Keyes and Burks[4] on mixtures of methane and nitrogen with good agreement between observed and calculated pressures.

Substitution of the relations (2) into (1) gives the general equation of state for gas mixtures. Since all of the integrations with which the present paper is concerned are carried out at constant temperature, it is more convenient to use the equation in its virial[5] form

$$pV=\textstyle\sum(n_1)RT+\beta_m/V+\gamma_m/V^2+\delta_m/V^3 \tag{3}$$

in which

$$\left.\begin{aligned} \beta_m&=\textstyle\sum(n_1)RT\sum(n_1B_{01})-[\sum(n_1A_{01}^{1/2})]^2-\sum(n_1)R\sum(n_1c_1)/T^2 \\ \gamma_m&=-\textstyle\sum(n_1)RT\sum(n_1B_{01})\sum(n_1b_1)+[\sum(n_1A_{01}^{1/2})]^2\sum(n_1a_1) \\ &\quad-\textstyle\sum(n_1)R\sum(n_1B_{01})\sum(n_1c_1)/T^2 \\ \delta_m&=\textstyle\sum(n_1)R\sum(n_1B_{01})\sum(n_1b_1)\sum(n_1c_1)/T^2 \end{aligned}\right\} \tag{4}$$

Certain derivatives of the virial parameters occur in the integration of the various equations. These are

[3] Beattie, to be published shortly.

[4] Keyes and Burks, Jour. Amer. Chem. Soc. **50**, 1100 (1928).

[5] The general virial equation in which the parameters are determined empirically at each temperature from the compressibility measurements has been extensively used for pure substances by Kamerlingh Onnes and his collaborators.

$$\left.\begin{aligned}
(\partial\beta_m/\partial T)_n &= \textstyle\sum(n_1)R\sum(n_1B_{01})+2\sum(n_1)R\sum(n_1c_1)/T^3 \\
(\partial\gamma_m/\partial T)_n &= -\textstyle\sum(n_1)R\sum(n_1B_{01})\sum(n_1b_1) \\
&\quad +2\textstyle\sum(n_1)R\sum(n_1B_{01})\sum(n_1c_1)/T^3 \\
(\partial\delta_m/\partial T)_n &= -2\textstyle\sum(n_1)R\sum(n_1B_{01})\sum(n_1b_1)\sum(n_1c_1)/T^3
\end{aligned}\right\} \quad (5)$$

$$\left.\begin{aligned}
(\partial\beta_m/\partial n_1)_T &= RT[\textstyle\sum(n_1B_{01})-\sum(n_1c_1)/T^3]+\sum(n_1)RT[B_{01}-c_1/T^3] \\
&\quad -2A_{01}^{1/2}\textstyle\sum(n_1A_{01}^{1/2}) \\
(\partial\gamma_m/\partial n_1)_T &= -RT\textstyle\sum(n_1B_{01})[\sum(n_1b_1)+\sum(n_1c_1)/T^3] \\
&\quad -B_{01}\textstyle\sum(n_1)RT[\sum(n_1b_1)+\sum(n_1c_1)/T^3] \\
&\quad -\textstyle\sum(n_1)RT\sum(n_1B_{01})[b_1+c_1/T^3] \\
&\quad +2A_{01}^{1/2}\textstyle\sum(n_1A_{01}^{1/2})\sum(n_1a_1)+a_1[\sum(n_1A_{01}^{1/2})]^2 \\
(\partial\delta_m/\partial n_1)_T &= \{\textstyle\sum(n_1b_1)\sum(n_1c_1)[RT\sum(n_1B_{01})+B_{01}\sum(n_1)RT] \\
&\quad +\textstyle\sum(n_1)RT\sum(n_1B_{01})[b_1\sum(n_1c_1)+c_1\sum(n_1b_1)]\}/T^3
\end{aligned}\right\} \quad (6)$$

The compositions of gas mixtures are usually expressed in terms of mole fractions. In Equations (2), (4), (5) and (6) the mole numbers $n_1, n_2, \cdots$ can be replaced by the mole fractions $x_1, x_2, \cdots$ and some simplification results since $\Sigma(x_1)=1$. When the virial parameters and their derivatives in terms of mole fractions are used in any equation, the volume must be expressed as the molal volume of the mixture $(V/\Sigma n_1)$ and the thermodynamic quantity which is thereby calculated is for an average mole of the mixture.

In Equation (3) the independent variables are V and T so that it is necessary to use the corresponding general equations developed in the first paper, which will be designated by writing the Roman numeral I before the number of the equation.

2. The Energy, Entropy, Thermodynamic Potential $F_{V,T}$ and Chemical Potential

The general expressions which have been derived for these quantities are

$$U=\int_V^\infty [p-T(\partial p/\partial T)_V]dV+\sum(n_1u_1) \qquad \text{(I 13)}$$

$$S=\int_V^\infty [\textstyle\sum n_1R/V-(\partial p/\partial T)_V]dV+\sum(n_1R\ln V/n_1)+\sum(n_1s_1) \qquad \text{(I 14)}$$

$$F_{V,T}=\int_V^\infty (p-\textstyle\sum n_1RT/V)dV-\sum[n_1RT\ln(V/n_1)]+\sum(n_1F_1) \qquad \text{(I 28)}$$

$$\mu_1=\int_V^\infty\left(\frac{\partial p}{\partial n_1}-\frac{RT}{V}\right)dV-RT\ln\frac{V}{n_1}+RT+F_1 \qquad \text{(I 36)}$$

$$u_1 = \int_{T_0}^{T} C_{V_1}^{*} dT + U_{01} \tag{I 10}$$

$$s_1 = \int_{T_0}^{T} C_{V_1}^{*} dT/T + S_{01} \tag{I 11}$$

$$F_1 = u_1 - Ts_1. \tag{I 29}$$

in which p, V and T are the total pressure, total volume and Kelvin temperature of the mixture and n_1 is the number of moles of Gas 1 in the mixture.

In a later paper, relations will be developed for evaluating $C_{V_1}^{*}$, the constant volume molal heat capacity of the pure Gas 1 at infinitely low pressure, which is a function of the temperature alone, and U_{01} and S_{01} the energy and entropy constants of Gas 1 at the temperature T_0. These expressions are

$$C_{V_1}^{*} = C_{V_1} - \frac{Rc}{V_1 T^3}\left[6 + \frac{3B_0}{V_1} - \frac{2B_0 b}{V_1^2}\right] \tag{7}$$

$$U_{01} = U_1 + \frac{A_0}{V_1}\left[1 - \frac{a}{2V_1}\right] + \frac{3Rc}{V_1 T_0^2}\left[1 + \frac{B_0}{2V_1} - \frac{B_0 b}{3V_1^2}\right] \tag{8}$$

$$S_{01} = S_1 - R\ln V_1 + \frac{RB_0}{V_1}\left[1 - \frac{b}{2V_1}\right] + \frac{2Rc}{V_1 T_0^3}\left[1 + \frac{B_0}{2V_1} - \frac{B_0 b}{3V_1^2}\right] \tag{9}$$

In Equation (7), C_{V_1} is the molal heat capacity of Gas 1 at the temperature T and the molal volume V_1. From measurements of C_{V_1} at different temperatures, a series of values of $C_{V_1}^{*}$ can be calculated, and these can be expanded in a power series of the temperature by means of which the expressions (I 10) and (I 11) can be integrated.

In (8) and (9), U_1 and S_1 are the energy and entropy of Gas 1 at T_0 and a molal volume V_1. The determination of the values of U_{01} and S_{01} for several different cases is considered in Section 5 of the present paper.

The general equations for the various thermodynamic quantities can be integrated by means of the virial Equation (3). We thus obtain[6]

$$U = \left[\beta_m - T\left(\frac{\partial \beta_m}{\partial T}\right)_n\right]\frac{1}{V} + \left[\gamma_m - T\left(\frac{\partial \gamma_m}{\partial T}\right)_n\right]\frac{1}{2V^2} + \left[\delta_m - T\left(\frac{\partial \delta_m}{\partial T}\right)_n\right]\frac{1}{3V^3} + \sum(n_1 u_1) \tag{10}$$

$$S = \sum\left(n_1 R \ln \frac{V}{n_1}\right) - \left(\frac{\partial \beta_m}{\partial T}\right)_n \frac{1}{V} - \left(\frac{\partial \gamma_m}{\partial T}\right)_n \frac{1}{2V^2} - \left(\frac{\partial \delta_m}{\partial T}\right)_n \frac{1}{3V^3} + \sum(n_1 s_1) \tag{11}$$

[6] The subscript n denotes differentiation at constant $n_1, n_2, n_3 \cdots$.

$$F_{V,T} = -\sum\left(n_1 RT \ln\frac{V}{n_1}\right) + \frac{\beta_m}{V} + \frac{\gamma_m}{2V^2} + \frac{\delta_m}{3V^3} + \sum(n_1 F_1) \tag{12}$$

$$\mu_1 = -RT \ln\frac{V}{n_1} + \left(\frac{\partial\beta_m}{\partial n_1}\right)_T \frac{1}{V} + \left(\frac{\partial\gamma_m}{\partial n_1}\right)_T \frac{1}{2V^2} + \left(\frac{\partial\delta_m}{\partial n_1}\right)_T \frac{1}{3V^3} + RT + F_1 \tag{13}$$

These equations could be used to calculate the desired thermodynamic quantities, provided that the virial parameters could be expressed as functions of the temperature and composition. One such method is given in the relations (4), and by substitution of the values of the virial parameters and their derivatives into the above relations, there are obtained expressions for the complete variation of the energy, entropy and thermodynamic potential of a gas mixture, and for the chemical potential of a gas in a mixture, with the temperature, volume and composition. For a mixture of given composition at a constant temperature all of the coefficients are constant and the expressions are quite simple. Since this is the usual experimental method of investigating gas mixtures the indicated substitutions will not be carried out, as it is more convenient to calculate the desired coefficients by means of Equations (4) to (6) and use the *numerical* results in the Equations (10) to (13).

Equation (12) gives a relation between the variables $F_{V,T}$, V, T, n_1, n_2, $\cdots$ and is a so-called fundamental equation.[7]

3. The Heat Content, Thermodynamic Potential $F_{p,T}$ and Fugacity

The heat content, H, and thermodynamic potential, $F_{p,T}$, are often expressed in terms of the independent variable p rather than V since they are zero for certain constant pressure processes. However they can be calculated for any state of a mixture of gases from the results of the previous section by means of the usual relations

$$H = U + pV \tag{14}$$

$$F_{p,T} = F_{V,T} + pV \tag{15}$$

$$= \sum(n_1\mu_1) \tag{16}$$

From (14) and (15) there results

$$H = \sum(n_1)RT + \left[2\beta_m - T\left(\frac{\partial\beta_m}{\partial T}\right)_n\right]\frac{1}{V} + \left[3\gamma_m - T\left(\frac{\partial\gamma_m}{\partial T}\right)_n\right]\frac{1}{2V^2} + \left[4\delta_m - T\left(\frac{\partial\delta_m}{\partial T}\right)_n\right]\frac{1}{3V^3} + \sum(n_1 u_1) \tag{17}$$

$$F_{p,T} = \sum(n_1)RT - \sum\left(n_1 RT \ln\frac{V}{n_1}\right) + \frac{2\beta_m}{V} + \frac{3\gamma_m}{2V^2} + \frac{4\delta_m}{3V^3} + \sum(n_1 F_1) \tag{18}$$

[7] Gibbs, Scientific Papers, Vol. I, p. 88. Longmans, Green and Co., New York (1906).

Equation (16) also leads to the relation (18). The partial molal thermodynamic potential $(\partial F_{p,T}/\partial n_1)_{p,T,n_2,n_3}\ldots$ cannot be obtained by differentiation of (18) because of the use of the independent variable V. By (16) however this quantity is equal to μ_1, an expression for which is given in Equation (13).

The fugacity[8] f is related to the chemical potential through the equation $d\mu_1 = RTd\ln f_1$ where μ_1 and f_1 refer to a pure substance or the value for one substance in a mixture. Integration at constant temperature gives

$$\mu_1 = RT\ln f_1 + k \tag{19}$$

The fugacity of a gas in a mixture is usually further defined so that at any temperature as the pressure approaches zero, $f_1 \doteq px_1$. At infinitely low pressures μ_1 from Equation (13) becomes $-RT\ln(RT/px_1)+RT+F_1$ whence $k = RT - RT\ln RT + F_1$ and on substitution of the value of μ_1 and k into (19) we obtain the complete expression for the isothermal variation of the fugacity of a gas in a mixture with the volume and composition

$$RT\ln f_1 = -RT\ln\frac{V}{n_1RT} + \left(\frac{\partial\beta_m}{\partial n_1}\right)_T \frac{1}{V} + \left(\frac{\partial\gamma_m}{\partial n_1}\right)_T \frac{1}{2V^2} + \left(\frac{\partial\delta_m}{\partial n_1}\right)_T \frac{1}{3V^3} \tag{20}$$

The differentials can be calculated by Equations (6).

4. The Mass Action Law

The general equations for the variation of $K_{\bar{p}}$ were derived in the first paper and are

$$\ln\frac{K_p}{K_{p_0}} = \sum\left[\nu_1\ln\frac{pV}{\sum(n_1)RT}\right] - \frac{1}{RT}\sum\left\{\nu_1\int_V^\infty\left[\left(\frac{\partial p}{\partial n_1}\right)_{T,V,n_2,\ldots} - \frac{RT}{V}\right]dV\right. \tag{I 45}$$

$$\ln K_{p_0} = \sum(\nu_1)[-1+\ln RT] - \frac{1}{RT}\sum(\nu_1F_1) \tag{I 43}$$

in which ν_1 is the number of moles of Gas 1 appearing in the stoichiometric equation expressing the chemical reaction, being negative when the substance disappears; $\ln K_p$ represents the expression $\Sigma(\nu_1\ln px_1)$; and K_{p_0} is the value of K_p at infinitely low pressures and is a function of the temperature alone.

When the isothermal variation of the equilibrium constant is being investigated, a value of K_{p_0} can be calculated from one known value of K_p and the corresponding temperature, volume and composition of the equilibrium mixture. If K_{p_0} is known at two temperatures, the two integration constants $\Sigma(\nu_1U_{01})$ and $\Sigma(\nu_1S_{01})$ which enter into the term $\Sigma(\nu_1F_1)$ through the relation (I 29) can be evaluated and K_p can then be calculated for the equilibrium mixture at any temperature and volume, provided that the integral in (I 45) can be evaluated, as for instance is done in Equations

[8] Lewis and Randall, Thermodynamics, p. 190. McGraw-Hall Book Company, New York (1923).

(21) and (22), and also that the constant volume heat capacities of the gases taking part in the reaction are known over the desired temperature range.

Carrying out the integration by use of the virial equation of state, we obtain

$$\ln \frac{K_p}{K_{p_0}} = \sum\left[\nu_1 \ln \frac{pV}{\sum(n_1)RT}\right] - \frac{1}{RT}\left\{\sum\left[\nu_1\left(\frac{\partial\beta_m}{\partial n_1}\right)_T\right]\frac{1}{V} + \sum\left[\nu_1\left(\frac{\partial\gamma_m}{\partial n_1}\right)_T\right]\frac{1}{2V^2} + \sum\left[\nu_1\left(\frac{\partial\delta_m}{\partial n_1}\right)_T\right]\frac{1}{3V^3}\right. \tag{21}$$

As before, it is possible to calculate $(\partial\beta_m/\partial n_1)_T$ from Equation (6), evaluate the summation $\nu_1(\partial\beta_m/\partial n_1)_T + \nu_2(\partial\beta_m./\partial n_2)_T + \cdots$ (ν being negative for gases on the left hand side of the chemical equation), and in this manner determine each of the three coefficients, which are constant for a given equilibruim mixture and at a constant temperature. However, in the case of this relation, it is somewhat more convenient to substitute the value of the virial coefficients into (21), the resulting equation being

$$\begin{aligned}
\ln \frac{K_p}{K_{p_0}} = {} & \sum(\nu_1)\ln\frac{pV_M}{RT} - \left\{\sum(\nu_1)\left[\sum(x_1B_{01}) - \frac{\sum(x_1c_1)}{T^3}\right]\right. \\
& + \left[\sum(\nu_1B_{01}) - \frac{\sum(\nu_1c_1)}{T^3}\right] - \left.\frac{2\sum(\nu_1A_{01}^{1/2})\sum(x_1A_{01}^{1/2})}{RT}\right\}\frac{1}{V_M} \\
& - \left\{-\left[\sum(\nu_1)\sum(x_1B_{01}) + \sum(\nu_1B_{01})\right]\left[\sum(x_1b_1) + \frac{\sum(x_1c_1)}{T^3}\right]\right. \\
& - \sum(x_1B_{01})\left[\sum(\nu_1b_1) + \frac{\sum(\nu_1c_1)}{T^3}\right] \\
& + \left.\frac{2\sum(\nu_1A_{01}^{1/2})\sum(x_1A_{01}^{1/2})\sum(x_1a_1) + \left[\sum(x_1A_{01}^{1/2})\right]^2\sum(\nu_1a_1)}{RT}\right\}\frac{1}{2V_M^2} \\
& - \left\{\sum(x_1b_1)\sum(x_1c_1)\left[\sum(\nu_1)\sum(x_1B_{01}) + \sum(\nu_1B_{01})\right]\right. \\
& + \left.\sum(x_1B_{01})\left[\sum(\nu_1b_1)\sum(x_1c_1) + \sum(x_1b_1)\sum(\nu_1c_1)\right]\right\}\frac{1}{3T^3V_M^3}
\end{aligned} \tag{22}$$

The composition of the equilibrium mixture is expressed in terms of mole fractions $x_1, x_2, \cdots$, and V_M is the volume of an average mole of the mixture. For a given equilibrium mixture, the five summations of the type $\Sigma(x_1 B_{01})$ and the five of the type $\Sigma(\nu_1 B_{01})$ involving the various equation of state constants can be calculated and all of the coefficients of the right hand side of Equation(22) evaluated. The quantity pV_M can be replaced by a function of V and T by use of the virial Equation (3).

The constants of the equation of state affect the calculation of the pressure in the descending order R, B_0, A_0, b, a, c. Thus products of the second order constants are in general small and the expressions (21) or (22) can

be simplified under certain conditions: (a) when the pressure is not too high, the term containing $1/V^3_M$ can be neglected, (b) at high temperatures, any term containing $1/T^3$ can usually be neglected, (c) at moderately low pressures, when a, b, and c can be neglected in the calculation of pressure a simple expression results

$$\ln \frac{K_p}{K_{p_0}} = \sum(\nu_1) \ln \frac{pV_M}{RT} - \left\{ \sum(\nu_1) \sum(x_1 B_{01}) + \sum(\nu_1 B_{01}) - \frac{2 \sum(\nu_1 A_{01}^{1/2}) \sum(x_1 A_{01}^{1/2})}{RT} \right\} \frac{1}{V_M} \tag{23}$$

5. Evaluation of the Integration Constants

The evaluation of the integration constants depends upon what changes in state of the gas mixture are to be studied. The determination of a consistent set of energy and entropy constants which will apply to all changes in state is outlined under I (a) below, but the necessary data a e not available for some gases, and such a complete system is not required in the case of many of the changes in state which it may be desired to study. The following cases may be considered:

I. *Chemical reactions between the component gases may take place.* (*a*) *The temperature of the system may change.* Arbitrary values may be assigned to the energy and entropy of all elementary substances at the standard temperature and some pressure (e.g. one atmosphere). The energy and entropy constants U_0 and S_0 for such elements as are gases under these conditions can be calculated from Equations (8) and (9) using the volume corresponding to the standard pressure. The energy and entropy for elements which are not gaseous under these conditions and for gases which are not elementary can be calculated for some volume at T_0 from thermodynamic data, and U_0 and S_0 determined from these values by (8) and (9).

(*b*) *Isothermal changes in state.* This case relates to the isothermal variation of K_p. A value of K_{p_0} at the temperature in question can be obtained from a given value of K_p for one equilibrium mixture.

II. No chemcial reactions occur. (*a*) *The temperature of the system may change.* Arbitrary values may be assigned to the energy and entropy of all of the pure gases composing the mixture for some volume (for instance, that corresponding to one atmosphere pressure) at the standard temperature T_0, and U_0 and S_0 calculated from Equations (8) and (9).

(*b*) *Isothermal changes in state.* Arbitrary values may be assigned to the energy or entropy of all of the pure gases for some volume and the temperature in question, from which u_1 and s_1 can be calculated from (8) and (9), by replacing U_{01}, S_{01}, and T_0 by u_1, s_1, and T.

Massachusetts Institute of Technology,
Cambridge, Mass.
July 11, 1928.

THE ENTROPY AND THERMODYNAMIC POTENTIALS OF REAL GASES AND MIXTURES OF REAL GASES AND A MASS ACTION LAW FOR CHEMICAL REACTION BETWEEN REAL GASES: III. RELATIONS FOR PURE GASES, AND THE EQUILIBRIUM PRESSURE OF A GAS IN A MIXTURE*

By James A. Beattie

Abstract

Thermodynamic relations.—Using the assumption that the pressure of a real gas approaches nRT/V as the volume approaches infinity, there are developed general thermodynamic equations for the energy, heat content, entropy, thermodynamic potentials $F_{V,T}$ and $F_{p,T}$, chemical potential and fugacity of a pure gas in terms of the appropriate independent variables V, T, n, or p, T, n. Each expression contains a definite integral which can be evaluated by use of an equation of state. The integrations are carried out by means of a new equation of state and all the thermodynamic quantities are expressed in terms of the variable V, T, n and the constants of the equation of the state.

Equilibrium pressures.—From the relations developed in this and a former paper for the chemical potential of a pure gas and of a gas in a mixture, there are obtained general expressions for the density and pressure of a gas which is in equilibrium at constant temperature through a semipermeable membrane with a mixture containing the gas in question. The integrations are again carried out by use of an equation of state for gases and gas mixtures.

Integration constants.—The evaluation of the various integration constants in briefly discussed.

1. Introduction

In the first two papers,[1] general and integrated equations were developed for the thermodynamic functions of mixtures of real gases. The derivations of the general equations depended upon two assumptions regarding the limiting values of the energy and equilibrium pressures of gases in mixtures of real gases as the total pressure approaches zero, and the integrations of these relations were carried out by means of a new equation of state for gas mixtures.

In the present paper, the method is used to derive general relations for the thermodynamic potentials of pure real gases, and for the equilibrium pressure of a gas in a mixture. Integrated expressions are obtained for all of the thermodynamic functions by means of an equation of state. Gibbs[2] has given the various thermodynamic functions for ideal gases and mixtures of ideal gases, but the method used by him cannot be applied directly to real gases.

* Contribution from the Research Laboratory of Physical Chemistry, Massachusetts Institute of Technology, No. 211.

[1] Beattie, (I) Phys. Rev. **31**, 680 (1928); (II) Phys. Rev. **32**, 691 (1928).

[2] Gibbs, Scientific Papers, Vol. 1, p. 150. Longmans, Green and Co., New York (1906).

2. General Thermodynamic Relations

The method used in deriving the general equations for a pure gas is the same as that outlined in the first paper: namely, in order to bring about any given change in state of a gas, all pressure or volume variations are carried out isothermally, and all temperature variations are made at infinitely low pressures. The equations for the isothermal variation of the desired thermodynamic quantities with pressure or volume are integrated from an infinitely low pressure to the variable pressure or volume. For the value of the thermodynamic quantity at the lower limit, there is substituted the ideal gas expression, with the exception that no assumption is made regarding the heat capacity of the gas at zero pressure, it being calculated from the measured heat capacity of the gas in question.

The application of this method requires only one assumption: that the pressure of a real gas approaches the perfect gas value nRT/V as the volume approaches infinity.[3] The following expressions can be derived:

(*a*) *When V and T are the independent variables.*

$$U=\int_V^\infty [p-T(\partial p/\partial T)_V]dV+nu \tag{1}$$

$$S=\int_V^\infty \left[\frac{nR}{V}-\left(\frac{\partial p}{\partial T}\right)_V\right] dV+nR\ln\frac{V}{n}+ns \tag{2}$$

$$F_{V,T}=\int_V^\infty \left[p-\frac{nRT}{V}\right] dV-nRT\ln\frac{V}{n}+nF \tag{3}$$

$$\mu=\int_V^\infty \left[\left(\frac{\partial p}{\partial n}\right)_{V,T}-\frac{RT}{V}\right] dV-RT\ln\frac{V}{n}+RT+F \tag{4}$$

$$RT\ln f=\int_V^\infty \left[\left(\frac{\partial p}{\partial n}\right)_{V,T}-\frac{RT}{V}\right] dV-RT\ln\frac{V}{nRT} \tag{5}$$

$$u=\int_{T_0}^T C_V^* dT+U_0 \tag{6}$$

$$s=\int_{T_0}^T C_V^* dT/T+S_0 \tag{7}$$

$$F=u-Ts \tag{8}$$

(*b*) *When p and T are the independent variables.*

$$H=\int_0^p [V-T(\partial V/\partial T)_p]dp+nh \tag{9}$$

[3] Gillespie and Lurie, Jour. Amer. Chem. Soc., **49**, 1146 (1927), have shown that if the equilibrium pressure of any gas in a mixture equals the product of its mole fraction times the total pressure, then the laws of Boyle and of Avagadro must hold for the pure gases present in the mixture. Thus a part of the assumption used here, namely that the pV product approaches a constant value as the volume approaches infinity at constant temperature, can be derived from one of the assumptions used for gas mixtures.

$$S=\int_0^p\left[\frac{nR}{p}-\left(\frac{\partial V}{\partial T}\right)_p\right]dp-nR\ln p+ns' \tag{10}$$

$$F_{p,T}=\int_0^p\left[V-\frac{nRT}{p}\right]dp+nRT\ln p+nF' \tag{11}$$

$$\mu=\int_0^p\left[\frac{V}{n}-\frac{RT}{p}\right]dp+RT\ln p+F' \tag{12}$$

$$h=\int_{T_0}^T C_V^*dT+RT+U_0 \tag{13}$$

$$s'=\int_{T_0}^T C_V^*dT/T+R\ln RT+S_0 \tag{14}$$

$$F'=h-Ts' \tag{15}$$

These equations express the variation of the energy U, heat content H, entropy S, thermodynamic potentials $F_{V,T}$ and $F_{p,T}$, chemical potential μ, and fugacity f, of a pure gas with the pressure p, total volume V, Kelvin temperature T, and number of moles n. C_V^* is the molal heat capacity at constant volume of the gas at infinitely low pressure. The quantities u, h, s, s', F and F' may be called the energy, heat content, entropy and thermodynamic potential constants at the temperature T and can be evaluated from the relations given; while U_0 and S_0 are the energy and entropy constants of the gas at the "standard temperature" T_0. The evaluation of these latter constants will be discussed in Section 4.

3. Integrated Equations

The general relations can be integrated by means of any equation of state. In the present paper the integrations are carried out by use of a new equation of state[4] which has been shown to reproduce the compressibility data on gases in a very satisfactory manner. The results are obtained most directly by using the equation in its virial form

$$p=nRT/V+n^2\beta/V^2+n^3\gamma/V^3+n^4\delta/V^4 \tag{16}$$

in which

$$\beta=RTB_0-A_0-Rc/T^2\ ;\quad \gamma=-RTB_0b+A_0a-RB_0c/T^2\ ;\quad \delta=RB_0bc/T^2 \tag{17}$$

R is the gas constant, and A_0, a, B_0, b and c are characteristic constants for a given gas.

Certain derivatives of the virial parameters will be used in the integration of the general equations. They are

$$\begin{aligned} &d\beta/dT=RB_0+2Rc/T^3\ ;\quad d\gamma/dT=-RB_0b+2RB_0c/T^3\ ;\\ &d\delta/dT=-2RB_0bc/T^3 \end{aligned} \tag{18}$$

[4] Beattie and Bridgeman, Jour. Amer. Chem. Soc., **49**, 1665 (1927); other papers to appear shortly.

The equation of state (16) has the independent variables V and T, so that it is necessary to use the corresponding general expressions which are given in Section 2 (a). Carrying out the integrations we obtain the relations

$$U=\left[\beta-T\left(\frac{d\beta}{dT}\right)\right]\frac{n^2}{V}+\left[\gamma-T\left(\frac{d\gamma}{dT}\right)\right]\frac{n^3}{2V^2}+\left[\delta-T\left(\frac{d\delta}{dT}\right)\right]\frac{n^4}{3V^3}+nu \tag{19}$$

$$S=nR\ln\frac{V}{n}-\left(\frac{d\beta}{dT}\right)\frac{n^2}{V}-\left(\frac{d\gamma}{dT}\right)\frac{n^3}{2V^2}-\left(\frac{d\delta}{dT}\right)\frac{n^4}{3V^3}+ns \tag{20}$$

$$F_{V,T}=-nRT\ln\frac{V}{n}+\frac{n^2\beta}{V}+\frac{n^3\gamma}{2V^2}+\frac{n^4\delta}{3V^3}+nF \tag{21}$$

$$\mu=-RT\ln\frac{V}{n}+\frac{2n\beta}{V}+\frac{3n^2\gamma}{2V^2}+\frac{4n^3\delta}{3V^3}+RT+F \tag{22}$$

$$RT\ln f=-RT\ln\frac{V}{nRT}+\frac{2n\beta}{V}+\frac{3n^2\gamma}{2V^2}+\frac{4n^3\delta}{3V^3} \tag{23}$$

The heat content and thermodynamic potential $F_{p,T}$ can be calculated by means of the usual equations and the relations given above. They are

$$H=U+pV=nRT+\left[2\beta-T\left(\frac{d\beta}{dT}\right)\right]\frac{n^2}{V}+\left[3\gamma-T\left(\frac{d\gamma}{dT}\right)\right]\frac{n^3}{2V^2}+\left[4\delta-T\left(\frac{d\delta}{dT}\right)\right]\frac{n^4}{3V^3}+nu \tag{24}$$

$$F_{p,T}=F_{V,T}+pV=nRT-nRT\ln\frac{V}{n}+\frac{2n^2\gamma}{V}+\frac{3n^3\gamma}{2V^2}+\frac{4n^4\delta}{3V^3}+nF \tag{25}$$

The various thermodynamic quantities can be expressed as functions of the temperature, volume and equation of state constants of the gas, by replacing the virial parameters and their derivatives by the relations (17) and (18). However, it is usually more convenient to calculate the values of these coefficients from (17) and (18) and substitute the numerical results into the Equations (19) to (25). The number of moles n, can be taken as unity by using the molal volume of the gas, and the thermodynamic quantity thereby calculated is for one mole.

4. The Molal Heat Capacity and the Energy and Entropy Constants

The quantity C_V* cannot be experimentally determined but it can be calculated from the measured constant volume heat capacity by means of the relation

$$(\partial C_V/\partial V)_T=T(\partial^2 p/\partial T^2)_V$$

which can be integrated by use of the equation of state (16), giving

$$C_V^* = C_V - \frac{nRc}{VT^3}\left[6 + \frac{3nB_0}{V} - \frac{2n^2B_0b}{V^2}\right] \tag{26}$$

where C_V is the molal heat capacity of the gas at T and the molal volume V/n. Hence a value of C_V^* can be calculated for each temperature at which a meaured value of C_V is available, and the resulting data expanded in a power series of the absolute temperature, which can be used to carry out the integration of Equations (6) and (7).

The molal energy and entropy constants, U_0 and S_0, can be referred to the energy and entropy of the gas in some "standard state." The temperature 0°C would be a convenient choice for the standard temperature T_0 In order to determine U_0 and S_0 we may make use of Equations (19) and (20) which on introduction of the equation of state constants give at the temperature T_0.

$$U_0 = U + \frac{nA_0}{V}\left[1 - \frac{na}{2V}\right] + \frac{3nRc}{VT_0^2}\left[1 + \frac{nB_0}{2V} - \frac{n^2B_0b}{3V^2}\right] \tag{27}$$

$$S_0 = S + \frac{nRB_0}{V}\left[1 - \frac{nb}{2V}\right] + \frac{2nRc}{VT_0^3}\left[1 + \frac{nB_0}{2V} - \frac{n^2B_0b}{3V^2}\right] - R\ln\frac{V}{n} \tag{28}$$

If one value of the molal energy U and molal entropy S is known at T_0 and a molal volume V/n, then U_0 and S_0 can be calculated by (27) and (28). For changes in state in which the gas does not undergo chemical reaction, arbitrary values may be assigned U and S for each gas at T_0 and a given value of V/n. A complete discussion of the determination of the energy and entropy constants for the various cases is given in Section 5 of the second paper of this series.

5. The Equilibrium Pressure of a Gas Through a Membrane

It is now possible to study the equilibrium relations through a semipermeable membrane. Consider a mixture of gases composed of n_1 moles of Gas 1, n_2 moles of Gas 2, etc., separated by means of a membrane which is permeable to Gas 1 alone, from a space containing pure Gas 1, the whole system being at constant temperature. At equilibrium the chemical potential of pure Gas 1 is equal to the value of the chemical potential of this gas in the mixture. Equations for the former have been obtained in the present paper; and equations for the latter were given in the second paper. We may use either set of independent relations V and T, or p and T in the expressions for μ, the two resulting relations being

(*a*) *When V and T are the independent variables*

$$\ln\frac{V_i/n_i}{V/n_1} = \frac{1}{RT}\int_{V_i}^{\infty}\left[\left(\frac{\partial p_i}{\partial n_i}\right) - \frac{RT}{V_i}\right]dV_i - \frac{1}{RT}\int_{V}^{\infty}\left[\left(\frac{\partial p}{\partial n_1}\right) - \frac{RT}{V}\right]dV \tag{29}$$

(b) When p and T are the independent variables

$$\ln\frac{p_i}{px_1}=\frac{1}{RT}\int_0^p\left[\left(\frac{\partial V}{\partial n_1}\right)-\frac{RT}{p}\right]dp-\frac{1}{RT}\int_0^{p_i}\left[\frac{V_i}{n_i}-\frac{RT}{p_i}\right]dp_i \tag{30}$$

The subscript i has been used to denote the value of a quantity for the pure Gas 1; no subscript denotes the value of a quantity for the whole mixture; and the subscript 1 refers to the value for Gas 1 in the mixture. Thus p_i and V_i are the pressure and volume of n_i moles of pure Gas 1, p and V the total pressure and volume of the mixture, and n_1 and x_1 the number of moles and mole fraction of Gas 1 in the mixture.

Equation (29) can be integrated by means of the equation of state for gases and gas mixtures, giving

$$RT\ln\frac{V_i/n_i}{V/n_1}=\frac{2n_i\beta_i}{V_i}+\frac{3n_i^2\gamma_i}{2V_i^2}+\frac{4n_i^3\delta_i}{3V_i^3}-\left(\frac{\partial\beta_m}{\partial n_1}\right)_T\frac{1}{V}-\left(\frac{\partial\gamma_m}{\partial n_1}\right)_T\frac{1}{2V^2}-\left(\frac{\partial\delta_m}{\partial n_1}\right)_T\frac{1}{3V^3} \tag{31}$$

Addition of a term $RT\ln p_i/px_1$, to both sides of (31) leads to the relation

$$RT\ln\frac{p_i}{px_1}=RT\ln\frac{p_iV_i/n_i}{pV/\sum(n_1)}-\frac{2n_i\beta_i}{V_i}-\frac{3n_i^2\gamma_i}{2V_i^2}-\frac{4n_i^3\delta_i}{3V_i^3}+\left(\frac{\partial\beta_m}{\partial n_1}\right)_T\frac{1}{V}+\left(\frac{\partial\gamma_m}{\partial n_1}\right)_T\frac{1}{2V^2}+\left(\frac{\partial\delta_m}{\partial n_1}\right)_T\frac{1}{3V^3} \tag{32}$$

The quantities β_i, γ_i, δ_i are the virial parameters for the pure Gas 1, and the three partial derivatives are obtained from the equation of state for the mixture. They are given in the second paper, the relations in terms of the equation of state constants of the gases composing the mixture the temperature and the composition being

$$\begin{aligned}
(\partial\beta_m/\partial n_1)_T&=RT\left[\sum(n_1B_{01})-\sum(n_1c_1)/T^3\right]+\sum(n_1)RT\left[B_{01}-c_1/T^3\right]\\
&\quad-2A_{01}^{1/2}\sum(n_1A_{01}^{1/2})\\
(\partial\gamma_m/\partial n_1)_T&=-\left[RT\sum(n_1B_{01})+B_{01}\sum(n_1)RT\right]\left[\sum(n_1b_1)+\sum(n_1c_1)/T^3\right]\\
&\quad-\sum(n_1)RT\sum(n_1B_{01})\left[b_1+c_1/T^3\right]\\
&\quad+2A_{01}^{1/2}\sum(n_1A_{01}^{1/2})\sum(n_1a_1)+a_1\left[\sum(n_1A_{01}^{1/2})\right]^2\\
(\partial\delta_m/\partial n_1)_T&=\left\{\sum(n_1b_1)\sum(n_1c_1)\left[RT\sum(n_1B_{01})+B_{01}\sum(n_1)RT\right]\right.\\
&\quad\left.+\sum(n_1)RT\sum(n_1B_{01})\left[b_1\sum(n_1c_1)+c_1\sum(n_1b_1)\right]\right\}/T^3
\end{aligned} \tag{33}$$

For a given system the values of the virial coefficients for Gas 1 and of the derivatives for the mixture can be calculated from (17) and (33), and the numerical results substituted in (31) or (32). The quantities p_iV_i and pV can be replaced by functions of the respective volumes and of the temperature by means of the virial equations.

From the relations (31) and (32) it is possible to calculate the density and pressure of a gas which is in equilibrium at constant temperature through a semipermeable membrane with a gas mixture containing this gas, the temperature, composition and volume of the mixture being known. The volume of the pure gas is contained implicitly in both expressions so that the calculation must be carried out by the method of successive approximations.

When two mixtures of gases are separated by means of a semipermeable membrane which is permeable to one or more of the gases, the chemical potential of each such gas is the same on both sides of the membrane. From the volume, temperature and composition of one of the mixtures, and the composition of the other, the density or pressure of this latter mixture can be calculated.

MASSACHUSETTS INSTITUTE OF TECHNOLOGY,
CAMBRIDGE MASS.
July 11, 1928.

BOOK REVIEWS

Handbuch der Elektrizität und des Magnetismus. L. GRAETZ. Band V, Lieferung 3. (Last issue of handbook.) Pp. 211 of text, pp. 21 of name index to vol. V, pp. 42 of subject index to vol. V. Johnan Ambrosius Barth, Leipzig, 1928. Price bound 39.50. R.M.

This issue is devoted to (1) electrical installations of batteries, machinery, etc., and (2) radio transmission and reception. Both subjects are treated very superficially. The treatment of electrical machinery is only sufficient to give one an idea of the types in use. It is quite useless to an engineer, and it would not enable a physicist to do away with an engineer. The radio parts of the book are somewhat fuller. However, they are decidedly inadequate. Most boys in this country know more circuits for reception than are given in the book. For some reason the intensity of radiation in different directions from different antennas is treated elaborately. The effects of the spherical shape of the earth, of the Kennelly-Heaviside layer, and of fading are listed among *special* effects (besondere Einflüsse). They are actually the most vital influences. The short paragraph on Sommerfeld's reciprocity theorem makes no mention of the effect of the Earth's magnetic field. van der Pol and G. N. Watson are not mentioned in connection with the spherical shape of the earth. Fortunately the index includes a reference to van der Pol in the first issue of volume V. H. A. Taylor and E. O. Hulbert do not seem to be mentioned at all. High-power, high-frequency alternators are discussed elaborately in comparison with tube-transmission. The modern systems of crystal-controlled short-wave sets are not discussed.

G. BREIT

La Théorie de la Relativité et la Méchanique Céleste. Vol. I. JEAN CHAZY. Pp. 261, figs. 139. Gauthier-Villars et Cie, Paris, 1928. Price 80fr.

In this volume the author is more concerned with the application of Einstein's theory to the problems of celestial mechanics than in the assumptions underlying that theory. Therefore he has little to say about curved time-space or covariant and contravariant tensors. Instead he makes Schwarzschild's expression for the line element his point of departure and gives a very thorough discussion of the minute divergences from Newton's law to which it leads and of its accordance with the observational evidence, in so far as the motions of the major planets are concerned.

The first chapter contains an unusually clear discussion of the Calculus of Variations and its applications to classical dynamics. In the next chapter Newton's law is formulated as representing motion along a geodesic in a three-dimensional representative space and then Schwarzschild's solution of Einstein's equations is considered as a generalization to four-dimensional space-time. It would have been illuminating if the author had included some comparison of the Hill-Jeffrey solution of Einstein's equations with that of Schwarzschild.

Next the author considers what modifications of the perturbation theory are made necessary by relativity. He finds that no sensible errors are incurred if Newton's inverse square law is replaced by Schwarzschild's law for the planet under consideration, and those corrections added which are required by the Newtonian theory of perturbations.

The next two chapters are devoted to the work of Le Verrier and of Newcomb and of the three discrepancies with Newton's law which they discovered. The author notes that while the relativity theory accounts most astonishingly well for the discrepancy in the advance of the perihelion of Mercury it is not so successful in accounting for the smaller discrepancy in that of Mars or for the motion of the node of Venus.

The last chapter treats the deflection of light passing through a gravitational field. No mention is made of the displacement toward the red of spectral lines originating on a gravitating mass.

The book is written with the clarity of exposition characteristic of the French, and should be very valuable to the student of celestial mechanics.

LEIGH PAGE